UNIVERSITY OF LONDON THESIS

Degree PhD Year 2008 Name of Author O'SHEA, MARIA.

Fine Mapping of Quantitative Trait Loci (QTL) and Identification of Candidate Genes for Prion Disease Incubation in Mice

A thesis presented in partial fulfilment of the requirements for the degree of Doctor of Philosophy to the University of London

Marie O'Shea
MRC Prion Unit
Institute of Neurology
University College London

ProQuest LLC
789 East Eisenhower Parkway
P.O. Box 1346
Ann Arbor, MI 48106-1346

Declaration

I, Marie O'Shea, confirm that the work presented in this thesis is my own. Where information has been derived from other sources, I confirm that this has been indicated in the thesis.

Abstract

Prion diseases are progressive neurodegenerative diseases which show characteristic prolonged incubation periods. Polymorphisms in the prion protein gene are known to influence incubation time but additional genetic loci have also been identified by quantitative trait locus mapping studies in mice. Genome-wide screening approaches using two-way crosses have identified broad regions of linkage with large confidence intervals on several mouse chromosomes. In order to reduce and fine map the regions, a genetically diverse heterogenous stock (HS) of mice has been utilized which provides a powerful tool for fine mapping at centimorgan (cM) intervals. Linkage analysis in the HS mice identified small (1-2cM), highly significant regions of linkage on chromosomes 8, 9 and 11. The predicted regulatory regions and entire mRNA transcript of candidate genes within these regions have been sequenced to identify polymorphisms between the parental strains of the cross. This variation may be indicative of genetic differences that influence prion disease incubation time. Linkage analysis was used to determine if identified polymorphisms correlated with the strain effects observed in the cross and resulting candidates were genotyped in the cross to assess association with incubation time. The expression of candidate genes was quantified in the parental strains of the cross to assess the regulatory control of polymorphisms identified. Attention on chromosome 11 has focused on Trans-acting Transcription Factor 6 (*Sp6*) and Monocyte Chemoattractant Protein 1 (*Mcp-1*), the latter having been assessed in a mouse model. A small group of genes on chromosome 8 have also been implicated as promising candidates. The identification of modifier genes influencing susceptibility to prion diseases will provide further insights into the pathogenesis of prion disease and identify ligands and pathways for the design of rational therapeutics.

Acknowledgements

Firstly I would like to thank my supervisors, Dr Sarah Lloyd and Professor John Collinge, for their essential help and guidance throughout my research and without whom this thesis would not have been possible. Thanks also for the hard work of Sebastian Brandner, Jackie Linehan, the histology team and the staff at Wakefield Street. Special thanks to comrade Emma Maytham for patiently teaching me everything I needed to know in the lab. A huge thank you to Ray Young for endless help with figures. Thanks also to Gareth Banks for help with tricky PCRs and to Mark Poulter for friendly technical advice.

A huge thank you to all of the past and present members of the Fisher group, with whom I was lucky enough to work with, and everyone else at the Prion Unit for friendship, fun, technical advice and moral support. It wouldn't have been the same without each and every one of you. Special thanks and love to Gaia and Emma for always believing in me. I would have never made it this far without you two. Thank you also to Dr Nick Parkinson and Dr James Stevens for the Croissant Appreciation Society, shame it had to fold so early on! You were a great lab buddy Nick and I learnt so much from you about being a good scientist. A heartfelt thank you to Professor Lizzy Fisher whose office door was always open and who gave me the confidence to carry on whenever I felt defeated. To my favourite lab girls, Ruth and Fran, thank you for the brilliant friendship we've shared and for our Friday afternoon coffee outings which were so good for the soul! A big hug and thank you to Mel for being a great housemate and an entertaining, supportive and inspiring friend! Thanks also to James and Gary for providing lab time entertainment and for all the sound effects! A special thanks also to Kevin for great chats about films and general nonsense and always being a friendly face at work.

Thanks and lots of love to Paresh, Fran and Si for an adventure I'll never forget. We have shared so many experiences along the way and your friendship will always be special to me. Go team! To Jess and Bev, thank you for beers and Gowlett pizza and for always being there throughout the dramas! To Tom, thanks for all the fun we had, for all the pool we played and for sticking with me when it was really hard. Thanks also to Bash and Nigel who were always available for hugs whether they liked it or not! A huge thank you to Yaz and Mal for sleepless nights, infinite wisdom and utter silliness.

To Tommy and Sara, thank you for countless beers, rubbish jokes and for providing me with a temporary home where I always felt welcome. I would also like to thank the numerous medical staff at Lincoln County Hospital, Dr Timothy Webber, The Wheelers (especially Keith Barnard and Karen Brooks) and Paul Smith who helped get me back on my feet, bike and thesis following my accident. Thanks also to Roger for a fresh perspective on 'the PhD' and to Emma for fish-finger sandwiches and for lending a friendly ear to listen to my PhD and broken body woes! Pep talks from Dr. T were also a massive help when viva nerves were getting the better of me. I am also very grateful for the kind support and friendship I recieved from my colleagues at Delta-Simons. Sarah, Laura, Mel, James, POB, Latho and Rammy B, thanks guys, you helped me get to the finish line.

To Hannah and Olivia, we did it all together girls! You guys are my very best friends no matter what I'm doing, where I am or what I'm going through. Thanks for being the best drinking buddies ever and for being my safe haven when I've needed you. Life would have been totally different now if it wasn't for our year away and you have made me who I am today.

I'd like to thank my whole family for their continued support, especially Mum and Dad. The unconditional love, support (financial and otherwise!) and advice you have given me has been essential in getting me to where I am today and I'll never be able to thank you enough. I couldn't have asked for better parents. Thanks for always being on my side. Thanks also to my brother, Kevin, you've been a great friend throughout, patiently listening to my grumbling and always being there for me. I feel like you've grown up much faster than me I'll always look to you for guidance in how to be a good person. Thanks also to Ali, you're part of the family mate and our friendship will always mean a lot to me. Thanks also to Lindsay for being there towards the end of my write-up and being a great listener and new friend!

Finally, I would like to dedicate this thesis to my wonderful grandma who has shared broken bones with me and provided me with an endless supply of tea and cheery anecdotes whilst I have been writing up. Knowing you were in the next room if I ever needed to escape from my studies was always great source of comfort.

'Courage is not the lack of fear. It is acting in spite of it.'
Mark Twain

Table of Contents

List of Figures

List of Tables

List of Appendices

Abbreviations

3'UTR	3' Untranslated Region
5'UTR	5' Untranslated Region
µg	Microgrammes
µl	Microlitre
µM	Micromolar
°C	Degrees centigrade
A	Adenine
A2M	Alpha(2)-Macroglobin
ACTB	Beta Actin
AD	Alzheimer's Disease
Adcy7	Adenylate Cyclase 7
AIL	Advanced Intercrossed Line
ALS	Amyotrophic Lateral Sclerosis
Apaf-1	Apoptotic Protease Activating Factor 1
APC	Antigen-Presenting Cells
ApoE	Apolipoprotein E
Arhgap23	Rho GTPase Activating Protein 23
ATP	Adenosine 5'-Triphosphate
BAC	Bacterial Artificial Chromosome
bp	Base Pair
Brd7	Bromodomain Containing 7
BSE	Bovine Spongiform Encehphalopathy
Bsx	Brain Specific Homeobox
C	Cytosine
cAMP	Cyclic 3', 5'-Adenosine Monophosphate
CARD	Caspase Recruitment Domain

Ccl2	Mouse Chemokine (C-C motif) Ligand 2
Cdk5rap3	Cyclin Dependent Kinase 5 Regulatory Associated Protein 3
cDNA	Complementary DNA
CJD	Creutzfeldt-Jakob Disease
cM	Centimorgan
CNS	Central Nervous System
Crtam	Cytotoxic and Regulatory T Cell Molecule
CSS	Chromosome Substitution Strain
Cul5	Cullin 5
CWD	Chronic Wasting Disease
Cyld	Cylindromatosis
Da	Daltons
ddH_20	Purified Deionised Water
Del	Deletion
DEPC	Diethyl Pyrocarbonate
DMSO	Dimethyl Sulphoxide
DNA	Deoxyribonucleic Acid
Dnaja4	Heat Shock Protein DNAJ-Like 4
dNTP	Deoxynucleotide Triphosphate
Dpl	Doppel
DRG	Dorsal Root Ganglia
dTTP	Deoxythymidine Triphosphate
EAE	Experimental Allergic Encephalomyeltis
EDRF	Erythroid Differentiation–Related Factor
EDTA	Ethylenediaminetetraacetic Acid
EGF	Epidermal Growth Factor
ELISPOT	Enzyme-Linked Immunospot Plate
ET	Energy Transfer

EtBr	Ethidium Bromide
EtOH	Ethanol
Ex	Exonic
FAM	6-Carboxy-Fluorescine
FDC	Follicular Dendritic Cells
FFI	Fatal Familial Insomnia
FTD	Frontotemporal Dementia
g	Acceleration Due to Gravity
G	Guanine
GAPDH	Glyceraldehyde 3-Phosphate Dehydrogenase
GFAP or *Gfap*	Glial Fibrilliary Acidic Protein
GPI	Glycosylphosphatidylinisotol
GRAM	Glucosyltransferases, Rab-Like GTPase Activators and Myotubularins
Gramd1b	GRAM Domain Containing 1B
GSS	Gerstmann-Straussler-Scheinker
GTP	Guanosine-5'-Triphosphate
HEAT	Huntingtin, Elongation Factor 3, Regulatory A Subunit of Protein Phosphatase 2A and TOR1
Heatr3	HEAT Repeat Containing 3
HEX	Hexachloro-6-Carboxyfluorescein
HD	Huntington's Disease
HDL	High-Density Lipoprotein
HLA	Human Leukocyte Antigen
HOCl	Hypochlorous Acid
HOX	Homeobox
HS	Heterogenous Stock
HSCC	Heterogenous Stock Collaborative Cross
HSE	Heat Shock Element

HSIBG	Boulder Heterogenous Stock
HSNPT	Northport Heterogenous Stock
Hsp	Heat Shock Protein
Hstf	Heat Shock Transcription Factor
Ig-SF	Immunoglobulin Superfamily
Il-10	Interleukin-10
Ins	Insertion
IT	Incubation Time
Intr	Intronic
kb	Kilobases
kDa	Kilodaltons
Kpnb1	Karyopherin (Importin) Beta 1
LOD	Logarithm of Odds
LPA	MegaBACE Linear Polyacrylamide
LRR	Leucine Rich Repeat
Lrrc46	Leucine Rich Repeat Containing 46
M	Molar
MAP	Microtubule-Associated Protein
Mapt or *Tau*	Microtubule-Associated Protein Tau
Mb	Mega Base
MCM	Multiple Cross Mapping
Mcp1	Monocyte Chemoattractant Protein 1
mg	Milligram
$MgCl_2$	Magnesium Chloride
MGB	Minor Groove Binder
MHC	Major Histocompatibility Complex
MM	Microsatellite Marker
mM	Millimolar

ml	Millilitre
Mllt6	Mixed Lineage-Leukaemia Translocation to 6 Homolog (Drosophila)
Mpo	Myeloperoxidase
mRNA	Messenger Ribonucleic Acid
Mrp	Mitochondrial Ribosomal Protein
NaAc	Sodium Acetate
NaCl	Sodium Chloride
NC	No Change
N-CAM	Neural Cell Adhesion Molecule
ND	Not Determined
Necl2	Nectin-Like 2
NF-κB	Nuclear Factor-Kappa B
ng	Nanogram
Ngfr	p75 Low Affinity Nerve Growth Factor Receptor
NK	Natural Killer
Nkd1	Naked Cuticle 1 Homolog
nm	Nanometre
NMR	Nuclear Magnetic Resonance
nNOS	Neuronal Nitric Oxide Synthase
NOD	Nucleotide Binding Oligomerization Domain
Npepps	Aminopeptidase Puromycin Sensitive
NTC	Non Template Control
Olfr	Olfactory Receptor
OPR	Octapeptide Repeat
OPRI	Octapeptide Repeat Insertion
ORF	Open Reading Frame
P140cap	P140 Caspase-Associated Protein
PBS	Phosphate Buffered Saline

Pcgf2/Mel-18	Polycomb Group Ring Finger
PCR	Polymerase Chain Reaction
PDGF	Platelet-Derived Growth Factor
Pid2	Prion Incubation Determinant-2
Pid3	Prion Incubation Determinant-3
PMCA	Prion Misfolding Cyclic Amplification
Prn	Prion Gene Complex
Prnd	Doppel
Prni	Prion Incubation Time Gene
Prnp or PRNP	Prion Protein
Pro	Promoter
PrP^{c}	Cellular Prion Protein
PrP^{Sc}	Abnormal Infectiouos Isoform of the Cellular Prion Protein
Psm	Proteasome (Prosome, Macropain) Subunit
PtdIns3P	Phosphatidylinositol 3-Monophosphate
PX	Phox Homology Domain
qRT-PCR	Quantitative Real Time-Polymerase Chain Reaction
QTG	Quantitative Trait Gene
QTL	Quantitative Trait Loci
QTN	Quantitative Trait Nucleotide
rcf	Relative Centrifugal Force
RFLP	Restriction Fragment Length Polymorphism
Rgs2	Regulator of G-Protein Signalling 2
RI	Recombinant Inbred
RIST	Recombination Inbred Segregation Test
RML	Rocky Mountain Laboratory
RNA	Ribonucleic Acid
RNAi	RNA Interference

rpm	Revolutions Per Minute
rRNA	Ribosomal RNA
RT-PCR	Real Time-Polymerase Chain Reaction
Sall1	Sal-Like 1
SCA	Scrapie Cell Assay
Scn3b	Sodium Channel, Voltage-Gated Type III, Beta
ScRG	Scrapie-Responsive Gene
Scrn	Secernin
Scya2	Small Inducible Cytokine A2
SDP	Strain Distribution Pattern
Sinc	Scrapie Incubation Time Gene
siRNAs	Small Interfering RNAs
Skt6	Serine-Threonine Kinase 6
Slic1	Selectin Ligand Interactor Cytoplasmic-1
Socs7	Suppressor of Cytokine Signalling 7
SOD	Super Oxide Dismutase
Sp6os	Non-Coding Opposite Strand Transcript of *Sp6*
SP/KLF	Specificity Protein/Krüppel-Like Factor
SNP	Single Nucleotide Polymorphism
SNX	Sorting Nexin
SNX-PX	SNX-PX Homology Domain
Sp	Sp Transcription Factor
SPF	Specific Pathogen Free
SYBR Green	Synergy Brands
T	Thymine
Ta	Annealing Temperature
TBE	Tris-Borate EDTA
Tbkbp1	TBK Binding Protein 1

Tbx21	T-Box 21
TE	Tris & EDTA Buffer
TET	Tetrachloro-6-Carboxyfluoresciene
TFSEARCH	Transcription Factor Search
T_m	Melting Temperature
TME	Transmissible Mink Encephalopathy
TNF-α	Tumor Necrosis Factor-Alpha
TRANSFAC	Transcription Factor Binding Site Database
TRI	Total RNA Isolation
TSE	Transmissible Spongiform Encephalopathies
Ube2	E2 Ubiquitin-Conjugating Enzyme
UCSC	University California Santa Cruz
UPS	Ubiquitin-Proteasome System
UTR	Untranslated Region
UV	Ultra Violet
V	Volts
vCJD	Variant Creutzfeldt-Jakob Disease
Vtn	Vitronectin
W	Watt
Zfp	Zinc Finger Protein

1
Introduction

1.1 Prion Diseases

Prion diseases, also known as Transmissible Spongiform Encephalopathies (TSEs), are fatal neurodegenerative disorders which show characteristic prolonged and clinically silent incubation periods. They include Creutzfeldt-Jakob disease (CJD), Gerstmann-Sträussler-Scheinker syndrome (GSS), Fatal Familial Insomnia (FFI), Kuru and variant CJD (vCJD) in humans and scrapie, bovine spongiform encephalopathy (BSE), transmissible mink encephalopathy (TME) and chronic wasting disease (CWD) in animals. A distinct neuropathology is seen in all of these diseases, the central feature being the post-translational conversion of a ubiquitous host-encoded, cellular 'prion' protein, (PrP^{C}), to an abnormal infectious isoform (PrP^{Sc}) (Prusiner, 1998) which accumulates in affected brains as insoluble aggregates (Figure 1.1b), sometimes within amyloid plaque deposits. Other histopathological hallmarks of prion disease include intracellular neuronal vacuolation (Figure 1.1a) and neuronal loss, giving the cerebral grey matter a microvacuolated or 'spongiform' appearance alongside severe astrocytic gliosis.

1.1.1 The Transmissible Nature of Prion Diseases

The transmissible nature of prion diseases was first demonstrated in scrapie, a disease endemic in European sheep populations and characterized by early behavioral signs of anxiousness, hypersensitivity, loss of co-ordination and an uncontrollable urge to scratch which are later followed by severe ataxia and death (Healy *et al.*, 2003). Accidental transmission of scrapie occurred through the use of a contaminated vaccination against looping ill virus which contained formalin-treated lymphoid tissue, providing one of the first demonstrations of the particular resistance of the infectious agent to chemical treatment (Gordon, 1946).

During the 1950s, Kuru, a progressive cerebellar ataxia accompanied by dementia in the later stages of disease (Collinge, 2001), reached epidemic proportions in the Fore highlanders of Papua New Guinea. The disease exhibited many similarities with scrapie pathology and this led to the suggestion that Kuru may also be an infectious transmissible disease (Hadlow, 1959). This hypothesis was subsequently validated by

Figure 1.1 Pathological hallmarks of prion disease
a) Section of medulla oblongata from a BSE-affected cow showing neuropil vacuolation (Haematoxylin and eosin; 400x). Taken from Gavier-Widen *et al.*, 2005.

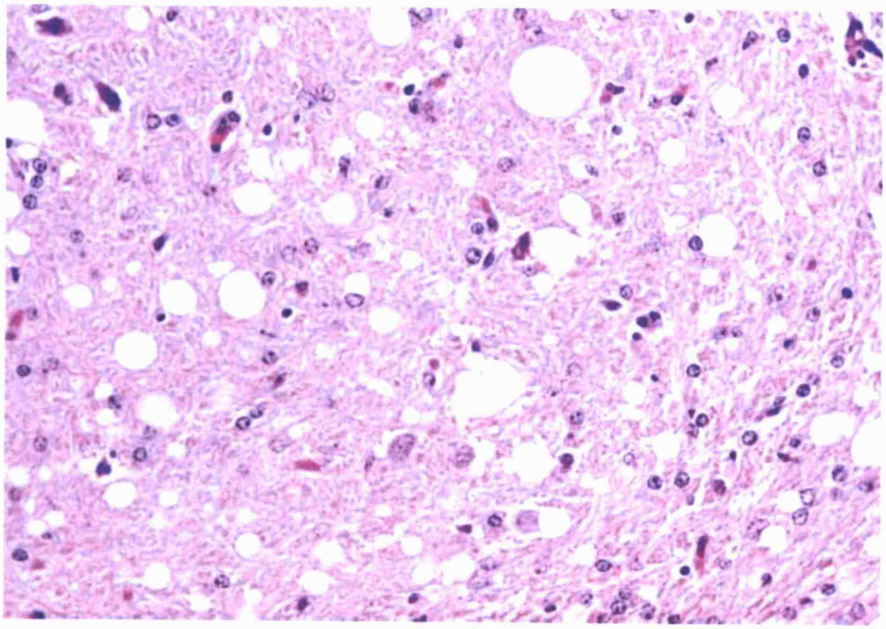

b) Unicentric plaques of abnormal prion protein in the human cortex. Immunohistochemistry with prion protein antibody ICSM35 is shown. Scale bar is 150μm. Taken from Mead, 2006.

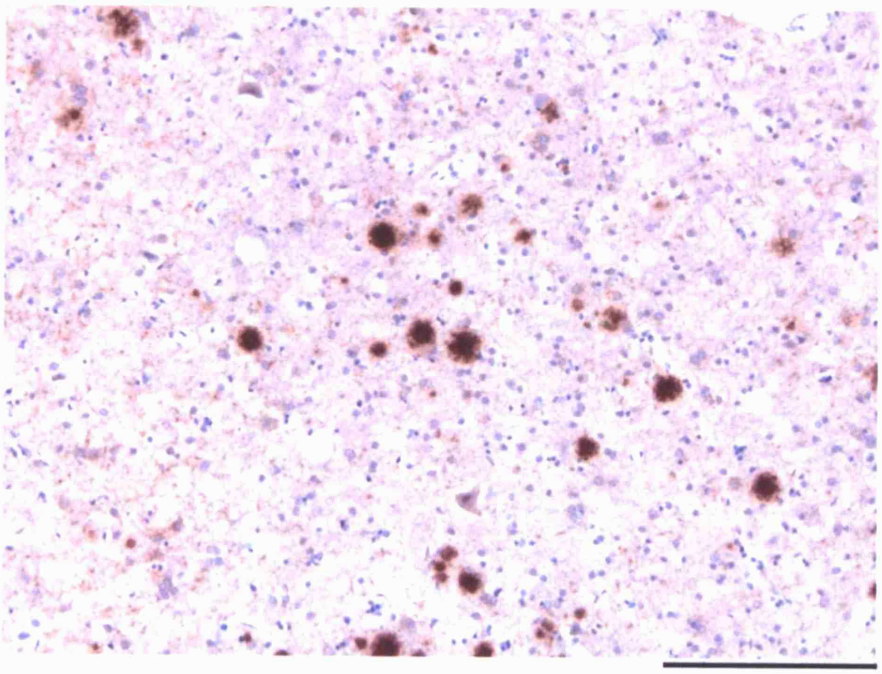

intracerebral inoculations of Kuru-infected brain homogenate in chimpanzees which produced a progressive neurodegenerative condition sharing many of the clinical and pathological features of the human form of the disease, including a prolonged incubation period (Gajdusek et al., 1966). Further neuropathological and clinical connections were made between Kuru and CJD following successful transmission of the latter to non-human primates (Gibbs *et al.*, 1968). The concept of 'transmissible dementias' was subsequently implemented to describe this group of diseases.

More recently, the 1986 UK BSE epidemic raised concerns about the transmission of disease to humans through dietary exposure to infected material. The origins of the BSE outbreak have not yet been fully established although it is generally believed that disease was transmitted to cattle through the consumption of animal feed prepared from scrapie-infected rendered sheep carcasses (Wilesmith et al., 1988). It has also been speculated that a rare sporadic form of BSE may have occurred within the bovine population and that the inclusion of contaminated cattle tissue alongside sheep offal in animal feed may have led to dietary recycling of infected material (Collinge, 1999; Prusiner, 1997). The significance of the BSE epidemic was realised in 1996 following the identification of a novel form of human prion disease, vCJD, whose neuropathological and molecular characteristics share many similarities with those of BSE providing a link between the two diseases (Bruce *et al.*, 1997; Collinge et al., 1996b; Hill *et al.*, 1997). The UK population was directly exposed to the BSE strain through the food chain until the statutory exclusion of specified bovine offal in 1989 which is consistent with an incubation period of between 5 and 10 years for the first recognised cases of vCJD (Will *et al.*, 1996). These findings have prompted intensified research into the pathogenesis and aetiology of prion diseases.

1.1.2 Human Prion Diseases

Human prion diseases are biologically unique in that they manifest as one of three different aetiologies; sporadic, inherited or acquired.

Sporadic Prion Disease

Sporadic CJD is the most common form of human prion disease, accounting for approximately 85% of cases, with a prevalence of 1 case per million per year worldwide. Its cause is unknown. The peak of onset of sporadic prion disease is between 60-65 years and 70% of affected individuals die within 6 months (Collinge,

2001). Progressive dementia is preceded by personality changes, psychiatric symptoms and sleep disturbance. It has been speculated that the disease originates following horizontal transmission of prions from humans or animals (Gajdusek, 1977), somatic mutations in the gene encoding human prion protein (*PRNP*) or as a result of a rare stochastic event which causes spontaneous conversion of PrP^{C} into PrP^{Sc} (Prusiner, 1989).

Inherited Prion Disease

Inherited prion diseases constitute around 10-15% of all human prion disease and include GSS, FFI and familial CJD. They exhibit autosomal dominant Mendelian inheritance with linkage to chromosome 20 (Hsiao *et al.*, 1989) and can range from a very rapid and aggressive disease to a more prolonged and slowly progressing dementia with clinical and neuropathological symptoms varying within a single family (Collinge et al., 1992). Over 30 coding mutations in the open reading frame (ORF) of the human prion protein gene (*PRNP*) are responsible for this group of diseases. These include nonsynonymous mutations, some of which cause a premature stop codon, and the insertion of additional octapeptide repeats (OPRI) found in the normal sequence of the prion protein (Collinge, 1997; Mead, 2006) (Figure 1.2).

Figure 1.2 Pathogenic mutations and polymorphic variants of the human prion protein. Pathogenic mutations and polymorphic variants are shown above and below the protein respectively. Octapeptide repeats are shown as black blocks. Numbers refer to codon numbers. Mutations are designated by the wild-type amino acid preceding the codon number. All residues are shown by single letter abbreviations of amino acids. Taken from Lloyd and Collinge, 2005.

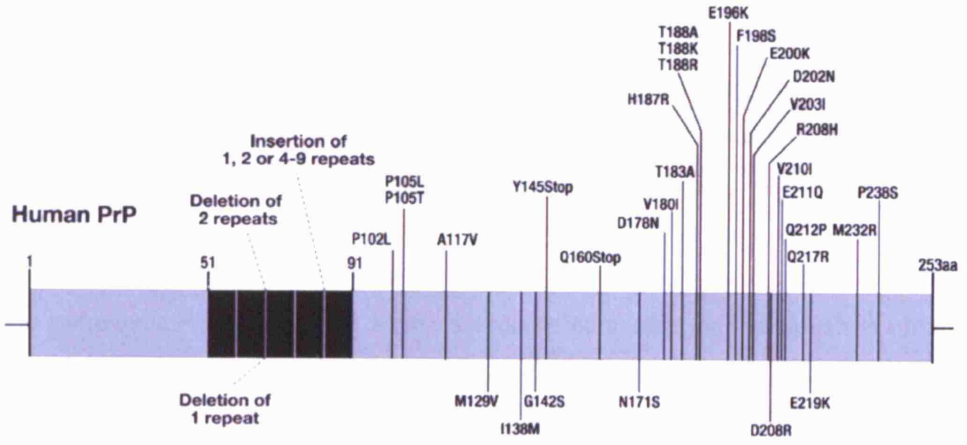

Acquired Prion Disease

Acquired prion diseases have resulted from exposure to infected material and include iatrogenic CJD, Kuru and vCJD. Iatrogenic CJD has occurred through a direct central nervous system (CNS) route following prion-infected dura mater tissue grafts (Yamada et al., 1994) and also via peripheral routes including treatment with prion-contaminated human cadaveric pituitary hormones (Gibbs et al., 1985). Intracerebrally acquired iatrogenic prion disease presents as a rapidly progressive dementia with a short incubation period of around 19-46 months whereas peripheral exposure produces a slower progressive ataxia and a much more prolonged incubation period of up to 15 years (Collinge, 2001).

Kuru is thought to have originated when a single case of sporadic CJD died and was consumed during endocannibalistic mortuary feasts, leading to subsequent horizontal recycling of infected tissue within this isolated population (Alpers and Rail, 1971). The disease is defined by progressive cerebellar ataxia with death usually occurring, often through starvation, after 6 to 9 months (Gajdusek, 1977). The incidence of Kuru dropped dramatically as a consequence of the mid-1950s prohibition of mortuary feasts by Australian authorities and is now currently only seen in individuals born before the cessation of cannibalism who represent the extreme end of the Kuru incubation time distribution, with incubation periods exceeding 50 years (Collinge et al., 2006). The experience and knowledge gained from research into Kuru provides a useful model of acquired human prion disease which may be important in predicting the possible epidemiological course of the novel prion disease, vCJD.

vCJD first attracted attention through its appearance in relatively young people with a mean age of onset of 29 and by its prolonged duration of illness before death (~14 months) compared to other CJD patients (Collinge, 2001; Will *et al.*, 1996). Behavioural and psychiatric disturbances are central clinical symptoms of vCJD, including depression and personality change (Hill *et al.*, 1999b; Zeidler *et al.*, 1997a). No pathogenic *PRNP* mutations have been identified in affected individuals (Collinge *et al.*, 1996a) and none have any known history of iatrogenic exposure to human prions (Will et al., 1996).

The transmission of acquired prion disease has mainly occurred through dietary exposure, as in the cases of Kuru and vCJD, although two recent cases of vCJD

infection have been reported in recipients of blood transfusions from a donor who subsequently developed vCJD following donation (Llewelyn *et al.*, 2004; Peden *et al.*, 2004; Wroe *et al.*, 2006).

1.1.3 The Nature of the Infectious Agent

It was first assumed that the causative agent of scrapie was a virus, leading to the use of the term 'slow virus', in reference to the observed characteristic prolonged incubation period. However, the low molecular weight of the scrapie agent, its notable resistance to high temperatures and the action of ionizing and ultra-violet radiation, known to destroy all other known viruses, led to the suggestion that the infectious agent was free of nucleic acid (Alper *et al.*, 1967; Pattison and Jones, 1967) and the transmission of disease was subsequently proposed to occur through a 'protein-only' mechanism (Griffith, 1967). This controversial theory of a 'protein-only' form of self-replication directly opposed the central dogma of molecular biology proposed following the elucidation of deoxyribonucleic acid (DNA). Further characterisation of the physicochemical properties of the purified scrapie agent, such as sensitivity to proteases and resistance to most procedures known to modify nucleic acids, provided support for the theory that a protein was required for infectivity and subsequently led to the proposal of the term "prion" to describe the causative agent as a small proteinaceous infectious particle (Prusiner, 1982). Further purification of infectious scrapie material (Prusiner *et al.*, 1982) identified a partially protease resistant 27-30kDa protein designated the prion protein (PrP) whose concentration was directly proportional to titers of infectivity, leading to the conclusion that it constitutes the major structural component of the scrapie agent (McKinley *et al.*, 1983) and providing support for the 'protein-only' hypothesis (Griffith, 1967).

Scrapie-infected mouse and Syrian hamster brain was later used to clone a cDNA encoding a single gene, *Prnp*, for PrP, present in both infected and uninfected animals (Oesch *et al.*, 1985). Antibodies against PrP were shown to react with proteins of 33,000 to 35,000 Daltons in crude extracts from both normal and scrapie-infected brain and were designated PrP^{C} for 'cellular' prion protein and PrP^{Sc} for the 'scrapie' associated form (Meyer *et al.*, 1986; Oesch et al., 1985). PrP^{C} was shown to be completely degraded following limited proteinase K digestion whereas PrP^{Sc} gave rise to a 27-30kDa fragment (PrP 27-30), identifying a protease resistant core in infected material. The fact that the two isoforms of PrP had identical primary structures

suggested a post-translational modification was taking place in PrP^{C} resulting in increased protease resistance in the scrapie-associated form and providing the first indication of the autocatalytic mechanism of prion propagation (Prusiner, 1989).

The exact identity of the infectious agent causing prion disease remains unclear amidst continuing strong support for the established role of the prion protein (Prusiner, 1998; Weissmann, 1999). In agreement with this hypothesis, recent intracerebral inoculations of synthetic mammalian prions have been shown to cause neurodegenerative disease in mice (Legname *et al.*, 2004; Legname *et al.*, 2005).

1.1.4 The Conversion of PrP^{C} to PrP^{Sc}

The conversion of PrP^{C} and replication of PrP^{Sc} within a host organism has been principally explained by two models which describe 'refolding' (Prusiner, 1991) and 'seeding' (Jarrett and Lansbury, 1993) mechanisms (Figure 1.3). In the 'refolding' model PrP^{Sc} recruits and binds PrP^{C} and acts as a template to drive the folding of the normal cellular form into the alternate pathological isoform, a process concluded by the dissociation of the two molecules which subsequently become available to recruit further PrP^{C} and thereby propagate infectivity. Alternatively, the seed polymerisation model proposes that an equilibrium existing between the two conformers of the prion protein is disrupted by mutations and/or the presence of stable aggregated seed material causing a shift in favour of PrP^{Sc}. This model provides a potential explanation for disease caused by spontaneous or known mutations in sporadic and inherited prion disease and also indicates how foreign PrP^{Sc} may act as the stable aggregated seed material to induce pathogenesis. Generated seeds are thought to produce oligomers of PrP^{Sc} which aggregate and form amyloid fibrils and then fracture to subsequently form multiple new seeds for further propagation of misfolded PrP (Jarrett and Lansbury, 1993).

Another proposed model of the conversion of cellular prion protein to the abnormal disease-associated form involves the production of an intermediate toxic species, designated PrP^{L} (L denoting lethal) (Collinge and Clarke, 2007). In this model PrP^{Sc} is not responsible for neurotoxicity but instead acts as a catalytic surface for the formation of toxic intermediate products prior to their maturation into PrP^{Sc}. Initially the relatively slow rate of conversion governed by a low level of PrP^{Sc} would in turn mean a low level of PrP^{L} present. A large amount of PrP^{Sc} and therefore, infectivity, would

Figure 1.3 Schematics of the 'refolding' and 'seeding' models of the conversion of PrP^{C} to PrP^{Sc}.

Refolding Model

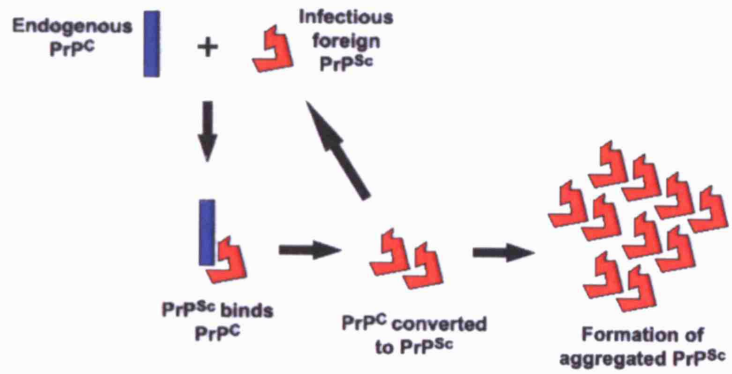

Seeding Model

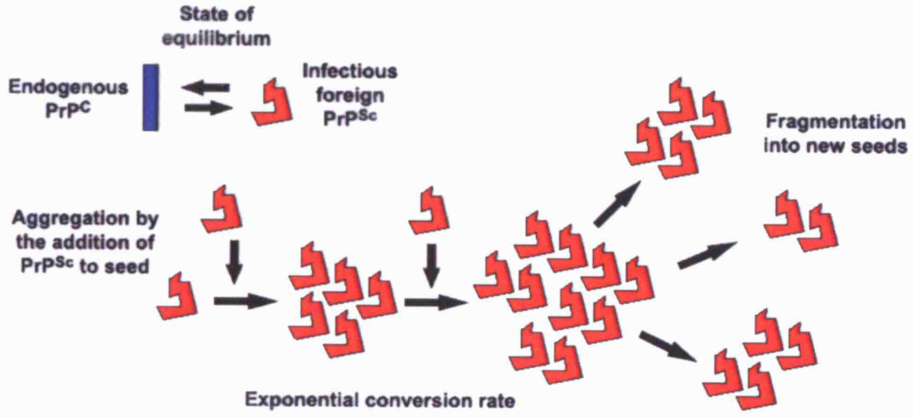

build up but the low level of PrP^{L} would not be sufficient to produce toxicity because of the rate of loss of this intermediate product through maturation. As the amount of final PrP^{Sc} product increases so does the level of PrP^{L} and therefore toxicity would become evident. This theory may explain observed decoupling between the level of PrP^{Sc} and observed pathology in subclinical prion infection (Hill and Collinge, 2003).

Conversion of PrP^{C} to PrP^{Sc} in cell-free systems in which infected hamster PrP^{Sc} has been mixed with PrP^{C} material from uninfected cultured cells (Kocisko *et al.*, 1994), and also using the prion misfolding cyclic amplification (PMCA) technique, which allows the rapid conversion of large excess PrP^{C} in the presence of minute quantities of PrP^{Sc} (Saborio *et al.*, 2001), have been successful in generating protease resistant material *in vitro* (Bieschke *et al.*, 2004; Hill *et al.*, 1999a) which has been shown to be infectious upon intracerebral inoculation in Syrian hamsters (Castilla *et al.*, 2005).

The study of yeast prions has provided evidence to support the heritable nature of proteins. The best-characterised yeast prion proteins are Sup35p, a translation termination factor and Ure2p, which is involved in nitrogen metabolism (Taylor and Wickner, 2001). The prion forms of Sup35p and Ure2p are known as [PSI+] and [URE3], respectively. A prion-like mechanism involving a self-perpetuating conformational change of Sup35p and Ure2p to their prion forms in the absence of nucleic acids is known to control the phenotypes controlled by these proteins (Liebman and Derkatch, 1999; Wickner, 1994). *In vivo* replication of infectivity using amyloid fibrils produced *in vitro* (King and Diaz-Avalos, 2004; Tanaka et al., 2004) further supports the mechanism of propagation suggested by the 'protein-only' hypothesis (Griffith, 1967).

1.1.5 The Prion Gene (*Prnp*) and Protein (PrP)

The prion protein gene is a single copy gene (Basler *et al.*, 1986; Oesch et al., 1985) located on the short arm of human chromosome 20 (Liao *et al.*, 1986) and on corresponding chromosome 2 in the mouse (Sparkes *et al.*, 1986). *Prnp* is widely expressed in mouse during embryogenesis, detectable by embryonic day 13.5 in the developing brain and spinal cord in addition to several tissues of the peripheral and sympathetic nervous systems and also in some non-neuronal cell populations (Manson *et al.*, 1992). In adult hamsters and mice, *Prnp* continues to be expressed at high levels in the brain, at intermediate levels in the heart and lung and at a lower level in the liver and spleen (Caughey *et al.*, 1988; Oesch et al., 1985). Human and hamster PrP share the same genomic structure with two exons and a single intron (Basler et al., 1986; Puckett *et al.*, 1991) whereas the mouse prion protein gene has three exons (Westaway *et al.*, 1994). The open reading frame is contained within the second exon in each case and encodes a 253-257 amino acid peptide (Puckett et al., 1991).

The cellular isoform of the prion protein is a widely expressed glycoprotein which is highly conserved throughout mammals and birds implying potential functional significance (Westaway and Prusiner, 1986; Wopfner *et al.*, 1999). Following translation a tightly packed hydrophobic core of twenty residues (Riek *et al.*, 1998) targets the peptide to the endoplasmic reticulum where the N terminal signal peptide is removed, as is a C terminal peptide which is replaced with a glycosylphosphatidylinisotol (GPI) anchor (Harris *et al.*, 1993; Stahl *et al.*, 1987). PrP is then trafficked to the Golgi body at which point the GPI anchor is modified and

glycosylation occurs (Stahl *et al.*, 1993). PrP contains two highly conserved N-glycan attachment sites which exist *in vivo* as un-, mono- and diglycosylated glycotypes (Rudd *et al.*, 2001). Structural analysis of recombinant prion protein in human, mouse and hamster using nuclear magnetic resonance (NMR) (Liu *et al.*, 1999; Riek *et al.*, 1996; Zahn *et al.*, 2000) showed that the unstructured N terminus of PrP contains a series of octapeptide repeats, which bind copper (Jackson *et al.*, 2001b) and also 3 regions of α-helices and two short anti-parallel β-sheet within the structured C terminal domain (Zahn et al., 2000). In contrast to the predominantly alpha helical PrP^{C}, disease associated misfolded PrP contains an increased proportion of β-sheets and it has been suggested that this is a consequence of the infective process (Pan *et al.*, 1993). A single internal disulphide bind is also formed in the C terminal creating a loop that contains both sites of N-linked carbohydrate (Rudd et al., 2001; Stahl and Prusiner, 1991).

PrP is clustered in discrete patches at relatively high density in cholesterol-rich and detergent resistant lipid rafts or microdomains in the plasma membrane (Madore *et al.*, 1999; Vey *et al.*, 1996) and is continually recycled within endosomes with a transit time of ~60 minutes via association with clathrin coated pits suggesting a putative role for PrP as a receptor for the uptake of molecules from the extracellular medium (Shyng *et al.*, 1993; Sunyach *et al.*, 2003).

1.1.6 The Normal Physiological Function of PrP

The exact physiological function of the normal cellular prion protein has not yet been established although several putative roles have been suggested. Observed alterations in calcium signalling and changes in hippocampal anatomy in PrP knockout mice suggest a potential role in synaptic transmission (Colling *et al.*, 1996; Collinge *et al.*, 1994; Mallucci *et al.*, 2002). It has been also suggested that PrP^{C} may target neuronal nitric oxide synthase (nNOS) to lipid rafts since this process is disrupted in mice with prion disease and also in PrP knockout mice (Keshet *et al.*, 1999). Disrupted circadian rhythms in PrP knockout mice are also noteworthy since sleep disorders are a central theme of FFI, although a link between the prion protein and the mechanisms enabling the normal transition to sleep have not been substantiated (Huber *et al.*, 2002). Other putative roles for the prion protein include copper transportation within the brain as PrP is known to bind copper with high affinity (Viles *et al.*, 1999) and copper levels have been shown to be decreased in PrP knockout mice (Brown, 2003).

PrP^C may function to protect neurons and other cells from stress or toxicity. Comparisons have been drawn between PrP and Super Oxide Dismutase (SOD) implicating a role for PrP in cellular resistance during oxidative stress (Brown *et al.*, 1999; Wong *et al.*, 2000), although there is conflicting evidence to suggest that PrP does not to contribute towards SOD activity (Hutter *et al.*, 2003). A protective effect of the prion protein has also been suggested based upon the observation that apoptosis occurs following serum removal in a neuronal cell line lacking normal PrP^C (Kuwahara *et al.*, 1999). Furthermore, overexpression of PrP^C has been found to prevent Bax-mediated cell death in cultured human neurons (Roucou *et al.*, 2003) and in also in yeast expressing mammalian Bax (Li and Harris, 2005).

A role in cell signalling and adhesion has also been suggested for PrP corresponding with its location and recycling in endosomes at the cell surface (Shyng et al., 1993). Overexpression of PrP has been shown to lead to neuroblastoma cell aggregation (Mange *et al.*, 2002) and PrP is also known to bind to isoforms of the Neural Cell Adhesion Molecule (N-CAM) (Schmitt-Ulms *et al.*, 2001) providing support for PrP as an intracellular adhesion molecule. An interaction between PrP^C and laminin and also with the human 37-kDa laminin receptor precursor has led to the suggestion that laminin may act as a receptor or co-receptor for PrP^C implying a further putative role in cell signalling (Graner *et al.*, 2000; Rieger *et al.*, 1997). Furthermore, reduced expression of the laminin receptor has been shown to inhibit the accumulation of PrP^{Sc} in scrapie-infected neuronal cells (Leucht *et al.*, 2003). PrP^C has also recently been shown to bind the extracellular matrix protein, vitronectin (VTN), with possible implications for a role in axonal growth (Hajj *et al.*, 2007).

1.1.7 PrP is required for Neurodegeneration in Prion Disease

Although the normal physiological function of PrP is still unclear there is much evidence to support the absolute requirement of the protein for disease susceptibility. Two mouse lines devoid of PrP, designated the 'Zurich I' knockout mice (*Prnp*$^{o/o}$) (Bueler *et al.*, 1992) and *Prnp*$^{-/-}$ (Manson *et al.*, 1994), have been shown to be viable and do not display any gross physical or behavioural abnormalities. Furthermore, postnatal abrogation of PrP expression, through Cre-mediated ablation of neuronal PrP in mice at 9 weeks of age, does not induce neurodegeneration and/or other histopathological changes (Mallucci et al., 2002). In line with the 'protein-only' hypothesis (Griffith, 1967; Prusiner, 1982) *Prnp*$^{o/o}$ mice challenged with prions do not

develop prion disease and fail to accumulate prions in the spleen and brain nor do they replicate infectivity (Bueler *et al.*, 1993; Sailer *et al.*, 1994). The introduction of murine transgenes into *Prnp*$^{o/o}$ mice restores disease susceptibility following challenge with prions, the shorter incubation times seen in those mice expressing the highest levels of PrP^{C} (Fischer *et al.*, 1996). The necessity for neuronal PrP^{C} in the neurodegenerative process in prion disease is also demonstrated by the reversal of spongiform change and the prevention of disease progression in prion infected mice following depletion of neuronal PrP^{C} despite a continued accumulation of PrP^{Sc} in non-neuronal tissues such as the glia (Mallucci *et al.*, 2003). Neurodegenerative phenotypes seen in alternate *Prnp* knockout mice which present with ataxia and cerebellar Purkinje cell degeneration (Moore *et al.*, 1999; Sakaguchi *et al.*, 1996) have been explained by ectopic expression of a novel PrP-like protein designated Doppel (Dpl) 16kb downstream of *Prnp* which is upregulated in these knockout lines (Moore et al., 1999). The structural similarities seen between Dpl and PrP in the C terminal region, suggests that they may share biological properties. Overexpression of Dpl in the brain of *Prnp*$^{o/o}$ mice (Moore et al., 1999; Moore *et al.*, 2001) and the Purkinje cells of transgenic mice (Anderson *et al.*, 2004) results in cerebellar ataxia associated with Purkinje cell degeneration. Again these results reflect the ectopic expression of Dpl in transgenic mice and do not represent the normal pattern of expression which is high in adult mouse testis but undetectable in the brain (Makrinou *et al.*, 2002; Moore et al., 1999). Dpl has been implicated in male fertility (Behrens *et al.*, 2002) but does not appear to have a role in prion disease (Mead *et al.*, 2000; Tuzi *et al.*, 2002).

1.1.8 Prion Strains

It is well established that prion diseases exhibit strain variation with well-defined heritable properties characterised by distinctive incubation times and neuropathology when passaged in a defined inbred mouse strain (Bruce, 1993; Bruce, 2003). The existence of multiple prion strains seemed to contradict the 'protein-only' hypothesis since PrP^{Sc} is thought to be the major component of the infectious unit. However, it is currently thought that structural variation in PrP^{Sc} provides the basis for prion strain specificity and this variation correlates well with the pathological characteristics observed between different forms of prion disease (Bessen and Marsh, 1992; Bessen and Marsh, 1994; Collinge et al., 1996b; Hill and Collinge, 2001; Telling *et al.*, 1996). Forms of prion disease are characterised by specific patterns of protease-resistant fragments of varying size and glycoform ratio following limited proteinase K digestion

(Collinge et al., 1996b). Prion strains are known to propagate their structural properties and phenotypes upon transmission to transgenic mice. The conformation of abnormally folded PrP also varies according to prion strain (Safar *et al.*, 1998; Telling *et al.*, 1996).

A molecular approach to prion strain typing based on susceptibility to proteinase K digestion and subsequent electrophoretic mobility and glycoform ratios has enabled the identification of four main types of CJD (Hill *et al.*, 2003) (Figure 1.4). Types 1-3 are signified by three different PrP^{Sc} glycoform ratios in cases of sporadic and iatrogenic CJD which show characteristic Western blot pattern of two large molecular-mass bands representing glycosylated PrP and a smaller unglycosylated form, of protease-resistant PrP. All variant CJD cases seen so far have been associated with a unique and highly consistent pattern showing a predominance of the diglycosylated band and has been designated PrP^{Sc} type 4 (Collinge et al., 1996b). This distinct molecular strain type is exclusive to BSE and vCJD providing compelling evidence for an aetiological link between the two diseases (Bruce et al., 1997; Collinge et al., 1996b; Hill et al., 1997).

Figure 1.4 Western blot illustrating typical type 1-4 PrP^{Sc} patterns.
Developed with monoclonal antibody 3F4. Adapted from Hill *et al.*, 2003.

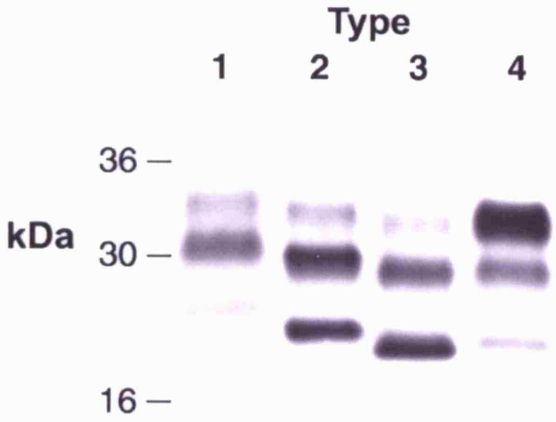

Transmission of BSE and vCJD to normal inbred mice (FVB) produces a type-4-like glycoform ratio pattern and fragment sizes which are indistinguishable between the two prion strains (Hill et al., 1997). Furthermore, glycoform patterns observed following experimental transmission of BSE in cynomolgus macaques (Lasmezas *et al.*, 1996) and in naturally acquired BSE in domestic cats (Wyatt *et al.*, 1991) match those of experimental murine BSE and vCJD. It has been suggested that the differences between PrP conformers may be the basis for specific neuropathological targeting in the brain as

observed in different strain types, with prions replicating most efficiently in those cell populations expressing a similarly glycosylated PrP (Collinge et al., 1996b; DeArmond *et al.*, 1997).

1.1.9 The Species or Transmission Barrier

It is well known that the transmission efficiency of prion disease between mammalian species is limited by a 'species barrier' characterised by differences in pathogenesis between first and subsequent passages in a new species (Dickinson, 1976; Kimberlin *et al.*, 1987). PrP^{Sc} glycoform pattern, three-dimensional structure and the compatibility of PrP between donor and recipient have also been implicated as major components of the species barrier (Moore *et al.*, 2005; Prusiner *et al.*, 1990). Transgenic mice expressing hamster PrP are highly susceptible to hamster prions compared to wild-type mice supporting the theory that prion propagation proceeds most efficiently when the primary structure of the interacting PrP^{Sc} and host PrP^{C} are identical (Prusiner *et al.*, 1990).

The transmission of vCJD prions across a species barrier to wild-type mice has been shown to be much more efficient than with other CJD prions, where transmission efficiency is more consistent with the presence of a species barrier, conferring low attack rates and prolonged incubation times (Hill et al., 1997). Intriguingly the transmission of vCJD prions to transgenic mice expressing human PrP ($HuPrP^{+/+}$ *Prn-p*$^{o/o}$) is paradoxically much less efficient than with other CJD strains (Hill et al., 1997). It has therefore been suggested that a description of a strain-species or transmission barrier would be more appropriate than simply a species barrier which does not take into account the specific effects of the prion strain in question (Collinge, 1999).

1.1.10 Mechanisms of Neurotoxicity and Cell Death in Prion Disease

The mechanisms of neurodegeneration in prion disease are not well understood although apoptotic cell death is known to be a central feature of pathogenesis (Cronier *et al.*, 2004; Hetz *et al.*, 2003). Several mechanisms of how neurotoxicity in prion disease leads to apoptotic cell death have been suggested including oxidative stress (Milhavet *et al.*, 2000) and migroglial-mediated damage (Betmouni *et al.*, 1996).

There is conflicting evidence for the role of altered cytosolic PrP^{C} trafficking in prion neurotoxicity in which impairment of the ubiquitin-proteasome system (UPS) results in

extensive accumulation of PrP^{C} in the cytoplasm and associated neuronal death suggesting a toxic gain of function for PrP^{C} (Kristiansen *et al.*, 2005; Rane *et al.*, 2004; Roucou et al., 2003). *In vitro* studies have implicated full length PrP^{Sc} as cytotoxic (Hetz et al., 2003). Shorter peptide fragments, especially those including residues 106 to 126, have also been shown to be cytotoxic *in vivo* (Ettaiche et al., 2000) and in primary cultured neurons (Forloni et al., 1993). However, there is conflicting evidence to suggest that PrP^{Sc} is not directly neurotoxic and that cellular PrP is required for the toxic effect since PrP^{C} null neuronal tissue exposed to PrP^{Sc} remains healthy and free of pathology despite accumulation of extraneuronal PrP^{Sc} (Brandner *et al.*, 1996; Mallucci et al., 2003). In addition, PrP^{Sc} is almost completely undetectable in some forms of FFI, yet disease is still transmissible (Collinge *et al.*, 1995; Tateishi *et al.*, 1995), and subclinical prion infection has been reported in which high level of PrP^{Sc} accumulates in the absence of clinical symptoms (Hill and Collinge, 2003). Furthermore, there is no direct correlation between neuronal loss and the presence of PrP^{Sc} plaques in CJD-affected brain tissue (Parchi *et al.*, 1996).

The process of prion replication itself and not the end product may induce toxicity. As previously described, a toxic oligomeric PrP intermediate species, PrP^{L}, has also been suggested as the causative agent of neurodegeneration (Collinge and Clarke, 2007; Hill and Collinge, 2003). In addition, small oligomeric species with common structural properties, formed prior to the generation of large protein aggregates have also been suggested to be the cause of cytotoxicity in several neurodegenerative diseases characterised by protein aggregation including prion disease, Alzheimer's Disease (AD) and Huntington's Disease (HD) (Bucciantini *et al.*, 2002; Kayed *et al.*, 2003) suggesting that the formation of fibrillar deposits may be a cellular self defence mechanism. This is supported by the protective effect of aggregated protein deposits in a cell model of HD (Arrasate *et al.*, 2004).

A role for aggresomes in the clearance of toxic cytoplasmic misfolded aggregates has also been implicated in prion disease (Garcia-Mata *et al.*, 2002; Kawaguchi *et al.*, 2003). Aggresome-like structures have recently been identified in the brains of scrapie-infected mice following mild inhibition of the proteasome, which contain PrP^{Sc}, heat shock protein 70, ubiquitin, proteasome subunits and vimentin (Kristiansen *et al.*, 2005). The formation of these aggresomes have been directly associated with apoptosis via caspase-3 and -8 activation.

1.2 Genetic Susceptibility to Prion Disease

1.2.1 Genetic Susceptibility to Prion Disease in Humans

Coding polymorphisms in the prion protein are well known to affect incubation time and susceptibility in prion disease. Codon 129 is the location of a common polymorphism in the human prion protein which encodes either a methionine or valine residue. It is a key determinant of genetic susceptibility to acquired and sporadic prion disease with homozygosity at this position a known risk factor (Cervenakova *et al.*, 1998; Palmer *et al.*, 1991; Windl *et al.*, 1996). Methionine homozygotes make up 37% of the UK Caucasian population, whereas valine homozygotes make up 12% and the remaining 51% are heterozygous (Collinge et al., 1991; Owen *et al.*, 1990).

Heterozygosity at codon 129 is associated with relative resistance to CJD and other prion diseases (Collinge, 2005). For example, in individuals affected by a form of inherited prion disease with a 144 base pair gene insertion heterozygosity increases life span (Baker *et al.*, 1991; Collinge et al., 1992). Heterozygosity also increases survival in iatrogenic CJD caused by exposure to contaminated pituitary hormones (Huillard d'Aignaux *et al.*, 1999) and in Kuru (Cervenakova et al., 1998). All identified cases of vCJD to date have been methionine homozygous at codon 129 (Collinge et al., 1996a; Hill *et al.*, 1999b; Zeidler *et al.*, 1997b) with the exception of a recent case of vCJD transmission in a codon 129 heterozygote individual which occurred following a contaminated blood transfusion (Peden et al., 2004). The individual died from an unrelated cause without evidence of any neurological disorder but post-mortem analysis revealed presence of PrP^{Sc} in lymphoreticular tissues consistent with prion infection.

It is thought that strong balancing selection pressure has occurred in the Fore population of Papua New Guinea as a result of the Kuru epidemic, due to a high disease incidence and the effect of heterozygosity in delaying disease onset (Cervenakova et al., 1998). A significant distortion of the population structure has essentially eliminated PrP codon 129 homozygotes (Mead *et al.*, 2003). The strong evolutionary selection pressure in favour of heterozygous prion disease resistance alleles may be explained in terms of the potential mechanisms by which prion strains are proposed to propagate as heterozygosity may reduce prion transmission efficiency and the rate of PrP^{Sc} accumulation by inhibiting homologous protein-protein interactions (Collinge, 1999; Moore et al., 2005; Prusiner et al., 1990). Intriguingly bovine PrP encodes a methionine

at the homologous amino acid to codon 129 in human suggesting a potential basis for the almost exclusive incidence of vCJD in methionine homozygotes (Wopfner et al., 1999). Codon 129 is not the only human PrP polymorphism which is known to control susceptibility in prion disease. Heterozygosity at codon 219 (E219K) is also thought to confer resistance to sporadic CJD in the Japanese population following a study of 85 sporadic CJD cases in which this genotype was absent (Shibuya *et al.*, 1998).

Human association studies have provided further support for the role of the *PRNP* locus in prion disease. Three polymorphisms identified in the promoter and a regulatory region of intron 1 were shown to be common to sporadic CJD patients (McCormack *et al.*, 2002). Furthermore a polymorphism ~23kb upstream of *PRNP* has been shown to be associated, independent of codon 129 genotype, with the risk of developing sporadic CJD but not vCJD, potentially reflecting the different aetiologies of prion disease (Mead *et al.*, 2001). Several polymorphisms have also been identified in the human *PRND* gene (Mead et al., 2000; Peoc'h et al., 2000), which encodes DPL and maps within 25kb of *PRNP*. There is also conflicting evidence of an association of a common coding polymorphism, M174T, with sporadic CJD (Croes *et al.*, 2004; Mead et al., 2000; Peoc'h et al., 2000; Schroder *et al.*, 2001).

The major histocompatibility complex (MHC) is well known to be associated with susceptibility in infectious diseases and has been implicated in prion disease incubation time in mouse studies (Kingsbury *et al.*, 1983). A study typing 50 vCJD patients and 26 sporadic CJD patients identified a significantly reduced frequency of the class II antigen HLA-DQ7 in vCJD patients relative to controls (Jackson *et al.*, 2001a) although subsequent work has failed to replicate these findings (Laplanche *et al.*, 2003; Pepys *et al.*, 2003).

The small samples sizes used in these studies, especially in the case of vCJD, make it difficult to assess whether an actual association between these non-*PRNP* candidate genes and prion disease exists. It is clear that prion protein gene polymorphisms remain the main genetic factor controlling susceptibility to prion disease in humans but there are other lines of evidence to suggest that it is not the sole genetic influence and this is supported by the identification of additional genetic factors in genome wide mapping studies in mice (Lloyd *et al.*, 2001; Lloyd *et al.*, 2002; Manolakou *et al.*, 2001; Moreno *et al.*, 2003; Stephenson *et al.*, 2000).

1.2.2 Prion Disease Incubation Time in Mice

The mouse has become a pre-eminent model for human physiology and disease. Mice provide an excellent model for the study of prion susceptibility genes because they are able to recapitulate the major characteristics of the disease phenotype such as the prolonged incubation time. The small size of the mouse, its high reproductive rate and short life span make it a feasible model of disease in terms of providing the substantial sample sizes required for statistical significance in genetic studies. The relatively high number of human sporadic CJD cases allows the application of association studies but the much smaller number of vCJD cases makes analysis problematic for this form of the disease. Furthermore, the high sequence conservation between mice and humans means that prion disease susceptibility genes identified in the mouse may also have potential relevance in the human population.

Prion diseases are characterised by prolonged, clinically silent incubation periods, defined in experimental transmission studies in mice, as the duration of time, measured in days, between inoculation with a prion strain and the onset of the clinical symptoms of disease. Genetic susceptibility is a major determinant of prion disease incubation period and different inbred mouse strains show well defined and reproducible incubation times when experimental conditions remain constant (Table 1.1). There are several additional factors which also influence incubation time including dose of infectious material, route of administration, level of host PrP^C, prion strain and the presence of a species barrier.

Dose of Infectious Agent

The dose of infectious agent is a key influence controlling incubation time with higher doses leading to shorter incubation times (Kimberlin and Walker, 1978b). It has been shown that differences in incubation time between different routes of administration can be compensated for by changes in dose (Kimberlin and Walker, 1978a).

Route of Administration

It is well established that peripheral inoculation or oral ingestion of prions produce a much longer incubation time than inoculation procedures directly targeting the CNS (Kimberlin and Walker, 1977). For example, in the C57BL mouse strain intracerebral challenge with the ME7 prion strain produces an incubation time of 168±2 days whereas intraperitoneal inoculation leads to a much more prolonged incubation time of

275±3 days (Bruce et al., 1991). Intravenous routes have been shown to be as efficient as intracerebral inoculation and subcutaneous routes are known to produce the longest incubation times (Kimberlin and Walker, 1978b).

Level of Host PrP^C

Incubation time is also influenced by the expression levels of host PrP^C. As described previously, mice devoid of PrP show normal development and behaviour but are known to be resistant to infection with prions due to their inability to replicate PrP^{Sc} (Bueler et al., 1993; Bueler et al., 1992). Hemizygous *Prn-p*$^{0/+}$ mice also show enhanced resistance to scrapie in comparison with mice carrying the usual two copies of the *Prnp* gene, giving incubation times around 125 days longer than wild-type controls (Bueler et al., 1993). Transgenic mice, designated Tg20, homozygous for a PrP-encoding construct, possess 60 copies of the gene and express high levels of PrP^C, up to 10-fold more than controls (Fischer et al., 1996). These mice have short incubation periods of 60±4 days following challenge with Chandler/RML consistent with similar studies showing that incubation times are inversely proportional to host PrP expression levels (Bueler *et al.*, 1993; Fischer *et al.*, 1996; Prusiner *et al.*, 1990).

Prion Strain

Different prion strains produce characteristic incubation times and neuropathology in defined inbred lines of mice (Bessen and Marsh, 1994; Bruce *et al.*, 1994; Bruce et al., 1991; Collinge et al., 1996b; Fraser and Dickinson, 1968; Telling et al., 1996). For example, C57BL mice have differing incubations times of 137±0, 158±2 and 469±22.3 days in response to intracerebral inoculations of Chandler/RML, ME7 and 22A mouse-passaged prion strains respectively (Dickinson and Mackay, 1964; Hunter *et al.*, 1992; Kingsbury *et al.*, 1983).

The Species Barrier

As previously described (Section 1.1.9), the species barrier is known to contribute towards the observed attack rate in prion disease and to affect the efficiency of transmission between mammalian species. It can be quantified by measuring the fall in mean incubation period on primary and secondary passage in the new host species. Transmission of prion disease between species produces much more prolonged incubation times than within species. In a study transmitting BSE and scrapie to four inbred lines of mice, initial prolonged incubation periods were shortened upon further

mouse-to-mouse passages (Bruce et al., 1994). For example, incubation times of 438±7 days and 404±5 days in C57BL mice challenged with BSE and scrapie respectively were reduced to 207±3 days and 164±4 days. As incubation times following primary passage of BSE and scrapie prions to mice are highly variable and prolonged they confound analysis between strains. Therefore, these prion strains have been passaged through mice to produce widely used mouse-adapted strains, such as the Chandler/RML and ME7 strains, which are transmitted to mice with high efficiency and reproducible incubation times.

1.2.3 Genetic Control of Prion Disease Incubation Time in Mice

The significance of mouse strain as a major determinant of incubation time was first described in 1964 by Dickinson and MacKay when they identified a stock of mice (VM/Dk) that had a greatly prolonged incubation time of 40 weeks following inoculation with the mouse-adapted scrapie isolate ME7, compared to other inbred mice, namely SM/JaxBt, BSVS/Sr, RIII/FaBt, C57BL/FaBt and LG/JaxBt, who had incubation times between 21 and 26 weeks (Dickinson and Mackay, 1964). Subsequent studies have reported a continuum of well defined incubation periods in several laboratory strains of mice which were originally classified into two groups; 'short' incubation time strains having incubation periods ranging from 100-200 days and 'long' incubation time strains having incubation periods greater than 225 days (Carlson *et al.*, 1988a; Carlson *et al.*, 1988b; Dickinson *et al.*, 1968; Kingsbury *et al.*, 1983; Westaway *et al.*, 1987).

Sinc and Prni

Further investigations of the prolonged incubation time observed in the VM mouse strain included classical genetic crosses between VM mice and RIII, a 'short' incubation time strain (Dickinson *et al.*, 1968). Crosses between 'long' and 'short' incubation time strains are useful in analysing the genetic control of incubation time as they provide maximal phenotypic difference for susceptibility. The F1 hybrid progeny of these two strains had incubation times which were intermediate between those of the two parental strains and subsequent backcrosses to either parent gave incubation times distributed from the mean F1 generation incubation time to that of the parent stock used. Furthermore, three distinct modes were seen in an F2 intercross corresponding to the ranges of the two parental strains and the F1 generation incubation times. These data led to the conclusion that the control of incubation time in the ME7 model was the

effect of an autosomal gene, designated *Sinc*, for scrapie incubation time. It was proposed that *Sinc* had a single pair of alleles, *s7* and *p7* denoting a short and prolonged incubation period respectively which showed no dominance and had a quantitative effect in controlling the incubation period phenotype in response to the ME7 prion strain. *Sinc* was found to control the incubation periods for all prion strains tested and distinct incubation times within each mouse strain were categorized into one of the three *Sinc* genotypes, *s7s7*, *s7p7* and *p7p7* (Dickinson and Meikle, 1971).

Surveys of inbred mouse strain incubation periods in response to a different mouse-passaged prion strain, Chandler/RML (Chandler, 1961), identified an exceptionally long incubation period of 200-385 days in *Sinc p7* strain, I/LnJ, and the shortest incubation time (<95 days) recorded for any murine host with scrapie in the NZW/LacJ *Sinc s7* strain (Kingsbury et al., 1983). F1 hybrid offspring of these two strains gave incubation periods of 223±2 days which were much longer than that of the NZW/LacJ parental strain indicating that the longer incubation period phenotype was dominant (Carlson *et al.*, 1986). Backcrossing the F1 generation to NZW/LacJ produced two phenotypic groups again suggesting single gene control of the scrapie incubation period in which the 'short' incubation period group is homozygous for the NZW/LacJ allele and the 'long' incubation period group is a product of both the I/LnJ and NZW/LacJ alleles. This single dominant gene was designated *Prni* (prion incubation time gene), with two alleles namely *I* and *N* to denote the I/LnJ and NZW/LacJ strains (Carlson et al., 1986). The similar properties of *Sinc* and *Prni* led to the suggestion that they were identical (Carlson et al., 1986; Carp *et al.*, 1987).

Prnp

The identification of a chromosomal gene encoding the only known functional component of infectious scrapie prions (Basler et al., 1986; Oesch et al., 1985) accelerated investigation into the genetic basis of prion disease and genetic linkage studies in mice produced the first evidence that *Prnp* is a major factor in controlling susceptibility to prion disease (Carlson *et al.*, 1986). Based upon their observations Carlson *et al.*, proposed the existence of a prion gene complex (*Prn*) on chromosome 2 which consisted of the prion incubation time gene (*Prni*) and the prion protein gene (*Prnp*).

Restriction fragment length polymorphism (RFLP) mapping of *Prnp* identified six

allelic RFLP patterns among 50 inbred lines of mice (Carlson et al., 1988a; Carlson et al., 1986; Carlson et al., 1988b). The identification of an XbaI restriction enzyme site which distinguished I/LnJ and NZW/LacJ, by giving 5.5kb and 3.8kb fragments respectively, led to the designation of the 'short' incubation time NZW/LacJ allele as *Prnp*^{a} and the 'long' incubation time allele of I/LnJ as *Prnp*^{b} (Carlson et al., 1986). It was subsequently found that most inbred lines of mice could be classified as *Prnp*^{a} and had 'short' incubation periods ranging from 105-158 days and that three inbred strains of mice with known incubation periods in excess of 200 days were of the *Prnp*^{b} allele (Carlson et al., 1988a; Carlson et al., 1988b). The association between incubation time and RFLP haplotype indicated that *Prni* and *Prnp* were closely linked genes. Subsequently RFLP typing of *Prnp* in *Sinc* congenic mice, expressing the *Sinc s7* allele on the background of 'long' incubation time *Sinc p7* strain, VM, and having a 185 day decrease in incubation time, identified the 3.8kb XbaI fragment which matched that of the *Sinc s7* donor strain, C57BL, demonstrating that *Sinc* and *Prnp* were closely linked or synonymous (Hunter *et al.*, 1987).

Codons 108 and 189

Observed variation in incubation periods was also hypothesised to be the result of sequence variation in coding or regulatory regions of the prion protein gene which would provide the molecular basis for variation through their effects on synthesis, translation, stability and/or the coding capacity of PrP messenger ribonucleic acid (mRNA). The mRNA and protein products of NZW/LacJ (*Prnp*^{a}) and I/LnJ (*Prnp*^{b}) mouse strains were found to be similar in size and abundance but further analysis of nucleotide variation between the two strains identified three nucleotide polymorphisms in the prion protein gene ORF which produced protein products harbouring different amino acid residues at codons 108 and 189 and these amino acid differences were found to segregate with incubation time phenotype (Westaway et al., 1987) (Figure 1.5). In 'short' to intermediate incubation time strains (*Prnp*^{a}) PrP codon 108 encodes a leucine residue and codon 189 a threonine and was designated PrPA. In 'long' incubation time strains (*Prnp*^{b}) with incubation periods of over 200 days, PrP codon 108 encodes phenylalanine residue and codon 189, a valine residue and was designated PrPB. The nucleotide polymorphism (AC to GT) causing threonine to be substituted by valine at codon 189 ablates a BstEII site at this position. Further screening of additional strains of inbred mice for the presence or absence of this restriction enzyme site led to the conclusion that the 189 threonine polymorphism correlates with 'short' incubation

Figure 1.5 Coding polymorphisms at codons 108 and 189 in the mouse prion protein. Octapeptide repeats are shown as black blocks. Numbers refer to codon numbers. All residues are shown by single letter abbreviations of amino acids.

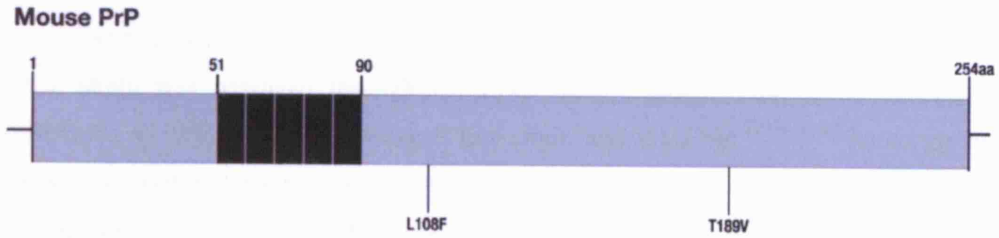

period (Westaway et al., 1987).

This discovery provided support for the idea that *Prnp* and *Prni* may be the same gene (Carlson et al., 1988a; Carlson et al., 1988b; Westaway et al., 1987). PrPA and PrPB were expressed in similar quantities and it seemed plausible that these amino acid substitutions may produce protein products with different activities that affect putative replication mechanisms and therefore directly influence incubation period phenotype between the $Prnp^a$ and $Prnp^b$ strains (Westaway et al., 1987). However, further investigation of the congruency of *Prnp* and *Sinc/Prni* failed to confirm that they were identical (Carlson *et al.*, 1993; Carlson et al., 1988a; Carlson et al., 1986; Carlson et al., 1988b; Hunter et al., 1992; Race *et al.*, 1990; Westaway *et al.*, 1991).

Confirmation that the specific amino acid residues at codons 108 and 189 are major determinants of prion disease incubation time came from a study where the endogenous $Prnp^a$ alleles were engineered, by gene targeting in an 129/Ola embryonic stem cell line, to produce the PrPB allotype instead of PrPA (Moore *et al.*, 1998). The transgenic mice had exactly the same genetic make up as $Prnp^a$ allele mice except at codons 108 and 189 of PrP where it expressed $Prnp^b$ amino acids. Mice homozygous for the modified *Prnp* coding region, $Prnp^{a[108F189V]}$ were bred and inoculated with 301V, a mouse-adapted BSE strain. Wild-type 129/Ola mice homozygous for the $Prnp^a$ allele confer a dominant prolonged incubation time of 244 days in response to this prion strain. The incubation times in mice expressing the modified $Prnp^b$ alleles were dramatically reduced to 133 days, 111 days shorter than the wild-type 129/Ola $Prnp^a$ mice. Congenic VM/Dk mice expressing two copies of the $Prnp^b$ alleles and PrPB allotype which are identical to the $Prnp^{a[108F189V]}$ homozygotes, also show similar short incubation times (119±2 days). This confirmed the importance of the 108 and 189

dimorphisms in controlling prion disease incubation time in the mouse. The resultant incubation time resembled that of a *Sinc p7 Prnp*^{b} allele mouse implying successful and independent control from this inserted locus. The single gene control over incubation time observed finally confirmed that *Sinc/Prni* and *Prnp* were congruent. The 301V prion strain was passaged through the *Prnp*^{b} mouse strain, VM/Dk, so the slight difference in incubation time between this strain and the *Prnp*$^{a[108F189V]}$ homozygous transgenic mice was not due to incompatibility between the donor and recipient, as both strains share identical PrP coding regions, but was suggested to be due to additional genetic elements outside of the *Prnp* coding region or to the different genetic background of the two strains.

A more recent study has evaluated the individual contributions of codons 108 and 189 (Barron *et al.*, 2005). Transgenic mice were generated by separately targeting the two amino acids at codons 108 and 189, specific to the PrPB allotype, onto a *Prnp*^{a} background. Inbred lines of mice of every possible allelic combination were generated to analyse the specific effects of each codon in co-isogenic mice. The ME7 and 301V prion strains were used to inoculate the resulting mice. As previously discussed the control of incubation time is thought to be a result of PrP sequence identity between the host and the donor of infectivity (Prusiner et al., 1990). Accordingly the shortest incubation times were seen when the host PrP sequence matched that of the inoculum and correspondingly the longest incubation times were observed where a mismatch occurred. Specifically, sequence identity between host and inoculum at codon 189 was found to be important in reducing incubation periods and homozygosity at codon 108 attenuated this effect. It has therefore been suggested that codon 108 may control the rate of conversion of PrP^{C} to PrP^{Sc} (Barron et al., 2005). Deletion mutants lacking residues 34-113 (MoPrPΔ34-113) still have the ability to bind to PrP^{C} but the conversion of PrP^{C} to PrP^{Sc} is seen to be much slower suggesting that this region, containing codon 108, is involved in the control of conversion but not binding (Lawson *et al.*, 2001). Barron *et al.*, conclude that codon 189 exerts major control over the scrapie incubation time through its initial interaction and binding with PrP but that efficiency of disease transmission is affected by codon 108 homozygosity, suggesting that distinct regions of PrP may play different roles in the disease process.

Identification of a Novel Prnp Allele

A recent survey of inbred and wild mice identified a new *Prnp* allele, *Prnp*^{c}, in MAI/Pas

mice (Lloyd *et al.*, 2004) derived from *M. m. musculus* wild mice trapped in Austria (Beck *et al.*, 2000). This invalidated the assumption that all mouse strains could be characterised as $Prnp^a$ or $Prnp^b$. The $Prnp^c$ allele mouse encodes a phenylalanine residue at codon 108 and a threonine residue at codon 189 and thus appears to be a hybrid of the $Prnp^a$ and $Prnp^b$ alleles. Southern blot analysis of restriction enzyme sites indicates that MAI/Pas mice share the polymorphisms 5' and 3' of the *Prnp* ORF with $Prnp^b$ mice. This implies that a *de novo* mutation has occurred upon a *b* allele background as opposed to a recombination event between an *a* and *b* allele mouse. The incubation time of 360±11 days in MAI/Pas far exceeds that of even the longest described $Prnp^b$ allele mouse incubation time phenotype, a probable consequence of its wild-derived genetic background. A congenic line was established whereby the $Prnp^c$ allele was expressed upon the genetic background of $Prnp^a$ strain, C57BL/6JOlaHsd, after nine generations of backcrossing. C57BL/6JOlaHsd have a mean incubation time of 143±1 days. These animals were crossed to produce homozygote mice and inoculated with Chandler/RML giving an incubation time of 255±12 days. The reduction in incubation time from that of the MAI/Pas strain indicates the importance of the modulating effects of differences in genetic background independent of PrP coding polymorphisms. The presence of the *c* allele is thought to be the primary cause of the increase in incubation time of the parental C57BL/6JOlaHsd strain although there is also the possibility that additional alleles in the MAI/Pas sequence flanking the *Prnp* locus which remained in the congenic mice, may be influencing the observed incubation time.

Additional Non-Prnp Candidate Genes

Early experiments attempting to elucidate *Sinc/Prni* and investigating variation in incubation time within given *Prnp* genotypes has suggested that genetic loci other than *Prnp* are involved (Carlson et al., 1988a; Carlson et al., 1986; Carlson et al., 1988b; Race et al., 1990; Westaway et al., 1987). Within both $Prnp^a$ and $Prnp^b$ allele groups a wide range of incubation times is seen with $Prnp^a$ ranging from 105±4 days to 221±5 days and $Prnp^b$ from 255±14 days to 313±3 days (Table 1.1), providing support for the involvement of genetic background in conferring the phenotype. It is clear that additional genetic factors are responsible for controlling incubation time in mice and the distinctive effects of PrP sequence polymorphisms are influenced by these modifiers.

Table 1.1 Incubation times following intracerebral inoculation with Chandler/RML mouse scrapie.
Adapted from Lloyd and Collinge, 2005. Incubation times taken from the following sources: Dickinson and MacKay 1964, Kingsbury et al., 1983, Carlson et al., 1986, Westaway et al., 1987, Carlson et al 1988, Lloyd et al., 2001, Lloyd et al., 2004 and Lloyd et al., 2005.

Strain	IT (Days) ± SEM
***Prnp*[a] (108-Leu & 189-Thr)**	
Laboratory strains	
SJL/J	105±4 (n=5)
NZW/OlaHsd	108±1 (n=38)
NZW/LaCJ	113±2 (n=20)
SWR/J	119±8 (n=6)
SJL/OlaHsd	122±1 (n=37)
AKR/J	123±4 (n=6)
BALB/cJ	124±11 (n=5)
FVB/NHsd	131±1 (n=33)
NZB	132 (n=5)
C3HeB/FeJ	132 ±4 (n=4)
SM/J	133±1 (n=47)
DBA/2J	134±3 (n=7)
SWR/OlaHsd	135±1 (n=36)
RIIIS/J	135±1 (n=34)
C57BL/6J	137 (n=2)
CBA/N	140±10 (n=3)
C57BL6/JOlaHsd	143±1 (n=42)
MA/MyJ	170 (n=6)
Wild-derived mice	
PERA/Kamei	151±1 (n=26)
CAST/Ei	188±12 (n=16)
PWK/Pas	221±5 (n=12)
***Prnp*[b] (108-Phe & 189-Val)**	
Laboratory strains	
JU/FaCt	313±3 (n=24)
VM/Dk	300±3
I/LnJ	255±14 (n=21)
P/J	295±9
***Prnp*[c] (108-Phe & 189-Thr)**	
Wild-derived mice	
MAI/Pas	360±11 (n=20)

1.2.4 Additional Candidate Genes in Mice

The first additional genetic locus identified as important in influencing prion disease incubation time in mice was the major histocompatibility complex (*H-2*) on mouse chromosome 17 (Kingsbury et al., 1983). Congenic strains differing only in their *H-2* haplotypes were used to successfully identify the D sub region of *H-2* as a susceptibility locus in mice.

Another murine prion disease incubation time candidate gene is Monocyte Chemoattractant Protein 1 (*Mcp1*), a CC chemokine which has a predominant pro-inflammatory action driving the recruitment of monocytes to the brain parenchyma and activating resident microglia during an inflammatory response (Gu *et al.*, 1997; Gu *et al.*, 1999). Recently *Mcp1* knockout mice have shown a 4 week delay in the late-stage clinical signs of prion disease and an increased survival time of 2-3 weeks compared to wild-type controls in response to intracerebral challenge with the ME7 prion strain (Felton et al., 2005) indicating a role for this gene in the pathogenesis of murine prion disease.

An anti-inflammatory cytokine, Interleukin-10 (*Il-10*), has also been implicated in the neuropathogenesis of prion disease (Thackray *et al.*, 2004). Mice deficient in *Il-10* have been shown to be highly susceptible to the development of prion disease and show markedly shortened incubation times compared with wild-type controls. For example, a reduction of 82 days is observed following intracerebral inoculation with the Chandler/RML prion strain and 186 days following peripheral inoculation with the ME7 prion strain. It has been suggested that anti-inflammatory cytokines play a significant role in the host defence response against prion pathology which is initiated and maintained by expression of pro-inflammatory cytokines.

The identification of both pro-inflammatory and anti-inflammatory cytokines as candidate genes for prion disease incubation time is noteworthy since lymphoid infectivity is found in most prion diseases, with an associated involvement of pro-inflammatory cytokines and immune cells in lymphoid prion replication (Aguzzi and Heikenwalder, 2005). Furthermore, a role for chronic inflammatory conditions has been suggested to affect prion pathogenesis and prion inoculation in mice with various naturally-occurring or induced inflammatory or autoimmune diseases has been shown to expand the normal tissue distribution of prions (Heikenwalder *et al.*, 2005).

Another candidate for prion disease incubation time is Clusterin, a heterodimeric glycoprotein known to have a role in spermatogenesis through the down-regulation of apoptosis (French *et al.*, 1994). Clusterin is seen to accumulate in significant quantities in prion protein lesions associated with BSE and knockout mice peripherally inoculated with BSE prions have a 40 day increase in mean incubation time compared to wild-type controls (Kempster *et al.*, 2004). It has been suggested that Clusterin alters the extracellular deposition of the disease-associated misfolded prion protein since reduced aggregation of this protein was found in the medulla of affected brain tissue. More recently Clusterin expression in FDCs has been associated with prion protein deposition and it has been suggested to be a chaperone-like molecule for PrP (Sasaki *et al.*, 2006).

1.2.5 Quantitative Trait Loci (QTL) for Prion Disease Incubation Time

The elucidation of other genetic loci contributing towards incubation time has been the aim of several recent genome-wide mapping studies in which the successful identification of 21 loci in eight different chromosomal regions has been achieved (Lloyd *et al.*, 2001; Lloyd *et al.*, 2002; Manolakou *et al.*, 2001; Moreno *et al.*, 2003; Stephenson *et al.*, 2000) (Table 1.2). The basic premise of these studies has been to utilise two-way crosses between unrelated mouse strains which exhibit significantly different incubation times following intracerebral inoculation with a defined prion strain. The two strains used in each case are of the same *Prnp* genotype to avoid any known effect of the coding region of the *Prnp* gene.

The F1 generations of each two-way cross were further employed in backcross strategies or bred to produce an F2 intercross. Backcrosses are advantageous as they provide only two genotypes segregating at each locus rather than three, as in the F2 intercross, and therefore simplify analysis, although a limitation of backcrossing is that dominant alleles can obscure the effect of recessive alleles. Four different combinations have been used: a CAST x NZW F2 intercross (Lloyd et al., 2001; Lloyd et al., 2002), a CAST x SJL F2 intercross (Stephenson et al., 2000) and a C57 x RIII reciprocal backcross and F2 intercross (Manolakou et al., 2001; Moreno et al., 2003). The resulting progeny of each were intracerebrally inoculated with a defined prion strain and phenotyped for incubation time. The prion strains used include the Chandler/RML and ME7 mouse-passaged scrapie strains, mouse-passaged BSE and BSE.

Table 1.2 Summary of identified QTL for mouse prion disease incubation time.
Adapted from Lloyd and Collinge 2005. [a]Lloyd et al 2001, [b]Stephenson et al 2000, [c]Lloyd et al 2002, [d]Manolakou et al 2001, [e]Moreno et al 2003 and *Females only.

Cross	Inoculum	Closest Marker and Map Position (cM)	Lod Score
CAST/Ei x NZW/OlaHsd F2 intercross[a] (n=1009)	Chandler/RML mouse scrapie	*D2Mit107* (61.2) *D2Mit194* (66.7) *D2Mit266* (98.4) *D11Mit36* (43.7) *D11Mit179* (49.2) *D12Mit97* (42.6) *D12Mit28* (47.0) *D12Mit141* (51.4)	8.15 4.51 4.6 56.41 53.91 5.86 7.55 5.68
CAST/Ei x SJL/J F2 intercross[b] (n=153)	Chandler/RML mouse scrapie	*D9Mit91* (17) *D11Mit260* (34.3) *D11Mit219* (43) *D11Mit213* (55)	5.7 5.44 5.66 4.88
CAST/Ei x NZW/OlaHsd F2 intercross[c] (n=124)	Mouse-passaged BSE	*D2Mit304* (59.0) *D2Mit106* (61.2) *D2Mit194* (66.7) *D11Mit36* (43.7)	5.57 5.91 5.9 3.96
RIII x C57 F1 x C57 backcross[d] (n=515)	BSE	*D2Mit61* (34) *D8Mit266* (43)	5.8 5.2
RIII x C57 F1 x RIII backcross[d] (n=512)		*D4Mit27* (42.5) *D15Mit159* (49.6)	4.5 3.8
RIII x C57 F2 intercross[e] (n=282)	ME7 scrapie	*D5Mit95* (68.0)	4.7*

Incubation times for F2 intercross mice show a near-normal distribution indicating that the phenotype is controlled by multiple genes which co-segregate independently in the cross. This observation characterises prion disease incubation time as a quantitative trait and it can be investigated using linkage analysis. QTL can be detected through genome-wide mapping to highlight chromosomal regions containing genes that are influencing the observed phenotype. No prior assumptions about the mechanisms of disease and the genes involved are required for analysis.

Knowledge of mouse strain genealogies is critical to the design of experiments mapping complex quantitative traits. Crosses were generated between unrelated parental strains of mice, in some cases from different subspecies that are genetically and phenotypically different. Maximising the genetic diversity between the parents is essential for mapping QTL because it relies upon polymorphic differences between the founder strains (Darvasi, 1998).

Chromosome 9 and 11 incubation time QTL were identified in F2 intercrosses between the 'short' incubation time inbred strains, SJL/J and NZW/OlaHsd, and the 'long' incubation time wild-derived strain, CAST/Ei (Lloyd et al., 2001; Lloyd et al., 2002; Stephenson et al., 2000). SJL and NZW are genetically divergent substrains but ancestral phylogenetic studies place them both within the ancestral *M. m. domesticus* subspecies fold (Beck et al., 2000; Silver, 1995). CAST/Ei is a wild-derived strain which has been bred to homozygosity from captured Asian wild mice. The CAST/Ei strain is derived entirely from the *M. m. castaneus* subspecies. *M. m. domesticus* and *M. m. castaneus* subspecies evolved apart from a common ancestor approximately one million years ago and therefore the level of polymorphisms between the two is much greater than that observed among strains that are predominantly derived from *M. m. domesticus* (Ferris *et al.*, 1983; Silver, 1995). Therefore, an F2 intercross produced between *M. m. domesticus* and *M. m. castaneus* subspecies strains maximises genetic diversity and this is hoped to capture numerous polymorphisms that potentially control the incubation time phenotype.

Chromosome 8 QTL were identified using an F2 intercross and a backcross population generated from RIII and C57 substrains (Manolakou et al., 2001; Moreno et al., 2003). RIII is an inbred strain of unknown origin whereas C57 is a commonly used laboratory inbred strain whose genetic background and phenotype has been well characterised

(Beck et al., 2000). RIII and C57 strains have very different incubation times indicating underlying genetic variation between these strains.

In each prion disease incubation time QTL mapping study genotyping was undertaken across the mouse genome at 10-20cM intervals using markers known to be polymorphic between the two mouse strains in question. Subsequent linkage analysis provided a statistical measurement of the correlation between incubation time phenotype and individual genotype. Genetic loci are seen to be linked to the phenotype in question when the contribution of each parental allele acts to modify the observed trait. Alleles can either show a completely dominant or recessive effect or an additive effect, in that the heterozygote phenotype is the mean of the homozygotes.

In all studies, with the exception of the Chandler/RML inoculated SJL/J x CAST/Ei F2 intercross, the genotyping strategy employed assessed the whole population (Lloyd et al., 2001; Lloyd et al., 2002; Manolakou et al., 2001; Moreno et al., 2003). Stephenson *et al.,* concentrated their analysis specifically on the phenotypic extremes of the population assessing ~20% of each end of the incubation time distribution (Stephenson et al., 2000) where most of the statistical power in linkage analysis is derived (Lander and Botstein, 1989). Significant linkage was indicated by lod scores of 4.3 or greater for an intercross and 3.3 or greater for a backcross with a genome-screen P value of <0.05 (Lander and Kruglyak, 1995) or in the case of Manolakou *et al.,* genome-wide significance levels were obtained by calculating permutations.

A possible limitation of using two-way combinations of inbred strains is that they represent limited genetic variability compared with that of natural populations and it is unlikely that all genes affecting the phenotype will be revealed. Two parental inbred mouse strains are unlikely to harbour all the possible alleles that modulate a phenotype and therefore incubation time QTL identified in two-way crosses may not be an accurate guide to QTL common in more outbred populations and furthermore in other species, a particularly relevant point if the identification of QTL in mice is exclusively relied upon to uncover homologous locations in humans.

The number of possible recombination events occurring in two-way crosses is limited and so mapping across the genome is carried out at low resolution. The resulting regions of linkage identified are extensive and have large confidence intervals that in

some cases span the majority of a chromosome. For example, a high level of significance was identified across the whole of chromosome 11 in a NZW x CAST F2 intercross identifying QTL for incubation time (Lloyd et al., 2001). Low resolution mapping may disguise the architecture of a QTL. In essence it is a genetic effect that is being mapped and not a gene and therefore an extensive region of linkage may turn out to be due to several separate loci which are physically linked (Darvasi and Soller, 1997; Flint, 2003; Flint et al., 2005). The architecture of a QTL may be obscured if genes exist in *trans* and cancel out their respective effects or the effect of a cluster of genes existing in *cis* may be amplified over the region and make a significant contribution to total variance. It is certainly true that genes of similar function or that work in the same pathways are known to cluster together in the mammalian genome (Cohen *et al.*, 2000), nicely illustrated by QTL studies looking at diverse phenotypes such as high-temperature growth in yeast (Steinmetz *et al.*, 2002) and seizure susceptibility (Legare et al., 2000), obesity (Stylianou *et al.*, 2004) and diabetes (Podolin et al., 1998) in mice. In general QTL are due to small genetic effects and may only contribute to 1-2% of the phenotypic variance hindering their elucidation with low resolution detection techniques (Flint et al., 2005).

It is difficult to compare all of the genetic loci which have been linked to prion disease incubation time as there are several experimental set-up differences between the studies and variation in key factors known to influence incubation time, such as the prion strain utilised. As previously discussed, prion strains are defined by the characteristic incubation times they confer and different QTL may be affected by different prion strains highlighting different regions of linkage in a given cross. Furthermore, the use of only two mouse strains in each cross limits the number of QTL that can be identified because it is unlikely that two parental strains of mice contain all the possible alleles modulating a phenotype and so chromosomal regions linked to prion disease incubation time in different mouse strains are potentially only relevant to those strains in question. Another source of QTL variation is a species or transmission barrier effect and the function of some genes may be exclusively related to the processes involved in overcoming this barrier. This factor is potentially most relevant to the study identifying QTL using BSE inoculum (Manolakou et al., 2001). The route of transmission is also another factor that would affect the QTL identified. All studies were carried out using intracerebral inoculations but it is possible that if they were repeated using peripheral or oral inoculation different QTL would be uncovered. It is the hope of the described

genome-wide mapping studies that the QTL identified will also be relevant to human prion disease. Therefore, in the case of acquired human prion disease, an oral route of transmission may be more relevant in attempts to elucidate genes controlling human susceptibility, since prion diseases such as vCJD and kuru are assumed to have arisen though oral exposure to prions. Oral challenge with vCJD prions in transgenic mice expressing human PrP may have been a more suitable and relevant model.

Although a frequent problem in QTL identification is the successful replication of results between studies due to differences in experimental set-up this variation can also be advantageous since it increases the overall number of identifiable QTL. It is certainly possible to draw conclusions from those studies sharing a common factor such as mouse strain, prion strain and/or type of genetic cross employed. For example, an NZWxCAST F2 intercross inoculated with Chandler/RML scrapie in one study and mouse-passaged BSE in another, identified similar regions of linkage on chromosome 2 and 11 which overlap considerably despite the use of different prion strains. This indicates that the genetic loci identified on each chromosome are acting independently of prion strain or perhaps that multiple loci within each regions are involved (Lloyd et al., 2001; Lloyd et al., 2002).

Another example of overlapping regions of linkage due to a common experimental variable is the identification of prion disease QTL on chromosome 11 in studies using the same prion strain, Chandler/RML, and the same 'long' incubation time mouse strain, CAST/Ei (Lloyd et al., 2001; Stephenson et al., 2000). The peaks of linkage identified in each study, *D11Mit36* 43.7cM (Lloyd et al., 2001) and *D11Mit219* 43cM (Stephenson et al., 2000), map very close together and due to the large 10-20cM confidence intervals associated with these peaks it is probable that the regions of linkage overlap. In addition, the *D11Mit36* locus is also seen at a suggestive level of linkage in the F2 intercross inoculated with mouse-passaged BSE (Lloyd et al., 2002). The CAST/Ei strain is common to all studies identifying linkage on chromosome 11 inferring that the strong affect of this locus may be derived from this mouse strain and that it is independent of prion strain. The identification of this locus in three independent studies provides support for the statistical significance of the data and such instances provide confirmation of the successful identification of a relevant QTL. This does not mean however that the regions identified in other studies are not valid. Aside from the identified chromosome 2 and 11 loci all other regions are represented only

once which may be explained by the specific effects of mouse strain, prion strain and a species barrier effect. In some instances studies have reported factors such as host environment, such as age of mother, age of host at infection and an x-cytoplasm interaction in the host (Manolakou et al., 2001) and one study observed a sex-dependent effect of linkage reporting statistical significance specifically for a group of female mice (Moreno et al., 2003). Further studies using a wider variety of inbred mouse strains which represent a larger proportion of allelic variation may reveal additional important QTL.

The regions of linkage identified on chromosome 2 in both studies carried out by Lloyd *et al.*, encompass the *Prnp* locus which would be an excellent candidate for this QTL. However, sequence analysis of the open reading frames of NZW and CAST *Prnp* did not reveal any variation between these $Prnp^a$ strains and no significant differences in PrP expression levels have been recorded (Lloyd et al 2001).

The identified regions of linkage for prion disease incubation time in mice provide a good starting point for the further elucidation of genes involved in controlling the phenotype but because they are large (~20cM) and contain numerous genes it is not feasible to utilise a candidate gene approach, assessing individual genes one by one. It is therefore necessary to use other genetic techniques to fine map and resolve these extensive regions of linkage into intervals in which the further characterisation of individual candidate genes can be undertaken and there are several different approaches by which this can be achieved.

1.2.6 Fine Mapping QTL

Congenics

A classical approach to fine mapping QTL is the use of congenic lines of mice. One mouse strain is repeatedly backcrossed onto another to create individuals that have a particular genomic region from one strain and the remainder of their genome from the other. Subsequent intercrossing makes the genomic segment homozygous and the mouse fully inbred. 10 generations of backcrossing are considered to achieve >99.9% homozygosity. Generating congenic mice is a lengthy and laborious process taking several years which is not ideal when measuring a phenotype such as incubation time which in itself is lethal and prolonged. The process has been accelerated by 'speed

congenics'. In marker-assisted breeding schemes interval specific congenics, generated by identifying individuals with recombinant chromosomes in regions previously identified as containing QTL, are backcrossed for several generations to remove other QTL and intercrossed for homozygosity (Darvasi, 1998; Markel *et al.*, 1997; Rikke and Johnson, 1998). Congenic mice may still give regions too large for a candidate gene approach requiring a further panel of subcongenics to continue to narrow the region of interest. It is necessary to phenotype established congenic lines to confirm that the transferred allele is still affecting the phenotype since there is a risk that several years of mouse breeding may obscure the small contribution of a single locus to total phenotypic variance. Another possible limitation of the use of congenics is the fact that QTL detection experiments do not map a gene but rather a genetic effect which may be the cumulative effect of multiple loci. Recently, a large effect QTL has been identified conferring seizure susceptibility in mice but it was not possible to capture the effects of this QTL within a set of nested subcongenics generated by further backcrossing because multiple loci acting together were found to be responsible (Legare *et al.*, 2000).

Most fine-mapping strategies have taken a single-locus approach assuming that a large-effect QTL harbours a large-effect gene and so have attempted to isolate even smaller chromosomal regions as in the case of congenics or by using crosses to determine the position of a QTL in relation to recombination events (Darvasi, 1998; Rikke and Johnson, 1998). It is becoming clear that large-effect QTL are actually rare and chromosome dissection has revealed more complex genetic effects which require sub-centimorgan resolution. Fine-mapping methods require recombinants to increase QTL resolution but this means great expense in terms of the number of markers for genotyping and animals involved. This has led to the use of advanced intercrossed lines (AIL) (Darvasi and Soller, 1995) and outbred stocks (Chia *et al.*, 2005; Demarest *et al.*, 2001; Mott and Flint, 2002; Mott *et al.*, 2000; Yalcin *et al.*, 2004b) which aid attempts to fine map by increasing the number of recombinations available for analysis in a single mouse. Both methods rely on multiple generations of mice.

Advanced Intercross Lines (AIL)

AILs rely on only two different parental lines and are initially generated by crossing two inbred strains to produce an F1 generation which is subsequently intercrossed to produce a further F2 generation from which the AIL is then derived by sequentially and randomly intercrossing for many generations so that only markers close to the QTL will

remain linked (Darvasi and Soller, 1995). The many recombination events required for QTL fine mapping are accumulated in a relatively small population over the course of many generations rather than by producing and examining many progeny in large F2 and backcross populations. The greatest gains in resolution in these populations occur in a breeding population size of ≥100 and at generations 8-10 after the initial F2 intercross (Darvasi and Soller, 1995; Xiong and Guo, 1997). A limitation of this method is the fact that genetic drift causes parts of the genome to become fixed over time reducing overall genetic variation and risking the attenuation or loss of the QTL (Flint and Mott, 2001). This is combated as much as possible by the use of a pseudo-random breeding design. As with congenics this method is time-consuming and it can take up to 5 years to achieve an appropriate AIL. Increasing the initial genetic diversity using a more complex initial pedigree has been suggested to accumulate recombinants more rapidly with less fixation of the genome. AILs have been successfully used to confirm and improve the mapping resolution of several QTL regulating high-density lipoprotein cholesterol (HDL) concentrations which are implicated in cardiovascular disease (Wang *et al.*, 2003).

Outbred Stocks

Outbred stocks are closed populations of genetically variable animals, bred for at least four generations to maximum heterozygosity, and maintained to minimize genetic change. Outbred stocks are more genetically diverse than AIL and accumulate many recombination breakpoints over time that split chromosomes into fine-grained mosaics, potentially comparable to the outbred human population, facilitating high resolution fine mapping (Chia *et al.*, 2005). Following identification of QTL in crosses between inbred strains, an outbred stock can be used to identifying the nucleotide sequence responsible for the effect by mapping the QTL within a 1cM interval, which in the mouse corresponds to 2Mb, with 1Mb containing 10 genes on average (Flint et al., 2005; Hitzemann *et al.*, 2002; Manenti *et al.*, 2003; Mott et al., 2000; Talbot *et al.*, 1999; Talbot *et al.*, 2003; Yalcin et al., 2004b). This method has been successful in the mapping and identification of a skin-tumour susceptibility gene, Serine-threonine kinase 6 (*Skt6*) in outbred *Mus spretus* (Ewart-Toland *et al.*, 2003; Nagase *et al.*, 1995; Nagase *et al.*, 1999), a susceptibility loci for pulmonary adenoma in outbred CD1 mice (Manenti et al., 2003) and a candidate gene, regulator of G-protein signalling 2 (*Rgs2*), controlling anxiety in outbred MF1 mice (Yalcin et al., 2004b).

Heterogenous Stocks

Heterogenous stocks (HS) are a type of outbred stock which have been derived from up to eight known founder inbred lines through a series of progressive intercrosses over multiple generations (30-60), following a pseudo-random breeding protocol to maximise diversity, and provide mapping resolution of less than 1cM (Flint et al., 2005; McPeek, 2000; Mott *et al.*, 2000; Talbot *et al.*, 1999) (Figure 1.6). Traits are mapped by association of allelic variants with the phenotype of interest. Two examples of such a cross include the Boulder HS (HSIBG) created from A/J, AKR, BALB/c, C3H, C57BL/6, DBA/2, Is/Bi and RIII inbred lines which has been bred for more than 60 generations (Flint et al., 2005) and also the Northport HS (HSNPT) generated from A/J, AKR/J, BALB/cJ, C3H/HeJ, C57BL/6J, CBA/J, DBA/2J and LP/J inbred strains (Demarest *et al.*, 2001). Robust and powerful QTL detection is possible in these strains by estimating the probability that an allele descends from each progenitor strain through the reconstruction of the genomic mosaic of each chromosome (Mott *et al.*, 2000). Theoretically the HS is proposed to offer at least a 30-fold increase in resolution for QTL mapping compared to an F2 intercross (Darvasi and Soller, 1995; Darvasi and Soller, 1997). HS mice have been used to successfully fine-map single QTL intervals controlling open field behaviour and conditioned fear responses in mice (Mott et al., 2000; Talbot et al., 1999; Talbot et al., 2003) and more recently to carry out genome-wide high-resolution mapping of multiple phenotypes (Valdar *et al.*, 2006b).

Figure 1.6 Schematic to illustrate the generation of a heterogenous stock (HS) of mice. Up to eight inbred strains are randomly bred over several generations to produce progeny whose chromosomes are a fine-grained mosaic of the founder strains and allow high resolution fine mapping at 1cM intervals.

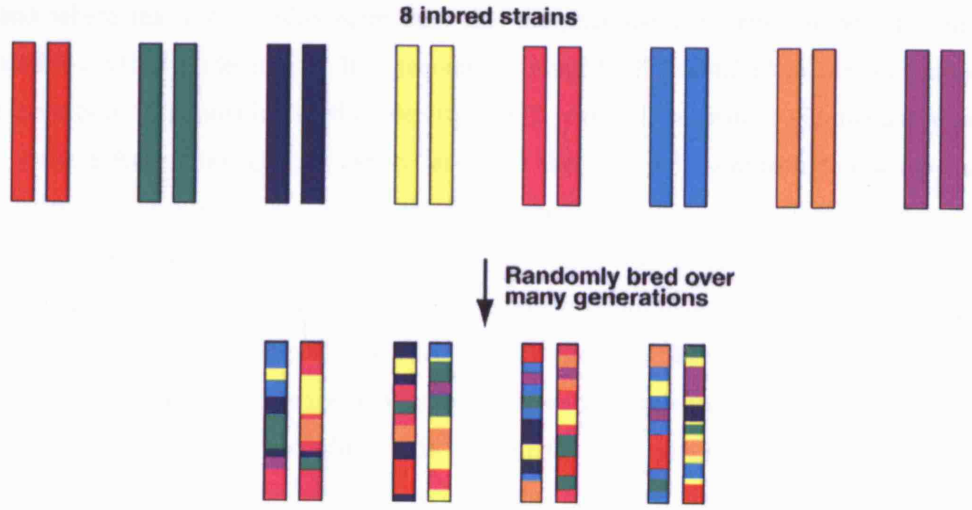

The fact that at any given locus on the genome there will be fewer alleles than the number of progenitor strains of a HS makes genetic mapping in these populations more complex than in inbred crosses since it is impossible to determine exactly which founder strain is the ancestor of the given allele (Flint et al., 2005; Mott and Flint, 2002; Mott et al., 2000). This confounds single maker association analysis in HS populations since it cannot distinguish between strains having different QTL effects but identical alleles. Multipoint analysis which is reliant upon predicting the probability that an individual is descended from a given progenitor strain at a particular locus on the genome overcomes the problem of QTL detection by single marker association in a HS (Mott et al., 2000). Following an additive model of genetic action the expected genetic effect for a diploid individual with ancestral founders *a* and *b* at the QTL will be the sum of the strain effects for these founders ($a + b$) of the QTL at the locus. Testing for differences between strain effects by analysis of variance is then the equivalent of testing for a QTL. This multipoint method, incorporating information from flanking markers and progenitor haplotypes, has been successfully used to identify QTL which have been missed using single marker association analysis because QTL are detected by testing for differences between the genetics effects of the progenitor haplotypes rather than by association at each locus.

HS progenitor strain sequence variant information has been incorporated with ancestral haplotype construction analysis in a HS population to identify quantitative trait nucleotides (QTN) within a previously identified QTL on mouse chromosome 1 which controls anxiety behaviour (Yalcin *et al.*, 2005). Allelic distribution across a panel of progenitor strains at a given locus is characterised by a strain distribution pattern (SDP) and where that pattern also correlates with the phenotypic distribution within those strains a QTL is identified. If a sequence variant SDP, identified in the progenitor strains of a HS population used to identify a QTL region, is consistent with the observed genetic effect of the QTL it can be assumed that any polymorphism following this pattern may be a potential QTN for the phenotype in question. A possible limitation of this method is the fact that important SDPs associated with a phenotype may be missed if complete sequence analysis of the whole region is not undertaken. Most sequence analysis of candidate genes is carried out in potential functional regions such as promoter and coding sequence and therefore important variants residing in non-coding regions may be missed. In addition, if multiple QTN are involved and are situated on the same SDP and in close proximity to each other then they will be equally ranked by

this analysis and be indistinguishable.

Inbred-Outbred Crosses

An extension of the fine-mapping capacity of the HS is seen in the use of inbred-outbred crosses (Mott and Flint, 2002). Following the same design as an F2 intercross an inbred line is crossed with an outbred population to produce F1 individuals which comprise homologous chromosomes entirely inbred or outbred. Subsequent intercrossing produces F2 individuals which contain a combination of inbred and outbred segments. The presence of two scales of recombinations makes it possible to carry out low and high resolution QTL mapping in the same animals.

Haplotype Analysis in Multiple Crosses

Multiple cross mapping (MCM) is a method of identifying haplotype blocks that segregate as expected in an initially defined QTL interval among multiple strains (Hitzemann et al., 2002). As previously discussed, QTL identified by two-way crosses between inbred strains are cross-dependent, that is, they reflect only a small fraction of the total natural variation for a phenotype because the two strains are unlikely to harbour all of the possible alleles for the trait in question. Overlapping QTL for behaviourally similar traits have been detected in genetically different mapping populations (Hitzemann *et al.*, 2000). Genes underlying a QTL are located in regions where the parental strains have different haplotypes, so by combining identified SDPs from different crosses with mapping data, regions of interest can be refined. Haplotype analysis in multiple crosses has been successfully used to confirm the identification of candidate genes underlying QTL associated with responses to ethanol and HDL levels in mice (Malmanger *et al.*, 2006; Wang *et al.*, 2004).

Collaborative Cross

An additional approach to the identification of QTL is the use of recombinant inbred (RI) strains, traditionally generated by repeated breeding from a second-generation hybrid of two inbred strains. The resulting progeny represent a collection of strains which are fully homozygous and contain 50% of each parental genome in different combinations. The Complex Trait Consortium have recently proposed and set in motion a project designated the Collaborative Cross to provide a reference panel of mice specifically for the analysis of complex traits and the elucidation of their genetic basis (Churchill *et al.*, 2004). When completed the Collaborative Cross is proposed to

provide a panel of RI strains derived from the correspondingly named Heterogenous Stock Collaborative Cross (HSCC) which include wild-derived strains such as CAST/Ei, PWK/Ph and WSB/Ei. The genomes of eight founder strains are combined and are then inbred to produce finished RI strains, each predicted to capture ~135 unique recombination events and retain segregating polymorphisms every 100-200bps. The purpose of the use of wild-derived strains is to maximise genetic diversity with the prospect of identifying numerous polymorphisms between strains which may provide the molecular basis for complex traits. It is estimated that ~1000 RI strains will be required to successfully map many of the 2,000 uncloned QTL into small genetic intervals (4cM). A simulation of the Collaborative Cross to investigate its power and ability to detect and map small genetic effects concluded that 500 RI lines are adequate to map a single additive locus that accounts for 5% of phenotypic variance to within 0.96cM but that mapping resolution may not be sufficient to identify individual genes (Valdar *et al.*, 2006a). HS mice are very useful in terms of the high number of recombination break points present, allowing mapping at 1cM intervals (Talbot et al., 1999) but these mice exist as an individual copy of a particular genotype whereas the advantage of the collaborative cross is that a strain of each unique cross generated is available providing high sample numbers for phenotyping and genotyping.

Recombination Inbred Segregation Tests (RISTs)

The usefulness of current projects like the Collaborative Cross to fine map QTL may be realised in the future through the use of generated RI strains in Recombination Inbred Segregation Tests (RISTs) (Darvasi, 1998; Flint et al., 2005). QTL identified in inbred strains could be further reduced in size by crossing the inbred parental lines with RI strains which are recombinant in the region of interest producing two segregating populations. In the first, if the RI and parental strain share the QTL alleles no QTL will segregate but in the second population the RI and parental strains may have different QTL alleles and therefore the QTL will segregate and is mapped to a position above or below the recombination breakpoint locating it within a smaller interval. As with congenics the effects of multiple linked QTL will provide a limitation for the use of this strategy but this analysis is faster and more economical to carry out than the production of congenic mice and multiple QTL could be tested using further RISTs assuming that appropriate recombinant lines are available.

Mouse SNP Databases & In Silico Mapping

Important aids in the continued mapping of QTL are current re-sequencing efforts which are providing detailed single nucleotide polymorphism (SNP) reference information for many mouse strains (Frazer et al., 2007; Shifman et al., 2006; Wade et al., 2002; Wiltshire et al., 2003; Yang et al., 2007) alongside established databases generated by Celera Genomics, the Mouse Genome Sequencing Consortium and the Jackson Laboratories. These publicly available resources provide the researcher with a more efficient way of identifying the underlying genetic basis of quantitative traits by reducing the need for individual *de novo* sequencing efforts. The increasing availability of mouse sequence-variation data for several different common laboratory strains has led to the use of dense SNP maps for *in silico* mapping of QTL (Pletcher *et al.*, 2004). This method relies on known phenotypic differences between inbred strains and requires a high density of markers to derive detailed SDPs (Grupe *et al.*, 2001). *In silico* mapping attempts to identify sequence variants that are shared by sets of inbred strains and correlate these with phenotype. A limitation of this method is that a shared sequence variant does not guarantee descent from a common ancestor although there is evidence to suggest that the genealogies of many inbred strains can be traced back to a relatively small number of animals (Beck et al., 2000). A further limitation of this method is that low resolution sequence maps often mask smaller blocks of haplotype difference and provide an oversimplification of SDP (Cuppen, 2005). This is supported by the recent finding of complex patterns within established haplotype blocks following high-density SNP screening in common inbred strains (Frazer *et al.*, 2004; Yalcin *et al.*, 2004a).

A problem facing researchers utilising published SNP datasets is that the specific mouse strains they are interested may not be included in the analysis or that the sequence available for that strain is not comprehensive enough. For example, the Wellcome-CTC Mouse Strain SNP Genotype Set (http://www.well.ox.ac.uk/mouse/INBREDS/) includes a large number of mouse strains but the level of sequence resolution is not as high as that of more recent re-sequencing projects (Frazer et al., 2007; Yang et al., 2007). However, these new sequencing efforts have focused on a smaller less comprehensive group of mouse strains.

Differential Gene Expression

Gene expression profiling can also be combined with genetic mapping data to identify

genes underlying QTL. This can be done on an individual gene basis using quantitative real-time PCR (qRT-PCR) or on a genome-wide scale via the use microarray technology investigating the expression of many thousands of transcripts simultaneously to identify potential functional differences between mouse strains. A possible limitation of the use of this method is the lack of knowledge regarding the stages of prion pathogenesis at which a given gene may be differentially expressed and in which specific tissues. Time-course studies would be therefore appropriate to discern which genes and their potentially related biochemical pathways are switched on and off throughout disease progression.

Knockout and Transgenic Mice

Other functional tests to confirm the roles of putative candidate genes include the generation of transgenic and knockout mice. Transgenic mice may be used to test the effect of overexpressing a candidate gene or involve the targeted interchange of nucleotides between two strains to prove that a sequence variant operates as a QTL. Knockout mice provide a powerful tool by which to elucidate the exact *in vivo* role of a gene in conferring a given phenotype (Flint et al., 2005). As previously described (Section 1.2.4), knockout technology has been recently employed to identify three mouse prion disease candidate genes; *Mcp-1*, *Il-10* and Clusterin (Felton *et al.*, 2005; Kempster *et al.*, 2004; Thackray *et al.*, 2004). Although published knockouts exist for approximately 10% of mouse genes there are future plans to produce a complete set knockouts for all known murine genes to provide a valuable resource for the testing of numerous phenotypes (Austin *et al.*, 2004).

Following the successful fine mapping of QTL into intervals small enough in which to analyse individual candidate genes, sequence comparisons between mouse strains may uncover genetic differences potentially contributing towards prion disease incubation time. Based upon the current limited knowledge of prion pathogenesis it would be intriguing to identify candidate genes which are expressed in the CNS or lymphoreticular system or perhaps have functions related to apoptosis or protein degradation. In the absence of a complete picture of the mechanisms of disease it is prudent to assess all candidate genes equally since the identification of genetic variants associated with incubation time in genes of unrelated function may in itself uncover novel biological pathways involved in prion disease. The identification of mouse candidate genes, and their alleles, accounting for variation in prion disease susceptibility

may be extended to humans to allow the identification of at-risk individuals within the populations and provide new targets for therapeutic strategies.

1.3 Aim of Project

Polymorphisms of the prion protein gene have an established role in conferring prion disease incubation time in mice but there are other lines of evidence indicating that additional genetic loci are involved in controlling susceptibility. Several extensive incubation time QTL have been identified in genome-wide mapping studies and the aim of this project is to fine map these regions of linkage in order to elucidate and further characterise candidate genes and their functional variants that may be influencing susceptibility to prion disease. Fine mapping will be undertaken by multipoint linkage analysis in a genetically diverse heterogenous stock of mice to allow high resolution mapping of chromosomal regions of interest. This method is proposed to reduce extensive QTL into intervals small enough in which to utilise a candidate gene approach. Subsequent sequence analysis of candidate genes may potentially uncover the genetic variation responsible for controlling incubation time. The identification of sequence variants and an assessment of their potential functional implications, alongside an analysis of mRNA expression, will be used to further characterise the most interesting candidate genes in terms of their relevance to prion pathogenesis.

2

Materials and Methods

2.1 Materials

2.1.1 Reagents and Commercial Kits

Absolute Ethanol 100% ('Analar')	VWR
Anti-GFAP Rabbit Polyclonal Antiserum	Dako
Anti-PrP Monoclonal Antibody ICSM35	D-Gen
Anti-Iba-1 Polyclonal Antibody	Wako
Better Buffer	Microzone
Big-Dye Terminator v1.1 Cycle Sequencing Kit	Applied Biosystems
ß-Mercaptoethanol	Sigma
Custom TaqMan Allele Discrimination Probes	Applied Biosystems
Diethyl Pyrocarbonate (DEPC) Treated H_20	Ambion
Electrophoresis Grade Ultra Pure Agarose	Invitrogen
Eosin Y Solution (0.5%)	VWR
ET-Dye Terminator Cycle Sequencing Kit	Amersham Biosciences
Ethanol (99.7-100%)	BDH
Ethidium Bromide (EtBr)	Sigma
Formic Acid (98%)	VWR
Harris Haematoxylin	BDH
Hyperladder I and IV	Bioline
Iso-Proply Alcohol (propan-2-ol 'Analar')	VWR
MegaBACE ET400-R Size Standard	Amersham Biosciences
MegaBACE Linear Polyacrylamide Buffer (10x)	Amersham Biosciences
MegaBACE Loading Solution	Amersham Biosciences
MegaBACE Long Read Matrix	Amersham Biosciences
MegaMix Blue PCR Master Mix	Microzone
microCLEAN	Microzone
Murine *Prnp* TaqMan® Gene Expression Assay	Applied Biosystems
Nuclei Lysis Solution	Promega
Oligonucleotide Primers	Sigma Genosys
Pertex Mounting Medium	Cox Scientific

Phosphate Buffered Saline (PBS)	VWR
Power Synergy Brands (SYBR) Green PCR Mix	Applied Biosystems
Proteinase K	BDH
Protein Precipitation Solution	Promega
Pure Paraffin Wax	RA Lamb
QuantiTect Probe PCR Master Mix	Qiagen
Reverse Transcription System	Promega
RNase-Free DNase Set	Qiagen
RNaseZap Refill Wipes	Ambion
RNaseZap Spray	Ambion
RNeasy® Mini, Midi and Maxi Preps	Qiagen
ROX MegaMix~Gold	Microzone
Sodium Acetate Buffer Solution (0.3M, pH 5.2)	Sigma
Sodium Hydroxide (2M)	VWR
Superfrost Microscope Slides	VWR
TaqMan Rodent Beta Actin (ACTB) (x20)	Applied Biosystems
TaqMan Rodent GAPDH	Applied Biosystems
Total RNA Isolation (TRI) Reagent	Ambion
Tris-Borate EDTA (x10) (TBE)	National Diagnostic
Xylene	TBS

2.1.2 Equipment

96-Well Optical Plate	Applied Biosystems
96-Well Seal Strips	Anachem
ABI Prism 7000 Sequence Detection System	Applied Biosystems
ABI Prism 7500 Fast Real-Time PCR System	Applied Biosystems
Adhesive PCR Film	ABgene
Benchmark Staining Machine	Ventana Medical Systems
Discovery Immunohistochemical Staining Machine	Ventana Medical Systems
Fast Optical 96-Well Reaction Plates	Applied Biosystems
Gel Doc EQ UV-Transilluminator	Bio-Rad Laboratories
MegaBACE 1000 DNA Analysis System	Applied Biosystems
Mitsubishi Thermal Printer Paper	Bio-Rad Laboratories
NanoDrop ND-1000 Spectrophotometer	NanoDrop
Optical Adhesive Covers	Applied Biosystems

Peltier Thermal Cycler PTC-225	MJ Research
Ribolyser	Hybaid Limited
Video Printer	Bio-Rad Laboratories

2.1.3 Prepared Solutions

Ethidium Bromide

10mg/ml in ddH_2O

Proteinase K

10mg/ml in ddH_2O

Tris-EDTA (TE)

10mM Tris-HCL, pH 7

1mM EDTA, pH 8

2.1.4 Computer Software

7500 Fast System SDS Software Version 1.3.1	Applied Biosystems
GraphPad InStat Version 3.05	GraphPad
HAPPY	www.well.ox.ac.uk/~rmott/
MegaBACE Genetic Profiler	Applied Biosystems
MegaBACE Sequence Analyser Version 3	Molecular Dynamics
Primer Express Software Version 2.0	Applied Biosystems

2.1.5 Websites

http://www.ebi.ac.uk/Tools/clustalw/index.html	ClustalW
http://www.ensembl.org/index.html	Ensemble Genome Browser
http://zeon.well.ox.ac.uk/git-bin/old_happy.cgi	HAPPY Web Server
http://www.informatics.jax.org/	Mouse Genome Informatics
http://www.ncbi.nlm.nih.gov/	NCBI
http://www.ncbi.nlm.nih.gov/BLAST/	NCBI BLAST
http://www.ncbi.nlm.nih.gov/gorf/gorf.html	ORF Finder
http://www.ncbi.nlm.nih.gov/gorf/gorf.html	Primer 3
http://www.repeatmasker.org/	RepeatMasker
http://www.cbrc.jp/research/db/TFSEARCH.html	TFSEARCH
http://genome.ucsc.edu/	UCSC Genome Browser

http://www.ebi.ac.uk/swissprot/	UniProtKB/Swiss-Prot
http://bimas.dcrt.nih.gov/molbio/proscan/	WWW Promoter Scan

2.2 Animal Procedures

2.2.1 Husbandry

Mice were housed in two types of facility; a conventional animal house and a Specific Pathogen Free (SPF) facility. Mice in the SPF facility were housed in individually ventilated cages. Breeding pairs and their litters were housed together until pups were weaned at around 3 weeks. Thereafter, mice were housed in same-sex groups of 5-7.

2.2.2 Identification

Breeding pairs and experimental mice were individually tagged with a Trovan transponder microchip that emits a code signal for processing by an appropriate reader. Mice were tagged in the scruff of the neck by subcutaneous injection under isofluorane anaesthesia and identification details recorded on a computer database. Tail biopsies of 0.5cm were taken for genomic DNA extraction (Section 2.4.1.1).

2.2.3 Biosafety

UK guidelines for the decontamination of prion-infected samples are detailed at http://www.archive.official-documents.co.uk/document/doh/spongifm/annex-b.htm. All procedures dealing with prion-infected tissue samples were performed within a Class 1 microbiological safety cabinet in a Level III containment laboratory. Decontamination of surgical instruments was carried out by soaking them in 2M sodium hydroxide.

2.2.4 Chandler/RML Mouse-Adapted Scrapie

The Chandler/Rocky Mountain Laboratory RML mouse-adapted scrapie inoculum (Chandler, 1961) was obtained from Adriano Aguzzi (Institute of Neuropathology, University of Zurich, Zurich) and passaged once in CD-1 Swiss mice to increase the quantity available. Brains from terminally sick mice were used to generate a 1% homogenate in PBS (Lloyd *et al.*, 2001).

2.2.5 Intracerebral Inoculations

Prior to inoculation mice were given general anaesthesia with isofluorane/O_2 in an inhalation chamber. Absence of the pedal withdrawal reflex was assessed by finger

pinch pressure between two digits on the hind limb to confirm surgical anaesthesia. 30µl of a 1% homogenate of Chandler/RML mouse-adapted scrapie was introduced by intracerebral injection, 3-4mm into the right parietal lobe of the brain avoiding vital centres, using a 25-gauge hypodermic needle. Mice were allowed to recover in a cage placed on a heated pad prior to being replaced in their home cage.

2.2.6 Diagnosis of Prion Disease

All animals inoculated with Chandler/RML mouse-adapted scrapie were observed daily by qualified and experienced animal technicians for signs and symptoms of illness (Table 2.1). Mice showing one or more non-specific signs of prion disease had their cages marked for closer observation in order to monitor progress. In the event of the observation of an early indicator of scrapie mice were placed under closer daily observation. The general condition of an animal was monitored with specific attention to weight loss, breathing, coordination, posture and gait. The animal was handled using forceps and picked up by the tail to assess clasping of hind limbs and the ability to grasp the bars of the cage. All symptoms were documented using a digital camera. Upon the observation of a confirmatory sign of prion disease the symptom was recorded using a digital camera and the animal was subsequently culled. Confirmatory symptoms of prion disease are considered to indicate a definite diagnosis and the experimental end point. In the case of the clinical course of illness proceeding at an unexpectedly fast rate with the animal showing severe signs of prion disease the symptoms were recorded and the animal was culled immediately. Mice were not deliberately allowed to progress to this stage to prevent unnecessary suffering. Prion disease incubation time was calculated retrospectively after a definite diagnosis had been made and defined as the number of days from inoculation to the onset of clinical signs.

2.2.7 Tissue Dissections

Tissue dissections were performed by fully trained animal technicians. The following tissues were harvested for analysis; spinal cord, liver, kidney, pituitary gland, adrenal gland, pancreas, thyroid gland, testes, spleen, thymus, lung, heart, stomach, small intestine, large intestine. The brain was also removed as a whole or with the cerebellum removed for separate analysis. Tissue dissections from Chandler/RML infected mice were taken in a Class 1 microbiological safety cabinet. All tissues were immediately snap frozen in liquid nitrogen and stored at -80°C.

Table 2.1 Signs and symptoms of prion disease in mice.

Non-Specific Signs
Head shake - Occasional shaking, as though clearing water from the ears **Head tilt** - Not holding the head erect and in the vertical plane **Agitation** - Inability to stay quiet in one place for several minutes, rest disturbed **Aggression** - Towards cage mates an/or animal technicians, when not previously noted **Disorientation** - Not moving in straight lines, knocking into objects **Unusual gait** - Walking movement is not fluid **Slight weight loss** - Compared to cage mates or that of age-matched controls **Eyes become dull** - Opaque glaze to the surface of the eye **Pale extremities** - Digits, ears or tail are noted as being paler than normal
Early Indicators
Erect ears **Slight loss of co-ordination** - Unsteady on legs **Slight piloerection** - Looking un-groomed **Slight hunched posture** - Back looks slightly arched **An altered breathing rate** - Slightly faster or slower **Erect penis** - Penis erect, red and swollen for more than a few minutes **Rigid tail** **Clasping hind legs** - When lifted by the tail
Confirmatory Signs
Ataxia - Animal looks drunk and grasps between bars on a grid **Generalised tremor** - Whole body shiver more than once every minute **Slight paralysis of limb** - Back legs begin to drag on the floor, some paralysis noticed **Loss of righting reflex** - Inability to right when placed on its back **Weight loss of up to 20%** - Of original body weight, or that of age-matched controls **Piloerection** - Hair sticking up and coat looking greasy **Hunched posture** - Arched back **Dyspnoea** - Difficult or laboured respiration
Severe Signs
Substantial ataxia - Losing balance and constantly falling over **Paralysis of limb** - Loss of function in two or more limbs and no response to stimulation by gentle handling **Unable to drink freely** - Cannot raise head to lick from water spout and will not take wet diet or water as a gel. Dehydrated mice exhibiting skin "tents" **Unable to eat freely** - Not raising head to food hopper and not eating food or dietary supplements placed on the cage floor **Extensive periods of prostration** - Animal on its side

2.3 Mice

2.3.1 The Northport Heterogenous Stock (HSNPT)

Generation 35 of the Northport HS were obtained as a kind gift of Robert Hitzemann (Portland Oregon, USA). As previously described (Section 1.2.6), this stock is derived from an 8-way cross of homozygous, inbred, unrelated parental lines of the following mouse strains; A/J, AKR/J, BALB/cJ, C3H/HeJ, C57BL/6J, CBA/J, DBA/2J and LP/J (Demarest *et al.*, 2001). The HS are maintained following a pseudo-random breeding protocol to maximise diversity and have genetic backgrounds which are fine grained genetic mosaics of the founder strains allowing high resolution fine mapping at centimorgan intervals (Talbot *et al.*, 1999). 49 breeding pairs from generation 36 were set up semi-randomly, to avoid shared 'grandparents', which produced >1000 mice (generation 37). These mice were inoculated intracerebrally with Chandler/RML mouse-adapted scrapie (Sections 2.2.4 and 2.2.5) and phenotyped for prion disease incubation time (Section 2.2.6). DNA was extracted from tail biopsies (Section 2.4.1.1) taken from each mouse and microsatellite markers were genotyped in these samples for linkage analysis, using fluorescently-labelled PCR primers (Section 2.4.4). DNA for the founder strains of the HS was purchased from The Jackson Laboratory.

2.3.2 *Mcp1* Knockout Mice

Mcp1 knockout mice (B6.129S4-*Ccl2*^{tm1Rol}/J) were purchased as homozygotes from The Jackson Laboratory. These mice were created by B. Rollins (Dana-Farber Cancer Institute, Harvard Medical School, Boston, USA). A targeting vector containing a PGK-neomycin resistance cassette, in a transcriptional orientation opposite to that of *Mcp1*, and a herpes simplex virus thymidine kinase gene was used to disrupt exon 2 introducing a small deletion and inserting an inframe stop codon into exon 1 (Lu *et al.*, 1998). The construct was electroporated into 129S4/SvJae derived J1 embryonic stem cells and correctly targeted ES cells were injected into C57BL/6J blastocysts. The resulting chimeric mice were crossed to C57BL/6J mice and then backcrossed to C57BL/6J mice for 10 generations. Secreted MCP1 protein was not detected in stimulated peritoneal macrophages from homozygous mutant mice (Lu et al., 1998). Mice homozygous for the targeted mutation are viable, fertile, normal in size and do not display any gross physical or behavioural abnormalities. Screening protocols for these mice are detailed in Section 2.4.2.4.

2.4 Methods

2.4.1 Extraction of DNA and RNA

2.4.1.1 Extraction of Genomic DNA

Genomic DNA was extracted, using a Promega DNA extraction kit, from thawed 0.5 cm mouse tail biopsies. 480µl nuclei lysis buffer and 28µl Proteinase K were added to each sample and mixed by gentle inversion. The mixture was then incubated overnight at 65°C in a water bath. The following day the samples were cooled on ice and spun briefly to remove liquid condensed on the lid. 160µl protein precipitation solution was added, mixed well by inversion and flicking and left to cool on ice for 5 minutes. The samples were then centrifuged at 16,100g for 4 minutes at room temperature. The supernatant was then removed to a fresh tube and 480µl isopropanol was added and mixed well by inversion and flicking. A DNA spool was visible at this point. The samples were centrifuged at 16,100g for 4 minutes at 4°C to pellet the DNA. The supernatant was discarded and the pellet was reformed and washed in 200µl 70% ethanol by centrifugation at 16,100g for 4 minutes at room temperature. The supernatant was discarded and the remaining pellet kept. Excess ethanol was removed with a pipette. The pellet was briefly air dried for approximately 10 minutes before being resuspended in 50µl 10mM TE and stored at 4°C for immediate use or at -20°C for archiving. A 1 in 10 dilution was made, in 10mM TE, of the stock DNA for amplification in polymerase chain reaction (PCR) (Section 2.4.2.2).

2.4.1.2 Extraction of Total RNA

Prior to working with RNA, RNaseZap spray and RNaseZap wipes were used to thoroughly clean laboratory bench surfaces and pipettes to destroy any RNases present. Gloves were treated with RNaseZap spray and changed regularly and fresh RNase-free tubes and filtered RNase-free pipette tips were used. Total RNA was extracted from thawed and weighed tissue samples using RNeasy Mini, Midi or Maxi Kit, depending on the size and nature of the tissue in question, following guidelines recommended by the manufacturer, and resuspended in an appropriate volume of RNase-free water. RNeasy kits utilise guanidine-isothiocyanate lysis and silica gel-membrane purification techniques which are less toxic and labour-intensive than traditional phenol/chloroform methods of extraction. RNA samples were purified using RNeasy mini columns and the RNase-Free DNase set. DNA contamination in samples was minimized following

manufacturer's recommendations by on-column DNase I treatment (2500 Kunitz units/mg) for 15 minutes at room temperature. RNA samples were kept on ice for immediate use or stored at -80°C. Prior to storage RNA quality and concentration was quantified using a NanoDrop spectrophotometer (Section 2.4.1.4).

2.4.1.3 Extraction of Total RNA from RML-Infected Tissue

Extra precautions were taken when extracting RNA from Chandler/RML-infected material to prevent transmission of infection. Two pairs of gloves were worn at all times with the outer glove being changed regularly and disposable sheaths were also worn over the arms. The protocol was carried out in a Class 1 microbiological safety cabinet until stated. The phenol/chloroform extraction method, which denatures proteins, was used to extract RNA from Chandler/RML-infected tissue in order to remove as much contaminated material as possible.

Mouse whole brain samples (~500mg) were cut into four segments on a petri dish using a sterile scalpel. Small ceramic rybolysing beads were placed in four 2ml screw cap microtubes filling the bevelled bottom of the tube. Individual segments of brain tissue were inserted into each tube and 1250µl Total RNA Isolation (TRI) Reagent (Phenol/Guanidine thiocyanate) was added. Tubes were rybolysed for 45 seconds after which two 500µl aliquots from each sample were transferred into fresh tubes and incubated at room temperature for 5 minutes. 100µl of chloroform was added to each sample and mixed thoroughly by inverting tubes. Samples were incubated at room temperature for 10 minutes and then centrifuged at 16,100g for 15 minutes at 4°C. The aqueous phase was then transferred into a fresh RNase-free 2ml screw cap tube. From this point onwards the protocol was carried out on a normal laboratory bench as infected protein material had been removed.

250µl of RNase-free DEPC-treated H_2O was added to each sample and mixed well by inverting the tube. 500µl of isopropanol was added to each sample and mixed well by inverting the tube. Samples were left to incubate at room temperature for 10 minutes. Tubes were then centrifuged at 16,100g for 15 minutes at 4°C to pellet the RNA. The RNA pellet was washed with 500µl 70% ethanol. Tubes were centrifuged at 16,100g for 5 minutes at 4°C to further pellet the RNA. The ethanol was then removed and the pellet was air dried for 10 minutes before being resuspended in 200µl RNase-free DEPC-treated H_2O. As previously described (Section 2.4.1.2), RNA samples were

purified using RNeasy mini columns and the RNase-Free DNase set. RNA concentration and quality was determined using a NanoDrop spectrophotometer (Section 2.4.1.4) and samples were stored at -80°C.

2.4.1.4 Spectroscopic Measurement of Nucleic Acids

The purity and concentration of nucleic acids extracted from mouse tissue was determined by spectroscopic analysis on a NanoDrop ND-1000 Spectrophotometer. 1µl samples of unknown RNA or DNA concentration were measured using the absorbance at 260nm and 280nm.

DNA concentration (µg/ml)= A_{260} x 50µg/ml

RNA concentration (µg/ml)= A_{260} x 40µg/ml

The 260/280nm absorbance ratio was also examined for assessment of nucleic acid purity. Samples with a ratio of ~1.8 for DNA or ~2.0 for RNA were considered sufficiently pure.

Nucleic acid purity = A_{260}/A_{280}

2.4.1.5 Reverse Transcription

Reverse transcription was performed, using a Promega Reverse Transcription System kit, to generate complementary DNA (cDNA) from RNA templates using the enzyme reverse transcriptase. All reverse transcription reactions were carried out in a total volume of 40µl. An appropriate volume of DEPC H_2O was added to samples to give 4µg of RNA in a total volume of 19.8µl. A master mix was prepared of 1µl RNasin (1u/µl), 8µl $MgCl_2$ (5mM), 4µl RT-buffer (10X), 4µl dNTPs (1mM each dNTP), 2µl random primers (500µg/ml) and 1.2µl AMV reverse transcriptase (12.5u/µl) per RNA sample. For each sample another mix was made up in which 1.2µl DEPC water substituted the AMV reverse transcriptase enzyme to test for successful generation of cDNA and to confirm the absence of DNA contamination. Samples were left at room temperature for 10 minutes and then incubated at 42°C for 1 hour and 95°C for 5 minutes. Samples were cooled on ice for 5 minutes after which 160µl of DEPC H_2O was added to each before storage at -20 °C.

2.4.2 Genomic DNA Amplification

2.4.2.1 Oligonucleotide Primer Design

Primers were designed for PCR amplifications (Section 2.4.2.1) manually or using Primer 3 software (Rozen and Skaletsky, 2000). When primers were designed manually the region of DNA sequence in question was screened for interspersed repeats and low complexity DNA sequences, which can be difficult to PCR amplify, using RepeatMasker software Version 3 (Smit *et al.*, 1996-2004).

Optional parameters for primer design included the following criteria;

i) Primer length – 20-30 nucleotides long to provide good specificity for unique target sequence.

ii) AT/GC ratio – Approximately equal AT/GC content. G and C have three hydrogen bonds compared to two for A and T. An excess of Gs and Cs reduces the detachability of the primer from the template.

iii) 3' end - Runs of three or more Gs or Cs at the 3' end were avoided to prevent mispriming in GC rich regions.

iv) Melting temperature (T_m) – A T_m range of 58-60°C was chosen with the temperature difference between primer pairs no more than 5°C.

v) Annealing temperature – 5°C less than the melting temperature.

vi) Secondary structure – Internal self-matching stretches of three bases or more were avoided to prevent the primer binding to itself and producing a hairpin structure.

vii) Primer dimers – 3' stretches of complementary sequence between primer pairs were avoided to prevent the primers binding to each other and creating a new template.

viii) Repetitive sequences and regions containing stretches of the same nucleotide were avoided to prevent slipping of the primer on the template leading to mispriming (G,C) or breathing (A,T).

ix) Amplicon size – Primers were designed to amplify amplicons no larger than 500bp. Products of this size are recommended by the manufacturer for optimal sequencing results (Section 2.4.3).

Freeze-dried primers were resuspended to a stock concentration of 100µM in 10mM TE and stored at -20°C. A 1 in 10 dilution to 10µM in 10mM TE was made for working

PCR primer stocks and these were stored at -20°C or 4°C dependent upon the regularity of use to avoid degradation through unnecessary freeze-thawing.

2.4.2.2 Polymerase Chain Reaction (PCR)

All PCR reactions were carried out in a total volume of 25µl unless otherwise stated. A master mix of 22µl MegaMix Blue PCR Master Mix, 1µl of forward primer (10µM) and 1µl of reverse primer (10µM) was scaled up appropriately according to the number of samples in question, mixed well and spun briefly at 16,100g. 24µl aliquots were transferred onto a 96-well plate per sample and 5-10ng/µl of DNA was added. 1µl of ddH_20 was added to a designated non-template control (NTC) for each primer set. Plates were sealed with an adhesive PCR film lid and spun briefly at 3007g. The samples were then subjected to a thermal cycling program on a PTC-225 thermal cycler. Cycling conditions were determined empirically but in general were as follows: Initial denaturation step at 95°C for 15 minutes and then 40-42 cycles of: DNA template denaturation at 94°C for 30 seconds, primer annealing at 50-65°C for 30 seconds, extension 72°C for 1 minute, and a final extension step at 72°C for 5 minutes. Upon completion of PCR plates were stored at 4°C for immediate analysis.

Primer annealing is dependent upon primer T_m and is optimal at 5°C below the lower of the PCR primer pair melting temperatures. The length of the extension step time was determined empirically based upon the size of the amplicon, allowing the amplification of 1kb per minute. An optimal cycle number was determined empirically by assessing the strength of PCR product signal observed on subsequent gel electrophoresis (Section 2.4.2.3). In the case of difficulty in amplifying PCR products a gradient PCR program was employed in which an annealing temperature range of 50-65°C was used across a plate of identical samples to identify an optimum temperature.

2.4.2.3 Gel Electrophoresis

Following PCR, amplified DNA fragments were separated according to size by electrophoresis on an agarose gels. 5µl PCR product was loaded onto a 1-2% TBE agarose gel depending upon the PCR product size under scrutiny. A 1% gel was used for products >500bp and a 2% gel for products <500bp. An appropriate amount of electrophoresis grade ultra pure agarose was melted in 1xTBE by heating for 30-60 seconds in a microwave oven. Once the gel had cooled ethidium bromide was added to a final concentration of 0.2µg/ml and the gel was left to set at room temperature before

being immersed in 1xTBE. 2µl of an appropriately sized DNA ladder of known concentration was used to confirm the size and estimate the DNA concentration of PCR amplicons. HyperLadder I was used for products ranging from 200bp to 10kb and HyperLadder IV was used for amplicons ranging in size from 100bp to 1kb. Electrophoresis was carried out at 100V for 15-30 minutes unless otherwise stated. The amplified products were visualised on a Gel Doc EQ UV-transilluminator and digital imaging system.

2.4.2.4 PCR Screening of Mcp1 Knockout and Wild-Type Mice

Two PCR reactions, A and B, were used to identify *Mcp1* wild-type and knockout mice respectively. Reaction A amplifies an 888bp wild-type product ($Mcp1^{+/+}$) using primers *a* and *b* (Table 2.2). Primers *a* and *c* are used in reaction B to amplify a 1350bp product which is present in the knockout mouse ($Mcp1^{-/-}$) and represents a neo cassette disrupting exon 2 (Section 2.3.2). Primers *a* and *b* were designed by The Jackson Laboratory. Primer *c* was designed manually.

Table 2.2 Primer sequences for screening *Mcp1* knockout and wild-type mice.

Reaction	Forward Primer	Reverse Primer
A (wt)	ggagcatccacgtgttggc (a)	acagcttctttgggacacc (b)
B (ko)		tcctcgtgctttacggtatcg (c)

All PCR reactions were carried out in a total volume of 10.5µl containing 8.5µl MegaMix Blue, 0.5µl forward primer (10µM), 0.5µl reverse primer (10µM) and 1µl of DNA per sample. Plates were sealed with adhesive PCR film and spun briefly at 3007g and subjected to the following PCR cycling conditions. Reaction A cycling conditions were: 94°C for 3 minutes, 45°C for 30 seconds, 72°C for 40 seconds and then 30 cycles of: 94°C for 1 minute, 55°C for 30 seconds and 72°C for 3 minutes after which 72°C for 2 minutes and finally 10°C for 5 minutes. For reaction B cycling conditions were: 94°C for 3 minutes, 45°C for 30 seconds, 72°C for 40 seconds and then 35 cycles of: 94°C for 1 minute, 62°C for 30 seconds and 72°C for 3 minutes after which 72°C for 2 minutes and finally 10°C for 5 minutes. 10µl of amplified PCR product was loaded onto a 1% agarose gel and run at 100V for 30 minutes to 1 hour.

2.4.3 Semi-Automated Sequencing of PCR Products

2.4.3.1 Purification of PCR Products for Sequencing

PCR product was purified and concentrated using microCLEAN following the manufacturer's instructions. microCLEAN removes reaction buffers, enzymes, primers, primer dimers and dNTPs. An equal volume of microCLEAN was added to each sample and mixed thoroughly. Samples were left at room temperature for 5 minutes before being spun at 3007g for 40 minutes. Plates were then placed upside down onto folded tissue paper in the centrifuge bucket and spun at 100g for 1 minute. The DNA concentration of PCR products was determined empirically through comparison of electrophoresed amplicons with an appropriately sized DNA ladder (Section 2.4.2.3). Pellets were resuspended in an appropriate amount of ddH_2O to give an approximate DNA concentration of 50-100ng/µl. Samples were mixed and allowed to resuspend and rehydrate at room temperature for 5 minutes. Plates were then spun briefly to remove bubbles and used immediately or stored at -20°C.

2.4.3.2 Sequencing of Purified Templates

Fluorescent sequencing of PCR fragments was carried out using BigDye Terminator v1.1 Cycle Sequencing Kit or DYEnamic ET Dye Terminator kit as described by the manufacturer. The starting template quantity for PCR products of 200-500bp is 3-10ng/µl for the BigDye terminator v1.1 kit and 50ng/µl for the DYEnamic ET terminator kit. The volume of PCR product and ddH_2O was varied as required to obtain these concentrations. All sequencing reactions were carried out in a total volume of 15µl.

For the BigDye terminator kit a master mix was prepared of 5µl Better Buffer, 1µl Big-Dye Terminator v1.1 Cycle Sequencing Mix and 7µl of ddH_2O per sample. Aliquots of master mix for specific PCR fragments were made in which 1.5µl of PCR product in ddH_2O and 0.5µl of the relevant primer (10µM) were added. Aliquots of the master mix were transferred onto a 96-well plate, sealed with an adhesive PCR film lid and spun briefly at 3007g. The samples were then subjected to the following thermal cycling program on a PTC-225 thermal cycler; 30 cycles of: 96°C for 30 seconds, 50°C for 15 seconds and 60°C for 3 minutes followed by a final hold step of 15°C for 5 minutes.

For the ET terminator kit a master mix was prepared of 6µl Better Buffer for the megaBACE, 1µl ET Dye Terminator Sequencing Mix and 3µl of ddH_2O per sample. Aliquots of this mix were made for specific PCR fragments in which 3.5µl PCR product in ddH_2O and 1.5µl of the relevant primer (10µM) were added. Aliquots of the master mix were transferred onto a 96-well plate, sealed with an adhesive PCR film lid and spun briefly at 3007g. The samples were then subjected to the following thermal cycling program on a PTC-225 thermal cycler; 25 cycles of: 95°C for 20 seconds, 50°C for 15 seconds and 60°C for 1 minute.

Sequencing products from both protocols were stored at 4°C until further processing by ethanol precipitation.

2.4.3.3 Purification of Sequencing Products

To purify sequencing products for analysis all samples were precipitated in 1µl 0.3M sodium acetate (pH 5.2) and 55µl 100% ethanol and centrifuged at 3007g for 45 minutes at 4°C. Plates were placed upside down on tissue paper in the centrifuge bucket and spun at 100g for 1 minute to discard the supernatant and then turned upright and spun at 3007g for 5 minutes to reform the pellet. The pellet was then resuspended in 150µl 70% ethanol and spun for 10 minutes at 3007g. The supernatant was discarded as before by inverting the plate and spinning for 1 minute at 100g. Plates were then turned upright and spun at 3007g for 5 minutes to reform the pellet after which the pellet was air dried for ~5-10 minutes. The plate was directly sealed with an adhesive PCR film lid and stored at -20°C.

2.4.3.4 Sequencing of PCR Products

PCR fragment sequencing was carried out using the semi-automated MegaBACE 1000 DNA Analysis System which employs capillary array electrophoresis to separate fluorescently labelled DNA fragments in 96 samples simultaneously. The manufacturer's guidelines were followed unless otherwise stated.

Prior to analysis the precipitated DNA samples with fluorescently labelled terminators were resuspended in 10µl megaBACE loading solution and mixed thoroughly to ensure the complete solubilization of the DNA. Samples were spun briefly. The 96 capillaries of the megaBACE 1000 instrument are injected by high pressure with MegaBACE Long Read Matrix. An electric field causes sequencing products to migrate towards the

capillaries by way of electrokinetic injection. This is controlled by a potential difference of 3kV for 40 seconds. Electrophoresis is then carried out in 1x MegaBACE LPA buffer at 9kV for 100 minutes. The DNA fragments in the sample separate by size with shorter fragments moving faster throughout the matrix than longer fragments. During electrophoresis, laser excitation and confocal optical detection excite and detect the dye-labelled DNA fragments of varying sizes as they migrate past the detection window. An electrophorogram is produced for each capillary/sample and these data were analysed using the MegaBACE Sequence Analyser Version 3.0 software package.

2.4.4 Genotyping and Linkage Analysis

2.4.4.1 Genotyping Microsatellite Markers for Linkage Analysis

Fine mapping in the HS was carried out using microsatellite markers mapping across identified QTL regions. Marker information was obtained from the Mouse Genome Informatics database. The length of these di-nucleotide repeats between homozygous inbred mouse strains is variable i.e., polymorphic. To give power to linkage analysis (Section 2.4.4.5) markers need to be informative in the HS, that is, they must be polymorphic between the founder strains of the cross (Mott *et al.*, 2000) and were therefore selected based upon this criteria. As previously described (Section 2.3.1), the HS allows fine mapping at high resolution (Talbot et al., 1999) and so markers were chosen at approximately 1cM intervals to provide regular and evenly spaced coverage across regions of interest.

Primer sequences for PCR amplification of microsatellite markers were obtained from UCSC Genome Browser. Full primer sequences are detailed in Appendix 1. Forward primers were labelled with 6-carboxyfluoresceine (FAM, blue), hexachloro-6-carboxyfluorescein (HEX, yellow) or tetrachloro-6 carboxyfluoresciene (TET, green) fluorescent dyes for semi-automated fluorescent genotyping of marker PCR fragments using the MegaBACE 1000 DNA Analysis System.

2.4.4.2 PCR Amplification of Microsatellite Markers

All PCR reactions for genotyping were carried out in a total volume of 5μl. A master mix was prepared of 4.3μl MegaMix Blue PCR master mix, 0.1μl of forward primer (10μM) and 0.1μl reverse primer (10μM). This mix was scaled up appropriately according to the number of samples for analysis, mixed well and spun briefly at

16,100g. 4.5µl aliquots of master mix per DNA sample were transferred onto a 96-well plate. 0.5µl of DNA was added per well with one sample per primer set designated as a NTC in which DNA was substituted by 0.5µl of ddH_2O. The plate was sealed with an adhesive PCR film lid and spun briefly at 3007g. Samples were then subjected to the following thermal cycling program on a PTC-225 thermal cycler: 94°C for 15 minutes followed by 40 cycles of; 94°C for 30 seconds, 55°C for 30 seconds, 72°C for 30 seconds and a final step of 72°C for 5 minutes.

2.4.4.3 Microsatellite Marker PCR Fragment Purification

Products were pooled in groups of 2-3 markers whose amplicon sizes and fluorescent dye emissions were suitably distinguishable. Samples were then precipitated in 2µl 0.3M sodium acetate (pH 5.2) and 55µl 95% ethanol and centrifuged at 3007g for 40 minutes. The plate was then placed upside down on tissue paper in the centrifuge bucket and centrifuged at 100g for 1 minute to discard the supernatant. The samples were washed in 150µl 70% ethanol and the plate was centrifuged for 10 minutes at 3007g. The supernatant was discarded by inverting the plate and spinning for 1 minute at 100g. Plates were spun at 3007g for 5 minutes to reform the pellet. The plate was sealed with an adhesive PCR film lid and stored at -20°C if not for immediate use.

For further processing and analysis samples were resuspended in 10µl ddH_2O, mixed well and spun briefly. The following master mix was then prepared per sample; 5.8µl MegaBACE loading solution, 0.2µl MegaBACE ET ROX 400-R size standard and 3µl ddH_2O, mixed well and spun briefly at 16,100g. 9µl aliquots of the master mix per sample were transferred onto a 96-well plate and 1µl PCR product was added to each. 10µl MegaBACE loading solution was added to any empty wells on the plate. Plates were spun briefly at 3007g to remove bubbles and then denatured for 2 minutes at 94°C.

2.4.4.4 Fluorescent Microsatellite Marker PCR Fragment Genotyping

As previously described (Section 2.4.3.4), the semi-automated MegaBACE 1000 DNA Analysis System uses capillary array electrophoresis to separate fluorescently labelled DNA fragments in 96 samples simultaneously. The manufacturer's guidelines were followed unless otherwise stated.

The mechanism of action of the megaBACE 1000 instrument has previously been described (Section 2.4.3.4). Important differences to note with this particular protocol

are a potential difference of 3kV for 45 seconds controlling electrokinetic injection and also that electrophoresis was carried out in MegaBACE LPA buffer at 10kV for 60 minutes. Electrophorograms were analysed using the MegaBACE Genetic Profiler Version 1.1 software package for allele calling. This software calculates the size of DNA fragments, identifying the peaks in the unknown sample data using an internal DNA standard of known fragment sizes 5'-labeled with energy transfer (ET) dyes. MegaBACE ET ROX 400-R was used as a size standard containing a set of 20 bands with an average spacing of 17 base pairs.

The protocol was initially carried out using amplified fluorescent PCR fragments from the founder strains of the HS to determine the size of each parental allele. This was carried out to optimise the PCR reaction and to check that the markers were suitably informative for the HS by being polymorphic between the founder strains of the cross. Upon confirmation of these criteria PCR fragments of microsatellite markers were used to genotype generation 37 HS mice.

2.4.4.5 HAPPY Linkage Analysis and Polymorphism Evaluation

Linkage analysis was performed using the HAPPY software package written by Richard Mott (Wellcome Trust Centre for Human Genetics, University of Oxford). This software detects small-effect QTL by multipoint mapping in genetically heterogenous animals (Mott and Flint, 2002; Mott et al., 2000; Valdar et al., 2006b; Valdar *et al.*, 2003). HAPPY analysis was used to fine map broad prion disease incubation time QTL in generation 37 of the HSNPT (Section 2.3.1). As previously described (Section 2.4.4), microsatellite markers were chosen to genotype the HS for linkage analysis. For each marker, knowledge of the ancestral alleles of the founder strains and the genotypes of the individuals in the generation of the cross are essential (Mott et al., 2000). HAPPY reconstructs ancestral haplotypes in the cross by predicting the probability of each founder strain being the ancestor of a given allele. QTL are then detected by testing the progenitor polymorphism haplotypes for differences between genetic effects rather than by association at each locus. Comparisons are drawn between the polymorphism haplotypes in the founder strains and the ancestral haplotypes predicted by HAPPY. The power of HAPPY relies upon the ability to distinguish ancestral haplotypes across regions of interest and therefore it is important that selected markers are informative and polymorphic between the parental strains of the HS.

2.4.5 Quantitative Real Time PCR and Allelic Discrimination

2.4.5.1 Primer and Probe Design

When possible, commercially available, pre-validated sets of primers and probes were used. All other primers and probes were designed using Primer Express software v2.0 following criteria detailed associated user manuals;

Probe design;

1. Probes were designed as short as possible without being less than 13 nucleotides in length.
2. Probe G-C content ranged from 30-80%.
3. Runs of an identical nucleotide in a probe were avoided. This is especially important for runs of four or more guanine bases.
4. Probes were designed to avoid the presence of a guanine residue at the 5' end because a guanine residue adjacent to the reporter dye quenches some of the reporter fluorescence, even after cleavage.
5. The reporter dye was located on the 5' end and the quencher dye on the 3' end. FAM and TAMRA were used in quantification assays and FAM or VIC were used for allele discrimination.
6. The strand (sense/anti-sense) giving the probe more Cs than Gs was selected.
7. Probe T_m was 68-70°C and 10°C higher than the T_m of the primers.
8. For allelic discrimination the polymorphic site was positioned near the centre of the probe. The site could be shifted towards the 3' end but must be located more than 2 nucleotides upstream from the 3' terminus.
9. For allelic discrimination both allele 1 and allele 2 probes annealed to the same strand (anti-sense/sense).
10. For allelic discrimination allele 1 and allele 2 probe melting temperatures (T_m) were within one degree of each other.

Primer design;

1. Primers were 20-24 bases in length.
2. Primers were designed as close to the probe as possible without overlapping it. For SYBR Green the primer pairs were designed as close to each other as possible without overlapping.

3. Primer G-C content ranged from 30-80%.
4. Runs of an identical nucleotide were avoided. This is especially important for runs of four or more guanine bases.
5. Primer T_m was 58-60°C.
6. The five nucleotides at the 3′ end had no more than two G and/or C bases.
7. Ideally primers ended in a G or C. This is known as a GC clamp and helps promote specific binding at the 3' end due to the stronger bonding of G and C bases.
8. The predicted occurrence of primer dimers were assessed using Primer Express software and primer sets showing the least dimerization were chosen.
9. The size of the PCR amplicon was restricted to 50-150bp as shorter amplicons work most efficiently.
10. For quantification the PCR amplicon was designed where possible to span one or more intronic regions to avoid amplification of any contaminating genomic DNA present in samples. As previously described DNase treatment was used to minimise the possibility of DNA contamination (Section 2.4.1.2).

Full primer and probe sequences are detailed in Appendix 3 for qRT-PCR and Appendix 4 for allelic discrimination.

2.4.5.2 Relative RT-PCR Quantitation

Quantitative real-time PCR was used to detect and quantify mRNA expression. As previously described (Section 2.4.1.5), reverse transcription was used to generate cDNA from RNA samples. qRT-PCR was performed using dual-labelled fluorogenic probes or SYBR Green Dye. qRT-PCR reactions using dual-labelled fluorogenic probes are based upon the 5' to 3' exonuclease activity of a Taq DNA polymerase to cleave the probe during PCR. The probe is a fluorescently tagged oligonucleotide hybridized to an internal region of the target amplicon. A fluorescent reporter dye, such as FAM, is attached to the 5' end of the probe which has its emission spectra quenched due to the spatial proximity of a second dye coupled to the 3' end. During PCR, cleavage of the probe decouples the fluorescent and quenching dyes allowing reporter fluorescence. Reporter fluorescence increases with each cycle of PCR, proportional to the amount of probe cleavage. SYBR Green is a fluorescent dye that binds to double stranded DNA, thus as PCR product accumulates, fluorescence increases. The intensity of fluorescence in both dual-labelled fluorogenic probe and SYBR Green methods was measured using an ABI Prism 7000 Sequence Detection System or ABI Prism 7500 Fast Real-Time

PCR System.

Endogenous controls were used to normalise expression data to correct for sample-to-sample variation to give relative quantification. Commercially available fluorescently VIC-labelled rodent GAPDH and β-Actin endogenous controls were used in TaqMan assays and primers for GAPDH were designed for SYBR Green assays following general guidelines stated in Section 2.4.5.1. Endogenous controls were duplexed alongside the gene of interest when dual-labelled fluorogenic probes were used whereas the target and endogenous control were measured separately in SYBR Green assays. All samples were tested in triplicate.

2.4.5.3 qRT-PCR using Dual-Labelled Fluorogenic Probes

Quantitative real-time PCR using dual-labelled fluorogenic probes was performed using QuantiTect Probe PCR Master Mix or ROX Mega-Mix Gold RT-PCR master mix. QuantiTect Probe PCR Master Mix contains HotStarTaq DNA polymerase, QuantiTect Probe PCR buffer and dNTPs. ROX Mega-Mix Gold RT-PCR master mix contains hot-start Taq, 400μM dNTPs and 6mM $MgCl_2$, in buffer with stabilizer. Both mixes also contain a passive reference ROX dye to provide an internal reference for normalisation of the reporter dye during data analysis to correct for well-to-well fluorescent fluctuations due to variable volumes or concentrations.

Standard curves were generated using a set of relative standards from which unknown samples are quantitated. Serial 1:2 dilutions of cDNA were generated and the concentration of each was quantified using the NanoDrop spectrophotometer (Section 2.4.1.4). The approximate concentrations of relative standards were 25, 50, 100, 200 and 400ng/μl. Dilutions of 50μl aliquots were stored at -20°C if not for immediate use. All quantitative real time PCR reactions were carried out in total volumes of 15μl. A master mix was prepared for each dilution sample containing 5.25μl cDNA standard, 0.6μl Forward primer (10μM), 0.6μl Reverse primer (10μM), 0.3μl TaqMan probe (10μM), 0.75μl rodent endogenous control and 7.5μl ROX MegaMix Gold per sample. The master mix was scaled up to allow samples to be tested in triplicate. 15μl aliquots of the master mix were transferred into 3 wells per cDNA standard onto an optical or fast optical 96-well reaction plate and these were sealed with an optical adhesive cover and spun briefly at 3007g. Samples were subjected to the following thermal cycling program using an ABI Prism 7000 Sequence Detection System or an ABI Prism 7500

Fast Real-Time PCR System;95°C for 15 minutes and then 40 cycles of 95°C for 15 seconds and 60°C for 1 minute.

Unknown mRNA levels in samples were quantified using the following protocol. A master mix was prepared containing 7.5µl ROX Mega-Mix Gold (X2), 0.6µl forward primer (10µM), 0.6µl reverse primer (10µM), 0.3µl labelled fluorogenic TaqMan probe (10µM), 0.45µl rodent endogenous control (20µM) and 4.35µl ddH_2O. The master mix was spun briefly at 16,100g and 13.8µl aliquots per sample were transferred into wells on a fast optical 96-well plate. 1.2µl cDNA (~400ng/µl) was added to each well and one well was designated as a negative control into which DNA was substituted by 1.2µl ddH_2O. The plate was spun briefly at 3007g and subjected to the following thermal cycling program using a ABI Prism 7000 Sequence Detection System or 7500 Fast Real-Time PCR System;95°C for 15 minutes followed by 40 cycles of 95°C for 15 seconds and 60°C for 1 minute.

2.4.5.4 qRT-PCR using SYBR Green

The Power SYBR green PCR master mix contains hot-start AmpliTaq Gold DNA Polymerase and SYBR Green I dye, dNTPs and a passive internal reference ROX dye.

Dissociation curves were generated to check for the absence of primer-dimer products. The dissociation curve identifies the melting temperature (T_m) of the specific product and of any primer dimers produced during the reaction, whose T_m are characteristically lower than that of the target amplicon. Primer dimers are most prevalent in NTC wells and sample wells containing low concentrations of template. Primers were titrated to find the optimum working concentration in the absence of primer-dimers (Table 2.3).

Table 2.3 Primer titrations to optimise reaction efficiency.

Primer Concentration and Direction	50µM Forward	300µM Forward	900µM Forward
50µM Reverse	50/50	300/50	900/50
300µM Reverse	50/300	300/300	900/300
900µM Reverse	50/900	300/900	900/900

As previously described (Section 2.4.5.3), standard curves were generated using a set of relative standards from which unknown samples are quantitated. Reactions were carried

out in total volumes of 15µl. A master mix was prepared for each dilution sample containing 5.25µl cDNA standard, 7.5µl Power SYBR Green PCR Master Mix and forward and reverse primers at their specific optimised concentrations. ddH_2O was added to make up a final reaction volume of 15µl.

Unknown mRNA levels in samples were quantified using the following protocol. Reactions were carried out in a 15µl volume in triplicate. A master mix was prepared containing 1.2µl cDNA (~400ng/µl), 7.5µl Power SYBR Green PCR Mix, appropriate volumes of forward and reverse primer were added in accordance with the titration concentrations and the total reaction volume per sample was made up to 15µl by the addition of ddH_2O. 15µl aliquots per sample were transferred onto a 96-well plate. One well was designated a negative control in which 1.2µl ddH_2O substituted cDNA. The plate was spun briefly at 3007g and subjected to the following thermal cycling program using a ABI Prism 7000 Sequence Detection System or 7500 Fast Real-Time PCR System;95°C for 15 minutes followed by 40 cycles of 95°C for 15 seconds and 60°C for 1 minute followed by a dissociation step of;95°C for 15 seconds, 60°C for 1 minute and 95°C for 15 seconds.

2.4.5.5 Allelic Discrimination

An allelic discrimination assay is a multiplexed, end point assay that detects variants of single nucleic acid sequence. The presence of two primer/probe pairs in each reaction allows genotyping of the two possible variants at a SNP site in a target template sequence. Like qRT-PCR, allelic discrimination relies upon the 5' nuclease activity of a Taq DNA polymerase to cleave probes during PCR. The PCR assay includes a specific, fluorescent dye labelled minor groove binder (MGB) probe for each allele of a sequence variant. A MGB is a small crescent-shaped molecule that stabilizes annealing during probe hybridization by folding into the minor groove of the duplex DNA created between the probe and the target sequence. The probes were labelled with either FAM or VIC fluorescent reporter dyes to differentiate the amplification of each allele. During PCR each probe anneals specifically to complementary sequences between the forward and reverse primer sites. The specific fluorescent signal generated by PCR amplification thus indicates the allele that is present in a given sample. The previously described (Section 2.4.5.3) ROX Mega-Mix Gold PCR master mix was used.

All reactions were carried out in a total volume of 15µl. A master mix was prepared

containing 0.7µl forward primer (10µM), 0.7µl reverse primer (10µM), 0.3µl allele 1 probe (10µM), 0.3µl allele 2 probe (10µM), 7.4µl ROX MegaMix Gold and 4.6µl ddH_2O per sample. The master mix was spun briefly at 16,100g and 14µl aliquots were transferred onto a fast optical 96-well plate. 1µl DNA was added per well and the plate was sealed with an optical adhesive cover and spun briefly at 3007g. Samples were subjected to the following thermal cycling program using the ABI Prism 7000 Sequence Detection System or 7500 Fast Real-Time PCR System;95°C for 15 minutes followed by 40 cycles of 95°C for 15 seconds and 60°C for 1 minute after which the allelic discrimination post-read program was applied which automatically subtracts the baseline fluorescence and assigns allele calls using the amplified data. Data from all allele discrimination assays was analysed using the ABI Prism 7000 Sequence Detection System or the 7500 Fast System Sequence Detection Software Version 1.3.1.

2.4.6 Immunohistochemistry

Immunohistochemistry on paraffin embedded slides was carried out by C. O'Malley and C. Powell and neuropathology was assessed by J. Linehan and Professor Sebastian Brandner.

2.4.6.1 Preparation of Fixed Brain Sections

Brains samples from mice culled by CO_2 asphyxiation were fixed in 10% buffered formal saline overnight and inactivation of prion infectivity was accomplished by incubation in 98% formic acid for 1 hour. Brains were then formalin post-fixed processed and paraffin wax-embedded. Nominal 4µm sections were cut and mounted onto Super-frost slides and allowed to dry overnight at room temperature, and then baked for 2 hours at 60°C.

2.4.6.2 Tissue Staining

Brain sections were de-waxed in three changes of xylene followed by rehydrating in sequential washing in ethanol (100 % x 2, 90% and 70%) and finally in running tap water before each staining protocol.

Haematoxylin and Eosin

Mouse brain sections were stained with haematoxylin and eosin to determine the integrity of the brain tissue, identify areas of the brain and to detect spongiosis, neuronal loss and inflammation. Haematoxylin is a basic dye which has affinity for acidic

structures such as nuclei, staining them deep blue whereas acidic eosin stains cytoplasm pink. Slides were placed in filtered Harris Haematoxylin solution for 5 minutes and then washed briefly in running tap water to removed excess dye and then differentiated in 1% acid alcohol for approximately 30 seconds. Slides were then washed well in running tap water to allow colour to develop. Slides were then stained with Eosin Y solution for 2-3 minutes. Sections were washed well in running tap water and then sequentially dehydrated through a series of alcohols (70 % ethanol, 90 % ethanol, 100 % ethanol) and finally through two changes of xylene. Slides were then mounted in Pertex, a xylene-based mounting medium.

Glial Fibrillary Acidic Protein (GFAP)

Slides were pre-treated by boiling in 1 litre of tris-EDTA-citrate buffer pH7.8 in a microwave for 25 min at 800W power followed by cooling in running cold tap water for 3 minutes. Immunohistochemical staining was performed with anti-GFAP rabbit polyclonal antiserum (1:1000 Dako), to assess the presence of reactive astrocytes, on an automated immunohistochemical staining machine using a diaminobenzidine detection system according to the manufacturers' instructions. Slides were then dehydrated in ethanol, cleaned in xylene and mounted in Pertex.

PrP

Slides were heat pre-treated by boiling in a pressure cooker containing 1.5 litres of tris-EDTA-citrate buffer for 5 minutes at high pressure and 5 minutes at low pressure. Slides were then held under running cold water for 5 minutes and treated with 98% formic acid for a further 5 minutes before washing in running water for 5 minutes to remove excess formic acid. Immunohistochemical staining was performed with anti-prion protein monoclonal antibody ICSM35 (Asante *et al.*, 2002) (1mg/ml concentration) to detect abnormal prion protein accumulation.

Iba-1

The anti-Iba1 polyclonal antibody was used to stain for activated microglia on the Discovery automated immunohistochemical staining machine. Slides were heat pre-treated, in buffer supplied by the manufacturer, at 95°C for 60 minutes and stained at a concentration of 1:250.

3

Chromosome 11 Candidate Genes

3.1 Introduction

The 'long' incubation time mouse strain, CAST/Ei, has a characteristic incubation period of 188±12 days when challenged intracerebrally with Chandler/RML mouse-adapted scrapie (Lloyd *et al.*, 2001). The incubation periods for this prion strain in 'short' incubation time strains is significantly shorter at 108 ± 4 days in NZW/OlaHsd (Lloyd et al., 2001) and 105 ± 4 days in SJL/J (Carlson et al., 1988a; Kingsbury et al., 1983). As previously described (Section 1.2.5), genome-wide mapping studies using Chandler/RML inoculated F2 intercrosses generated between NZW/OlaHsd and CAST/Ei (Lloyd et al., 2001) and also SJL/J and CAST/Ei (Stephenson *et al.*, 2000) have identified extensive significant QTL for prion disease incubation time on chromosomes 2, 9, 11 and 12, in addition to regions of suggestive linkage on chromosomes 6 and 7. Interestingly the chromosome 11 QTL (Figure 3.1), identified in these separate mapping studies, overlap considerably (Figure 3.2). This is a likely consequence of the use of the same prion strain and also the same 'long' incubation time mouse strain, CAST/Ei, in both F2 intercrosses and provides validation of the identification of genuine QTL on this chromosome. The aim of this chapter is the further elucidation of candidate genes within identified QTL which may potentially be controlling prion disease incubation time.

3.2 Candidate Genes

As described above, the identified chromosome 11 prion disease incubation time QTL (Lloyd et al., 2001; Stephenson et al., 2000) are extremely broad and it is necessary to resolve these loci into intervals small enough in which to analyse and identify individual genes contributing towards the incubation time phenotype. Further characterisation of chromosome 11 QTL regions by fine mapping is described later in Chapter 5. In addition to this analysis, several candidate genes (Table 3.1), of potential functional relevance to prion disease were assessed to identify sequence variants potentially responsible for the observed variation in phenotype between 'short' and 'long' incubation time strains. Candidate gene locations within the QTL were determined using NCBI, Ensembl and UCSC gene annotation databases (Section 2.1.5). All candidate genes mapped within 32Mb of the peaks of linkage.

Figure 3.1 Chromosome 11 LOD score plots for Chandler/RML incubation periods.
A) NZW/OlsHsd x CAST/Ei F2 intercross and (B) SJL/J x CAST/Ei F2 intercross. The x axes display relative positions of markers along the chromosome in cM. Dotted lines intersecting the y axis in represents a statistical significance threshold of (A) 4.3 and (B) suggestive (2.39), significant (3.97) and highly significant (5.99) linkage. Figures adapted from Lloyd *et al.*, 2001 (A) and Stephenson *et al.*, 2000 (B).

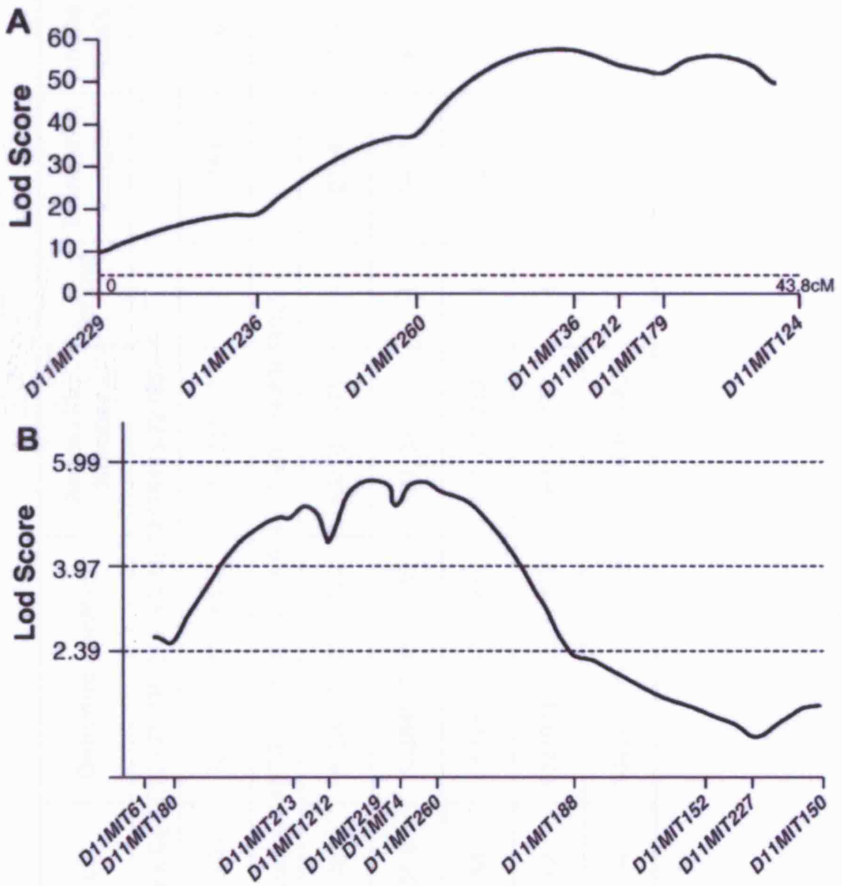

Figure 3.2 Schematic of overlapping chromosome 11 QTL.
The horizontal red and blue lines signify regions of linkage identified by Lloyd *et al.*, 2001 and Stephenson *et al.*, 2000, respectively. Flanking markers, genomic location, size and peaks of linkage for both regions are labelled in corresponding colours.

Table 3.1 Chromosome 11 candidate gene positions.
Peaks of linkage are detailed in bold.

Gene Name (Symbol)	cM	Genomic Location	Accession Number	Strand	Transcript Length	Amino Acids	Exons
SJL/J x CAST/Ei - *D11Mit219* (43cM) 72135165-72135296							
Vitronectin (*Vtn*)	45.09	78315315-78318518	NM_011707	1	1743	478	8
NZW/OlaHsd x CAST/Ei - *D11Mit36* (47.6cM) 83658789-83659021							
Myeloperoxidase (*Mpo*)	49	87609776-87620592	NM_010824	1	2734	718	14
Nerve Growth Factor Receptor (*Ngfr*)	55.6	95384908-95403788	NM_033217	-1	3409	427	6
Cyclin Dependent Kinase 5 Regulatory Associated Protein 3 (*Cdk5rap3*)	58	96724147-96732289	NM_030248	-1	1509	502	13
Glial Fibrillary Acidic Protein (Gfap)	62	102703437-102713221	NM_010277	-1	2637	430	9
Microtubule-associated Protein Tau (*Mapt*)	64	104047526-104148186	NM_001038609	1	6296	733	14

Vitronectin (Vtn)

VTN also known as serum spreading factor, is an extracellular matrix protein expressed in the central nervous system during development (Preissner, 1991; Seiffert *et al.*, 1995) and has been shown to support proliferation and differentiation of cultured neurons (Martinez-Morales *et al.*, 1995). VTN may be functionally relevant to prion disease as recently it has been shown to interact, at residues 307-320, with PrP^C (Hajj *et al.*, 2007). This candidate maps within 3cM of the peaks of linkage identified within overlapping QTL for prion disease incubation time (Lloyd et al., 2001; Stephenson et al., 2000) (Table 3.1).

Myeloperoxidase (Mpo)

MPO is a heme protein expressed in phagocytic cells such as neutrophils, monocytes and microglia (Klebanoff, 2005). MPO is present in the human brain and also in tissue showing AD neuropathology where its increased expression is predominantly localised with amyloid plaques and also in granule and pyramidal neurons of the hippocampus as well as in activated microglia (Green *et al.*, 2004; Reynolds *et al.*, 1999). This increased expression has been suggested to contribute towards the oxidative stress implicated in the pathogenesis of AD. Both prion disease and AD are neurodegenerative diseases and may have common biochemical pathways. Therefore, highlighting pathways involved in AD may potentially indicate those also important in prion disease. An association between AD and a functional *MPO* promoter region polymorphism has been established (Crawford *et al.*, 2001; Reynolds *et al.*, 1999) which interacts with another polymorphism in alpha(2)-macroglobin (A2M) and is known to increase the risk of the development of sporadic AD in southern Italy (Zappia *et al.*, 2004). Both genes are involved in molecular pathways leading to beta-amyloid deposition (Du *et al.*, 1998; Smith *et al.*, 1998). These findings make *Mpo* an interesting modifier candidate gene for analysis since prion disease is also characterised by the deposition of amyloid plaques which can contain insoluble aggregates of prion protein. This candidate maps within 2cM of the QTL peak of linkage identified by the NZW/OlaHsd x CAST/Ei F2 intercross (Lloyd et al., 2001) (Table 3.1).

p75 Low Affinity Nerve Growth Factor Receptor (Ngfr or $p75^{NTR}$)

NGFR belongs to the family of death receptors which trigger apoptosis (Nagata, 1997). A prion protein fragment, PrP-(106-126), has been shown to cause neuronal death through binding to the extracellular region of NGFR, inducing the signalling function of

the intracytoplasmic region of the receptor and activating caspase-8, consequently leading to the production of oxidant species (Della-Bianca *et al.*, 2001). The mediation of PrP-related neuronal death by human NGFR suggests that this gene may be a potential modifier of prion disease incubation time.

Cyclin Dependent Kinase 5 Regulatory Associated Protein 3 (Cdk5rap3)

CDK5RAP3 is a potential regulator of Cyclin Dependent Kinase 5 (CDK5), a proline-directed serine/threonine kinase, which is highly expressed in the brain and is associated specifically with neuronal development and function (Gilmore *et al.*, 1998). CDK5 has also been implicated in several murine models of neurodegenerative disease including Niemann-Pick type C, Parkinson's disease and Amyotrophic Lateral Sclerosis (ALS) (Bu *et al.*, 2002; Nguyen *et al.*, 2001; Smith *et al.*, 2003). The potential role of CDK5RAP3 in pathways involved in neurodegeneration highlights it as a possible modifier of prion disease incubation time.

Glial Fibrillary Acidic Protein (Gfap)

GFAP is the principal component of glial filaments, 8-10 nm fibres that constitute the cell cytoskeleton alongside microtubule and actin microfilaments, and represents a specific marker for astroglial cells in the mammalian nervous system (Bignami *et al.*, 1972). A major pathological hallmark of prion diseases is astrogliosis in response to the presence of PrP^{Sc} or as a response to neuronal damage. High expression of *Gfap* mRNA is observed at sites of astrogliosis in prion disease (Manuelidis *et al.*, 1987). *Gfap* has also been shown to be differentially expressed between scrapie-infected golden Syrian hamsters and age-matched controls using subtractive cDNA cloning (Duguid *et al.*, 1988). GFAP is not thought to have a causative effect in prion disease (Prusiner, 1998) and primarily indicates associated astrogliosis. However, its involvement in prion pathogenesis and its close genomic location, approximately 14-19cM, to the peaks of linkage identified on chromosome 11 makes it a potentially interesting modifier candidate gene for analysis.

Microtubule-associated Protein Tau (Mapt)

MAPT or TAU is a member of the microtubule-associated protein (MAP) family expressed in neurons, oligodendrocytes and astrocytes which promote microtubule assembly and stability by binding to tubulin (Binder *et al.*, 1985; LoPresti *et al.*, 1995). The aggregation of MAPT into paired helical filaments is a hallmark of several

neurodegenerative diseases, including AD (Goedert *et al.*, 1988), highlighting this gene as a potential candidate for prion disease. A recent study has confirmed MAPT pathology as a consistent feature of vCJD identifying the presence of phosphorylated TAU immunoreactive structures in the brains of vCJD patients and in also in a mouse model of vCJD (Giaccone *et al.*, 2007).

Monocyte Chemoattractant Protein 1 (Mcp1)

An additional chromosome 11 candidate, MCP1 has recently been shown to have a role in the murine ME7 mouse model of prion disease (Felton *et al.*, 2005). A more detailed assessment of this candidate is described in Chapter 4.

Candidate gene information was obtained from Ensembl and UCSC mouse genome sequence annotation databases (Section 2.1.5). UCSC and Ensembl known protein-coding genes are based on protein data from the UniProt (SWISS-PROT and TrEMBL) protein database and mRNA data from the NCBI reference sequences collection (RefSeq) and GenBank. Ensembl and UCSC also detail RIKEN gene sequences for predicted genes which are obtained from the RIKEN Mouse Gene Encyclopaedia Project (Kawai *et al.*, 2001).

3.3 Candidate Gene Sequence Polymorphisms

Sequence analysis of candidate genes was undertaken to identify polymorphisms between 'short' and 'long' incubation time mouse strains which may be indicative of genetic differences controlling the incubation time phenotype (Figure 3.3). Sequence information was obtained from NCBI, Ensembl and UCSC gene annotation databases (Section 2.1.5) to carry out oligonucleotide primer design (Section 2.4.2.1) for PCR (Section 2.4.2.2) and sequencing (Section 2.4.3) in SJL/J, NZW/OlaHsd and CAST/Ei mouse strains. Genomic sequence of potential functional significance such as protein coding regions or motifs controlling gene expression were prioritised for analysis. In addition, ~10bp of intronic sequence directly flanking exons was analysed to identify potential splice site polymorphisms. Characterised promoter regions for *Mapt* (Gao *et al.*, 2005) and *Vtn* (Miyamoto *et al.*, 1998; Seiffert *et al.*, 1996) were analysed. Putative promoter motifs were determined for *Ngfr* and *Cdk5rap3* using WWW Promoter Scan software (Section 2.1.5) which predicts promoter regions based on scoring homologies with putative eukaryotic Pol II promoter sequences including TATA-box, cap signal, CCAAT- and GC-box sequences (Prestridge, 1995). 2kb of genomic database sequence

Figure 3.3 Example comparision of electrophorogram sequence showing a SNP between traces from different mouse strains.
The black arrow and boxes indicate the position of a SNP between sequences.

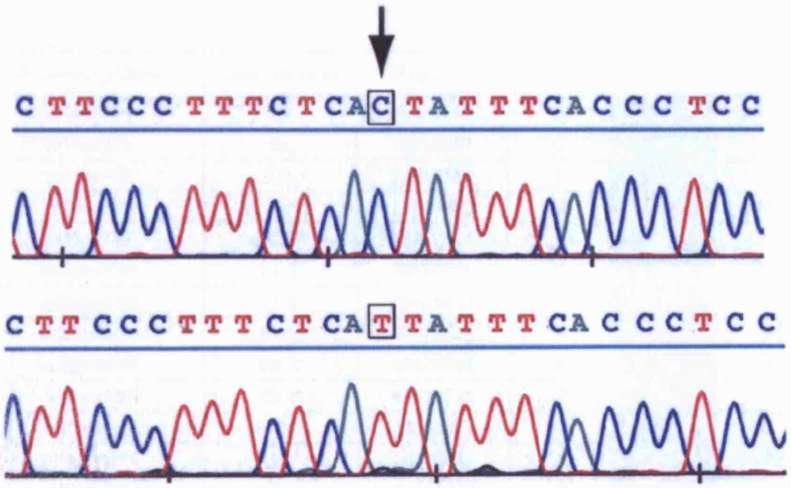

upstream of candidate gene transcription start sites was analysed using this software. Details of PCR primer sequences and conditions for use are listed in Appendix 2.1. Sequence polymorphism data is listed in Table 3.2.

Perhaps the most interesting polymorphisms are those that have common alleles in the 'short' incubation time strains, SJL/J and NZW/OlaHsd, and contrast with the 'long' incubation time strain CAST/Ei. The majority of polymorphisms (53/91) followed this pattern (Table 3.2). This segregation may indicate genetic variants important in controlling the phenotype in both F2 intercrosses used to identify chromosome 11 incubation time QTL (Lloyd et al., 2001; Stephenson et al., 2000).

3.4 Potential Functional Properties of Observed Polymorphisms

It is difficult to predict the exact functional significance of polymorphisms identified between mouse strains but the natural variation observed may potentially contribute towards prion disease incubation time. To further characterise those polymorphisms potentially making the most significant contribution the possible functional effects of each were considered.

Polymorphisms located in predicted promoter regions have the potential to produce variation in gene expression. Differential gene expression is examined in Section 3.5.

Table 3.2 Chromosome 11 candidate gene sequence polymorphisms.
Ex=Exonic, Pro=Promoter, 3'=3'UTR, 5'=5'UTR and Intr=Intronic. Nonsynonymous polymorphisms are indicated by amino acid abbreviations flanking the relevant codon number. Shading illustrates polymorphism SDP.

Polymorphism	Description	Position	SJL	CAST	NZW
m*Vtnx*1#1	Ex	78315553	C	T	C
m*Vtnx*1#2	Ex	78315562	C	A	C
m*Vtnx*1#3	F7L	78315563	T	C	T
m*Vtnx*5#1	Ex	78316725	G	A	G
m*Vtnx*7#1	N337D	78317801	A	G	A
m*Mpox*5'#1	Ex 5'	88570658	C	T	C
m*Mpox*5'#2	Ex 5'	88570689	C	T	C
m*Mpox*5'#3	Ex 5'	88570693	T	C	T
m*Mpox*5'#4	Ex 5'	88570704	A	G	A
m*Mpox*5'#5	Ex 5'	88570712	T	C	T
m*Mpox*4#1	A121S	88572587	G	T	G
m*Mpox*5#1	Ex	88572822	T	C	T
m*Mpox*5#2	Ex	88572843	C	T	C
m*Mpox*5#3	S182A	88572865	T	G	T
m*Mpox*5#4	Ex	88572876	T	C	T
m*Mpox*5#5	Ex	88572888	A	C	A
m*Mpox*6#1	Ex	88573019	T	C	T
m*Mpox*6#2	Ex	88573061	C	T	C
m*Mpox*6#3	Ex	88573112	C	T	C
m*Mpox*6#4	Ex	88573142	C	G	C
m*Mpox*6#5	Ex	88573169	C	T	C
m*Mpox*7#1	Ex	88574101	T	C	T
m*Mpox*7#2	Q280P	88574130	A	C	A
m*Mpox*7#3	Ex	88574233	T	C	T
m*Mpox*7#4	Ex	88574236	G	A	G
m*Mpox*9#1	Ex	88577870	G	A	G
m*Mpox*9#2	Ex	88577927	T	C	T
m*Mpox*9#3	Ex	88578050	T	C	T
m*Mpox*11#1	Ex	88579327	T	C	T
m*Mpox*11#2	Ex	88579441	G	A	G
m*Mpox*11#3	Ex	88579450	A	G	A
m*Mpox*12#1	Ex	88580348	C	T	C
m*Ngfr*3'#3	Ex 3'	95386362	G	A	G
m*Ngfr*3'#2	Ex 3'	95386369	C	C	T
m*Ngfr*3'#1	Ex 3'	95386453	T	T	A
m*Ngfrx*5#1	G329D	95387915	G	A	G
m*Ngfrx*4#2	Ex	95390409	A	G	G
m*Ngfrx*4#1	I227V	95390432	G	A	A
m*Ngfrx*3#1	Ex	95394176	G	A	G
m*Ngfr*Pro#3	Pro	95403715	A	C	C
m*Ngfr*Pro#2	Pro	95403727	G	A	G
m*Ngfr*Pro#1	Pro	95403749	G	C	G
m*Cdk5rap3* 3'#6	Ex 3'	96723933	T	C	C
m*Cdk5rap3* 3'#5	Ex 3'	96723981	C	C	T
m*Cdk5rap3* 3'#4	Ex 3'	96724048	C	C	T
m*Cdk5rap3* 3'#3	Ex 3'	96724049	G	G	A

Polymorphism	Description	Position	SJL	CAST	NZW
m*Cdk5rap3* 3'#2	Ex 3'	96724119	C	C	T
m*Cdk5rap3* 3'#1	Ex 3'	96724146	C	T	C
m*Cdk5rap3*x12#2	T400M	96724876	T	C	C
m*Cdk5rap3*x12#1	Ex	96724962	T	T	C
m*Cdk5rap3*x9#1	V281I	96727223	G	G	A
m*Cdk5rap3*x8#1	Ex	96727684	A	G	G
m*Cdk5rap3*x7#2	A190T	96728042	G	G	A
m*Cdk5rap3*x7#1	Ex	96728052	A	G	G
m*Cdk5rap3*x6#3	Ex	96728316	T	C	C
m*Cdk5rap3*x6#2	Ex	96728328	C	T	T
m*Cdk5rap3*x6#1	Ex	96728370	T	C	C
m*Cdk5rap3*x3#1	Ex	96729810	T	T	C
m*Cdk5rap3*Pro#4	Pro	96732675	G	C	C
m*Cdk5rap3*Pro#3	Pro	96732761	T	T	C
m*Cdk5rap3*Pro#2	Pro	96732815	A	A	C
m*Cdk5rap3*Pro#1	Pro	96732855	C	C	T
m*Gfap*3'#7	Ex 3'	102703752	G	T	T
m*Gfap*3'#6	Ex 3'	102703871	C	T	C
m*Gfap*3'#5	Ex 3'	102703906	T	C	C
m*Gfap*3'#4	Ex 3'	102703922	A	A	T
m*Gfap*3'#3	Ex 3'	102703933	C	A	C
m*Gfap*3'#2	Ex 3'	102703955	A	A	G
m*Gfap*3'#1	Ex 3'	102704008	C	G	C
m*Gfapx*4#3	Ex	102710522	C	C	T
m*Gfapx*4#2	Ex	102710549	G	T	G
m*Gfapx*4#1	Ex	102710585	C	C	T
m*Gfapx*3#3	Intr	102711555	C	C	T
m*Gfapx*3#2	Ex	102711632	T	A	T
m*Gfapx*3#1	Intr	102711661	C	T	T
m*Gfapx*2#1	Ex	102711849	G	G	A
m*Gfapx*1#4	F141L	102712787	T	C	C
m*Gfapx*1#3	Ex	102712917	A	A	G
m*Gfapx*1#2	Ex	102713016	G	A	G
m*Gfapx*1#1	Ex	102713102	T	C	C
m*Mapt*Pro#1	Pro	104047567	T	G	G
m*Maptx*5#1	Ex	104110965	C	T	C
m*Maptx*5#2	Ex	104110977	G	A	G
m*Maptx*5#3	Ex	104110989	C	T	C
m*Maptx*5#4	A50S	104110996	G	T	G
m*Maptx*8#1	Ex	104126432	G	A	G
m*Maptx*8#2	Ex	104126441	A	T	A
m*Maptx*8#3	Ex	104126453	A	G	A
m*Maptx*8#4	Ex	104126543	T	A	T
m*Maptx*8#5	Ex	104126549	C	G	C
m*Maptx*9#1	Ex	104134309	T	C	C

Polymorphisms in 5'- and 3'-untranslated (UTR) regions may also have an effect on gene expression as these are known to contain important regulatory regions. The Transcription Factor Search (TFSEARCH) program (Section 2.1.5) which searches highly correlated sequence fragments against the transcription factor binding site database, TRANSFAC (Heinemeyer *et al.*, 1999; Heinemeyer *et al.*, 1998), was also used to assess the location of predicted transcription factor binding sites in 5'- and 3'UTR regions.

Nonsynonymous polymorphisms may have potential functional significance especially if the amino acid changes they produce occur in highly conserved residues within the functional domains of a protein. When amino acid residues are highly conserved across several distantly related species homologs it is indicative of potential functional constraint since preservation of the residue has occurred throughout evolution. Conserved residues usually reside in important functional domains where changes in the physicochemical properties of residues are not well tolerated. Nonsynonymous polymorphisms producing amino acid substitutions in such important domain regions may affect protein function and activity. Conformational changes in tertiary structure may also be brought about by substitutions at certain residues where a change in physicochemical property, such as hydrophobicity to hydrophillicity, may cause the protein to fold in alternate ways perhaps affecting the function of important active regions. The ClustalW sequence alignment software program (Section 2.1.5) was utilised to compare homolog protein sequence and identify amino acid similarities and differences for each of the candidate genes where nonsynonymous changes were observed. The following symbols *, : and . denote identical, conserved and semi-conserved amino acids, respectively within an alignment of homologs. The absence of a symbol denotes a lack of conservation for the residue in question.

3.4.1 Promoter Polymorphisms

Sequence analysis of *Vtn* did not identify polymorphisms in two characterised promoter regions (Miyamoto et al., 1998; Seiffert et al., 1996) (Table 3.2). A polymorphism located within a characterised promoter region for *Mapt* (m*Mapt*Pro#1) did not occur in known AP-2 binding sites (Gao et al., 2005). Furthermore, polymorphisms located in putative promoter regions for *Cdk5rap3* (m*Cdk5rap3*Pro#1-4) and *Ngfr* (m*Ngfr*Pro#1-3), did not occur in any transcription factor binding sites within these regions as determined by WWW Promoter Scan software (Section 2.1.5).

3.4.2 5' and 3'UTR Polymorphisms

A 3'UTR polymorphism in *Ngfr* (m*Ngfr*3'#1), between NZW/OlaHsd and CAST/Ei, and in *Gfap* (m*Gfap*3'#6), between 'short' and 'long' incubation time strains occurs in putative *Gata-1* transcription factor binding site (Figure 3.4). *Gata-1* belongs to a family of transcription factors which are essential for normal erythroid development (Pevny *et al.*, 1995). The same *Gfap* 3'UTR polymorphism is also predicted to be located within another erythrocyte-specific transcription factor binding site, namely *Nf-e2* (Figure 3.5). *Nf-e2* is an erythroid-specific nuclear factor that binds AP-1-like recognition sites to control the expression of globin genes (Andrews *et al.*, 1993).

Figure 3.4 *Ngfr* and *Gfap* 3'UTR polymorphisms in putative *Gata-1* binding sites.
The sequence comprising the putative transcription factor binding site is illustrated by a broken arrow and the position of the polymorphism and its alternative nucleotide bases are highlighted in red.

Figure 3.5 *Gfap* 3'UTR polymorphism in a putative *Nf-e2* binding site.
The sequence comprising the putative transcription factor binding site is illustrated by a broken arrow and the position of the polymorphism and its alternative nucleotide bases are highlighted in red.

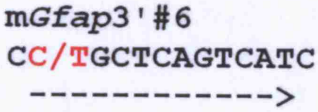

Mpo (m*Mpo*x5'#1-5) and *Cdk5rap3* (m*Cdk5rap3* 3'#1-6) 5' and 3'UTR polymorphisms were not assessed as being located within any putative transcription factor binding sites.

3.4.3 Intronic Polymorphisms

Two intronic polymorphisms identified in *Gfap* (m*Gfap*x3#1 and m*Gfap*x3#3) (Table 3.2) are not located in intronic 5' or 3' splicing signal sequences and are therefore unlikely to effect splicing of this gene between mouse strains.

3.4.4 Nonsynonymous Polymorphisms

Twelve nonsynonymous candidate gene polymorphisms were identified between SJL/J,

NZW/OlaHsd and CAST/Ei mouse strains (Table 3.2). For seven of these substitutions, amino acids segregated in the 'short' incubation time strain contrasting with that of the 'long' incubation time strain.

Vtn

Two *Vtn* polymorphisms cause amino acid substitutions between the 'short' and 'long' incubation time strains at codons 7 (m*Vtn*x1#3) and 337 (m*Vtn*x7#1) (Table 3.2). These codons are located outside of those VTN residues critical for interaction with cellular prion protein (PrP^C) (Hajj *et al.*, 2007). Codon 7 resides in the signal peptide region of the VTN precursor protein, as determined by UniProt (SWISS-PROT and TrEMBL) protein database, and is therefore cleaved to generate the functional mature VTN protein. SJL/J and NZW/OlaHsd strains code for a phenylalanine residue at codon 7 whereas a leucine residue is seen at this position in CAST/Ei. Codon 7 is conserved throughout the homologs (Figure 3.6) featured suggesting potential evolutionary significance although mouse and rat differ from the other homologs suggesting that a leucine residue at this position is not essential for protein functionality. Phenylalanine and leucine are both non-polar hydrophobic residues. Due to the common physicochemical properties of the alternate amino acids occurring at this codon substantial structural changes in the protein are unlikely.

SJL/J and NZW/OlaHsd also share the same residue, asparagine, at codon 337 contrasting with CAST/Ei which has an aspartic acid residue at this position (Table 3.2). Codon 337 is also conserved between the homologs shown (Figure 3.6) and occurs in the C-terminal region of VTN in a plasminogen-binding site (Hajj *et al.*, 2007). Plasminogen is the inactive precursor of plasmin, a potent serine protease involved in the dissolution of fibrin blood clots. The role of plasminogen in the propagation of scrapie has been investigated but was found to have no major effect on the survival of the scrapie infected mice (Salmona *et al.*, 2005). Since asparagine and aspartic acid share physicochemical properties, both being small polar amino acids, they are unlikely to causes changes in protein tertiary structure which would affect the activity of this binding site.

Mpo

Three amino acid substitutions occur between the 'short' and 'long' incubation time strains in MPO occurring at codons 121 (m*Mpo*x4#1), 182 (m*Mpo*x5#3) and 280

Figure 3.6 VTN homolog protein sequence alignment.
Codons 7 and 337 are highlighted in red and the amino acid substitution observed in mouse (C57BL/6J) is labelled above.

```
                                F7L
Mus musculus                [1] MAPLRPF-FILAL [12]
Rattus norvegicus           [1] MASLRPF-FILAL [12]
Homo sapiens                [1] MAPLRPL-LILAL [12]
Pan troglodytes             [1] MAPLRPL-LILAL [12]
Macaca mulatta              [1] MAPLRPL-LMLAL [12]
Bos taurus                  [1] MTSLRPL-LMLAL [12]
Canis familiaris            [1] MAFPRPL-LVLAL [12]
Monodelphis domestica       [1] RRDMSPLSLLVIL [13]
                                *: ::: *

                                N337D
Mus musculus              [329] REPQFISRNWHGVPGKV [345]
Rattus norvegicus         [340] KGPQFISRDWHGVPGKV [356]
Homo sapiens              [330] RQPQFISRDWHGVPGQV [346]
Pan troglodytes           [330] RQPQFISRDWHGVPGQV [346]
Macaca mulatta            [330] RQPQLISRDWHGVPGQV [346]
Bos taurus                [326] GQPQLISRNWFGLPGRL [342]
Canis familiaris          [323] GEPGFISQDWPGLPRQV [339]
Monodelphis domestica     [320] SGPWFISQDWHGVPNRV [336]
                                :**::* *:* ::
```

(m*Mpo*x7#2) which are identical throughout all the homologs featured in the alignment implying significant evolutionary constraint (Table 3.2 and Figure 3.7). Codon 121 is located in the MPO propeptide domain which in human MPO has been shown to have a critical role in late processing of the protein and also in targeting it for storage in granules (Andersson *et al.*, 1998). A change from an alanine residue in SJL/J and NZW/OlaHsd to serine in CAST/Ei is observed which are both small amino acids but differ in polarity which may affect the direction in which this residue prefers to face in terms of its aqueous environment. Codon 182 and 280 are situated in the 14-kDa light and 57-kDa heavy chains of MPO, respectively, as determined by UniProt (SWISS-PROT and TrEMBL) protein database. Mature MPO is a tetramer composed of two glycosylated heavy subunits and two unglycosylated light subunits linked together by a disulphide bond (Nauseef *et al.*, 1988). MPO requires heme as its co-factor for enzymatic activity and each heavy chain subunit carries a covalently bound heme prosthetic group (Andrews and Krinsky, 1981) and therefore an amino acid substitution occurring here may have important implications in terms of the function of MPO. At codon 182 SJL/J and NZW/OlaHsd code for a serine residue and CAST/Ei codes for an alanine residue thus the same residue property changes are seen here as in codon 121. At codon 280 a glutamine residue is coded for in SJL/J and NZW/OlaHsd whereas a proline residue is observed at this position in CAST/Ei. Glutamine is a hydrophilic

Figure 3.7 MPO homolog protein sequence alignment.
Codons 121, 182 and 280 are highlighted in red and the amino acid substitution observed in mouse (C57BL/6J) is labelled above.

```
                                  A121S
Homo sapiens          [137] PFNVTDVLTPAQLNVLSKSSG [157]
Pan troglodytes       [137] PFNVTDVLTPAQLNVLSKSSG [157]
Macaca mulatta        [137] SFNVTDVLTPAQLNLLSKSSG [157]
Mus musculus          [111] PFNVTDVLTPAQLNLLSVSSG [131]
Rattus norvegicus     [111] PFNVTDVLTPAQLNLLSVSSG [131]
Bos taurus            [123] RFNVTDVLTPAQLNLLSKTSG [143]
                            ************:** :**
                                  S182A
Homo sapiens          [198] WLPAEYEDGFSLPYGWTPGVK [218]
Pan troglodytes       [230] WLPAEYEDGFSLPYGWTPGVK [250]
Macaca mulatta        [229] WLPAEYEDGFSLPYGWTPGVK [249]
Mus musculus          [172] WLPAEYEDGVSMPFGWTPGVN [192]
Rattus norvegicus     [172] WLPAEYEDGISLPFGWTPKVN [192]
Bos taurus            [215] WLPAEYEDGFSLPFGWTPRVK [235]
                            *********.*:*:**** *:
                                  Q280P
Homo sapiens          [296] IPPNDPRIKNQADCIPFFRSC [316]
Pan troglodytes       [328] IPPNDPRIKNQADCIPFFRSC [348]
Macaca mulatta        [327] IPPNDPRIKNQADCIPFFRSC [347]
Mus musculus          [270] IPPNDPRIKNQKDCIPFFRSC [290]
Rattus norvegicus     [270] IPPNDPRIKNQKDCIPFFRSC [290]
Bos taurus            [313] IPPNDPRIKNQQDCIPFFRSS [333]
                            ********** ********.
```

uncharged polar residue whereas proline is a hydrophobic non-polar residue so the difference in the preferences of these amino acids in facing towards or away from aqueous surroundings may have possible implications for tertiary protein structure and heme-binding activity.

Ngfr

Two nonsynonymous polymorphisms in *Ngfr* cause amino acid substitutions at codons 227 (m*Ngfr*x4#1) and 329 (m*Ngfr*x5#1) which are not well conserved residues (Table 3.2 and Figure 3.8) and are located outside important functional domains (Kanning *et al.*, 2003) including the cysteine-rich repeat motifs in the extracellular domain which, in human NGFR, have been implicated in meditating PrP-(106-126) neuronal damage (Della-Bianca et al., 2001).

Cdk5rap3

Functional domain regions in CDK5RAP3 are not well characterised and therefore it is

Figure 3.8 NGFR homolog protein sequence alignment.
Codons 227 and 329 are highlighted in red and the amino acid substitution observed in mouse (C57BL/6J) is labelled above.

```
                                    I227V
Mus musculus                [218] PEAPPERDLIASTVADTVT [236]
Rattus norvegicus           [216] PEVPPEQDLVPSTVADMVT [234]
Homo sapiens                [215] PEAPPEQDLIASTVAGVVT [233]
Bos taurus                  [215] PEAPPEQDLIASTVAGVVT [233]
Pan troglodytes             [215] PEAPPEQDLIASTVAGVVT [233]
Monodelphis domestica       [217] PPEPPEPEAEASTVADVVT [235]
                                  *  *** :  .****. **
                                    G329D
Mus musculus                [320] QQTHTQTASGQALKGDGNL [338]
Rattus norvegicus           [318] QQTHTQTASGQALKGDGNL [336]
Homo sapiens                [317] QQPHTQTASGQALKGDGGL [335]
Bos taurus                  [317] QQPHTQTASGQALKGDGGL [335]
Pan troglodytes             [317] QQPHTQTASGQALKGDGGL [335]
Monodelphis domestica       [319] QQPQTQTAQVQALKGDGGL [337]
                                  **.:****. *******.*
```

difficult to ascertain the significance of the amino acids substitutions observed between mouse strains in this candidate gene (Table 3.2). The first occurs in conserved codon 190 (m*Cdk5rap3*x7#2) (Figure 3.9) at which SJL/J and CAST/Ei code for an alanine residue and NZW/OlaHsd codes for a threonine. Alanine and threonine are both small amino acids and thus a change in residue size is not observed. However, alanine is a non-polar, hydrophobic molecule whereas threonine has polar physicochemical properties which may be have implications for tertiary protein structure as the preferences of these residues to be facing towards or away from aqueous surroundings differ. At codon 281 (m*Cdk5rap3*x9#1) a valine residue is seen in SJL/J and CAST/Ei whereas NZW/OlaHsd codes for isoleucine. This residue shows no conservation between the homolog sequences (Figure 3.9) and as both amino acids are aliphatic and non-polar this substitution would produce minimal changes in physicochemical property. The final amino acid polymorphism is seen at codon 400 (m*Cdk5rap3*x12#2) where SJL/J codes for polar threonine, and NZW/OlaHsd and CAST/Ei strains code for non-polar methionine. This residue is semi-conserved and therefore the changes in polarity observed may have implications for protein structure and function reliant upon the positioning of this residue facing towards the inwardly folded regions of the protein or towards its aqueous surroundings.

Gfap

A single nonsynonymous polymorphism was identified in *Gfap* between mouse strains

Figure 3.9 CDK5RAP3 homolog protein sequence alignment.
Codons 190, 281 and 400 are highlighted in red and the amino acid substitution observed in mouse (C57BL/6J) is labelled above.

```
                                    A190T
Macaca mulatta              [93]  ALVKDLPSQLAEIGAAAQQSL [113]
Homo sapiens                [182] ALVKDLPSQLAEIGAAAQQSL [202]
Pan troglodytes             [182] ALVKDLPSQLAEIGAAAQQSL [202]
Gallus gallus               [289] ALVKDLPSQLAEIGAAAQQSL [309]
Mus musculus                [180] ALVKDLPSQLAEIGAGAQS-L [199]
Monodelphis domestica       [181] ALVKDLPSLLTETGAKVES-L [200]
                                  ******** *:* ** .:. *
                                    V281I
Macaca mulatta              [188] AVSEGTDSGISAEAAGIDWGV [208]
Homo sapiens                [277] AVSEGTDSGISAEAAGIDWGI [297]
Pan troglodytes             [277] AVSEGTDSGISAEAAGIDWGI [297]
Gallus gallus               [384] AVSEGTDSGISAEAAGIDWGI [404]
Mus musculus                [274] AVSD---SGIVAETPGIDWGI [291]
Monodelphis domestica       [275] STSEGINYGTSAETDEIDWGI [295]
                                  :.*:    *  **:  ****:
                                    T400M
Macaca mulatta              [306] TKEKMVTMVSVLDNLIGKLTN [326]
Homo sapiens                [395] TKEKMVTMVSVLEDLIGKLTS [415]
Pan troglodytes             [395] TKEKMVTMVSVLEDLIGKLTS [415]
Gallus gallus               [502] TKEKMVTMVSVLEDLIGKLTS [522]
Mus musculus                [390] TKEKMLSLVSTLQQLIGRLTS [410]
Monodelphis domestica       [394] TKARVVAMVSALQDLIGQLTS [414]
                                  ** ::::::**.*::***:**.
```

(Table 3.2). At codon 141 (m*Gfap*x1#4) in *Gfap* SJL/J codes for phenylalanine whereas NZW/OlaHsd and CAST/Ei code for leucine (Table 3.2). This codon is situated in the large rod-like domain of several α-helices in GFAP which are known to be extensively conserved (Geisler *et al.*, 1982). The hydrophobic backbone of these helices is proposed to cause aggregation of monomers into coiled coils which then polymerize into filaments. Phenylalanine and leucine are both non-polar amino acids so no change in polarity occurs at this conserved residue (Figure 3.10) but a difference in structure is seen between the two residues as phenylalanine is an aromatic amino acid whereas leucine is aliphatic.

Mapt

A single nonsynonymous polymorphism was identified in *Mapt* (m*Mapt*x5#4) causing an amino acid change at codon 50 (Table 3.2). SJL/J and NZW/OlaHsd code for alanine at this residue whilst CAST/Ei codes for serine. Alanine and serine residues are both small amino acids but differ in polarity which may affect the direction in which this residue prefers to face, towards the aqueous surroundings of the protein or its

Figure 3.10 GFAP homolog protein sequence alignment.
Codons 141 are highlighted in red and the amino acid substitution observed in mouse (C57BL/6J) is labelled above.

```
                                    F141L
Homo sapiens                [134] SARLEVERDNLAQDLATVRQK [154]
Macaca mulatta              [134] SARLEVERDNLAQDLGTVRQK [154]
Pan troglodytes             [134] SARLEVERDNLAQDLATVRQK [154]
Bos taurus                  [130] SARLEVERDNLAQDLGTLRQK [150]
Mus musculus                [131] SARLEVERDNFAQDLGTLRQK [151]
Rattus norvegicus           [132] SARLEVERDNLTQDLGTLRQK [152]
Monodelphis domestica       [131] SARLEIERDNLAEDLTTLRQK [151]
Danio rerio                 [146] KARLEIERDNLASDLGTLKQR [166]
                                  .****:****::.** *::*:
```

inwardly folded areas. Codon 50 is conserved across the homolog sequences featured (Figure 3.11) and located in the variable N-terminal domain of MAPT whose function is not well understood but has been proposed to be involved in microtubule bundling (Kanai *et al.*, 1992) and in binding to different antigens or ligands (Himmler *et al.*, 1989). Codon 50 is located outside of three important 18 amino acid repeated sequences responsible for the central role of MAPT in tubulin binding (Himmler et al., 1989; Lee *et al.*, 1989) and the polymerisation of tubulin into microtubules (Ennulat *et al.*, 1989).

Figure 3.11 MAPT homolog protein sequence alignment.
Codon 50 is highlighted in red and the amino acid substitution observed in mouse (C57BL/6J) is labelled above.

```
                                S50A
Mus musculus                [44] GAEEP----GSETS--DAKST [58]
Rattus norvegicus           [44] GSEEP----GSETS--DAKST [58]
Homo sapiens                [55] GSEEP----GSETS--DAKST [69]
Pan troglodytes             [55] GSEEP----GSETS--DAKST [69]
Bos taurus                  [44] GSEEP----GSETS--DAKST [58]
Monodelphis domestica       [45] AISEALRHYGAEAIGQDAINM [65]
                                  . .*.    *:*:   ** .
```

3.5 Gene Expression

Another means by which to identify important candidates for prion disease incubation time is by examining differential gene expression to investigate a correlation between candidate gene expression and incubation time to assess the effect of predicted promoter and regulatory region polymorphisms. Gene expression was investigated for those candidates considered to have the most functional relevance to prion disease, specifically *Mapt*, *Vtn* and *Ngfr*. As previously described (Section 3.4), polymorphisms were identified in predicted promoter regions for *Mapt* and *Ngfr* in addition to a 3'UTR polymorphism in *Ngfr* (Table 3.2). Sequencing of all of the possible regulatory regions

for candidate genes was not exhaustive as it is possible that some are not yet fully characterised. It was therefore prudent to assess candidate gene expression as polymorphisms controlling gene regulation may not have been identified in this analysis. Candidate gene expression was quantified by SYBR Green real-time PCR (Section 2.4.5) using cDNA generated from whole brain RNA extracted from 8-week old mice (Sections 2.4.1.2-5). Due to availability, the SJL/JOlaHsd mouse strain was used as a substitute in place of the SJL/J strain used in the original mapping studies to identify linkage (Stephenson et al., 2000). Gene expression in normal and Chandler/RML infected (Sections 2.2.4) mice was also quantified to assess if candidates are differentially regulated in the prion disease state which may highlight a potential functional role in prion pathogenesis. GAPDH was used as an endogenous control to normalise expression data (Sections 2.4.5.4). Full details of primer sequences for RT-PCR can be found in Appendix 3. *Ngfr* expression in normal and Chandler/RML infected mice was too low to quantify accurately.

3.5.1 *Vtn* mRNA Expression

A significant difference in *Vtn* expression was observed between normal SJL/JOlaHsd and CAST/Ei mice ($p=0.006$, unpaired two-tailed t test) (Figure 3.12) but not between NZW/OlaHsd and CAST/Ei. If the *Vtn* sequence variants identified in this study were responsible for the expression differences seen between SJL/JOlaHsd and CAST/Ei then the same effect would be seen between NZW/OlaHsd and CAST/Ei because SJL/JOlaHsd and NZW/OlaHsd share the same alleles and contrast with those of CAST/Ei. Therefore, the expression differences seen between SJL/JOlaHsd and CAST/Ei must be regulated by other sequence variants, perhaps within intronic regions, not analysed in this study, or possibly in more remote regions of the genome. The identification of differential expression implicates *Vtn* as a potential quantitative trait gene (QTG) within the QTL identified in the SJL/J and CAST/Ei F2 intercross (Stephenson et al., 2000). *Vtn* expression was not detectable in Chandler/RML infected mice suggesting that this candidate is significantly down-regulated in prion disease.

3.5.2 *Mapt* mRNA Expression

No significant difference in *Mapt* expression was observed between normal mice from 'short' and 'long' incubation time strains (Figure 3.13). These data suggest that *Mapt* expression levels in 'short' and 'long' incubation time strains do not correlate with phenotype and sequence data. A significant difference in *Mapt* mRNA expression was

Figure 3.12 *Vtn* mRNA expression.
'Short' incubation time strains are signified by blue bars and the 'long' incubation time strain by white. All samples were tested in triplicate. Units are arbitrary and represent quantity of *Vtn* transcript normalised by quantity of GAPDH. N=6 for all strains. Error bars represent SEM. * signifies p<0.01.

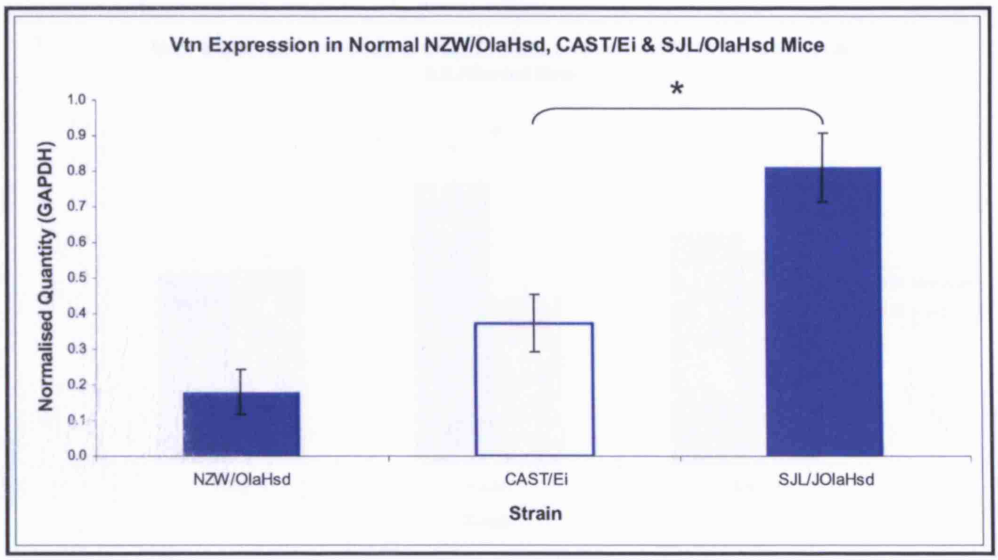

identified between normal and sick CAST/Ei mice (p=0.05, unpaired two-tailed t test) suggesting that *Mapt* is downregulated in prion disease in this mouse strain. No significant difference in *Mapt* expression was observed between normal and Chandler/RML infected groups within SJL/J and NZW/OlaHsd strains. Finally, no significant difference in *Mapt* expression was observed in Chandler/RML infected mice between 'short' and 'long' incubation time strains.

3.6 Conclusion

In summary, six candidate genes considered to have a particular functional relevance to prion pathogenesis and mapping within incubation time QTL identified on chromosome 11 have been sequenced to identify polymorphisms between 'short' and 'long' incubation time strains. The majority of polymorphisms identified had alleles common to the two 'short' incubation time strains which contrasted with the 'long' incubation time strain implicating potential QTN relevant for both F2 intercrosses used in the original mapping studies. The potential functional significance of polymorphisms were assessed highlighting 3'UTR polymorphisms residing in putative transcription factor binding sites in *Ngfr* and *Gfap,* which may have implications for downstream gene expression pathways, and several nonsynonymous polymorphisms in *Mpo*, *Gfap* and *Mapt* which may have functional implications at the protein level since they are located

Figure 3.13 *Mapt* mRNA expression.
N=6 for all groups except Chandler/RML infected NZW/OlaHsd where n=5 and Chandler/RML infected CAST/Ei where n=4. All samples were tested in triplicate. Units are arbitrary and represent quantity of *Mapt* transcript normalised by quantity of GAPDH. Error bars represent SEM. * signifies $p<0.05$.

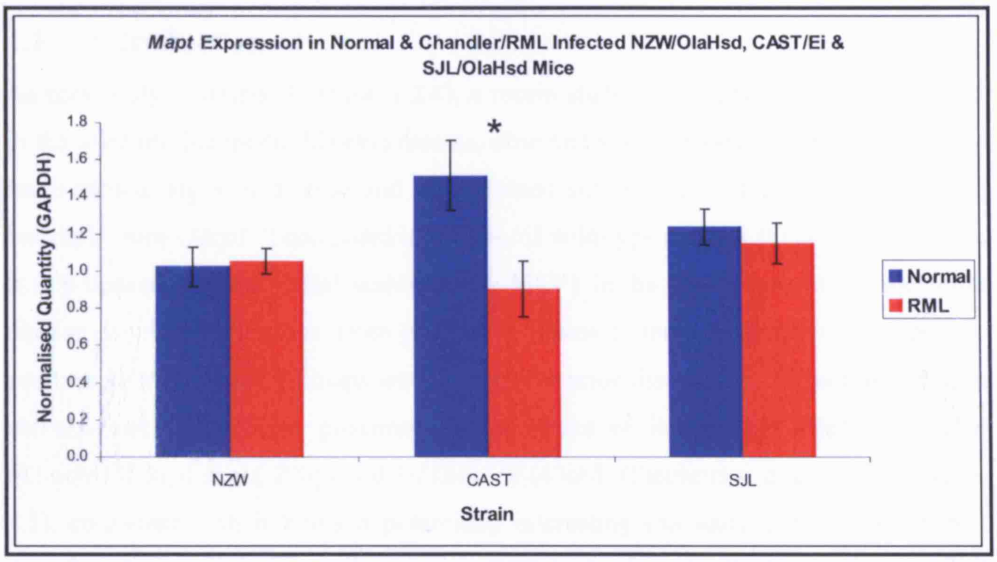

in known or putative functional domains. Several nonsynonymous polymorphisms in *Cdk5rap3* may prove promising following further characterisation of the function and domain structure of the protein product of this gene. In addition to the potential structural and functional changes caused by nonsynonymous polymorphisms in *Vtn,* differential expression of this gene correlates with incubation time phenotype in SJL/OlaHsd and CAST/Ei mice suggesting that this candidate may be an important QTG. Furthermore the observation that *Vtn* mRNA is downregulated in Chandler/RML infection provides further support for a potential role in prion disease. *Mapt* mRNA expression also appears to be downregulated in prion disease, specifically in the CAST/Ei strain. In conclusion, *Mpo*, *Gfap*, *Mapt* and *Vtn* remain the most promising candidates for incubation time and require further investigation.

4

Monocyte Chemoattractant Protein 1 (*Mcp1*)

4.1 Introduction

As previously described (Section 1.2.4), a recent study investigating the role of MCP1 in the ME7 murine model of prion disease, observed a 4-week delay in the onset of late-stage clinical signs of disease and an increased survival time of 2-3 weeks in *Mcp1* knockout mice (*Mcp1*$^{-/-}$) compared to C57BL/6J wild-type controls (Felton *et al.*, 2005). It is proposed that microglial activation by MCP1 in the later stages of murine prion disease drives the transition from preclinical illness to terminal disease. The genetic position of *Mcp1*, 46.5cM, maps within extensive prion disease incubation time QTL on chromosome 11 in close proximity to the peaks of linkage identified, *D11Mit36* (47.6cM) (Lloyd et al., 2001) and *D11Mit219* (43cM) (Stephenson et al., 2000) (Figure 4.1), consistent with it being a potentially interesting candidate gene. This chapter describes the investigation of the role of MCP1 in the Chandler/RML murine model of prion disease.

Figure 4.1 Schematic representation of the position of *Mcp1* on chromosome 11.
The purple box illustrates the combined regions of the published QTL for chromosome 11. The related peaks of linkage, *D11Mit36* and *D11Mit219*, and the location of *Mcp1* are labelled in black.

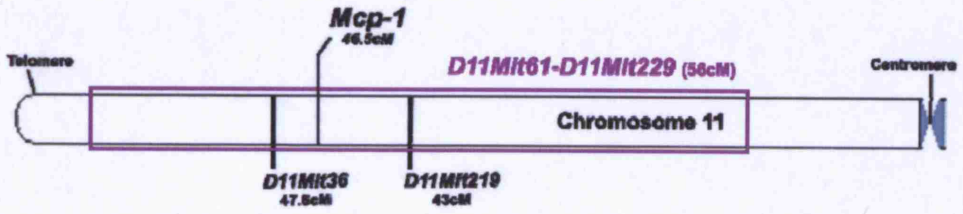

4.2 *Mcp1* Sequence Polymorphisms

As previously described (Section 3.2), sequence information for *Mcp1* (NCBI accession number NM_011333) was obtained from mouse genome sequence annotation databases. Alternate names for this gene are Chemokine (C-C motif) Ligand 2 (*Ccl2*) and Small Inducible Cytokine A2 (*Scya2*). *Mcp1* spans 1.65kb, has an 806bp mRNA transcript and a 148 amino acid peptide. It has both 5'- and 3'-UTR and three exons. As previously described (Section 3.3), sequence analysis of *Mcp1* was undertaken to identify polymorphisms between 'short' and 'long' incubation time mouse strains which

may be indicative of genetic differences controlling the phenotype. The sequence of two platelet-derived growth factor (PDGF)-responsive promoter motifs were also analysed (Freter *et al.*, 1995). These motifs are located in a 240bp enhancer region 2.3kb upstream of the *Mcp1* transcription site and are known to bind the transcription factor, Nuclear Factor-Kappa B (NF-κB). Details of PCR primer sequence and conditions for use are listed in Appendix 2.1.

Ten exonic polymorphisms were identified between NZW/OlaHsd, SJL/J and CAST/Ei (Table 4.1). Seven polymorphisms occur between NZW/OlaHsd and CAST/Ei and nine between SJL/J and CAST/Ei. Five polymorphisms had alleles common to the 'short' incubation time strains, contrasting with CAST/Ei. No polymorphisms were identified in the PDGF-responsive promoter motifs. Two polymorphisms were identified in the 5'-UTR region, one a SNP between the 'short' and 'long' incubation time strains and a second characterised by a 6bp deletion (CAST/Ei) or insertion (SJL/J) of sequence. Of the eight SNPs located in the three exons of *Mcp1*, three were nonsynonomous.

The potential functional significance of each *Mcp1* polymorphism was assessed to further characterise those which may be making the most significant contributions towards prion disease incubation time.

4.2.1 5'UTR Polymorphisms

A SNP and 6bp deletion (CAST/Ei) or insertion (SJL/J) polymorphism in the 5'UTR are both located within a putative transcription factor binding site for *α-Cp2*, a transcriptional activator of the α-globin gene (Kim *et al.*, 1990) (Figure 4.2) and may have the potential to influence the regulation of gene expression.

Figure 4.2 *Mcp1* 5'UTR polymorphisms in a putative *α-Cp2* binding site.
The sequence comprising the putative transcription factor binding site is illustrated by a broken arrow and the positions of m*Mcp1* 5'#1 (blue), showing alternative nucleotide bases, and m*Mcp1* 5'#2 defined by a 6bp deletion (red) or insertion (green) polymorphism (See Table 4.1).

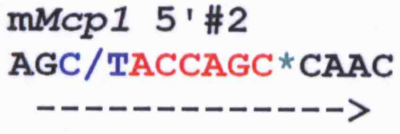

4.2.2 Nonsynonymous Polymorphisms

Three nonsynonomous polymorphisms in *Mcp1* cause substitutions at codons 6 (m*Mcp1*x1#1), 50 (m*Mcp1*x2#3) and 92 (m*Mcp1*x3#3) between NZW/OlaHsd, SJL/J and CAST/Ei (Table 4.1). A methionine residue in both NZW/OlaHsd and SJL/J is substituted by a threonine residue in CAST/Ei at codon 6. It is possible that the important QTN for prion disease incubation time may be the same in both F2 intercrosses used to identify linkage on chromosome 11 (Lloyd et al., 2001; Stephenson et al., 2000) with 'short' incubation time strains sharing the same amino acid residue and contrasting with that of the 'long' incubation time strain. At codon 6 the amino acid pattern mirrors that of the strain incubation time phenotype pattern, consistent with methionine conferring a short incubation time and threonine contributing towards a long incubation time.

It is also possible that separate QTN are important in controlling incubation time in each F2 intercross (Lloyd et al., 2001; Stephenson et al., 2000). At codon 50, serine in NZW/OlaHsd is substituted by glycine in CAST/Ei and SJL/J strains implying a potential QTN for the NZW/OlaHsd x CAST/Ei F2 intercross (Lloyd et al., 2001) and likewise the substitution of arginine in NZW/OlaHsd and CAST/Ei to glutamine in SJL/J at codon 92 may be an important QTN for the SJL/J x CAST/Ei F2 intercross (Stephenson et al., 2000). Furthermore, a combined effect of all of the affected codons may be important, conferring three different haplotypes (MSR, TGR and MGQ) and incubation times for the three mouse strains.

As previously described (Section 3.4), the conservation of amino acid residues affected by nonsynonymous polymorphisms in SJL/J, NZW/OlaHsd and CAST/Ei were assessed by aligning human, chimpanzee, macaque, dog, cow, mouse and rat MCP1 protein sequence (Figure 4.3).

Codon 6 is not a well conserved residue between the species featured. A change from non-polar, hydrophobic methionine to polar, hydrophilic threonine occurs between the 'long' and 'short' incubation time strains. This change may potentially affect tertiary protein structure since hydrophobic residues prefer to reside in internally folded domains which are protected from aqueous surroundings whereas a hydrophilic residue would rather be in externally facing regions. However, as this residue does not appear to be well conserved between species a change in physicochemical

Table 4.1 *Mcp1* nucleotide polymorphisms.
Amino acids are shown for nonsynonomous polymorphisms. NC=No change when compared to database sequence for *Mcp1*, Del=Deletion and Ins=Insertion.

Region	Polymorphism ID	Position	Codon	Polymorphism (Amino Acid)		
				NZW/OlaHsd	CAST/Ei	SJL/J
5'UTR	m*Mcp1* 5'#1	81851811	-	C	T	C
	m*Mcp1* 5'#2	81851812-81851817	-	NC	ACCAGC Del	ACCAGC Ins
Exon 1	m*Mcp1*x1#1	81851873	6	T (Met)	C (Thr)	T (Met)
	m*Mcp1*x1#2	81851887	11	C	C	T
Exon 2	m*Mcp1*x2#1	81852688	29	C	C	T
	m*Mcp1*x2#2	81852742	47	G	A	G
	m*Mcp1*x2#3	81852749	50	A (Ser)	G (Gly)	G (Gly)
Exon 3	m*Mcp1*x3#1	81853194	90	C	T	C
	m*Mcp1*x3#2	81853199	91	T	C	T
	m*Mcp1*x3#3	81853201	92	G (Arg)	G (Arg)	A (Gln)

Figure 4.3 MCP1 homolog protein sequence alignment.
Mouse sequence is for the C57BL/6J strain. Amino acid residues affected by nonsynonomous polymorphisms are highlighted in red with the corresponding polymorphism in mouse detailed directly above. ClustalW consensus symbols indicate the degree of conservation observed at each amino acid residue. * = residues are identical in all sequences of the alignment, : = conserved residue and . = semi-conserved residue.

```
                          M6T                                                S50G
Homo sapiens              MKVSAALLCLLLIAATFIPQGLAQPDAINAPVTCCYNFTNRKISVQRLASYRRITSSKCP 60
Pan troglodytes           MKVSAALLCLLLIAATFIPQGLAQPDAINAPVTCCYNFTNRKISVQRLASYRRITSSKCP 60
Macaca mulatta            MKVSAALLCLLLIAATFSPQGLAQPDAINAPVTCCYNFTNRKISVQRLASYRRITSSKCP 60
Canis familiaris          MKVSAALLCLLLIAAALTTQVLTQPDAINSPVTCCYTLTNKKISIQRLASYKRVTSSKCP 60
Bos taurus                MKVSAVLLCLLLTATLCSIQVLAQPASI--PTICCFNMSKKKISIQRLQSYRKITSSKCP 58
Mus musculus              MQVPVMLLGLLFTVAGWSIHVLAQPDAVNAPLTCCYSFTSKMIPMSRLESYKRITSSRCP 60
Rattus norvegicus         MQVSVTLLGLLFTVAACSIHVLSQPDAVNAPLTCCYSFTGKMIPMSRLENYKRITSSRCP 60
                          *:*.. ** **: .:    : *:** ::  *  **:.:: : *.:.** .*:::***:**
                                                  R92Q
Homo sapiens              KEAVIFKTIVAKEICADPKQKWVQDSMDHLDK--QTQTPKT------------------- 99
Pan troglodytes           KEAVIFKTIVAKEICADPKQKWVQDSMDHLDK--QTQTPKT------------------- 99
Macaca mulatta            KEAVIFKTIVAKEICADPKQKWVQDSMDHLDK--QIQTPKP------------------- 99
Canis familiaris          KEAVIFKTVLNKEICADPKQKWVQDSMAHLDKKSQTQTAKP------------------- 101
Bos taurus                QKAVIFNTKQNKKICVDPQEKWVQNAMEYLNQ--KSQTLKS------------------- 97
Mus musculus              KEAVVFVTKLKREVCADPKKEWVQTYIKNLDR-NQMRSEPTTLFKTASALRSSAPLNVKL 119
Rattus norvegicus         KEAVVFVTKLKREICADPNKEWVQKYIRKLDQ-NQVRSETTVFYKIASTLRTSAPLNVNL 119
                          ::**:* *   :::*.**:::***  :  *::  : ::  .

Homo sapiens              ----------------------------
Pan troglodytes           ----------------------------
Macaca mulatta            ----------------------------
Canis familiaris          ----------------------------
Bos taurus                ----------------------------
Mus musculus              TRKSEANASTTFSTTTSSTSVGVTSVTVN 148
Rattus norvegicus         THKSEANASTLFSTTTSSTSVEVTSMTEN 148
```

properties at this position may be negligible.

Codon 50 is a semi-conserved residue at which the polar amino acid serine is substituted with non-polar glycine. Both residues are classed as tiny amino acids and are generally well conserved in most proteins possibly due to the fact that substitution with larger residues would almost certainly disrupt protein structure. The change in polarity between these amino acids may bring about similar changes to those at codon 6 in terms of the type of environment these residues would prefer to be situated in.

Murine MCP1 is comprised of two functional domains, an N-terminal domain responsible for monocyte chemoattractant activity and a heavily glycosylated C terminal domain whose function is not yet clear (Gu *et al.*, 1999). Mutational analysis has demonstrated that all of MCP1 chemoattractant activity resides in the first 73 amino acids of the protein (Ernst *et al.*, 1994) where codons 6 and 50 are located. This N-terminal domain is associated with MCP1 receptor binding (Baggiolini *et al.*, 1997). The murine N-terminal domain shares 62% amino acid homology with human MCP1 and its specific *in vitro* activity is identical to that of human MCP1 (Gu et al., 1999). The potential effects of amino acid substitutions at codons 6 and 50 in affecting tertiary structure in this region of the protein may therefore have implications for chemoattractant activity and receptor binding.

At codon 92, a nonsynonymous polymorphism causes arginine, a basic charged polar and hydrophilic residue to be converted to glutamine, also polar and hydrophilic but neutral and an amide. It is possible that because both of these residues are hydrophilic little conformation change will occur upon substitution of either as they both prefer to be on the outside surface of a protein where they can interact with the polar environment. This residue is conserved, although not identical, beween species suggesting that a change in property may have important functional implications at this position. Codon 92 resides in the C-terminal region of the molecule. This serine- and threonine- rich murine MCP1 domain has no counterpart in human MCP1 and contains the largest amount of O-linked carbohydrate known in chemokines of any species (Ernst *et al.*, 1994).

To further investigate the contribution of these nonsynonomous changes to prion disease incubation time mutational analysis in amino acid targeted transgenic mice

would be a useful model to consider. Significant variation in incubation time between prion inoculated mice expressing different amino acid residues at the described positions within MCP1 would determine if these substitutions constituted functional sequence variants responsible for the disparity in incubation times observed between the 'long' and 'short' incubation time strains. This line of investigation was beyond the scope of the current study where the primary consideration was to examine the overall candidacy of the *Mcp1* gene.

4.3 Quantitative Complementation

Mcp1 knockout mice (*Mcp1*$^{-/-}$) (Section 2.3.2) were used to investigate the candidacy of *Mcp1* in prion disease incubation time as part of a quantitative complementation experimental design, also known as a QTL-knockout interaction test, to ascertain whether *Mcp1* is a QTG or influences the phenotype independently of identified QTL (Flint and Mott, 2001; Flint *et al.*, 2005; Mackay, 2001). This method involves a systematic series of crosses between QTL alleles and the null allele of the gene of interest to test for an interaction. Quantitative complementation is oblivious to the nature and position of the responsible sequence variant except that it lies within a designated QTL interval. In addition, this test gives no information about the molecular nature of a QTL, and only identifies a gene under the influence of a QTL. This strategy has recently been successfully used to confirm the candidacy of *Rgs2,* a quantitative trait gene for anxiety in mice (Yalcin et al., 2004a).

Mcp1 knockout mice which are homozygous for the targeted mutation and generated on a C57BL/6J background (Section 2.3.2) were utilised in this investigation. To generate the necessary offspring for the experimental design, *Mcp1*$^{-/-}$ mice were mated with co-isogenic C57BL/6J mice to produce mice hemizygous for the *Mcp1* gene (Figure 4.4). Subsequent breeding pairs were set up between the C57BL/6J hemizygous mice and 'short' (NZW/OlaHsd or SJL/JOlaHsd) and 'long' (CAST/Ei) incubation time strains to produce four types of offspring; 'short' (NZWxC57BL/6J F_1 or SJLxC57BL/6J F_1) WT/WT and WT/KO and 'long' (CASTxC57BL/6J F_1) WT/WT and WT/KO (Figure 4.4). The resulting progeny harbour 50% of the genetic background of the 'short' or 'long' incubation time strain in question and 50% is derived from C57BL/6J. Each individual will contain one copy of *Mcp1* derived from the 'short' or 'long' incubation time strain but will differ genetically by the presence or absence of the wild-type *Mcp1* copy derived from C57BL/6J.

Figure 4.4 Quantitative complementation breeding scheme.
Coloured rectangles represent pairs of chromosomes with the *Mcp1* gene region illustrated by a box. Crossed boxes represent the PGK-neomycin resistance cassette introduced to produce the knockout mouse by targeted disruption of exon 2 in *Mcp1*. IT = Incubation time, WT = wild-type and KO = knockout.

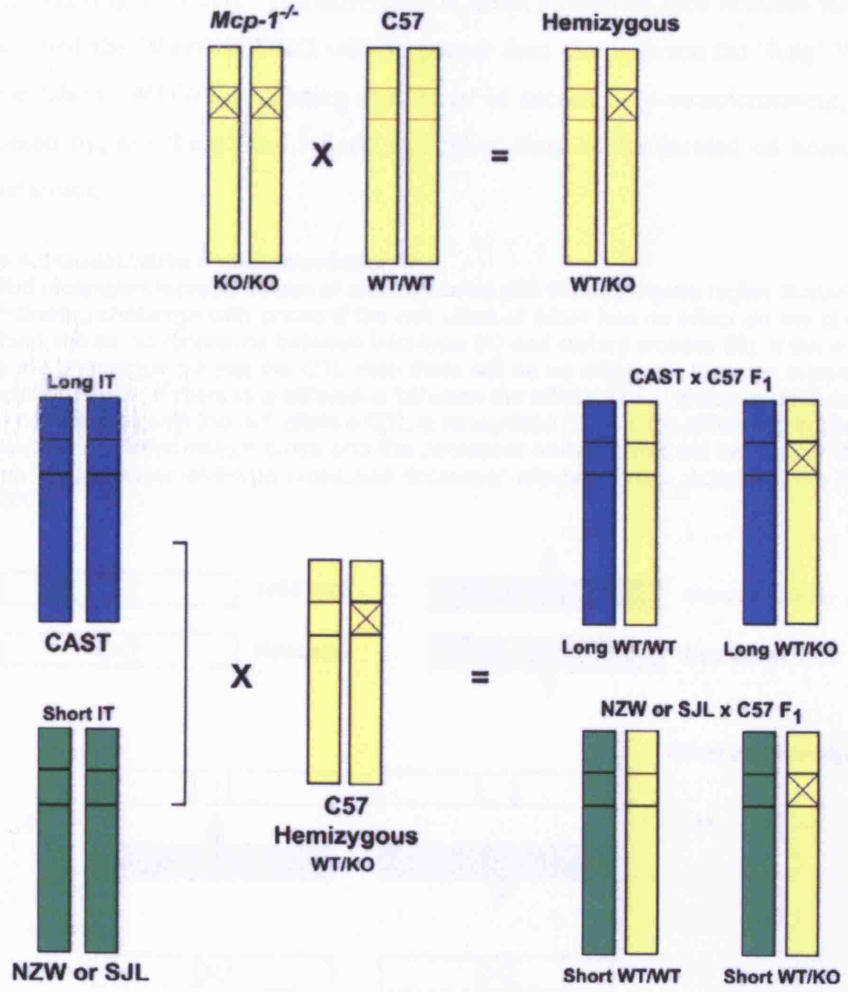

The mean incubation time of *Mcp1*$^{-/-}$ mice was compared with that of C57BL/6J wild-type and the hemizygous mice to determine if there was a significant difference between these groups which differ only in the number of *Mcp1* copies they have. To further confirm *Mcp1* as a candidate for prion disease incubation time, an interaction between the null allele of *Mcp1* and the 'long' and 'short' incubation time strain alleles must be observed (Flint and Mott, 2001; Flint et al., 2005). Following challenge with prions, if the null allele has no effect on the phenotype then there will be no difference in incubation time between wild-type (WT/WT) (Figure 4.5A) and mutant crosses (WT/KO) (Figure 4.5B) within each mouse strain. If the null allele of *Mcp1* effects the phenotype but not the QTL then there will be no difference in incubation time between

'long' (CAST/Ei) and 'short' (NZW/OlaHsd or SJL/JOlaHsd) strains (Figure 4.5C). If *Mcp1* affects the QTL there will not only be a difference between the wild-type and hemizygous mice but also be a difference between the effects of the 'long' and 'short' QTL alleles (Figure 4.5D). The difference in mean incubation time between the 'long' WT/KO and the 'short' WT/KO will be greater than that between the 'long' WT/WT and the 'short' WT/WT indicating that *Mcp1* is successfully complementing, and is modulated by, the 'long' and 'short' incubation time alleles located on homologous chromosomes.

Figure 4.5 Quantitative complementation test.
Coloured rectangles represent pairs of chromosomes with the *Mcp1* gene region illustrated by a box. Following challenge with prions if the null allele of *Mcp1* has no effect on the phenotype then there will be no difference between wild-type (A) and mutant crosses (B). If the null allele effects the phenotype but not the QTL then there will be no difference between increaser and decreaser QTL (C). If there is a difference between the effects of the increaser and decreaser QTL in combination with the null allele a QTL is recognised (D) and the difference in phenotype between the increaser mutant cross and the decreaser mutant cross will be greater than that between the increaser wild-type cross and decreaser wild-type cross. Adapted from Flint and Mott, 2001.

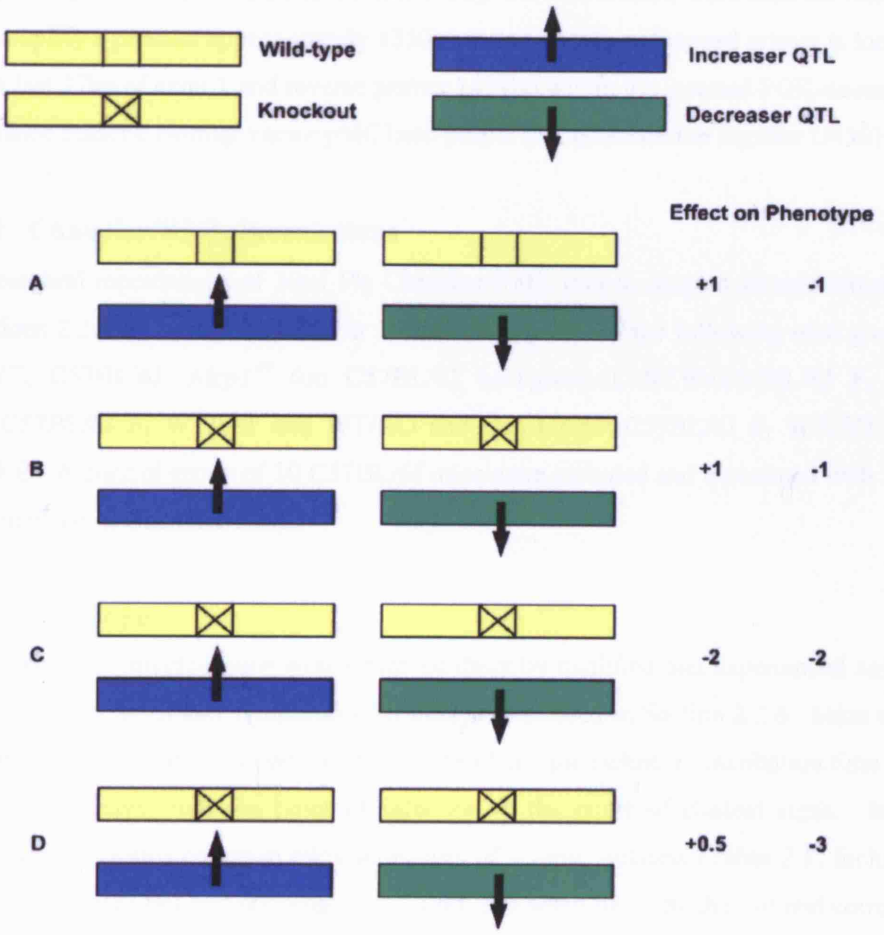

4.3.1 Screening *Mcp1*$^{-/-}$ and Wild-Type Mice

Genomic DNA was extracted (Section 2.4.1.1) from tail biopsies (Section 2.2.2) to screen for the presence or absence of the *Mcp1* gene using two optimized genotyping PCR protocols, namely reaction A and B using primers *a*, *b* and *c* (Section 2.4.2.4). Full primer sequences for both wild-type and knockout amplicons are detailed in Section 2.4.2.4. The co-isogenic C57BL/6J strain was used as a control in genotyping assays. Both PCR amplicons from reaction A and B are amplified in hemizygous mice.

Primers *a* and *b* were used for reaction A to amplify an 888bp wild-type product spanning 27bp at the end of exon 1, across 745bp of intronic sequence and 115bp of exon 2 (Figure 4.6). As previously described (Section 2.3.2), *Mcp1*$^{-/-}$ mice were generated using a targeting vector containing a PGK-neomycin resistance cassette, in a transcriptional orientation opposite to that of *Mcp1*, and a herpes simplex virus thymidine kinase gene which disrupts exon 2 and introduces a small deletion causing an inframe stop codon into exon 1 (Lu *et al.*, 1998). Primers *a* and *c* were used for reaction B to amplify a product approximately 1350bp in length whose forward primer is located in the last 27bp of exon 1 and reverse primer 1459bp within the inserted PGK-neomycin resistance cassette cloning vector pMC1neo-polyA (NCBI accession number U43612).

4.3.2 Chandler/RML Inoculations

Intracerebral inoculations of 30µl 1% Chandler/RML mouse-adapted scrapie inoculum (Sections 2.2.4-5) were performed in 10 mice from each of the following nine groups; *Mcp1*$^{-/-}$, C57BL/6J, *Mcp1*$^{-/+}$ (on C57BL/6J background), NZWxC57BL/6J F_1 and SJLxC57BL/6J F_1 WT/WT and WT/KO and also CASTxC57BL/6J F_1 WT/WT and WT/KO. A control group of 10 C57BL/6J mice were included and inoculated with 30µl PBS in place of Chandler/RML.

Scrapie phenotype

Chandler/RML infected mice were observed daily by qualified and experienced animal technicians for signs and symptoms of illness as described in Section 2.2.6. Mice were culled upon presentation of confirmatory signs of scrapie sickness. Incubation time was measured in days from the point of infection to the onset of clinical signs. In all experimental groups common early indicators of scrapie sickness (Table 2.1) included erect ears, a rigid tail and clasping of the hind legs when lifted by the tail and common confirmatory signs included piloerection, hunched posture, mild ataxia and abnormal

Figure 4.6 *Mcp1* screening primers.
Numbered blue boxes indicate the three exons of *Mcp1*. The red arrow indicates the neo cassette disrupting exon 2 in a transcriptional orientation opposite to that of *Mcp1*. The position of primers *a*, *b* and *c* are illustrated by labelled black arrows. A = Reaction A for amplification of 888bp wild-type *Mcp1* amplicon. B = Reaction B for amplification of 1350bp knockout product comprising part of a neomycin resistance cassette. bp= base pairs, HIV = HyperLadder IV and HI = HyperLadder I.

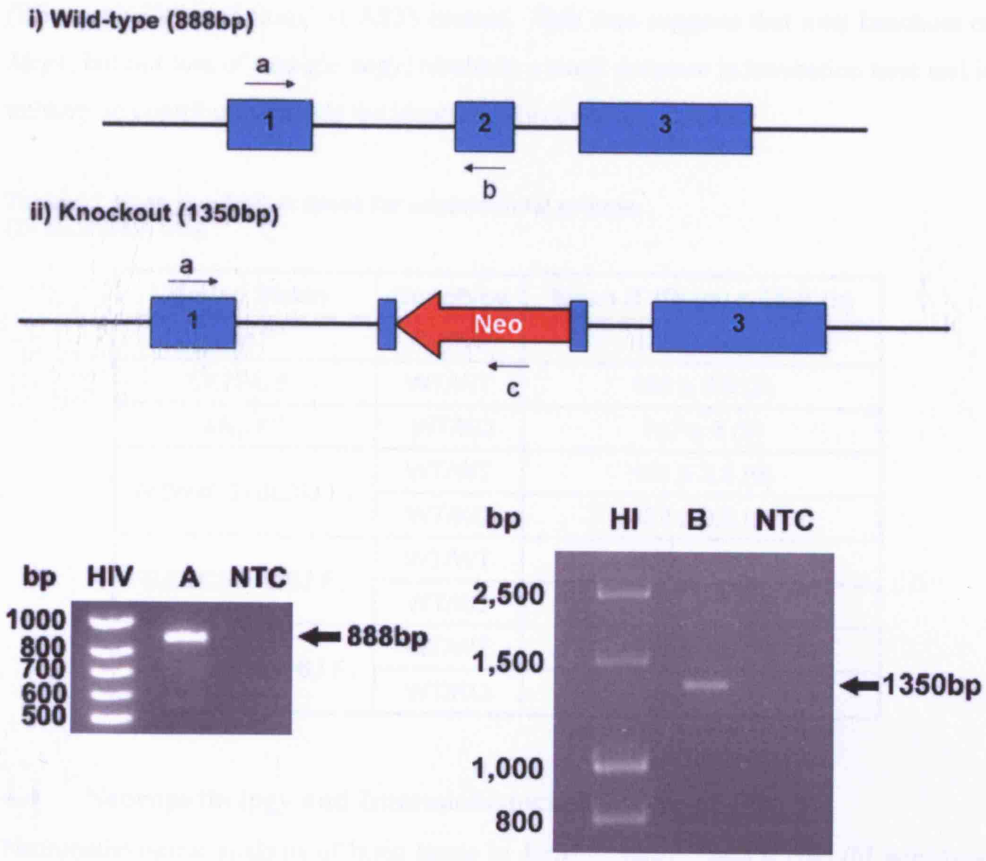

respiration. In total, 83 of the 90 mice inoculated with Chandler/RML were confirmed as scrapie sick and culled for this reason. 7 mice were culled due to other non-specific illness or were found dead and were excluded from the analysis. No clinical signs or symptoms of scrapie sickness were recorded in the PBS control group.

Incubation time phenotype

Group incubation times (Table 4.2) were compared by Kaplan-Meier log-rank survival analysis. The mean incubation times for the *Mcp1*$^{-/-}$, C57BL/6J and *Mcp1*$^{-/+}$ groups were 161±0.5 (n=10), 166±3.9 (n=8) and 167±3 (n=9) days respectively. A statistically significant mean difference of 5 days was seen between the *Mcp1*$^{-/-}$ mice compared to

wild-type controls (P=0.0175) contrasting with the findings of Felton *et al.*, which describe a significant increase in survival for knockout mice in the ME7 model of murine prion disease. The incubation times of *Mcp1*$^{-/+}$ and *Mcp1*$^{-/-}$ groups were also significantly different (P=0.0027). No significant differences were observed between the incubation times of the hemizygous and *Mcp1* wild-type mice for each of the 'short' (SJL and NZW) and 'long' (CAST) crosses. This data suggests that total knockout of *Mcp1*, but not loss of a single copy, results in a small decrease in incubation time and is unlikely to contribute towards the identified chromosome 11 QTL.

Table 4.2 Mean incubation times for experimental groups.
IT= Incubation time.

Mouse Strain	Genotype	Mean IT (Days) ± SEM (n)
Mcp1$^{-/-}$	KO/KO	161 ± 0.5 (10)
C57BL/6J	WT/WT	166 ± 3.9 (8)
Mcp1$^{-/+}$	WT/KO	167 ± 3 (9)
NZWxC57BL/6J F_1	WT/WT	181 ± 3.8 (9)
	WT/KO	178 ± 9.5 (9)
SJLxC57BL/6J F_1	WT/WT	148 ± 2.6 (10)
	WT/KO	152 ± 4.3 (10)
CASTxC57BL/6J F_1	WT/WT	206 ± 5.8 (9)
	WT/KO	205 ± 2 (9)

4.4 Neuropathology and Immunohistochemistry

Neuropathological analysis of brain tissue in *Mcp1*$^{-/-}$, *Mcp1*$^{-/+}$ and C57BL/6J wild-type mice was carried out to confirm the presence of Chandler/RML prion pathology (Section 2.4.6). Following a definitive diagnosis of scrapie sickness (Section 2.2.6) mice were culled and brains were removed for analysis (Section 2.2.7). The monoclonal antibody ICSM35 was used to determine deposition of abnormal PrP (Asante *et al.*, 2002). This was diffuse and did not vary between strains (Figure 4.7M-O). In all three groups the characteristic Chandler/RML prion strain PrP^{Sc} distribution pattern was seen with the cortex, hippocampus and thalamus showing intense staining and the cerebellum, brain stem, tectum and basal ganglia showing light staining (Figure 4.7P-R). Gliosis and spongiosis, determined by GFAP immunohistochemistry (Figure 4.7J-L) and hematoxylin and eosin staining (Figure 4.7D-F) respectively, was consistent with the pattern of PrP^{Sc} distribution and did not differ between groups. An anti-Iba1 polyclonal antibody was used to specifically detect the distribution of activated

Figure 4.7 Neuropathology and immunohistochemistry for *Mcp1*$^{-/-}$, *Mcp1*$^{-/+}$ and C57BL/6J wild-type mice.
Hematoxylin and eosin stained sections show no evidence of neuronal loss in the hippocampus (A-C). Panels D-F, stained with hematoxylin and eosin show evidence of spongiform neurodegeneration. Staining with the polyclonal antibody Iba1 shows the distribution of activated microglia in panels G-I. Panels J-L show GFAP immunohistochemistry indicating reactive astrocytes and gliosis. PrP immunohistochemistry with monoclonal antibody ICSM35 is shown in panels M-O highlighting the distribution pattern of abnormal PrP. The schematic representation of PrP deposition in the brain is shown in panels P-R. Red represents areas of intense staining, dark pink areas of moderate staining and light pink areas of light staining. No significant differences are seen between the groups. Schematic representation of mouse brain regions is shown in panel S (1=cortex, 2=hippocampus, 3=thalamus, 4=cerebellum, 5=brain stem, 6=tectum and 7=basal ganglia). The scale bar represents 200μm (A-C), 50μm (D-F) and 2mm (G-O).

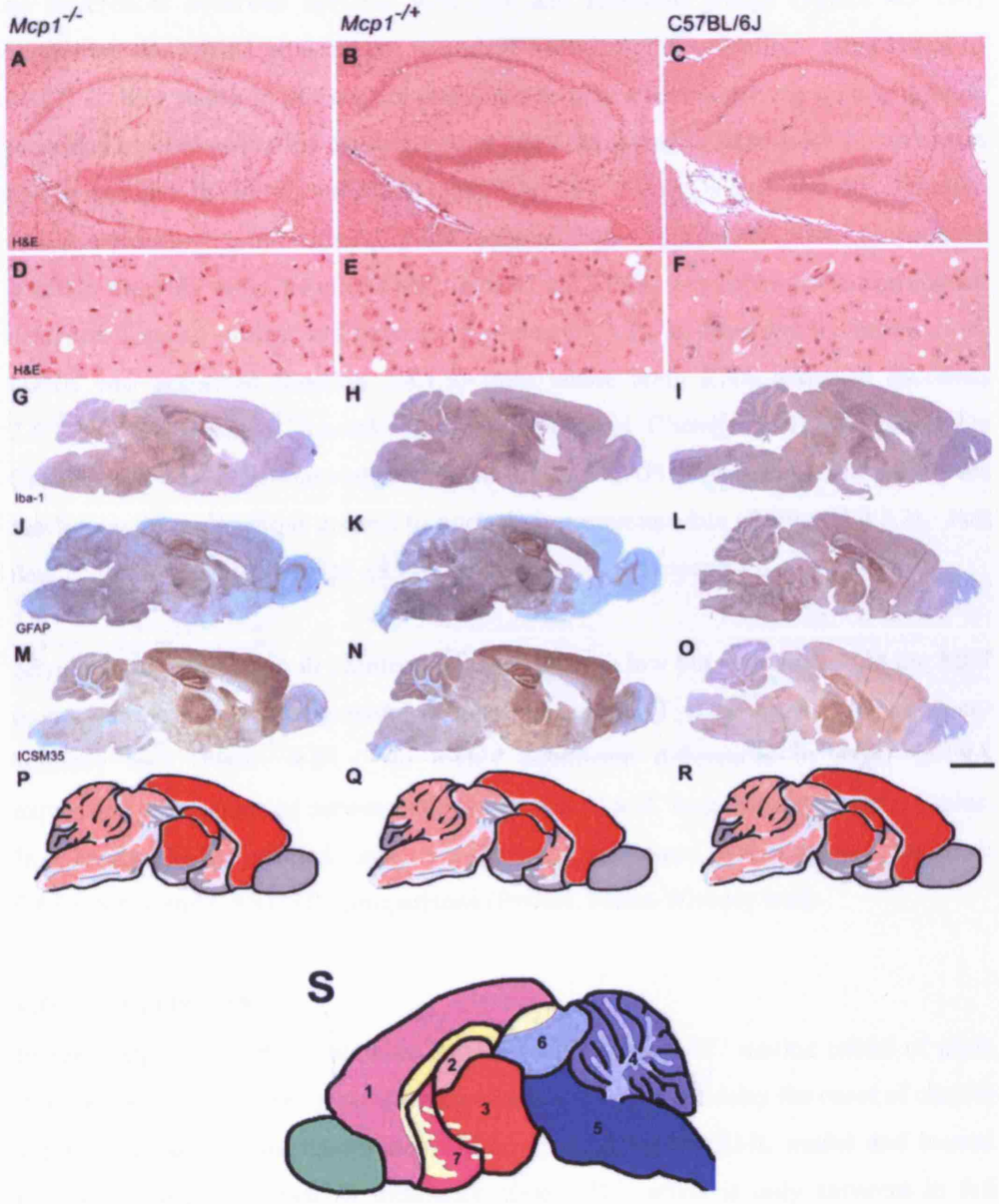

microglia (Figure 4.7G-I) which mirrored the pattern of general gliosis and PrP^{Sc} deposition with no difference observed between groups. No neuronal loss was detected in the hippocampus by staining with hematoxylin and eosin (Figure 4.7A-C).

4.5 *Mcp1* Expression

MCP1 is thought to activate microglia which exacerbates neuronal injury in the later stages of prion disease (Felton et al., 2005). As in the ME7 model of murine prion disease, microglial activation was detected in mice inoculated with Chandler/RML with no differences observed between wild-type and knockout groups (Figure 4.7 G-I) suggesting that MCP1 alone is not necessary for microglial activation. High levels of MCP1 in later stages of disease are postulated to play a role in driving microglia to an increased level of activation causing further neuronal damage. *Mcp1* mRNA expression was quantified in uninfected C57BL/6J, CAST/Ei, NZW/OlaHsd and SJL/JOlaHsd strains and following inoculation at the terminal stage of disease to draw comparisons between the ME7 and Chandler/RML models. qRT-PCR was performed using custom designed Taqman probes and primers (Sections 2.4.5.3), as described by Felton *et al.* cDNA was generated (Section 2.4.1.5) from whole brain RNA extracted (Sections 2.4.1.2-3) from normal 8-week old male mice and Chandler/RML infected mice (Section 2.2.4-5). Commercially available murine GAPDH was duplexed within the reaction as an endogenous control to normalise expression data (Section 2.4.5.2). Full details of primer sequences for qRT-PCR are detailed in Appendix 3.

Mcp1 mRNA expression in uninfected mice was very low but consistent with the ME7 model, was significantly increased in terminal disease ($P \leq 0.01$ for all strains, Mann-Whitney test) (Figure 4.8). No highly significant differences in *Mcp1* mRNA expression were observed between uninfected 'short' and 'long' incubation time strains. In Chandler/RML infected mice a significant difference was observed for both CAST/NZW and CAST/SJL comparisons ($P=0.01$, Mann-Whitney test).

4.6 Conclusion

In summary, despite the established role of MCP1 in the ME7 murine model of prion disease (Felton et al., 2005), the absence of this gene does not delay the onset of clinical signs of disease nor increase survival time in the Chandler/RML model and instead produces a small decrease in incubation time. This effect is only apparent in full knockout and not hemizygous mice. No significant differences in incubation time were

Figure 4.8 *Mcp1* mRNA expression.
Black and grey bars represent normal and terminal stage Chandler/RML infected mice respectively. N=6 for each group except CAST-RML (n=4) and NZW-RML (n=5). All samples were tested in triplicate. Arbitrary units represent the quantity of *Mcp1* transcript normalised by quantity of GAPDH. Error bars represent SEM. ★ signifies P=0.01 when compared to other strains for infected samples only (Mann-Whitney test).

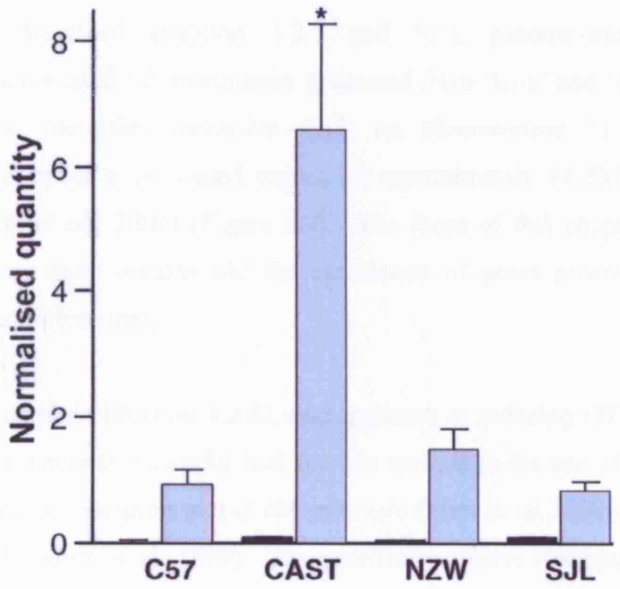

observed between wild-type and knockout crosses in a quantitative complementation test suggesting that *Mcp1* does not affect the phenotype nor contribute towards the QTL. Significant differences in *Mcp1* mRNA expression were seen between Chandler/RML infected mouse strains at the terminal stage of disease but did not correlate with incubation time as the highest expression was observed in CAST/Ei. This finding is inconsistent with the model of MCP1 action in which increased *Mcp1* expression would be expected to reduce incubation time. In conclusion, it appears that the role of MCP1 may be exclusive to the specific pathogenesis of the ME7 prion strain.

5

Fine Mapping Chromosome 11 QTL

5.1 Introduction

As previously described (Section 1.2.5 and 3.1), genome-wide mapping in Chandler/RML inoculated F2 intercrosses generated from 'long' and 'short' incubation time strains has identified extensive QTL on chromosome 11 which overlap considerably and cover a combined region of approximately 86.5Mb (Lloyd *et al.*, 2001; Stephenson *et al.*, 2000) (Figure 3.2). The focus of this chapter is the further characterisation of these regions and the elucidation of genes potentially controlling prion disease incubation time.

As previously described (Section 1.2.6), one approach to reducing QTL regions is fine mapping and a potentially powerful tool for this method is the use of HS mice which allow high resolution mapping at 1-2 cM intervals (Flint *et al.*, 2005; McPeek, 2000; Mott *et al.*, 2000; Talbot *et al.*, 1999). The genetically diverse Northport HS (Demarest *et al.*, 2001) (Section 2.3.1) was utilised in this study to fine map chromosome 11 QTL. A potential limitation of this method is the absence of the mouse strains used in the original mapping studies (SJL/J, NZW/OlaHsd and CAST/Ei) from the panel of parental strains used to generate the Northport HS (A/J, AKR/J, BALB/cJ, C3H/HeJ, C57BL/6J, CBA/J, DBA/2J and LP/J). It is possible that the chromosome 11 QTL identified may be mouse strain specific and not be present in the progenitor strains of the HS. However, the potential gains to be made from the use of the HS in reducing the regions of linkage and enabling the identification of individual genes controlling prion disease incubation time outweighed the possible risk that linkage would not be reproducible in the HS.

5.2 HAPPY Linkage Analysis

In previous work (Lloyd *et al.*, unpublished data), 1052 generation 37 HS mice (Section 2.3.1) were challenged intracerebrally with Chandler/RML mouse-adapted scrapie (Sections 2.2.4-5) and phenotyped for incubation time (Section 2.2.6). Fluorescently-labelled microsatellite markers (Table 5.1), polymorphic between the parental strains of the HS and thus informative in the cross, were selected from the Mouse Genome Informatics database (Section 2.1.5) at approximately 1cM intervals within the flanking

Table 5.1 HS progenitor strain allele sizes for chromosome 11 microsatellite markers. cM=centimorgan and bp=base pairs.

Marker	Position (cM)	Marker Sizes (bp)							
		A	AKR	BALB	C3H	C57	CBA	DBA	LP
D11Mit260	34.4	97	107	97	97	97	97	73	112
D11Mit5	37	218	218	182	182	222	182	184	182
D11Mit278	40	135	119	115	115	113	115	133	139
D11Mit90	42	153	153	155	155	153	155	179	155
D11Mit320	43	118	124	134	134	118	134	116	134
D11Mit194	44	135	123	123	123	129	123	123	125
D11Mit40	46	206	204	204	204	206	204	208	206
D11Mit326	49	95	66	93	95	93	95	66	95
D11Mit36	49.1	243	235	237	243	237	243	221	243
D11Mit212	50	155	155	153	155	139	155	155	155
D11Mit41	50.3	165	165	175	133	165	165	165	165
D11Mit179	52	136	138	134	136	161	138	136	136
D11Mit70	54	128	128	140	128	142	128	142	140
D11Mit288	54.5	106	106	124	106	126	106	126	124
D11Mit289	55	119	119	133	119	127	119	127	127
D11Mit263	55.6	164	164	150	164	146	164	156	146
D11Mit54	56	111	111	141	141	141	111	138	141
D11Mit67	57	176	176	134	124	132	176	124	124
D11Mit145	57.5	136	136	136	152	152	136	152	152
D11Mit124	57.8	128	124	124	122	118	124	122	122
D11Mit132	58	130	123	117	138	119	117	138	138
D11Mit99	59.5	124	120	122	107	124	122	107	107

markers of chromosome 11 QTL (*D11Mit260* to *D11Mit99).* Prior to analysis in the HS, markers were used to genotype (Sections 2.4.4.1-4) the founder strains of the cross to establish allele size and confirm that they were polymorphic between these strains (Table 5.1). Markers were then used to genotype approximately 400 mice from the extreme ~20% of each end of the Chandler/RML incubation time distribution. This subpopulation was selected for analysis based upon estimates that the majority of statistical power in linkage analysis is derived from the tails of the phenotypic distribution (Lander and Botstein, 1989). PCR primer sequences and fluorescent labelling information for microsatellite markers are detailed in Appendix 1.1.

Multipoint QTL mapping in the subpopulation described above was undertaken using HAPPY linkage analysis software (Mott et al., 2000) (Section 2.4.4.5). Linkage analysis LOD score values of 2.8 and 4.3 were assigned as the thresholds for 'suggestive' and 'significant' linkage respectively, based upon thresholds suggested for mapping complex trait loci in an intercross population (Lander and Kruglyak, 1995).

A minimal region of significant linkage was successfully identified in a single microsatellite marker interval spanning approximately 708kb and defined by the flanking markers *D11Mit67* and *D11Mit145* (-logP=4.39) (Lloyd *et al.*, unpublished data) (Figure 5.1). A second region, approaching the threshold level for significant linkage, spanning approximately 1.2Mb across two microsatelitte marker intervals, namely *D11Mit288* and *D11Mit289* (-logP=4.07) and *D11Mit289* and *D11Mit263* (-logP=4.19), was also identified. The smaller and more significant region of linkage was the subject of further analysis in this study. Overall the critical region for analysis has been reduced by approximately 85.8Mb (Figure 5.2) resolving the QTL into a small enough interval in which to identify potential candidate genes for prion disease incubation time.

Figure 5.1 Chromosome 11 HAPPY linkage analysis –logP plot.
The x axis represents 21 microsatellite marker intervals across chromosome 11. Dotted line intersecting the y axis indicates the –logP value representing a statistical significance threshold of 4.3.

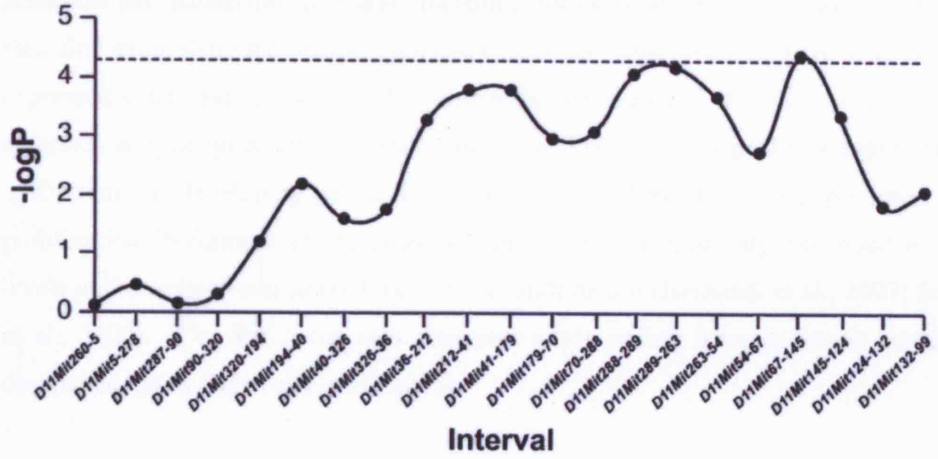

Figure 5.2 Chromosome 11 schematic.
The purple box illustrates the combined chromosome 11 QTL with the peaks of linkage detailed in black. The red box indicates the new region of linkage spanning between the markers *D11Mit67* and *D11Mit145*.

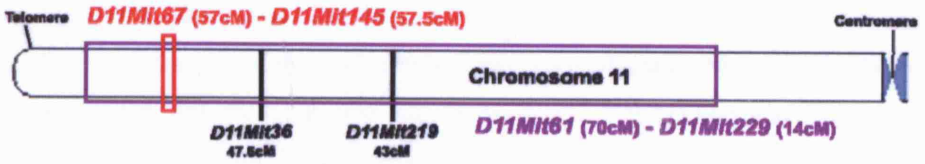

5.3 Candidate Genes

As previously described (Section 3.2), information for seventeen candidate genes mapping within the new region of linkage was obtained from genome sequence annotation databases (Table 5.2). Candidate genes which have a particular relevance to prion pathogenesis in terms of their function are noteworthy but since the mechanisms of prion disease are not yet completely understood it is prudent to assess all genes systematically assigning equal value to each as potential candidates.

Transacting transcription factor 6 (Sp6)

Sp6 is a member of the Specificity Protein/Krüppel-like Factor (SP/KLF) transcription factor family which bind GC/GT boxes (Hagen *et al.*, 1992) and interact with DNA through an 81 amino-acid DNA-binding domain with 3 highly conserved tandem C2H2-type (Krüppel-like) zinc finger motifs at the C-terminus (Kadonaga *et al.*, 1988; Kadonaga and Tjian, 1986; Scohy *et al.*, 2000; Suske *et al.*, 2005). The *Sp6* locus generates two transcripts, *Sp6* and epiprofin, from distinct promoters, which differ in their first exon, share the second exon and encode the same protein but are differentially expressed (Hertveldt *et al.*, 2007). Currently the sequence databases use *Sp6* and epiprofin as synonyms and they share the same first exon. Epiprofin is expressed by epithelium of developing teeth, hair follicles and limb buds and promotes cell proliferation (Nakamura *et al.*, 2004) whereas *Sp6* is ubiquitously expressed at high levels in the embryo and lower levels in the adult mouse (Hertveldt et al., 2007; Scohy et al., 2000). The *Sp6* locus also generates a non-coding opposite strand transcript designated *Sp6os* (Hertveldt et al., 2007).

Secernin 2 (Scrn2)

SCRN2 is not well characterised in mice but may have related function to a novel 50-kDa cytosolic protein, Secernin 1 (SCRN1), which is proposed to be involved in regulating exocytosis in permeablised mast cells (Way *et al.*, 2002).

Leucine Rich Repeat Containing 46 (Lrrc46)

LRRC46 is characterized by leucine rich repeat (LRR) domains which are 20-29 residue protein recognition motifs (Kobe and Deisenhofer, 1995; Kobe and Kajava, 2001) which provide a structural framework for the formation of protein-protein interactions which are known to allow the regulation of neural development (Mutai *et al.*, 2000), gene expression (Linhoff *et al.*, 2001) and apoptosis signaling (Inohara *et al.*, 1999).

Table 5.2 Chromosome 11 candidate genes (*D11Mit67-D11Mit145*).
AK030625 clone will be labelled as *AK* and Hypothetical protein LOC103551 as *HypPro* from this point onwards.

Gene Name (Symbol)	Accession Number	Strand	Genomic Location	Transcript Length	Amino Acids	Exons
Transacting transcription factor 6 (*Sp6*)	NM_031183	1	96829659-96840824	3371	376	1
Secernin 2 (*Scrn2*)	NM_146027	1	96846091-96850040	1278	425	8
Leucine Rich Repeat Containing 46 (*Lrrc46*)	NM_027026	-1	96850692-96857459	1298	323	8
Mitochondrial Ribosomal Protein L10 (*Mrpl10*)	NM_026154	1	96857676-96865303	1682	262	5
T-box 21 (*Tbx21*)	NM_019507	-1	96914097-96931418	2549	530	6
TBK1 Binding Protein 1 (*Tbkbp1*)	NM_198100	-1	96952261-96966138	1893	601	9
Karyopherin (Importin) Beta 1 (*Kpnb1*)	NM_008379	-1	96975800-97003982	5909	876	21
Aminopeptidase puromycin sensitive (*Npepps*)	NM_008942	-1	97021944-97096666	4143	920	23
Mitochondrial Ribosomal Protein L45 (*Mrpl45*)	NM_025927	1	97131946-97146010	2291	306	8
AK030625 clone (*AK030625 or AK*)	AK030625	-1	97152033-97168106	2647	333	2
Suppressor of cytokine signalling 7 (*Socs7*)	NM_138657	1	97178641-97214632	7015	579	9
Rho GTPase activating protein 23 (*Arhgap23*)	NM_021493	1	97282114-97318492	3096	352	1
P140 Caspase-associated protein (*P140cap*)	NM_018873	-1	97327759-97390009	4592	1248	20
Hypothetical Protein LOC103551 (*E130012A19Rik or HypPro*)	NM_175332	-1	97444262-97445371	1110	396	1
Mixed Lineage-Leukaemia Translocation to 6 Homolog (Drosophila) (*Mllt6*)	NM_139311	1	97479567-97498621	4279	1079	20
Polycomb group ring finger (*Pcgf2*)	NM_009545	-1	97505910-97516587	1755	342	13
Proteasome (Prosome, Macropain) Subunit, Beta Type 3 (*Psmb3*)	NM_011971	1	97519524-97529590	731	205	6

Mitochondrial Ribosomal Protein L10 (Mrpl10) and L45 (Mrpl45)

MRPL10 and MRPL45 are precursor protein components of the mitochondrial ribosome large subunit (39S) which comprises a 16S ribosomal RNA (rRNA) and approximately 50 distinct proteins and is responsible for synthesis of 13 mitochondrial components involved in oxidative phosphorylation (Mears *et al.*, 2006).

T-box 21 (Tbx21)

The T gene encodes proteins characterised by the presence of a 'T-box' which is a 200-conserved amino-acid sequence involved in DNA binding (Smith, 1999). *T-box* genes play a role in the activation of transcription and several of these genes have been implicated in developmental abnormalities (Bamshad *et al.*, 1997; Li *et al.*, 1997). *Tbox21* is predominantly expressed in spleen and lung and in natural killer cells (Zhang and Yang, 2000).

TBK1 Binding Protein 1 (Tbkbp1)

TBKBP1 is not well characterised in mice but human TBKBP1 is an adaptor protein with a potential role in the TNF-α/NF-κB signal transduction pathway (Bouwmeester *et al.*, 2004).

Karyopherin (Importin) Beta 1 (Kpnb1)

KPNB1 plays a key role in nuclear protein import and mediates the targeting of nuclear localization signal substrates bound to adaptor proteins (Gorlich *et al.*, 1994; Imamoto *et al.*, 1995).

Aminopeptidase puromycin sensitive (Npepps)

NPEPPS is involved in protein degradation. It is a widely expressed aminopeptidase thought to be involved in the degradation of enkephalins (de la Baume *et al.*, 1983). As previously described (Section 3.2), there is evidence that TAU pathology is a feature of vCJD (Giaccone *et al.*, 2007). A genomic screen for modifiers of tauopathy has identified murine NPEPPS as an inhibitor of TAU -induced neurodegeneration (Karsten *et al.*, 2006) and it has also been shown to degrade TAU *in vitro* (Sengupta *et al.*, 2006). Therefore the function of NPEPPS may be related to prion pathology via an involvement with TAU.

Suppressor of cytokine signalling 7 (Socs7)

Human SOCS7 may have a potential role in adhesion-dependent signalling and cytoskeletal remodelling as it has been shown to interact with the cytoskeletal molecule vinexin (Martens *et al.*, 2004). SOCS7 deficiency in mice leads to the development of hydrocephalus (Krebs *et al.*, 2004) and enhanced insulin action (Banks *et al.*, 2005) suggesting an important role for this candidate in the brain and also in regulating insulin signalling.

Rho GTPase activating protein 23 (Arhgap23)

A RIKEN cDNA gene, 4933428G20Rik, provisionally named Rho GTPase activating protein 23 (*Arhgap23*) is not well characterised but belongs to a family of 22 small GTPases responsible for the regulation of cytoskeleton organization, gene transcription, cell cycle entry and cell survival (Etienne-Manneville and Hall, 2002).

P140 gene (P140cap)

P140CAP (Caspase-associated protein) is a tyrosine phosphorylated p130Cas-associated protein which plays a role in cytoskeletal organisation and is involved in intergrin- and epidermal growth factor (EGF)-dependent signalling (Di Stefano *et al.*, 2004).

Mixed Lineage-Leukaemia Translocation to 6 Homolog (Drosophila) (Mllt6)

Chromosomal translocations at 11q23 are associated with human acute leukaemias. The MLL fusion gene spans the breakpoint in 11q23 and is frequently rearranged leading to different fusion genes (Mitterbauer-Hohendanner and Mannhalter, 2004; Ziemin-van der Poel *et al.*, 1991). MLLT6 is a partner gene of MLL and the mouse homolog, MLLT6, is investigated in this study.

Polycomb group ring finger (Pcgf2)

PCGF2, also known as MEL-18, belongs to a RING-finger motif family and has a role in cell proliferation and tumorigenesis (Kanno *et al.*, 1995). PCGF2 has recently been shown to transcriptionally downregulate an important regulator of cell proliferation, BMI-1 (Guo *et al.*, 2007).

Proteasome (Prosome, Macropain) Subunit, Beta Type 3 (Psmb3)

PSMB3 is a subunit of the 20S proteasome, the catalytic portion of the 26S mammalian proteasome, involved in the degradation of misfolded and short-lived regulatory

proteins (Elenich *et al.*, 1999). As previously discussed (Section 1.1.10), proteasome dysfunction is thought to play a central role in prion pathogenesis (Kristiansen *et al.*, 2005) and so this gene is a potentially interesting candidate for analysis.

The function of the clone *AK030625 (AK)* and hypothetical Protein LOC103551 (*HypPro*) are unknown as these genes and their protein products are currently not well characterised.

5.4 Candidate Gene Sequence Polymorphisms

As previously described (Section 3.3), sequence analysis of candidate genes was undertaken in order to identify polymorphisms, indicative of genetic differences controlling incubation time, between the founder strains of the HS and also between the 'short' and 'long' incubation time strains used to originally identify chromosome 11 QTL (Lloyd et al., 2001; Stephenson et al., 2000). Sequence analysis of the whole 708kb region of interest would be ideal for completeness but such a detailed analysis, including genomic regions between candidate genes, would be time-consuming and laborious. Instead sequence of potential functional significance, i.e., protein coding sequence or genomic motifs potentially controlling gene expression were prioritised over less well characterised regions. Details of PCR primer sequence and conditions for use are listed in Appendix 2.1. Sequence polymorphism data is listed in Table 5.3.

Candidate genes within the region of interest proved not very polymorphic between the parental strains of the HS as only 79 polymorphisms were identified in total. 2 polymorphisms were identified in predicted promoter regions, 5 in introns and 72 in exons, of which 7 were nonsynonymous. Most polymorphisms identified were SNPs (n=75) with only a small number involving deletion (n=2) or insertion (n=2) of sequence. Three haplotype patterns were observed across the region of interest (Table 5.3). The most common SDP includes 48 polymorphisms throughout *Sp6*, *Scrn2*, *Lrrc46*, *Mrpl10*, *Tbx21*, *Tbkbp1*, *Kpnb1* and *Psmb3* whose alleles segregated into one group containing A/J, AKR/J and CBA/J and another containing the remaining parental strains. Two other haplotype patterns were also seen with a smaller number of polymorphisms. 7 polymorphisms in *Sp6* had alleles segregating into one group of A/J, AKR/J, CBA/J, C3H/HeJ, DBA/2J and LP/J and another including BALB/cJ and C57BL/6J. 13 polymorphisms identified throughout *Npepps*, *Mrpl45*, *AK*, *P140*, *HypPro*, *Mllt6* and *Psmb3* segregated into a first group including A/J, AKR/J BALB/cJ

Table 5.3 Haplotype pattern of alleles mapping between *D11Mit67* and *D11Mit145*.
Ex=Exonic, Pro=Promoter, 3'=3'UTR, 5'=5'UTR, Intr=Intronic, Del=Deletion, MM=Microsatellite Marker, Ins=Insertion, NC=No Change (compared to NCBI, Ensembl and UCSC database sequence), ND=Not Determined and bp=base pair. Nonsynonymous polymorphisms are indicated by amino acid abbreviations flanking the relevant codon number. Shading illustrates polymorphism haplotype patterns. –logP values are derived from HAPPY analysis.

Marker/Polymorphism Description		Position	A	AKR	CBA	C3H	DBA	LP	BALB	C57	NZW	CAST	SJL	-logP
D11Mit67	MM	96822957	176	176	176	124	124	124	134	132	ND	ND	ND	4.55
m*Sp6*Intr#2	Intr	96837488	T	T	T	T	T	T	A	A	T	T	A	4.87
m*Sp6* 5'#1	Ex5'	96837538	C	C	C	C	C	C	T	T	C	C	T	4.87
m*Sp6*x1#2	Ex	96837765	A	A	A	G	G	G	G	G	A	G	G	1.79
m*Sp6*x1#4	Ex	96838209	T	T	T	A	A	A	A	A	T	T	A	1.79
m*Sp6*x1#5	Ex	96838321	C	C	C	T	T	T	C	C	C	C	C	4.53
m*Sp6*x1#6	Ex	96838627	G	G	G	G	G	G	A	A	G	G	A	4.87
m*Sp6* 3'#1	Ex3'	96838757	G	G	G	G	G	G	C	G	G	G	G	3.32
m*Sp6* 3'#3	Ex3' Ins	96839048	1bp	1bp	1bp	NC	NC	NC	NC	NC	1bp	NC	NC	1.79
m*Sp6* 3'#4	Ex3'	96839277	C	C	C	C	C	C	T	T	C	C	C	4.87
m*Sp6* 3'#8	Ex3'	96839761	G	G	G	G	G	G	A	A	G	G	A	4.87
m*Sp6* 3'#9	Ex3'	96839954	C	C	C	C	C	C	T	T	C	C	T	4.87
m*Sp6* 3'#11	Ex3'	96840256	T	T	T	C	C	C	C	C	T	C	C	1.79
m*Sp6* 3'#12	Ex3'	96840344	T	T	T	A	A	A	A	A	T	A	A	1.79
m*Sp6* 3'#13	Ex3'	96840494	G	G	G	G	G	G	A	A	G	G	A	4.87
m*Sp6* 3'#14	Ex3'	96840549	T	T	T	C	C	C	C	C	ND	C	C	1.79
m*Sp6* 3'#16	Ex3'	96840769	C	C	C	T	T	T	C	C	C	C	C	4.53
m*Scrn2*x5#1	T199A	96848883	G	G	G	A	A	A	A	A	G	A	A	1.79
m*Scrn2*x5#2	Ex	96848921	C	C	C	T	T	T	T	T	C	C	T	1.79
m*Scrn2*Intr#2	Intr	96849119	C	C	A	A	A	A	A	A	A	C	A	1.22
m*Scrn2*Intr#3	Intr	96849142	T	T	T	C	C	C	C	C	T	C	C	1.79
m*Scrn2*x7#1	Ex	96849508	G	G	G	A	A	A	A	A	G	G	A	1.79
m*Scrn2*x7#2	Ex	96849583	C	C	C	T	T	T	T	T	C	C	T	1.79
m*Scrn2*x8#2	Ex	96849833	C	C	C	G	G	G	G	G	C	G	G	1.79
m*Scrn2*x8#3	A406P	96849852	C	C	C	G	G	G	G	G	C	C	G	1.79
m*Lrrc46* 3'#1	Ex3'	96850740	G	G	G	A	A	A	A	A	G	A	A	1.79
m*Lrrc46*x8#3	T279S	96850893	T	T	T	A	A	A	A	A	T	T	A	1.79
m*Lrrc46*x8#2	Ex	96850987	C	C	C	T	T	T	T	T	C	T	T	1.79
m*Lrrc46*x7#1	Ex	96851640	A	A	C	C	C	A	C	C	A	A	C	0.70
m*Lrrc46*x5#2	Ex	96852253	T	T	T	C	C	C	C	C	T	C	C	1.79
m*Lrrc46*Intr#1	Intr	96854985	C	C	C	T	T	C	T	T	C	C	T	1.43
m*Lrrc46* 5'#3	Ex5'	96857269	G	G	G	A	A	A	A	A	G	G	A	1.79
m*Lrrc46* 5'#2	Ex5'	96857316	T	T	T	C	C	C	C	C	T	C	C	1.79
m*Mrpl10*x1#1	Intr	96857670	T	T	T	G	G	G	G	G	T	T	G	1.79
m*Mrpl10*x2#1	Ex	96860679	G	G	G	A	A	A	A	A	G	A	A	1.79
m*Mrpl10*x2#2	Ex	96860742	T	T	T	C	C	C	C	C	T	C	C	1.79
m*Mrpl10*x4#1	R141Q	96863537	A	A	A	G	G	G	G	G	A	A	G	1.79
m*Mrpl10*x5#1	Ex	96864176	T	T	T	C	C	C	C	C	T	C	C	1.79
m*Mrpl10*x5#2	G262C	96864420	T	T	T	G	G	G	G	G	T	G	G	1.79
m*Mrpl10* 3'#1	Ex 3'	96864482	T	T	T	C	C	C	C	C	T	C	C	1.79
m*Mrpl10* 3'#2	Ex3'	96864606	G	G	G	C	C	C	C	C	G	G	C	1.79
m*Mrpl10* 3'#3	Ex3'	96864719	T	T	T	G	G	G	G	G	T	G	G	1.79
m*Mrpl10* 3'#4	Ex3'	96864771	C	C	C	A	A	A	A	A	C	A	A	1.79
m*Mrpl10* 3'#5	Ex3'	96864826	G	G	G	C	C	C	C	C	G	G	C	1.79
m*Mrpl10* 3'#6	Ex3'	96864844	A	A	A	C	C	C	C	C	A	C	C	1.79
m*Mrpl10* 3'#7	Ex3'	96864875	T	T	T	A	A	A	A	A	T	T	A	1.79
m*Mrpl10* 3'#8	Ex3'	96864878	T	T	T	C	C	C	C	C	T	C	C	1.79
m*Mrpl10* 3'#9	Ex3'	96865008	T	T	T	C	C	C	C	C	T	T	C	1.79
m*Mrpl10* 3'#11	Ex3'	96865048	A	A	A	G	G	G	G	G	A	G	G	1.79
m*Mrpl10* 3'#12	Ex3'	96865129	G	G	G	T	T	T	T	T	G	G	T	1.79
m*Mrpl10* 3'#13	Ex3'	96865234	T	T	T	A	A	A	A	A	T	ND	A	1.79
m*Mrpl10* 3'#14	Ex3' Ins	96865276	2bp	2bp	2bp	NC	NC	NC	NC	NC	2bp	2bp	NC	1.79
m*Mrpl10* 3'#15	Ex3' Del	96865280	5bp	5bp	5bp	NC	NC	NC	NC	NC	5bp	NC	NC	1.79
m*Mrpl10* 3'#16	Ex3'	96865296	A	A	A	T	T	T	T	T	A	A	T	1.79
m*Tbox21* 3'#5	Ex3'	96914318	C	C	C	T	T	T	T	T	C	C	T	1.79
m*Tbox21* 3'#4	Ex3'	96914385	A	A	A	G	G	G	G	G	A	G	G	1.79
m*Tbox21* 3'#1	Ex3'	96914595	T	T	T	C	C	C	C	C	T	C	C	1.79
m*Tbox21*x6#6	Ex	96914976	A	A	A	G	G	G	G	G	A	A	G	1.79
m*Tbox21*x4#1	Ex	96916077	G	G	G	A	A	A	A	A	G	G	A	1.79
m*Tbkbp1* 5'#1	Ex5'	96966138	G	G	G	A	A	A	A	A	G	G	A	1.79
m*Kpnb1*x17#1	Ex	96981484	A	A	A	G	G	G	G	G	G	G	G	1.79
m*Npepps* 3'#1	Ex3'	97022754	C	C	C	A	A	A	C	A	C	C	C	3.06
m*Npeppsx*23#1	Ex	97023289	C	C	C	C	C	T	C	T	C	C	C	0.68

Marker/Polymorphism Description		Position	A	AKR	CBA	C3H	DBA	LP	BALB	C57	NZW	CAST	SJL	-logP
m*Mrpl45*x4#1	Ex	97139980	G	G	G	A	A	A	G	A	G	G	G	3.06
m*Mrpl45* 3'#8	Ex3'	97145285	G	G	G	A	A	A	G	A	A	G	G	3.06
m*Mrpl45* 3'#9	Ex3'	97145357	T	A	T	A	A	A	T	A	A	A	T	3.60
*AK*x2#2	P308L	97165763	T	T	T	C	C	C	T	C	C	C	T	3.06
*AK*x2#1	Ex	97165867	T	T	T	C	C	C	T	C	T	C	T	3.06
*AK*Pro#1	Pro Del	97166576	1bp	1bp	1bp	NC	NC	NC	1bp	NC	NC	ND	1bp	3.06
m*P140*x8#5	R487M	97350859	T	T	T	T	T	G	T	G	T	T	G	0.68
m*P140*x6#1	Ex	97352493	G	G	G	T	T	T	G	T	G	G	G	3.06
m*P140*x2#6	Ex	97367809	C	G	C	C	C	C	C	C	C	T	C	0.92
m*P140*x2#1	Ex	97368034	C	C	C	A	A	A	C	A	C	C	C	3.06
m*HypProx*1#2	Ex	97445220	T	T	T	C	C	C	T	C	C	C	T	3.06
m*HypProx*1#1	Ex	97445267	T	T	T	C	C	C	T	C	C	C	T	3.06
m*Mllt6*x18#1	Ex	97495080	T	T	T	C	C	C	T	C	C	C	T	3.06
m*Mllt6* 3'#4	Ex3'	97498499	C	T	T	T	T	T	T	T	T	C	T	1.48
m*Mllt6* 3'#7	Ex3'	97498625	A	A	A	T	T	T	A	T	A	A	A	3.06
m*Psmb3*Pro#1	Pro	97518684	T	T	T	C	C	C	T	C	C	C	T	3.06
m*Psmb3*x5#1	Ex	97528574	A	A	A	G	G	G	G	G	G	G	G	1.79
D11Mit145	MM	97530769	136	136	136	152	152	152	136	152	ND	ND	ND	2.67

and CBA/J and a second containing C3H/HeJ, C57BL/6J, DBA/2J and LP/J. The further characterisation of polymorphisms potentially controlling prion disease incubation time was undertaken using HAPPY linkage analysis software and is described in the next section.

5.5 HAPPY Analysis of Polymorphisms

Using the confirmed allele sizes of selected microsatellite markers in the progenitor strains of the HS (Table 5.1) HAPPY linkage analysis software (Section 2.4.4.5) attempts to reconstruct ancestral haplotypes associated with prion disease incubation time in the cross by calculating the probability that an allele is descended from one of the eight founder strains at any given locus (Mott et al., 2000). The SDP of polymorphisms identified in the parental strains of the HS were analysed using HAPPY to find matches with its simulated reconstruction, therefore identifying polymorphisms potentially associated with incubation time (Figure 5.3).

24 polymorphisms identified between the parental strains of the HS reached a threshold value for 'suggestive' linkage (-logP >2.8) and 9 of these reached the threshold level for 'significant' linkage (-logP >4.3) (Lander and Kruglyak, 1995) (Figure 5.3 and Table 5.3). All polymorphisms reaching a threshold of significant linkage were identified in *Sp6* and therefore this candidate has been highlighted by HAPPY as the most promising candidate gene for the HS within the new region of linkage. The most significant polymorphisms (-logP=4.87), which are the focus of further analysis, had a SDP dividing A/J, AKR/J, CBA/J, C3H/HeJ, DBA/2J and LP/J in one group and BALB/cJ and C57BL/6J into another. This was the general haplotype pattern seen in *Sp6*,

Figure 5.3 HAPPY analysis output for polymorphisms identified between *D11Mit67* and *D11Mit145*.
The x axis measures distance along the chromosome between the flanking markers (vertical lines) of the region of significant linkage. The y axis indicates –logP values. Each polymorphism is identified as a black dot on the plot. Polymorphism –logP values of >2.8 reach the threshold for suggestive linkage or and those >4.3 reach a significant linkage threshold and are highlighted within red boxes.

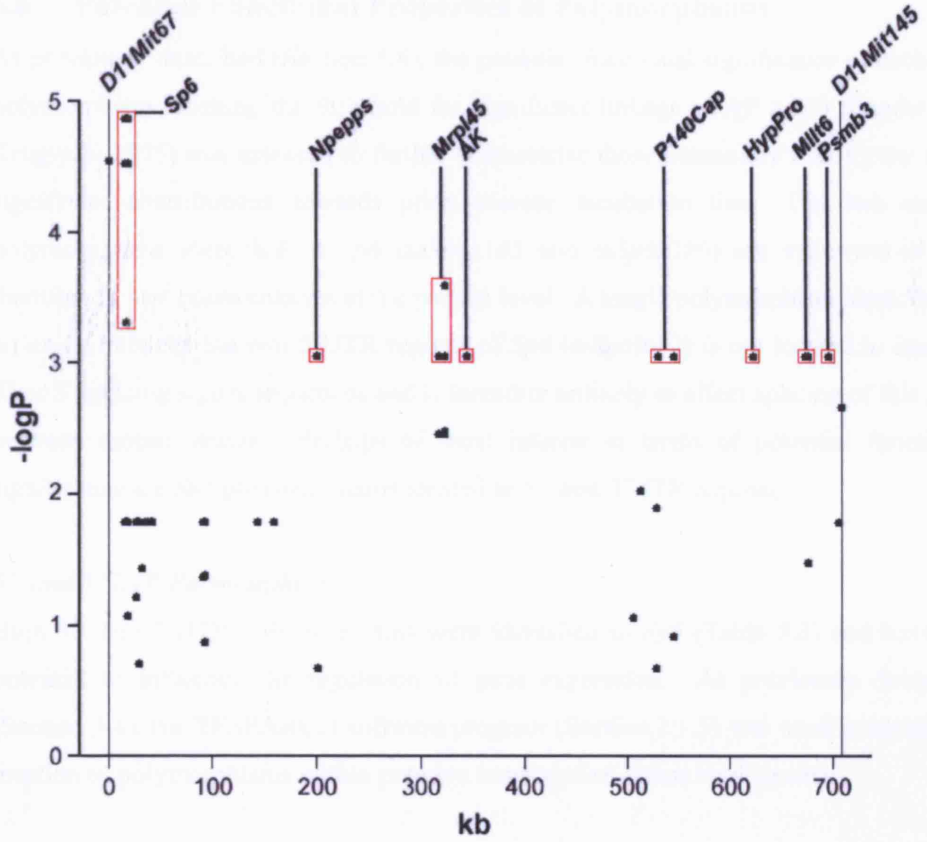

occurring in seven polymorphisms. A second SDP (-logP=4.53) was observed in two polymorphisms (m*Sp6*x1#5 and m*Sp6* 3'#16) which segregated C3H/HeJ, DBA/2J and LP/J in one group and the remaining parental strains in another.

Based on an assumption that the new region of interest identified in the HS is the same QTL as identified in original mapping studies, polymorphisms identified between the parental strains of the HS must also be polymorphic between the 'short' and 'long' incubation time strains, therefore containing genetic differences that potentially underpin the observed phenotypic variation between these strains. Of the nine *Sp6* polymorphisms observed between the parental strains of the HS and reaching a threshold of significant linkage, six were also polymorphic between SJL/J and CAST/Ei

strains but none were polymorphic between NZW/OlaHsd and CAST/Ei (Table 5.3). This implies that *Sp6* is a potential QTG for the SJL/J and CAST/Ei F2 intercross (Stephenson et al., 2000) but not for the NZW/OlaHsd and CAST/Ei F2 intercross (Lloyd et al., 2001).

5.6 Potential Functional Properties of Polymorphisms

As previously described (Section 3.4), the potential functional significance of each *Sp6* polymorphism reaching the threshold for significant linkage (-logP >4.3) (Lander and Kruglyak, 1995) was assessed to further characterise those potentially making the most significant contributions towards prion disease incubation time. The two exonic polymorphisms identified in *Sp6* (m*Sp6*x1#5 and m*Sp6*x1#6) are synonymous and therefore do not cause changes at the protein level. A single polymorphism identified in an intron between the two 5'UTR regions of *Sp6* (m*Sp6*In#2) is not located in intronic 5' or 3' splicing signal sequences and is therefore unlikely to effect splicing of this gene between mouse strains. Perhaps of most interest in terms of potential functional significance are *Sp6* polymorphisms located in 5'- and 3'UTR regions.

5'- and 3' UTR Polymorphisms

Both 5'- and 3'UTR polymorphisms were identified in *Sp6* (Table 5.3) and have the potential to influence the regulation of gene expression. As previously described (Section 3.4), the TFSEARCH software program (Section 2.1.5) was used to assess the location of polymorphisms within putative transcription factor binding sites.

A polymorphism identified in the 5'UTR (m*Sp6* 5'#1) and one in the 3'UTR (m*Sp6* 3'#13) of *Sp6* are located in a putative binding site for the previously described (Section 3.4.2) transcription factor, *Gata-1*, involved in erythroid development (Pevny et al., 1995) (Figure 5.4).

Figure 5.4 *Sp6* 5'- and 3'UTR polymorphisms in putative *Gata-1* binding sites.
The sequence comprising the putative transcription factor binding site is illustrated by a broken arrow and the position of the polymorphisms and their alternative nucleotide bases are highlighted in red.

A second 3'UTR SNP (m*Sp6* 3'#9) is located in a putative binding site for Heat Shock Transcription Factor 1 (*Hstf1*) and 2 (*Hstf2*) which are the transcriptional activators responsible for the inducible expression of heat shock genes such as HSP70 (Abravaya *et al.*, 1991) (Figure 5.5). This is noteworthy since heat shock proteins are an established feature of prion pathogenesis (Kenward *et al.*, 1994; Kenward *et al.*, 1996; Kovacs *et al.*, 2001; Laszlo *et al.*, 1992; Tatzelt *et al.*, 1998).

Figure 5.5 *Sp6* 3'UTR polymorphism in putative *Hstf1* and *Hstf2* binding sites.
The sequence comprising the putative transcription factor binding sites are illustrated by a broken arrow for the sense and anti-sense strand for both *Hstf1* and *Hstf2*. The position of the polymorphism and its alternate nucleotide bases are highlighted in red.

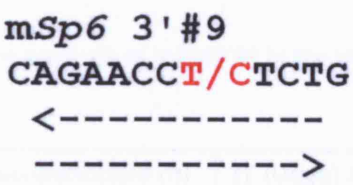

5.7 Testing Individual Polymorphisms for Linkage

It is necessary to test HAPPY's simulation of the polymorphism SDPs associated with prion disease incubation time because HAPPY can only predict the position of recombination points in the HS based upon its reconstruction of ancestral haplotypes using progenitor strain microsatellite marker genotypes. The exact points of recombination within the HS are unknown and may occur within marker intervals defined by HAPPY as associated with incubation time. In addition, numerous cycles of breeding to generation 37 in the HS may have caused some of the polymorphisms present in the progenitor strains to have been lost in the cross.

To verify the accuracy of HAPPY's prediction and confirm an association between genotype and incubation time, a *Sp6* 3'UTR polymorphism (m*Sp6*3'#9) which is representative of the most significant SDP across the region of interest (-logP=4.87) (Table 5.3) was tested in 944 generation 37 HS mice by allelic discrimination (Sections 2.4.5.1, 2.4.5.5 and Table 5.4). This polymorphism was chosen because of its potential functional significance based upon its location within a putative transcription factor binding site for *Hsf1* and *Hsf2* (Section 5.6). Details of primer and fluorescently labelled probe sequences for allelic discrimination are listed in Appendix 4.

The individual T and C alleles of m*Sp6*3'#9 are associated with a mean incubation time of 152±1.1 days and 147±0.4 days, respectively (Table 5.4). A significant difference of 5 days in mean incubation time is observed between these alleles ($p<0.0001$, Mann Whitney non-parametric ANOVA). The mean incubation time of m*Sp6*3'#9 TT, CT and CC genotypes are 150±5.8 days, 152±1.1 days and 146±0.6 days respectively (Table 5.4). A significant association between m*Sp6*3'#9 genotype and incubation time is observed ($p<0.0001$, One-way ANOVA). A significant difference of 6 days was seen between CT and CC genotypes ($p<0.001$, Tukey-Kramer Multiple Comparisons test) but no significant difference was observed between TT and CT. The T allele is dominant conferring long incubation times in heterozygote mice.

Table 5.4 Genotype/phenotype analysis of m*Sp6*3'#9 in the HS.
IT=incubation time.

Allele/Genotype (n)	IT (Days) SEM
C (1680)	147 ± 0.4
T (208)	152 ± 1.1
CC (745)	146 ± 0.6
CT (190)	152 ± 1.1
TT (9)	150 ± 5.8

A significant association between incubation time and the alleles and genotypes of m*Sp6*3'#9, a representative SNP of the most significant SDP has been established confirming the prediction of HAPPY linkage analysis (Section 5.5). It is likely that the same association can be extended to other *Sp6* polymorphisms characterised by this SDP and the association may also be true for SJL/J and CAST/Ei strains since they are polymorphic at these loci (Table 5.3).

5.8 *Sp6* Expression

As previously described (Section 3.5), another means by which to identify important candidates controlling prion disease incubation time is by examining differential gene expression to investigate a correlation between expression and genotype. 5'- and 3'-UTR polymorphisms in *Sp6* reaching the threshold for significant linkage (-logP >4.3) (Table 5.3), may be potential candidates influencing prion disease incubation time through their propensity to affect regulation of gene expression.

As previously described (Section 3.5) qRT-PCR was performed for *Sp6*, using custom designed Taqman probes and primers (Sections 2.4.5.1), to assess mRNA expression. cDNA was generated (Section 2.4.1.5) from whole brain RNA extracted (Sections 2.4.1.2-3) from 8-week old male mice. Mouse strains included the parental strains of the HS, with the exception of LP/J which was unavailable, and also the 'short' and 'long' incubation time strains used in the original mapping studies. Due to availability, the SJL/JOlaHsd mouse strain was used as a substitute in place of the SJL/J strain used in the original mapping studies to identify linkage (Stephenson et al., 2000). *Sp6* expression in normal and Chandler/RML infected (Section 2.2.4-5) NZW/OlaHsd, SJL/OlaHsd and CAST/Ei mice in the terminal stages of disease (Section 2.2.6) were also quantified to investigate whether this candidate gene is differentially regulated in prion disease. Commercially available murine GAPDH (Section 2.1.1) was duplexed within reactions as an endogenous control to normalise expression data (Section 2.4.5.2). Full details of primer sequences for qRT-PCR can be found in Appendix 3.

HS parental strains

A significant difference in *Sp6* expression was observed between the parental strains of the HS when they were grouped by allele for the most significant SDP (P=0.05, Mann Whitney Test) (Figure 5.6).

Figure 5.6 *Sp6* mRNA expression in the parental strains of the HS.
Shading of bars refers to Table 5.3. All samples were tested in triplicate. Units are arbitrary and represent quantity of *Sp6* transcript normalised by quantity of GAPDH. Error bars represent SEM. * indicates P=0.05.

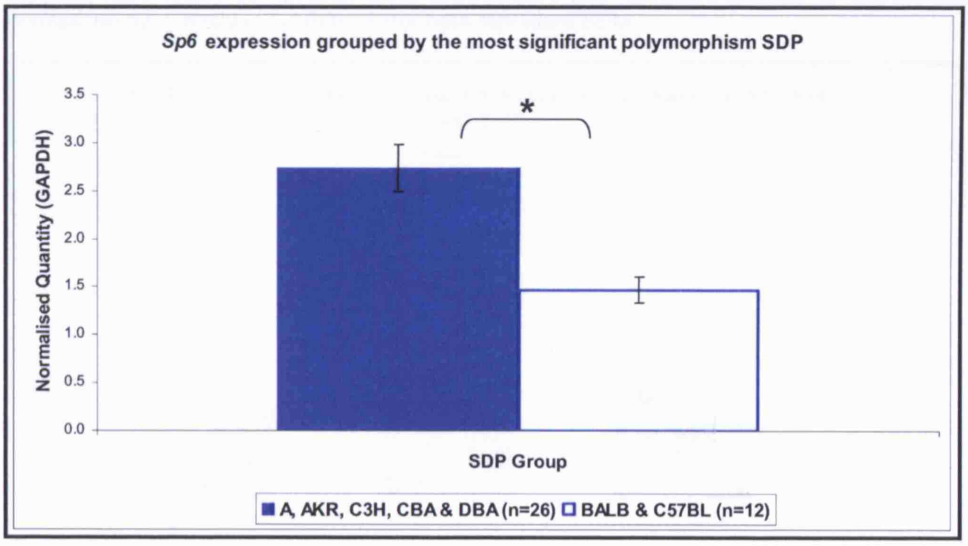

Normal and Chandler/RML infected SJL, NZW and CAST strains

A significant difference in *Sp6* expression was observed between normal SJL/OlaHsd and CAST/Ei strains (P<0.0001, two-tailed unpaired t test) but not between NZW/OlaHsd and CAST/Ei (Figure 5.7). The difference in *Sp6* expression between these 'short' and 'long' incubation time strains is noteworthy since these data are consistent with the SDP previously identified as associated with incubation time (Section 5.7) and provides further support for *Sp6* as a potential QTG for the SJL/J and CAST/Ei F2 intercross (Stephenson et al., 2000). A significant difference in *Sp6* expression was observed between normal CAST/Ei and Chandler/RML infected CAST/Ei mice (P=0.0238, Mann-Whitney Test) (Figure 5.7) but no significant differences were observed between normal and Chandler/RML infected mice within SJL/OlaHsd and NZW/OlaHsd strains. It is unlikely that the *Sp6* sequence variants identified in this study are responsible for the significant upregulation of *Sp6* mRNA expression in Chandler/RML infected CAST/Ei because NZW/OlaHsd shares the same alleles as CAST/Ei but does not also share the same expression profile. Upregulation in CAST/Ei is therefore, likely to be regulated by other sequence variants such as those potentially residing within unanalysed intronic regions or more remote regions of the genome. In Chandler/RML infected mice a significant difference was observed for both CAST/NZW (P=0.04, Mann-Whitney test) and CAST/SJL comparisons (P=0.005, two-tailed unpaired t test).

Figure 5.7 *Sp6* mRNA expression in normal and Chandler/RML infected mice.
N=6 for all groups except normal NZW (n=5), NZW RML (n=5) and CAST RML (n=3). All samples were tested in triplicate. Units are arbitrary and represent quantity of *Sp6* transcript normalised by quantity of GAPDH. Error bars represent SEM.

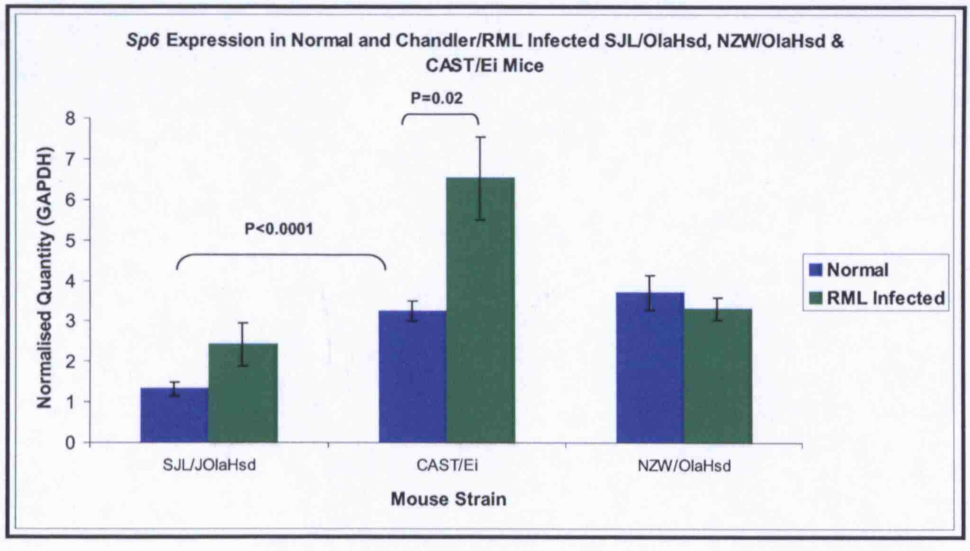

5.9 *Sp6* and *Prnp*

It is plausible to suggest that if *Sp6* is a promising candidate gene for prion disease incubation time its function and activity may be linked to that of *Prnp*, the primary candidate gene involved in prion disease. In its role as a transcription factor, *Sp6* may regulate the expression of genes in biochemical pathways central to prion pathogenesis, potentially including *Prnp*. TFSEARCH analysis (Section 2.1.5) did not identify any putative *Sp6* binding sites for *Prnp*. However, it is possible that there are more remote *Sp6* binding sites elsewhere in the genome which are controlling the expression of *Prnp*. A possible correlation between *Sp6* and *Prnp* expression profiles was investigated.

5.9.1 *Sp6* Expression Profile

The expression profile of *Sp6* in various brain and body tissues was assessed to investigate whether it was comparable to *Prnp*. Co-expression of *Sp6* and *Prnp* in similar tissues may imply a link between the two genes. *Prnp* is expressed ubiquitously at especially high levels in adult mouse brain, intermediary levels in heart and lung, and lower levels in the spleen (Caughey *et al.*, 1988; Oesch *et al.*, 1985). *Sp6* is reported to be ubiquitously expressed in adult mice throughout bladder, skeletal muscle, kidney, testis, lung, spleen, brain, liver and heart (Scohy et al., 2000).

qRT-PCR was performed as previously described (Section 5.8), in several brain and body tissues (Section 2.2.7) of 7-week old male C57BL/6J mice. *Sp6* was expressed at relatively high levels in the lung and spleen compared to other tissues and at relatively low levels in the brain, heart, kidney, liver, large intestine, adrenal gland and thyroid gland (Figure 5.8). Intermediary levels of expression were observed in the thymus, testes and pituitary gland. Overall no direct correlation between the expression profile of *Sp6* and the reported expression profile for *Prnp* (Caughey *et al.*, 1988; Oesch *et al.*, 1985) was observed.

5.9.2 *Prnp* Expression

qRT-PCR was performed for *Prnp* as previously described (Section 3.5), to investigate a correlation between *Sp6* and *Prnp* expression in the parental strains of the HS and also in SJL/OlaHsd, NZW/OlaHsd and CAST/Ei strains. The commercially available, pre-validated TaqMan Gene Expression Assay for the murine prion protein was used to quantify *Prnp* expression (Section 2.1.1).

Figure 5.8 *Sp6* mRNA expression profile.
Expression was quantified in C57BL/6J mice. N=6 per tissue. All samples were tested in triplicate. Units are arbitrary and represent quantity of *Sp6* transcript normalised by quantity of GAPDH. Error bars represent SEM. Brain=brain tissue minus cerebellum.

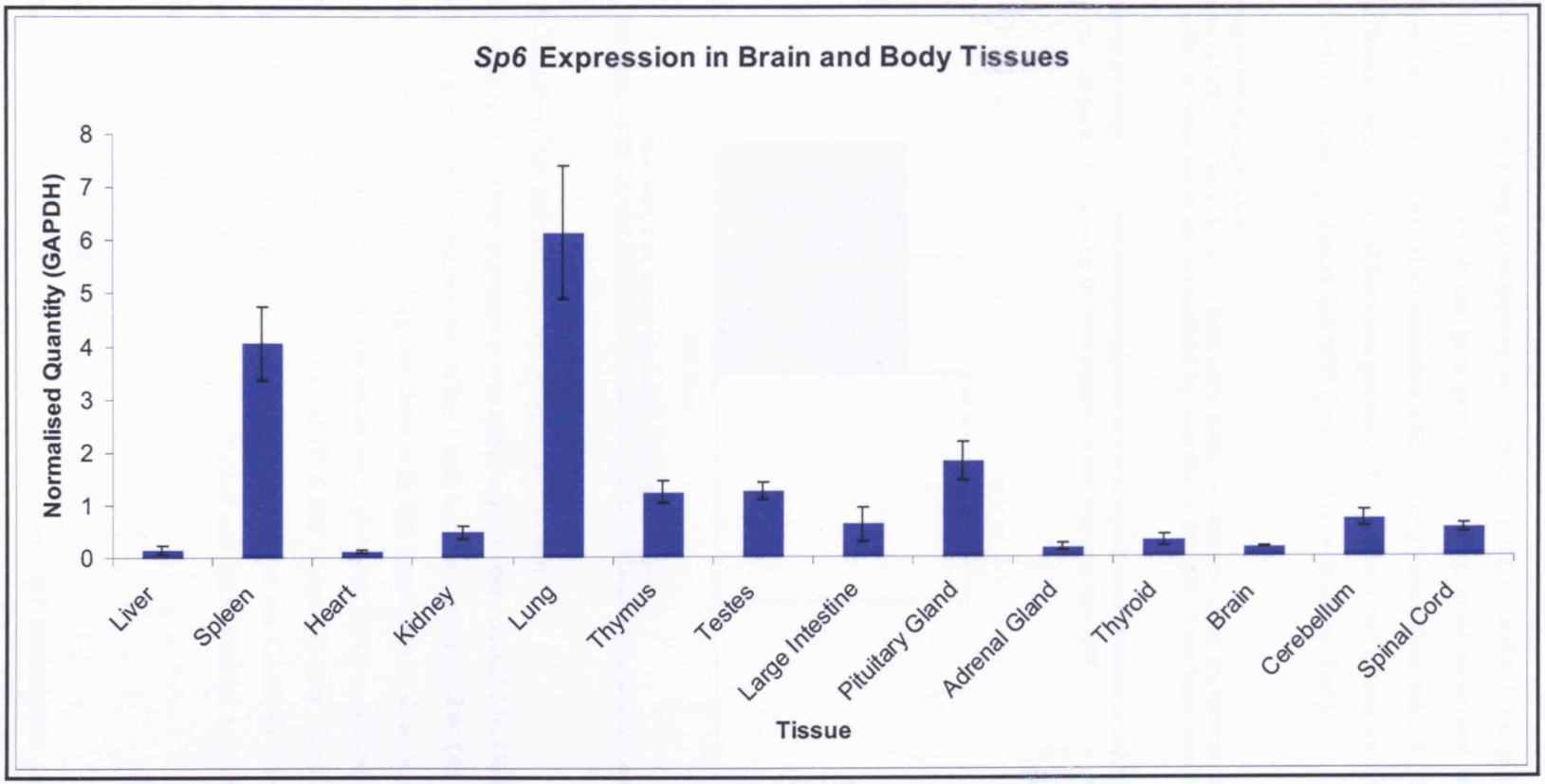

HS parental strains

Prnp expression data was grouped according to the most significant *Sp6* polymorphism SDP, -logP=4.87 (Table 5.3), which has been previously shown to be associated with incubation time (Section 5.7) and also correlates with *Sp6* expression (Section 5.8). No significant difference was observed between groups and therefore *Prnp* expression does not correlate with the most significant *Sp6* SDP (P=0.77, Mann-Whitney Test).

Figure 5.9 *Prnp* mRNA expression.
Shading of bars refers to Table 5.3. All samples were tested in triplicate. Units are arbitrary and represent quantity of *Prnp* transcript normalised by quantity of GAPDH. Error bars represent SEM.

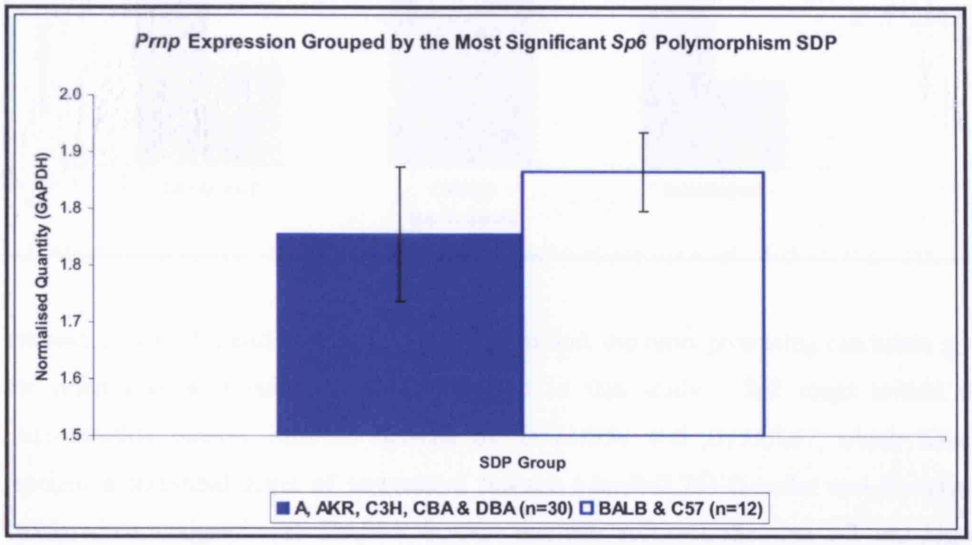

Normal and Chandler/RML infected SJL, NZW and CAST strains

A significant difference in *Prnp* expression was observed between normal SJL/OlaHsd and CAST/Ei mice (p=0.002, unpaired two-tailed t test) but not between NZW/OlaHsd and CAST/Ei (Figure 5.10). This finding correlates with *Sp6* expression in these strains (Section 5.8). Significant differences in expression were also seen between normal and Chandler/RML infected mice within SJL/OlaHsd (P=0.002 Mann Whitney Test) and NZW/OlaHsd (P=0.0008, unpaired two-tailed t test) strains but not CAST/Ei (Figure 5.10). *Prnp* appears to be downregulated in SJL/OlaHsd and NZW/OlaHsd as a result of prion infection.

5.10 *Sp2* Transcription Factor (*Sp2*)

Interestingly a SP/KLF transcription factor family member, *Sp2* transcription factor (*Sp2*), maps 23.9kb away from the flanking microsatellite marker of the region of

Figure 5.10 *Prnp* expression in normal and Chandler/RML infected mice.
N=6 for all groups except Chandler/RML infected CAST/Ei where n=4 and Chandler/RML infected NZW/OlaHsd where n=5. All samples were tested in triplicate. Units are arbitrary and represent quantity of *Prnp* transcript normalised by quantity of GAPDH. Error bars represent SEM.

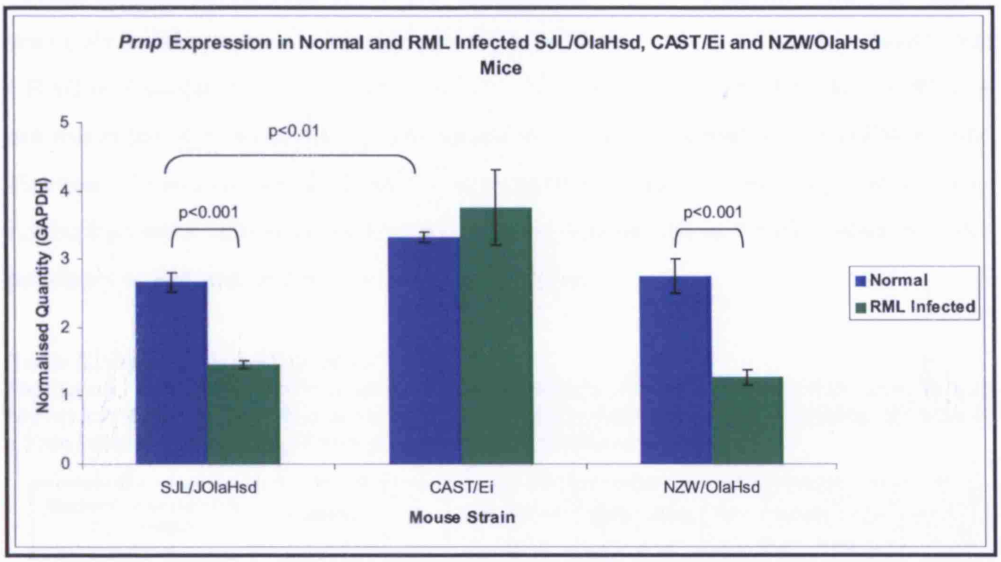

interest, *D11Mit67*, and also 30.6kb away from *Sp6,* the most promising candidate gene for prion disease incubation time identified in this study. *Sp2* maps within the microsatellite marker interval flanked by *D11Mit54* and *D11Mit67* which almost reached a threshold level of suggestive linkage (-logP=2.75) (Lander and Kruglyak, 1995) when analysed with HAPPY linkage analysis software (Section 5.2 and Figure 5.1). *Sp2* is a related partner of *Sp6* and the gene products show similarity with each other at their DNA-binding domains, although *Sp6* is different in terms of nucleotide and amino acid sequences over the remainder of the molecule (Scohy et al., 2000). *Sp6* and *Sp2* are also closely linked in rat and human and it has been suggested that these genes probably evolved following a duplication of an ancestral gene (Scohy *et al.*, 1998). The close proximity and related function of *Sp2* to *Sp6* made it an interesting additional candidate for analysis. As previously described, putative promoter regions and the exons of *Sp2* (NCBI accession number NM_030220) were PCR amplified (Section 2.4.2) for sequencing (Section 2.4.3) in the parental strains of the HS to identify sequence variants which may be controlling prion disease incubation time in these strains. 14 *Sp2* SNPs were found (Table 5.5), 13 of which are located in exons, one causing an amino acid substitution at codon 161. A single intronic SNP was identified in intron 1.

As previously described (Section 5.5), HAPPY linkage analysis was used to ascertain whether there is an association between the SDP of these polymorphisms and incubation time. No SNPs reached a threshold of suggestive (>2.8) or significant (>4.3) linkage (Lander and Kruglyak, 1995). A general SDP was observed across the region with polymorphism alleles segregating into two groups, one including A/J, AKR/J and CBA/J and another C3H/HeJ, DBA/2J, LP/J, BALB/cJ and C57BL/6J. This SDP does not match the significant SDP in *Sp6* established to be associated with incubation time (Section 5.7) and correlating with *Sp6* expression (Section 5.8) implying that *Sp2* may not be a potential candidate for prion disease incubation time in the HS despite its close proximity to *Sp6* and related structure and function.

Table 5.5 Haplotype pattern of *Sp2* alleles.
Ex=Exonic, 3'=3'UTR, Intr=Intronic, MM=Microsatellite Marker and ND=Not Determined. Nonsynonymous polymorphisms are indicated by amino acid abbreviations flanking the relevant codon number. Shading illustrates polymorphism haplotype patterns.

Marker/Polymorphism Description		Position	A	ARK	CAB	C3H	DAB	LP	BLAB	C57	-logP
D11Mit54	MM	96101729	111	111	111	141	138	141	141	141	4.23
m*Sp2* 3'#11	Ex 3'	96769854	C	C	C	T	T	T	T	T	1.22
m*Sp2* 3'#10	Ex 3'	96769857	C	C	C	T	T	T	T	T	1.22
m*Sp2* 3'#9	Ex 3'	96769880	T	T	T	C	C	C	C	C	1.22
m*Sp2* 3'#8	Ex 3'	96770023	G	G	G	A	A	A	A	A	1.22
m*Sp2* 3'#6	Ex 3'	96770146	C	C	C	G	G	G	G	G	1.22
m*Sp2* 3'#4	Ex 3'	96770342	T	T	T	C	C	C	C	C	1.22
m*Sp2* 3'#3	Ex 3'	96770411	A	A	A	G	G	G	G	G	1.22
m*Sp2*x8#1	Ex	96770605	T	T	T	C	C	C	C	C	1.22
m*Sp2*x7#1	Ex	96772031	T	T	T	C	C	C	C	C	1.22
m*Sp2*x6#1	Ex	96772323	C	C	C	T	T	T	T	T	1.22
m*Sp2*x5#1	Ex	96773782	A	A	A	C	C	C	C	C	1.22
m*Sp2*x4#5	T161I	96777687	T	T	T	T	T	T	T	C	1.88
m*Sp2*x4#1	Ex	96778088	G	G	G	A	A	A	A	A	1.22
m*Sp2*x2#1	Intr	96779446	A	A	A	G	G	G	G	A	2.15
D11Mit67	MM	96822957	176	176	176	124	124	124	134	132	4.55

5.11 Conclusion

In summary, the fine mapping of chromosome 11 QTL has been successfully achieved and described in this chapter. The region of interest has been reduced from 86.5Mb to 0.7Mb, allowing the further characterisation of individual candidate genes for prion disease incubation time. Sequence variants identified between the parental strains of the HS were assessed for linkage by HAPPY which highlighted a single candidate, *Sp6*. Polymorphisms identified in the 3'UTR of *Sp6* are located in putative transcription

factor binding sites for *Hsf1* and *Hsf2* suggesting possible implications for differential regulation of gene expression between mouse strains. A correlation between *Sp6* genotype and mRNA expression has also been established. *Sp6* may also be an important candidate within the QTL identified using an SJL/J x CAST/Ei F2 intercross since these strains are polymorphic throughout *Sp6* and show significant differences in *Sp6* expression.

6

Fine Mapping Chromosome 8 QTL

6.1 Introduction

C57BL/Fa/Dk and RIII/Fa/Dk, 'long' and 'short' incubation time mouse strains respectively, show a 100-day difference in incubation time following primary intracerebral challenge with BSE prions (Bruce *et al.*, 1994; Fraser *et al.*, 1992). Linkage analysis in a backcross population, generated from these strains and challenged intracerebrally with BSE prions has identified extensive QTL for prion disease incubation time on chromosomes 2, 8, 4 and 15 (Manolakou *et al.*, 2001). This study identified dominant QTL, only detectable in one direction of the cross, with C57BL alleles contributing to a longer incubation time and RIII alleles contributing to a shorter incubation time. The QTL reflect large regions of linkage (10-20cM) which require fine mapping in order to further characterise individual candidate genes controlling the phenotype. The smallest QTL, identified on chromosome 8, was chosen for further analysis in this study. It is defined by a highly significant region of linkage flanked by the microsatellite markers *D8Mit104* and *D8Mit211*, and spans 20.8Mb with 95% confidence intervals (Figure 6.1). The focus of this chapter is the elucidation of the candidates which map within this region and may be controlling prion disease incubation time.

Figure 6.1 Chromosome 8 LOD score plot.
Plot represents the BSE incubation period in a backcross population generated from C57BL/Fa/Dk and RIII/Fa/Dk strains. The x axis shows the position of genotyped markers across the chromosome. The dotted line intersecting the y axis represents a statistical significance threshold of 2.71. One lod, 95% confidence intervals, are indicated by the double-headed arrows. Adapted from Manolakou *et al.*, 2001.

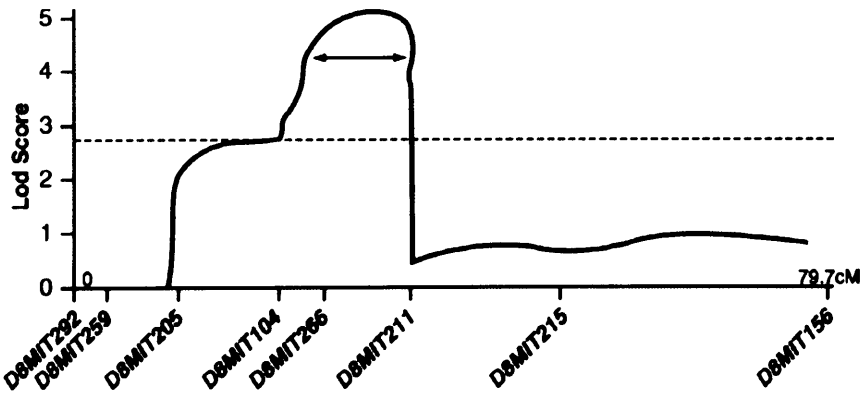

As previously described (Chapter 5), fine mapping with the genetically diverse Northport HS (Section 2.3.1) (Demarest *et al.*, 2001) has been successfully used to resolve extensive chromosome 11 QTL into smaller intervals. As previously described (Section 5.1), a potential limitation of this method is the absence of those mouse strains used to identify chromosome 8 QTL from the panel of parental strains used to generate the HS. It is possible that the identified QTL may be mouse strain specific and only observable in C57BL/Fa/Dk and RIII/Fa/Dk strains. C57BL/Fa/Dk and C57BL/6J, the latter featured in the Northport HS, are closely related substrains and it can therefore be argued that C57BL/6J is an appropriate substitute for the C57BL/Fa/Dk strain.

Another potential limitation of using the HS was the possibility that chromosome 8 QTL, identified in a BSE inoculated population, may also be prion strain specific and not be reproducible in the HS which was challenged with the Chandler/RML prion strain (Section 2.2.4). Challenging mice with BSE prions also represents a primary transmission of prions from one species to another and therefore a species barrier is present and may have implications for the identification of separate incubation time QTL. Other experimental factors important in defining incubation time, such as the chosen route of infection, are common between the original mapping study and this investigation, and similarities in clinical and neuropathological features of disease produced following challenge with Chandler/RML and BSE suggest that the identification of shared QTL is possible despite the use of alternate prion strains. The potential risk of not reproducing linkage in the HS was outweighed by the potential gains to be made in fine mapping the extensive QTL.

6.2 HAPPY Linkage Analysis

As described previously (Section 5.2), fluorescently-labelled microsatellite markers (Table 6.1), mapping at approximately 1cM intervals between the flanking markers of chromosome 8 QTL (Manolakou et al., 2001), were selected to genotype (Sections 2.4.4.1-4) approximately 400 generation 37 HS mice (Section 2.3.1) for HAPPY linkage analysis (Section 2.4.4.5) (Mott *et al.*, 2000). This population represents the extreme ~20% of each end of the Chandler/RML incubation time distribution. PCR primer sequence and fluorescent labelling information for microsatellite markers are detailed in Appendix 1.2.

Table 6.1 HS progenitor strain allele sizes for chromosome 8 microsatellite markers. cM=centimorgan and bp=base pairs.

Marker	Position (cM)	Marker Sizes (bp)							
		A	AKR	BALB	C3H	C57	CBA	DBA	LP
D8Mit104	37.0	138	132	130	138	144	138	138	130
D8Mit236	38.1	85	89	89	85	115	85	85	89
D8Mit105	38.6	131	129	129	131	120	131	131	129
D8Mit45	40.0	129	125	123	129	119	129	129	123
D8Mit57	41.0	153	163	163	153	161	163	163	163
D8Mit81	41.5	135	149	149	135	135	147	147	149
D8Mit197	42.6	113	103	103	113	113	99	99	103
D8Mit267	43.0	102	85	90	102	104	90	90	85
D8Mit109	43.7	135	133	135	135	137	135	135	133
D8Mit164	44.8	140	140	142	146	146	146	146	146
D8Mit183	47.0	156	156	154	158	152	158	158	152
D8Mit85	47.3	122	122	134	126	126	126	126	126
D8Mit211	49.0	167	167	165	163	153	163	163	161

A minimal region of significant linkage was successfully identified in a single interval defined by the flanking markers *D8Mit81* and *D8Mit197* (-logP=4.55) (Figure 6.2). The –logP score of the preceding interval, spanning within *D8Mit57* to *D8Mit81* (–logP=4.27), almost reached the suggested threshold value for significant linkage (Lander and Kruglyak, 1995) and was also included in further analysis. The minimum region of interest is therefore defined by the flanking markers *D8Mit57* and *D8Mit197* spanning a 2.2Mb region which is an 18.6Mb reduction in size from the original chromosome 8 QTL (Manolakou et al., 2001) (Figure 6.3).

6.3 Candidate Genes

As previously described (Section 3.2), information for eight candidate genes mapping within the new region of linkage was obtained from mouse genome sequence annotation databases (Table 6.2). No known or predicted genes have been identified between the flanking markers of the most significant interval of linkage, *D8Mit81* and *D8Mit197*, therefore candidate gene analysis focused between *D8Mit57* and *D8Mit81*. As previously described (Section 5.3), all genes were assessed systematically with equal value assigned to each as potential candidates for controlling prion disease incubation time.

Figure 6.2 Chromosome 8 HAPPY linkage analysis –logP plot.
The x axis represents 11 microsatellite marker intervals across chromosome 8. The dotted line intersecting the y axis indicates the –logP value representing a statistical significance threshold of 4.3.

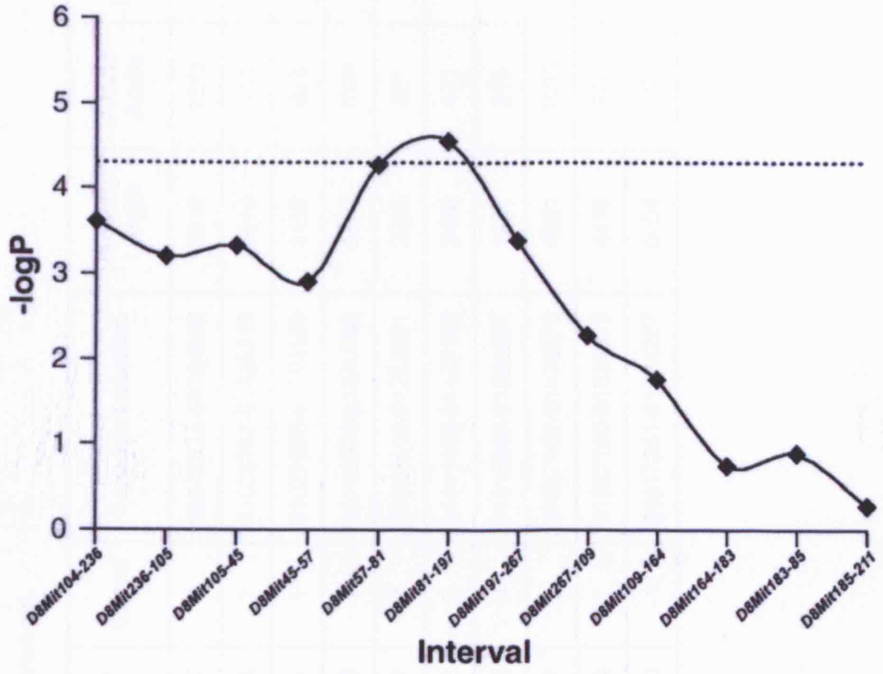

Figure 6.3 Chromosome 8 schematic.
The horizontal red line signifies the original chromosome 8 QTL and the horizontal blue line signifies the reduced region of linkage identified by fine mapping in the HS. The flanking markers and sizes of both regions are labelled in corresponding colours.

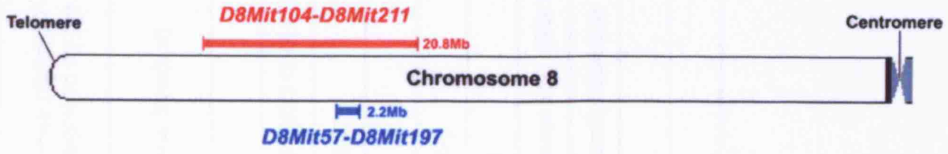

Table 6.2 Chromosome 8 candidate genes (*D8Mit57-D8Mit81*).
Hypothetical protein LOC382030 will be signified by the symbol *HypP* from this point onwards.

Gene Name (Gene Symbol)	Accession Number	Strand	Genomic Location	Transcript Length	Amino Acids	Exons
Zinc Finger Protein 423 (*Zfp423*)	NM_033327	-1	90576534-90794663	3819	1273	8
Hypothetical Protein LOC382030 (*5033428A16Rik or HypP*)	NM_029074	1	91008892-91025213	1616	106	4
HEAT Repeat Containing 3 (*Heatr3*)	NM_172757	1	91027990-91062103	3192	679	15
Adenylate Cyclase 7 (*Adcy7*)	NM_007406	1	91162508-91220066	5198	1099	25
Bromodomain Containing 7 (*Brd7*)	NM_012047	-1	91222416-91252261	2335	651	17
Naked Cuticle 1 Homolog (*Nkd1*)	NM_027280	1	91411459-91483156	2468	471	9
Selectin Ligand Interactor Cytoplasmic-1 (*Slic1*)	NM_027840	-1	91516890-91526207	1451	313	3
Caspase Recruitment Domain Family Member 15 (*Card15*)	NM_145857	1	91537452-91578579	4621	1015	12
Cylindromatosis (*Cyld*)	NM_173369	1	91587180-91638573	4489	952	16
Sal-Like 1 (*Sall1*)	NM_021390	-1	91917351-91934267	5254	1323	3

Zinc Finger Protein 423 (Zfp423)

ZFP423 is one of two members of a novel transcription factor family of zinc finger proteins with 30 Krüppel-like zinc finger (ZF) domains. ZFP423 has an essential role in the development of the cerebellum (Warming *et al.*, 2006) by controlling proliferation and differentiation of neural precursors in cerebellar vermis formation (Alcaraz *et al.*, 2006).

HEAT Repeat Containing 3 (Heatr3)

HEATR3 is currently not well characterised. The acronym, HEAT, was coined to describe tandem arrays of a repeat in Huntington's disease in four functionally characterised proteins, namely huntingtin, elongation factor 3 (EF3), the regulatory A subunit of protein phosphatase 2A and TOR1 (Andrade and Bork, 1995). HEAT repeats vary in length between 37-43 amino acids, consist of two α-helices and occur in at least 3 consecutive repeats. Most of the well characterised HEAT proteins containing HEAT repeats are regulatory cytoplasmic proteins involved in cytoplasmic transport processes.

Adenylate Cyclase 7 (Adcy7)

Adcy7 is widely expressed in mouse tissues (Watson *et al.*, 1994) and is one isoform of a family of enzymes responsible for converting ATP to cyclic AMP, a second messenger involved in intracellular signal transduction, and who also play an important role in G-protein-regulated signal transduction systems.

Bromodomain Containing 7 (Brd7)

BRD7 is a ubiquitously expressed 75kDa protein that has been shown to regulate *Wnt* signalling, which plays a pivotal role in animal development and tumorigenesis, through interactions with Dishevelled-1 (Kim *et al.*, 2003). The bromodomain is defined as a conserved sequence of approximately 110 amino acids that is found in over 40 proteins, several of which are involved in transcriptional regulation (Jeanmougin *et al.*, 1997). Recently human BRD7 has been shown to confer its role as a transcriptional regulator through binding to acetylated histones (Peng *et al.*, 2006).

Naked Cuticle 1 Homolog (Nkd1)

Nkd1 is one of two mouse homologs of Drosophila naked cuticle and is, like *Brd7*, involved in regulation of the *Wnt* signalling pathway. During mouse embryogenesis

Nkd1 is expressed in multiple tissues in *Wnt*-like patterns suggesting possible roles in mouse development (Wharton *et al.*, 2001). Recently a targeted mutation of *Nkd1* has been shown to impair mouse spermatogenesis (Li *et al.*, 2005).

Selectin Ligand Interactor Cytoplasmic-1 (Slic1)

Slic1 is a provisionally named RIKEN cDNA which is suggested, by UniProt (SWISS-PROT and TrEMBL) database information, to have putative sorting-nexin (SNX) domains. Sorting-nexins are an emerging family of peripheral membrane proteins which have been implicated in regulating membrane traffic (Haft *et al.*, 1998; Kurten *et al.*, 1996; Ponting, 1996). Sorting nexins are thought to be involved in pro-degradative sorting, internalisation, endosomal recycling or simply in endosomal sorting (Worby and Dixon, 2002). A suggested role for this RIKEN cDNA as a member of a family involved in protein trafficking is interesting in terms of prion pathology because as previously described (Section 1.1.5), the cellular prion protein is located at the surface of neuronal cells in detergent-insoluble lipid rafts, bound by a glycophosphatidylinositol (GPI) anchor (Stahl *et al.*, 1987), and is known to leave these rafts to recycle every few minutes via clathrin coated pits between the cell surface and recycling endosomes (Shyng *et al.*, 1993; Sunyach *et al.*, 2003).

Caspase Recruitment Domain Family Member 15 (Card15)

Card15 encodes nucleotide binding oligomerization domain 2 (NOD2) (Ogura *et al.*, 2001b) which belongs to the NOD-LRR family of proteins. This family are characterised by a tripartite domain structure consisting of a carboxy-terminal recognition LRR domain, a central NOD domain and an amino-terminal domain composed of protein-protein interaction cassettes, such as caspase recruitment domains (CARDs) or pyrin domains (Strober *et al.*, 2006; Watanabe *et al.*, 2005). NOD2 is an activator of NF-κB transcription pathways and enhances apoptosis and/or caspase activation (Ogura et al., 2001b). Mutations in this gene have been implicated in Crohn's disease (Hampe *et al.*, 2002; Hugot et al., 2001; Ogura et al., 2001a).

Cylindromatosis (Cyld)

Cyld was originally identified as a tumor suppressor gene mutated in familial cylindromatosis (Bignell *et al.*, 2000), an autosomal dominant predisposition to benign tumours of the skin appendages (Lian and Cockerell, 2005). More recently CYLD has been identified as a de-ubiquitinating enzyme (Trompouki *et al.*, 2003), a family of

cysteine proteases that digest ubiquitin chains. This is noteworthy as the prion protein is known to be ubiquitinated after developing protease resistance in the brain of ME7 scrapie infected mice (Kang *et al.*, 2004).

Sal-Like 1 (Sall1)

In drosophila *sal* is a region containing specific homeotic genes characterised by unique multiple double-zinc finger motifs (Kuhnlein *et al.*, 1994). The mouse has three homolog *Sal* genes, one of which, *Sall1*, is involved in kidney development (Nishinakamura *et al.*, 2001).

The function of the hypothetical protein LOC382030 (*HypP*) is unknown as this gene and its protein product are currently not well characterised.

6.4 Candidate Gene Sequence Polymorphisms

As previously described (Sections 3.3 and 5.4) sequence analysis of candidate genes was undertaken in order to identify polymorphisms between the founder strains of the HS and also between C57BL/6J and RIIIS/J, which are related to those strains originally used to identify the QTL (Manolakou *et al.*, 2001). Details of PCR primer sequence and conditions for use are listed in Appendix 2.2. Sequence polymorphism data is detailed in Table 6.3.

In total, 168 polymorphisms were identified between the parental strains of the HS (Table 6.3). 8 polymorphisms were identified in predicted promoter regions, 22 in introns and 138 in exons, of which 19 were nonsynonymous. Most polymorphisms identified were SNPs (n=158) with only a small number involving deletion (n=7) or insertion (n=3) of sequence.

6.5 HAPPY Analysis of Polymorphisms

As previously described (Section 5.5) HAPPY linkage analysis software (Section 2.4.4.5) was used to assess whether identified polymorphisms were potentially associated with incubation time. 134 polymorphisms identified between the parental strains of the HS, within the flanking markers *D8Mit57* and *D8Mit81*, reached a 2.8 –logP threshold value for 'suggestive' linkage one of which, a single exonic polymorphism in *Sall1* (m*Sall1*x2#8), reached a 4.3 –logP threshold for 'significant' linkage (Lander and Kruglyak, 1995) (Figure 6.4 and Table 6.3). At least one of these

Figure 6.4 HAPPY analysis output for polymorphisms identified between *D8Mit57* and *D8Mit81*.
The x axis measures distance along the chromosome between the flanking markers (vertical lines) of the region of significant linkage. The y axis measures polymorphism –logP values. Each polymorphism is identified as a black dot on the plot. Polymorphism –logP values of >2.8 and >4.3 reach the threshold for 'suggestive' and 'significant' linkage and are highlighted by red boxes.

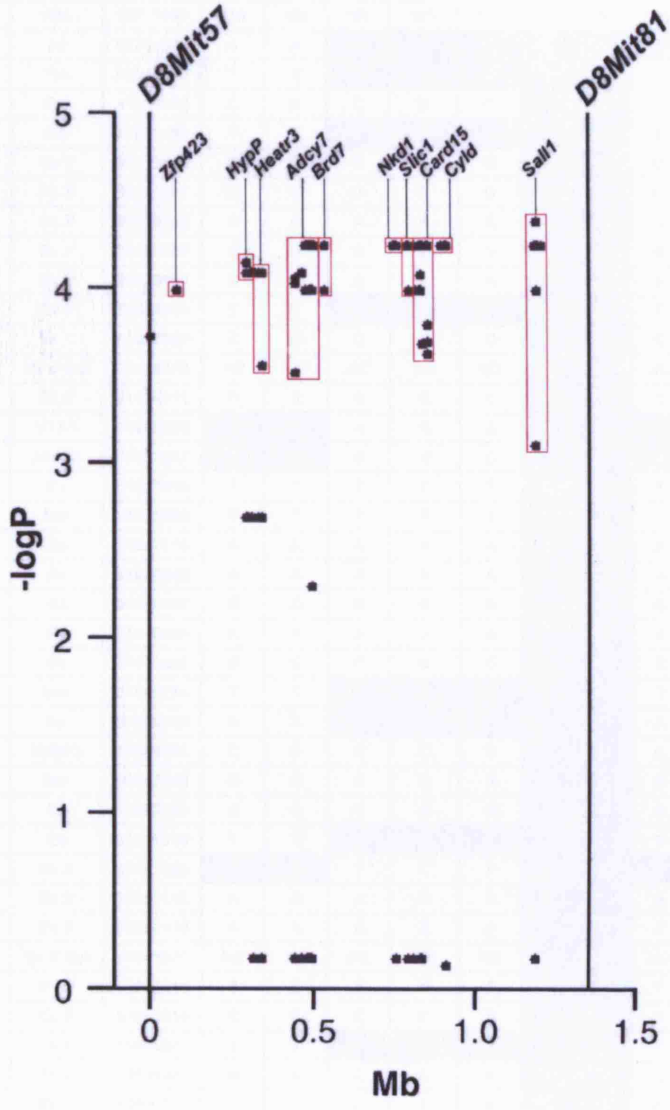

polymorphisms was identified in every candidate gene mapping within the region of interest. 6 polymorphisms were identified in predicted promoter regions, 113 in exonic regions of which 12 were nonsynonymous, 15 were identified in intronic regions, 7 were deletion polymorphisms and 2 were characterised by an insertion of sequence.

Table 6.3 Haplotype patterns of alleles mapping between *D8Mit57* and *D8Mit81*.
Ex=Exonic, Pro=Promoter, 3'=3'UTR, 5'=5'UTR, Intr=Intronic, Del= Deletion, MM=Microsatellite Marker, Ins=Insertion, NC=No Change (compared to NCBI, Ensembl and UCSC database sequence), ND=Not Determined and bp=base pair. Nonsynonymous polymorphisms are indicated by amino acid abbreviations flanking the relevant codon number. Shading illustrates polymorphism SDP.

Marker/Polymorphism Description		Position	CBA	DBA	AKR	BALB	LP	A	C3H	C57	RIIIS	-logP
D8Mit57	MM	90710987	163	163	163	163	163	152	152	161	ND	3.69
m*Zfp423*x2#1	Ex	90794625	A	A	G	G	G	G	G	G	G	3.96
m*HypP*Pro#1	Pro	91008711	T	T	C	C	C	C	C	T	T	2.66
m*HypP*Pro#2	Pro	91008838	C	C	C	C	C	G	G	C	C	4.06
m*HypP*x3#1	Intr	91015183	T	T	C	C	C	C	C	T	T	2.66
m*HypP*3'#1	Ex 3'	91019976	G	G	G	G	G	A	A	G	G	4.06
m*HypP*3'#2	Ex 3'	91020081	G	G	G	G	G	A	A	G	G	4.06
m*HypP*3'#3	Ex 3'	91020142	A	A	A	A	A	G	G	A	A	4.06
m*HypP*3'#4	Ex 3'	91020157	G	G	G	G	G	A	A	G	G	4.06
m*HypP*3'#5	Ex 3'	91020384	A	A	A	A	A	T	T	A	A	4.06
m*Heatr3*x1#1	Ex 5'	91028003	T	T	C	C	C	C	C	T	T	2.66
m*Heatr3*x1#2	Ex 5'	91028009	C	C	C	C	C	T	T	C	C	4.06
m*Heatr3*x1#3	Ex 5' Del	91028013	NC	NC	NC	NC	NC	2bp	2bp	NC	NC	4.06
m*Heatr3*x1#4	Ex 5'	91028111	C	C	C	C	C	T	T	C	C	4.06
m*Heatr3*x3#1	V114I	91030025	G	G	A	A	A	G	G	G	G	0.11
m*Heatr3*x4#2	A142E	91031803	A	A	C	C	C	A	A	A	A	0.11
m*Heatr3*x4#3	Ex	91031825	T	T	T	T	T	C	C	T	T	4.06
m*Heatr3*x4#4	Intr	91031899	T	T	T	T	T	C	C	T	T	4.06
m*Heatr3*x6#1	Ex	91037716	A	A	A	A	A	G	G	A	A	4.06
m*Heatr3*x7#1	Ex	91040342	A	A	A	A	A	G	G	A	A	4.06
m*Heatr3*x7#2	Ex	91040447	G	G	G	G	G	A	A	G	G	4.06
m*Heatr3*x7#3	Ex	91040453	A	A	A	A	A	G	G	A	A	4.06
m*Heatr3*x7#4	Ex	91040462	C	C	C	C	C	A	A	C	C	4.06
m*Heatr3*x9#1	Intr	91046763	T	T	C	C	C	C	C	T	T	2.66
m*Heatr3*x9#2	Ex	91046800	A	A	G	G	G	G	G	A	A	2.66
m*Heatr3*x9#3	H406Q	91046863	C	C	C	C	C	G	G	C	C	4.06
m*Heatr3*x10#1	Intr	91047254	G	G	G	G	G	A	A	G	G	4.06
m*Heatr3*x11#1	Ex	91048249	G	G	G	G	G	A	A	G	ND	4.06
m*Heatr3*x11#2	Ex	91048318	T	T	C	C	C	C	C	T	ND	2.66
m*Heatr3* 3'#2	Ex 3'	91061142	C	C	T	T	T	C	C	C	C	0.11
m*Heatr3* 3'#4	Ex 3'	91061158	A	A	A	A	A	G	G	A	A	4.06
m*Heatr3* 3'#6	Ex 3'	91061178	A	A	A	A	A	G	G	A	A	4.06
m*Heatr3* 3'#8	Ex 3' Del	91061236	NC	NC	NC	NC	NC	1bp	1bp	NC	NC	4.06
m*Heatr3* 3'#9	Ex 3'	91061241	T	T	T	T	T	G	G	T	T	4.06
m*Heatr3* 3'#11	Ex 3'	91061514	C	C	C	C	C	T	T	C	C	4.06
m*Heatr3* 3'#12	Ex 3'	91061535	T	T	C	C	C	C	C	T	T	2.66
m*Heatr3* 3'#14	Ex 3'	91061927	A	A	A	A	A	T	T	A	A	4.06
m*Heatr3* 3'#15	Ex 3'	91061932	A	A	A	A	A	G	G	A	ND	4.06
m*Heatr3* 3'#16	Ex 3'	91061940	G	G	G	G	G	A	A	G	ND	4.06
m*Adcy7* 5'1#1	Intr Del	91162505	NC	NC	NC	NC	NC	1bp	NC	NC	NC	4.00
m*Adcy7* 5'1#2	Ex 5'	91162554	C	C	G	G	G	C	C	C	C	0.11
m*Adcy7* 5'1#3	Ex Ins 5'	91162583	NC	NC	1bp	1bp	1bp	NC	NC	NC	NC	0.11
m*Adcy7* 5'2#1	Ex 5'	91185134	A	A	A	A	A	G	G	A	A	4.06
m*Adcy7* 5'2#3	Ex 5'	91185220	A	A	A	A	A	G	G	A	A	4.06
m*Adcy7* 5'2#4	Ex 5'	91185222	C	C	C	C	C	A	A	C	C	4.06
m*Adcy7* 5'3#1	Ex 5'	91185716	C	C	T	T	T	C	C	C	C	0.11
m*Adcy7* 5'4#1	Ex 5'	91196607	T	T	A	A	A	A	A	A	T	3.96
m*Adcy7* 5'4#2	Ex 5'	91196618	G	G	G	G	G	A	A	A	G	4.22

Marker/Polymorphism Description		Position	CBA	DBA	AKR	BALB	LP	A	C3H	C57	RIIIS	-logP
m*Adcy7*x3#2	A150V	91199870	T	T	T	T	T	C	C	C	T	4.22
m*Adcy7*x4#1	Ex	91200659	T	T	T	T	T	C	C	C	T	4.22
m*Adcy7*x4#2	Ex	91200785	G	G	A	A	A	G	G	G	G	0.11
m*Adcy7*x7#1	Ex	91204229	T	T	C	C	C	C	C	C	T	3.96
m*Adcy7*x7#3	Ex	91204259	G	G	A	A	A	G	G	G	G	0.11
m*Adcy7*x7#4	Intr	91204330	C	C	C	C	C	A	A	A	C	4.22
m*Adcy7*x9#1	Intr	91205850	T	T	T	T	T	C	C	C	T	4.22
m*Adcy7*x9#2	Ex	91205901	C	C	C	C	C	T	T	T	C	4.22
m*Adcy7*x10#1	Ex	91208074	C	C	C	C	C	A	A	A	C	4.22
m*Adcy7*x12#1	Ex	91208913	C	C	C	C	C	T	T	T	C	4.22
m*Adcy7*x12#2	Ex	91208970	G	G	T	T	T	T	T	T	G	3.96
m*Adcy7*x12#3	Intr	91208991	C	C	G	G	G	G	G	G	C	3.96
m*Adcy7*x13#1	Intr	91209257	G	G	A	A	A	G	G	G	G	0.11
m*Adcy7*x14#3	Intr	91210241	G	G	A	A	A	A	A	A	G	3.96
m*Adcy7*x14#4	Intr	91210244	T	T	C	C	C	C	C	C	T	3.96
m*Adcy7*x17#2	Intr	91213032	C	C	T	T	T	C	C	C	C	0.11
m*Adcy7*x17#3	Y707C	91213125	G	G	A	A	A	G	G	G	G	0.11
m*Adcy7*x19#1	Q791R	91214601	G	G	A	A	A	G	G	G	G	0.11
m*Adcy7*x20#1	Ex	91214977	A	A	G	G	G	G	G	G	A	3.96
m*Adcy7*x21#1	Ex	91215519	T	T	C	C	C	C	C	C	T	3.96
m*Adcy7*x22#1	Intr Del	91216178	17bp	17bp	17bp	17bp	17bp	NC	NC	NC	17bp	4.22
m*Adcy7*x22#2	Ex	91216221	C	C	C	C	C	T	T	T	C	4.22
m*Adcy7* 3'#2	Ex 3'	91218009	T	T	C	C	C	C	C	C	T	3.96
m*Adcy7* 3'#3	Ex 3'	91218069	C	C	C	C	C	A	A	A	C	4.22
m*Adcy7* 3'#4	Ex 3'	91218259	G	G	T	T	T	G	G	G	G	0.11
m*Adcy7* 3'#5	Ex 3'	91218261	C	C	T	T	T	C	C	C	C	0.11
m*Adcy7* 3'#6	Ex 3'	91218318	T	T	T	T	T	C	C	C	T	4.22
m*Adcy7* 3'#7	Ex 3'	91218573	T	T	T	T	T	G	G	G	T	4.22
m*Adcy7* 3'#8	Ex 3'	91218673	G	G	G	G	G	A	A	A	G	4.22
m*Adcy7* 3'#9	Ex 3'	91218743	T	T	T	T	T	C	C	C	T	4.22
m*Adcy7* 3'#10	Ex 3'	91218818	T	T	T	T	T	A	A	A	T	4.22
m*Adcy7* 3'#12	Ex 3'	91218932	G	T	G	G	G	T	T	T	T	2.26
m*Adcy7* 3'#13	Ex 3'	91218933	A	A	A	A	A	G	G	G	A	4.22
m*Adcy7* 3'#15	Ex 3'	91218959	A	A	A	A	A	G	G	G	A	4.22
m*Adcy7* 3'#16	Ex Ins 3'	91219096	2bp	2bp	2bp	2bp	2bp	NC	NC	NC	2bp	4.22
m*Brd7*x17#1	Intr	91222405	C	C	C	C	C	T	T	T	C	4.22
m*Brd7*Pro1#2	Pro	91253497	C	C	T	T	T	T	T	T	C	3.96
m*Brd7*Pro1#1	Pro	91253502	T	T	C	C	C	C	C	C	T	3.96
m*Nkd1*x4#1	Ex	91473330	C	C	C	C	C	T	T	T	C	4.22
m*Nkd1*x5#1	Ex	91475264	A	A	A	A	A	G	G	G	A	4.22
m*Nkd1*x5#2	Intr	91475363	G	G	G	G	G	A	A	A	G	4.22
m*Nkd1*x9#1	Intr	91481650	C	C	T	T	T	C	C	C	C	0.11
m*Nkd1*x9#2	V440M	91482159	G	G	A	A	A	G	G	G	G	0.11
m*Nkd1* 3'#1	Ex 3'	91482236	T	T	T	T	T	C	C	C	T	4.22
m*Nkd1* 3'#3	Ex 3'	91482490	A	A	A	A	A	C	C	C	A	4.22
m*Nkd1* 3'#7	Ex 3'	91482785	C	C	T	T	T	C	C	C	C	0.11
m*Slic1* 3'#4	Ex 3'	91517036	G	G	G	G	G	A	A	A	G	4.22
m*Slic1* 3'#3	Ex 3' Del	91517175	10bp	10bp	10bp	10bp	10bp	NC	NC	NC	10bp	4.22
m*Slic1* 3'#2	Ex 3'	91517219	C	C	C	C	C	T	T	T	C	4.22
m*Slic1* 3'#1	Ex 3'	91517257	A	A	C	C	C	C	C	C	A	3.96
m*Slic1*x3#2	A136T	91517800	A	A	A	A	A	G	G	G	A	4.22
m*Slic1*x3#1	Intr	91517945	C	C	C	C	C	G	G	G	C	4.22
m*Slic1*x1#3	P39S	91521880	T	T	C	C	C	C	C	C	T	3.96
m*Slic1*x1#2	Ex	91521887	C	C	C	C	C	T	T	T	C	4.22
m*Slic1*x1#1	P29L	91521909	C	C	T	T	T	C	C	C	C	0.11

Marker/Polymorphism Description		Position	CBA	DBA	AKR	BALB	LP	A	C3H	C57	RIIIS	-logP
m*Card15*Pro#1	Pro	91537265	A	A	A	A	A	G	G	G	A	4.22
m*Card15*Pro#2	Pro	91537325	C	C	C	C	C	G	G	G	C	4.22
m*Card15*Pro#4	Pro	91537455	G	G	A	A	A	G	G	G	G	0.11
m*Card15*x2#4	Intr	91543442	C	G	C	C	C	C	C	C	C	3.96
m*Card15*x3#2	Ex	91550721	G	G	G	G	G	A	A	A	G	4.22
m*Card15*x4#1	T205A	91553850	G	G	G	G	G	A	A	A	G	4.22
m*Card15*x4#2	Ex	91553885	A	A	G	G	G	G	G	G	A	3.96
m*Card15*x4#3	Q233R	91553935	G	G	G	G	G	A	A	A	G	4.22
m*Card15*x4#5	Ex	91554470	C	C	C	C	C	T	T	T	C	4.22
m*Card15*x4#6	Ex	91554473	T	T	T	T	T	C	C	C	T	4.22
m*Card15*x4#7	L415C	91554481	G	G	G	G	G	T	T	T	G	4.22
m*Card15*x4#8	L415C	91554482	C	C	C	C	C	G	G	G	C	4.22
m*Card15*x4#11	Ex	91554654	T	T	C	C	C	C	C	C	T	3.96
m*Card15*x4#12	G478V	91554670	T	T	G	G	G	G	G	G	T	3.96
m*Card15*x4#14	Ex	91555019	G	G	A	A	A	A	A	A	G	3.96
m*Card15*x4#15	Ex	91555022	A	A	A	A	A	G	G	G	A	4.22
m*Card15*x4#16	A596V	91555024	C	C	T	T	T	T	T	T	C	3.96
m*Card15*x4#17	Ex	91555172	G	G	G	G	G	A	A	A	G	4.22
m*Card15*x4#19	V668I	91555239	A	A	A	A	A	G	G	G	A	4.22
m*Card15*x4#20	Ex	91555247	G	G	A	A	A	G	G	G	G	0.11
m*Card15*x4#21	Ex	91555253	G	G	G	G	G	A	A	A	G	4.22
m*Card15*x4#22	Ex	91555283	G	G	A	A	A	G	G	G	G	0.11
m*Card15*x4#23	Ex	91555334	G	G	T	T	T	G	G	G	G	0.11
m*Card15*x4#24	Ex	91555373	C	T	T	T	T	C	C	C	T	4.05
m*Card15*x4#25	Ex	91555388	G	G	G	G	G	T	T	T	G	4.22
m*Card15*x4#26	Ex	91555499	G	G	G	G	G	A	A	A	G	4.22
m*Card15*x4#27	Ex	91555571	C	C	C	C	C	T	T	T	C	4.22
m*Card15*x7#1	Intr	91562772	C	C	T	T	T	C	C	C	C	0.11
m*Card15*x7#2	Intr	91562773	C	C	T	T	T	C	C	C	C	0.11
m*Card15*x8#3	Intr	91565097	G	G	G	G	G	A	A	A	G	4.22
m*Card15*x10b#1	Ex	91574594	T	T	T	T	T	C	C	C	T	4.22
m*Card15* 3'#8	Ex 3'	91577599	A	A	A	A	A	T	T	T	A	4.22
m*Card15* 3'#10	Ex 3' Del	91577714	12bp	12bp	12bp	12bp	12bp	NC	NC	NC	12bp	3.76
m*Card15* 3'#12	Ex 3'	91577905	C	C	C	C	C	T	T	T	C	4.22
m*Card15* 3'#13	Ex 3'	91577943	T	T	T	T	T	C	C	C	T	4.22
m*Card15* 3'#14	Ex 3'	91577998	C	C	C	C	C	T	T	T	C	4.22
m*Card15* 3'#15	Ex 3'	91578251	G	G	G	G	G	G	A	A	G	3.60
m*Card15* 3'#16	Ex 3'	91578375	T	T	T	T	T	C	C	C	T	4.22
m*Cyldx*7#1	Ex	91620904	G	G	G	G	G	A	A	A	G	4.22
m*Cyldx*13#1	Intr	91632387	T	T	T	T	T	G	G	G	T	4.22
m*Cyldx*16#1	Ex	91637028	C	C	C	C	C	T	T	T	C	4.22
m*Cyld* 3'#1	Ex 3'	91637563	A	A	A	A	A	G	G	G	A	4.22
m*Cyld* 3'#2	Ex 3'	91637578	G	G	G	G	G	A	A	A	G	4.22
m*Cyld* 3'#5	Ex 3'	91637866	G	G	G	G	G	A	A	A	G	4.22
m*Cyld* 3'#6	Ex 3'	91637899	T	T	T	T	T	C	C	C	T	4.22
m*Cyld* 3'#7	Ex 3'	91637997	C	C	C	C	C	T	T	T	C	4.22
m*Cyld* 3'#8	Ex 3'	91637998	C	C	C	C	C	T	T	T	C	4.22
m*Cyld* 3'#9	Ex 3'	91638087	C	C	C	C	C	T	T	T	C	4.22
m*Cyld* 3'#10	Ex 3'	91638282	T	T	T	T	T	C	C	C	T	4.22
m*Sall1* 3'#4	Ex 3' Del	91917447	1bp	1bp	1bp	1bp	1bp	NC	NC	NC	1bp	4.22
m*Sall1* 3'#1	Ex Ins 3'	91918492	NC	NC	4bp	4bp	4bp	NC	NC	NC	NC	3.35
m*Sall1*x3#1	Ex	91918777	C	C	C	C	C	T	T	T	C	4.22
m*Sall1*x2#20	Ex	91920714	A	A	G	G	G	G	G	G	A	3.96
m*Sall1*x2#19	Ex	91920769	T	T	T	T	T	C	C	C	T	4.22

Marker/Polymorphism Description		Position	CBA	DBA	AKR	BALB	LP	A	C3H	C57	RIIIS	-logP
m*Sall1*x2#17	Ex	91921327	T	T	T	T	T	C	C	C	T	4.22
m*Sall1*x2#15	Ex	91921537	G	G	T	T	T	G	G	G	G	0.11
m*Sall1*x2#13	Ex	91921750	C	C	C	C	C	T	T	T	C	4.22
m*Sall1*x2#12	Ex	91921759	C	C	C	C	C	T	T	T	C	4.22
m*Sall1*x2#11	Ex	91921792	T	T	T	T	T	C	C	C	T	4.22
m*Sall1*x2#10	Ex	91922149	G	G	G	G	G	A	A	A	G	4.22
m*Sall1*x2#9	E388A	91922417	C	C	A	A	A	C	C	C	C	0.11
m*Sall1*x2#8	Ex	91922629	T	T	C	T	T	C	C	C	T	4.36
m*Sall1*x2#4	Ex	91923295	T	T	T	T	T	C	C	C	T	4.22
m*Sall1*x2#3	T84A	91923330	A	A	A	A	A	G	G	G	A	4.22
m*Sall1*x2#2	Ex	91923379	A	A	A	A	A	G	G	G	A	4.22
m*Sall1*Pro2#1	Pro	91935042	C	C	C	C	C	G	G	G	C	4.22
D8Mit197	MM	92915060	99	99	103	103	103	113	113	113	ND	4.45

For those polymorphisms reaching a level of 'suggestive' linkage, three general haplotype patterns were observed across the region of interest (Table 6.3 and Table 6.4). The most significant SDP gave a –logP value of 4.22 and divided the mouse strains into one group featuring A/J, C3H/HeJ and C57BL/6J and another including CBA/J, DBA/J, AKR/J, BALB/cJ and LP/J. These polymorphisms were located in *Adcy7*, *Brd7*, *Nkd1*, *Slic1*, *Card15*, *Cyld* and *Sall1* in a 1.2Mb region next to the flanking marker *D8Mit81* (Figure 6.4). In *HypP*, *Heatr3* and the 5'UTR of *Adcy7*, the first 0.5Mb of the region next to flanking marker *D8Mit57*, polymorphisms segregated into a SDP of A/J and C3H/HeJ in one group and AKR/J, BALB/cJ, C57BL/6J, CBA/J, DBA/J and LP/J in another giving a –logP value of 4.06. An SDP giving a –logP value of 3.96 was seen in polymorphisms located in *Zfp423*, *Adcy7*, *Brd7*, *Slic1*, *Card15* and *Sall1* which segregated CBA/J and DBA/J from the remaining strains.

Based on an assumption that the new region of interest identified in the HS is the same QTL as identified in the original mapping study (Manolakou et al., 2001), polymorphisms identified between the parental strains of the HS must also be polymorphic between RIIIS/J and C57BL/6J, therefore containing genetic differences that are potentially responsible for the observed variation in incubation time between these 'short' and 'long' incubation time strains. Of the 134 polymorphisms reaching threshold for suggestive and significant linkage, 100 were also polymorphic between C57BL/6J and RIIIS/J (Table 6.3). 5 polymorphisms are located in predicted promoter regions, 11 in introns and 84 in exonic regions, 11 of which were nonsynonymous. Most polymorphisms identified were SNPs (n=95) with only a small number involving deletion (n=4) or insertion (n=1) of sequence. These polymorphisms are located in every gene with the exception of *Zfp423*, *HypP* and *Heatr3*, and therefore these

Table 6.4 Chromosome 8 polymorphism SDPs.

-logP (No. of Polymorphisms)	SDP		Gene (No. of Polymorphisms)
	Group 1	Group 2	
4.22 (n=77)	CBA/J DBA/2J AKR/J BALB/cJ LP/J	A/J C3H/HeJ C57BL/6J	*Adcy7* (n=19) *Brd7* (n=1) *Nkd1* (n=5) *Slic1* (n=6) *Card15* (n=23) *Cyld* (n=11) *Sall1* (n=12)
4.06 (n=30)	CBA/J DBA/J AKR/J BALB/cJ LP/J C57BL/6J	A/J C3H/HeJ	*HypP* (n=6) *Heatr3* (n=21) *Adcy7* (n=3)
3.96 (n=21)	AKR/J BALB/cJ LP/J A/J C3H/HeJ C57BL/6J	CBA/J DBA/2J	*Zfp423* (n=1) *Adcy7* (n=9) *Brd7* (n=2) *Slic1* (n=2) *Card15* (n=6) *Sall1* (n=1)

candidates were removed from further analysis. A further six polymorphisms were also discounted based upon this criteria. These included m*Adcy7*5'1#1, m*Adcy7*5'2#1, m*Adcy7*5'2#3, m*Adcy7*5'2#4, m*Card15*x2#4 and m*Sall1*3'#1.

Following HAPPY analysis *Adcy7*, *Brd7*, *Nkd1*, *Slic1*, *Card15*, *Cyld* and *Sall1* remain potential candidate genes controlling prion disease incubation time. *Card15* and *Adcy7* have been highlighted as the most polymorphic genes featuring 31 and 28 sequence variants respectively (Table 6.3 and 6.4). The fourth exon of *Card15* contains the majority of the polymorphisms identified within this gene (n=22), six of which cause amino acid substitutions.

6.6 Potential Functional Properties of Observed Polymorphisms

As previously described (Section 3.4), the possible functional implications of polymorphisms were considered to further characterise those potentially making the most significant contributions towards prion disease incubation time. The potential functional properties of polymorphisms in the most common SDP (–logP=4.22) were prioritised.

6.6.1 Promoter Polymorphisms

Two polymorphisms identified in a predicted promoter region in *Card15* (m*Card15*Pro#1 and m*Card15*Pro#2) and one in *Sall1* (m*Sall1*Pro2#1) (Table 6.3) were not located in any transcription factor binding sites within these regions as determined by WWW Promoter Scan software (Section 2.1.5).

6.6.2 5' and 3'UTR Polymorphisms

As previously described (Section 3.4), the TFSEARCH software program (Section 2.1.5) was used to assess the location of 5' and 3'UTR polymorphisms within putative transcription factor binding sites. Following this analyses several transcription factors and functional pathways have been highlighted (Table 6.5). However, it is difficult to define which of the polymorphisms located in putative transcription factor binding sites may be influencing incubation time via differential gene regulation since a complete understanding of all the biochemical pathways involved in prion disease has not been reached.

6.6.3 Intronic Polymorphisms

Intronic polymorphisms identified in *Adcy7*, *Brd7*, *Nkd1*, *Slic1*, *Card15* and *Cyld* (Table 6.3) are not located in intronic 5' or 3' splicing signal sequences and are therefore unlikely to effect splicing of this gene between mouse strains.

6.6.4 Nonsynonymous Polymorphisms

Seven nonsynonymous polymorphisms giving –logP values of 4.22 were identified in *Adcy7* (n=1), *Slic1* (n=1), *Card15* (n=4) and *Sall1* (n=1) (Table 6.3).

Adcy7

A SNP in exon 3 of *Adcy7* (m*Adcy7*x3#2) causes an amino acid substitution at codon 150 from valine to alanine (Table 6.3). NCBI RefSeq *Adcy7* sequence for human, cow and mouse was aligned with novel transcripts for chimp, macaque, opossum and rat to assess the conservation of this amino acid (Figure 6.5). Codon 150 of murine *Adcy7* is located in a region predicted to form one of 12 membrane-associated helices (Watson et al., 1994). In support, the UniProt (SWISS-PROT and TrEMBL) protein database details a potential 21 residue transmembrane domain spanning codons 147 to 167 in murine *Adcy7* (accession number P51829). Both valine and alanine are hydrophobic and non-polar amino acids thus the physicochemical property of this semi-conserved

Table 6.5. Chromosome 8 candidate gene 3' and 5'UTR polymorphisms located in putative transcription factor binding sites.
The sequence comprising the putative transcription factor binding site is illustrated by a broken arrow and the position of the polymorphisms (SNPs or deletions) and their alternative nucleotide bases are highlighted in red. ID=Identification and TFBS = Transcription Factor Binding Site.

Polymorphism ID	Transcription factor	Function	Location Within TFBS
m*Adcy7* 3'#6	*S8* homeobox gene	DNA-binding regulator expressed during embryogenesis and important in controlling developmental processes (de Jong *et al.*, 1993).	ATTCTC/TTCAATTAGGCAT ---------->
m*Adcy7* 3'#10			AGA/TGTTTCAATTACAGAT ---------->
m*Adcy7* 3'#9	Homeodomain factor *Nkx-2.5/Csx* (Drosophila homolog, *Tinman)*	Expressed in myocardiogenic progenitor cells preceding differentiation and known to be involved in cardiac mesoderm formation (Lints *et al.*, 1993).	GC/TACTTTAT <--------
m*Adcy7* 3'#15			CCACTTGG/AC <--------
m*Cyld* 3'#1	*Oct-1*	Characterised by a conserved ~160 amino acid POU domain (Sturm and Herr, 1988). The POU domain gene family are expressed during embryogenesis and have critical roles in developmental regulation (Rosenfeld, 1991).	GATTTTATTAAGAG/AT <----------
m*Cyld* 3'#7			GATCT/CTATTACAGAT <----------
m*Cyld* 3'#8			GATCTT/CATTACAGAT <----------
m*Card15* 3'#13	*Ik-2*	One of four alternatively spliced products of the Ikaros gene (Molnar and Georgopoulos, 1994), a zinc finger DNA-binding protein expressed in early lymphocytes and mature T cells essential for the development of all lymphoid lineages (Georgopoulos *et al.*, 1994).	GGC/TCATCCCACTCT <----------
m*Slic1* 3'#4			GGA/GATGGGAAGGAC ---------->
m*Slic1* 3'#3	CCAAT/enhancer binding protein (*C/EBPalpha*)	High expression in tissues important in the uptake, metabolism and storage of physiological fuels has implicated a role for C/EBP in the regulation of energy homeostasis (Birkenmeier *et al.*, 1989).	CGGCTTTGGACAAGCC ---------->

Polymorphism ID	Transcription factor	Function	Location Within TFBS
m*Cyld* 3'#6	*Gata-1, Gata-2* & *Gata-3*	Family of transcription factors including four *Gata*-binding proteins, (designated *Gata-1* to *Gata-4*) each with a different tissue and developmental profile which control gene expression and development of haematopoietic cells (Orkin, 1992; Pevny et al., 1995).	GC/TGATAAGTAAAT ---------->
m*Cyld* 3'#9			GAGCT/CATCTCTC <----------
m*Card15* 3'#13			AGGC/TCATCCCAC <----------
m*Cyld* 3'#2	*Sry*	Y chromosomal gene which determines testis formation during mammalian embryogenesis (Koopman *et al.*, 1990).	CCAA/GTTGTTGAA <----------
	Sox-5	*Sox5* is a Sry-related gene which shares considerable homology with *Sry* over a conserved DNA–binding region known as the HMG-box (Jantzen *et al.*, 1990). *Sox5* is expressed during spermatogenesis and thought to be involved in transcriptional regulation in the testis (Denny *et al.*, 1992).	
m*Cyld* 3'#6	*Nf-e2*	Erythrocyte-specific transcription factor which binds AP-1-like recognition sites to control the expression of globin genes (Andrews *et al.*, 1993).	AATGACTGAGC/TGA <----------
m*Sall1* 3'#4	*c-Rel*	Member of the Rel/NF-κB family which are key regulators of innate and adaptive immune responses and of several cellular processes, including survival, growth and proliferation (Bonizzi and Karin, 2004).	AGGGGGGGGTTCCA ---------->

residue remains constant between mouse strains.

Figure 6.5 *Adcy7* homolog protein sequence alignment.
Codon 150 is highlighted in red with the amino acid substitution in mouse (C57BL/6J) labelled above.

```
                                    V150A
Homo sapiens              [140] LPFSMRGAVAVGAVSTASHLL [160]
Pan troglodytes           [140] LPFSMRGAVAVGAVSTASHLL [160]
Macaca mulatta            [140] LPFSMRGAIAVGAVSTASHLL [160]
Bos taurus                [161] LPFSMWGAVTAGLVSSISHLL [181]
Mus musculus              [140] LPLSRRAAIVVGVTSTVSHLL [160]
Monodelphis domestica     [140] LPFEMKDAIVVNVLSTLSYLL [160]
Rattus norvegicus        [1163] CACCGTCAAGTGTATCCAGAT [1184]
                                  .    *  ..  :  :
```

Slic1

A SNP in exon 3 of *Slic1* (m*Slic1*x3#2) causes an amino acid substitution at codon 136 from alanine to threonine (Table 6.3). As this gene and its functional domains have not yet been well characterised NCBI RefSeq sequence is only available for human and mouse and other featured homologs were supported by Ensembl novel transcripts (Figure 6.6). The UniProt (SWISS-PROT and TrEMBL) protein database ascribes murine *Slic1* (accession number Q9D2Y5) codons 1 to 313 as a sorting-nexin-20 chain and codons 71 to 188 as the PX domain, common to sorting nexin proteins, which is a lipid-binding module that aids the association of host protein with membrane enriched phosphoinositides during membrane trafficking events (Ponting, 1996). Both of these domains encompass codon 136. Codon 136 does not appear to be a well conserved residue and thus differences in charge between polar threonine and non-polar alanine, are likely to be well tolerated in terms of protein structure and function.

Figure 6.6 *Slic1* homolog protein sequence alignment.
Codon 136 is highlighted in red with the amino acid substitution in mouse (C57BL/6J) labelled above.

```
                                  A136T
Homo sapiens              [97]  ---KSRPGEMTYP-----GSR [109]
Macaca mulatta            [97]  ---KSRAGEVTHP-----GSH [109]
Pan troglodytes          [129]  KTFREEIEDVEFPRKYLTGNF [149]
Mus musculus             [126]  KRFGPELEDVAFPRKRLTGNL [146]
Monodelphis domestica    [132]  KNFSEEIEDIIFPKKYLTGNF [152]
                                     .  :: .*     *.
```

Card15

Four amino acid substitutions are located in exon 4 of *Card15* at codons 205 (m*Card15*x4#1), 233 (m*Card15*x4#3), 415 (m*Card15*x4#7 and m*Card15*x4#8), and

688 (m*Card15*x4#19) (Table 6.3). NCBI RefSeq sequence for human and mouse were aligned with novel transcripts for chimp, macaque and opossum (Figure 6.7). Codon 415 is of particular interest because it is the only codon of the four residing in an important functional domain. Of the other codons, 205 is conserved while 233 and 688 show no conservation. An amino acid substitution from leucine to cysteine occurs at this position. This change resides within the NOD binding domain which is involved in self-oligomerization after the binding of a ligand at leucine rich repeat domains and in turn activates downstream effectors molecules through the caspase-recruitment domains (Inohara and Nunez, 2001). Codon 415 is only semi-conserved between homologs. Leucine and cysteine are both hydrophobic non-polar amino acids and it is therefore unlikely that a significant change in the physicochemical property of this residue occurs as a result of the substitution. However, covalent intrachain disulfide bonds (S-S bonds) are often formed between the two -SH groups of neighbouring cysteine residues and serve to stabilise the three dimensional structure of a protein. Therefore the substitution of cysteine for a leucine residue would potentially reduce the number of disulfide bonds governing the tertiary structure of NOD2 and in turn, possibly affect its function.

Figure 6.7 *Card15* homolog protein sequence alignment.
Codon 415 is highlighted in red with the amino acid substitution in mouse (C57BL/6J) labelled above.

```
                                    L415C
Homo sapiens              [432] AFLRKYIRTEFNLKGFSEQGI [452]
Pan troglodytes           [432] AFLRKYIRTEFNLKGFSEQGI [452]
Macaca mulatta            [436] AFLRKYIRTEFNLKGFSEQGI [456]
Mus musculus              [405] ALLRKFVRTELQLKGFSEEGI [425]
Monodelphis domestica     [406] PSLRKYVRKELSLMGFSQDGI [426]
Danio rerio               [251] PSLKRYLRKEVLLKGFSPGGI [271]
                                . *:::*.*. * ***  **
```

Sall1

A nonsynonymous polymorphism in exon 2 of *Sall1* (m*Sall1*x2#3) causes a threonine to alanine substitution at codon 84 (Table 6.3). This residue is identical throughout the featured homolog species suggesting potential functional significance (Figure 6.8). Both residues are small amino acids so a significant change in size would not occur as a result of the substitution. However a change in charge would be observed as threonine is polar and alanine is non-polar. As this codon is not located in characterised zinc finger motifs (Nishinakamura et al., 2001) its propensity to effect protein binding activity or function is unclear.

Figure 6.8 *Sall1* homolog protein sequence alignment.
Codon 84 is highlighted in red with the amino acid substitution in mouse (C57BL/6J) labelled above.

```
                                    T84A
Homo sapiens              [74]  VNENPASPPETFSPSP-PPDN [93]
Macaca mulatta            [74]  VNENPASPPETFSPSP-PPDN [93]
Pan troglodytes           [93]  VNENPASPPETFSPSP-PPDN [112]
Rattus norvegicus         [74]  VNESPASPPKTFPPGPPSLNN [94]
Mus musculus              [74]  VNESPASPAKTFPPGP-SLND [93]
Gallus gallus             [74]  VNENPASPPETFPPRS-PSDN [93]
                                ***.****.:**.* . . ::
```

6.6.5 Deletion and Insertion Polymorphisms

All deletion and insertion polymorphisms were identified in the 5' and/or 3'UTR of candidate genes of which none were assessed to be located within putative transcription factor binding sites as determined by TFSEARCH (Section 2.1.5).

In summary, *Adcy7*, *Cyld*, *Card15*, *Slic1* and *Sall1* remain interesting candidates for further analysis. *Adcy7*, *Card15* and *Slic1* are particularly intriguing having both 3'UTR polymorphisms within putative transcription factor binding sites and also nonsynonymous polymorphisms that cause amino acid substitutions in known and putative functional domains. While it is difficult to distinguish which 3'UTR polymorphisms are the most potentially interesting in terms of functional relevance to prion disease, two nonsynonymous polymorphisms residing in *Slic1* and *Card15*, although occurring at residues which are not highly conserved, may affect functional domain regions important in regulating membrane trafficking and apoptosis. These processes are known to be important in the regulating the normal location of the cellular prion protein (Section 1.1.5) and also in the mechanisms of prion pathogenesis (Section 1.1.10). The potential functional implications of exonic and intronic polymorphisms residing in *Brd7* and *Nkd1* are unclear because they are not located within known functional domains or putative transcription factor binding sites and therefore these genes were removed from further analysis.

6.7 Testing Individual Polymorphisms for Linkage

As previously described (Section 5.7), it is necessary to verify the accuracy of HAPPY's prediction of an association between polymorphism SDP and incubation time. Polymorphisms representative of the common SDP reaching a –logP value of 4.22, from *Adcy7* (m*Adcy7*x3#2) and *Card15* (m*Card15*x4#1), were chosen for analysis. These genes contain several sequence variants residing in putative

transcription factor binding sites and in known functional domains and therefore have implications for gene regulation and protein function and structure which may be influencing incubation time. As previously described (Section 6.6.4), m*Adcy7*x3#2 is a nonsynonymous polymorphisms located in a region predicted to form one of 12 membrane-associated helices (Watson et al., 1994). m*Card15*x4#1 is also nonsynonymous and although not located within a known functional domain, produces a change in residue polarity at codon 205 which may have implications for protein structure and therefore function. m*Adcy7*x3#2 and m*Card15*x4#1 were tested by allelic discrimination (Sections 2.4.5.1 and 2.4.5.5) in approximately 400 generation 37 HS from the 20% extremes of the prion disease incubation time distribution. Details of primer and fluorescently labelled probe sequences for allelic discrimination are listed in Appendix 4.

m*Adcy7*x3#2

The individual C and T alleles of m*Adcy7*x3#2 (Table 6.3) are associated with a 'long' and 'short' mean incubation time of 151±2 days and 144±1 days, respectively (Table 6.6). A significance difference of 7 days in mean incubation time is observed between these alleles ($p<0.0001$, Mann-Whitney Test). The mean incubation times of TT, TC and CC genotypes are 140±2 days, 150±2 days and 151±3 days respectively (Table 6.6). A significant association between m*Adcy*x3#2 genotype and incubation time has been identified ($p<0.0001$, Kruskal-Wallis ANOVA). The 'long' incubation time C allele is dominant conferring long incubation times in heterozygote mice.

m*Card15*x4#1

The individual G and A alleles of m*Card15*x4#1 (Table 6.3) are associated with a 'short' and 'long' mean incubation time of 143±1 days and 151±2 days, respectively (Table 6.6). A significant difference of 8 days in mean incubation time is seen between these alleles ($p<0.0001$, Mann-Whitney Test). The mean incubation times of GG, GA and AA genotypes are 140±2 days, 151±2 days and 150±4 days respectively (Table 6.6). A significant difference is observed between m*Card15*x4#1 genotype and mean incubation time ($p<0.0001$, Kruskal-Wallis ANOVA). The A allele shows dominance conferring longer incubation times in heterozygote mice.

Extremely significant associations, between both allele and genotype, with incubation time were observed for both polymorphisms in the HS verifying the prediction of

Table 6.6 Genotype/phenotype analysis of m*Adcy7*x3#2 and m*Card15*x4#1 in the HS. IT=incubation time.

Polymorphism	Allele/Genotype	IT (Days) ± SEM (n)
m*Adcy7*x3#2	C	151 ± 2 (262)
	T	144 ± 1 (502)
	CC	151 ± 3 (49)
	TC	150 ± 2 (164)
	TT	140 ± 2 (169)
m*Card15*x4#1	G	143 ± 1 (506)
	A	151 ± 2 (256)
	GG	140 ± 2 (173)
	GA	151 ± 2 (160)
	AA	150 ± 4 (48)

HAPPY analysis. Since the SDP represented by these polymorphisms is common across the region of interest (Table 6.3) it is possible that the association with incubation time can be extended to others whose alleles segregate accordingly.

6.8 Gene Expression

As previously described (Section 3.5), differential gene expression is another means by which to further characterise candidates. As previously described (Section 6.6.2), *Adcy7*, *Cyld*, *Sall1*, *Slic1* and *Card15* contain 3'-UTR region polymorphisms reaching a threshold for 'suggestive' linkage (–logP=4.22) (Table 6.3) and are therefore all good candidates for analysis of differential gene expression.

As previously described (Section 3.5), Candidate gene expression was quantified by SYBR Green real-time PCR (Section 2.4.5.1-2 and 2.4.5.4) using cDNA generated from whole brain RNA extracted from 8-week old mice (Sections 2.4.1.2 and 2.4.1.4-5). Expression was quantified in the parental strains of the HS, with the exception of LP which was unavailable, and also in RIIIS/J for comparison with C57BL/6J. GAPDH was used as an endogenous control to normalise expression data (Sections 2.4.5.4). Full details of primer sequences for qRT-PCR can be found in Appendix 3. Gene expression data for mouse strains was grouped according to the polymorphism SDP (-logP=4.22) previously established (Section 6.7) as being associated with incubation time. All gene expression data was analysed using an unpaired, two-tailed t test unless stated otherwise. *Slic1* and *Card15* expression levels were too low to quantify accurately in all mouse strains.

Adcy7

No significant difference in *Adcy7* expression was observed between the SDP groups (p=0.45, Mann-Whitney Test) (Figure 6.9). However, a significant difference was identified between C57BL/6J and RIIIS/J (p=0.04) (Figure 6.10).

Figure 6.9 *Adcy7* mRNA expression grouped by SDP.
Shading of bars refers to Table 6.3. All samples were tested in triplicate. Units are arbitrary and represent quantity of *Adcy7* transcript normalised by quantity of GAPDH. N=6 for all strains except CBA where n=5. Error bars represent SEM.

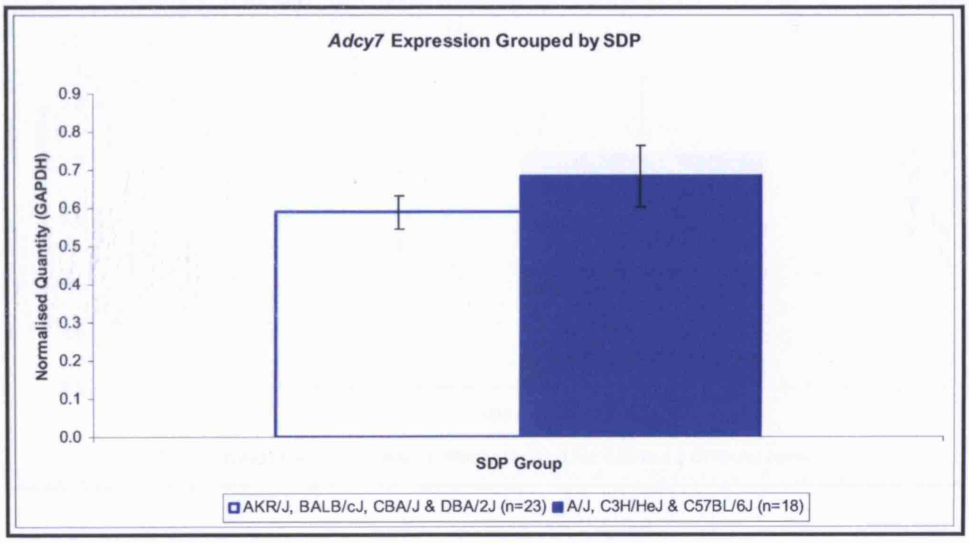

Figure 6.10 *Adcy7* mRNA expression in C57BL/6J and RIIIS/J.
Shading of bars refers to Table 6.3. All samples were tested in triplicate. Units are arbitrary and represent quantity of *Adcy7* transcript normalised by quantity of GAPDH. N=6 for all strains. Error bars represent SEM. * signifies p=0.042.

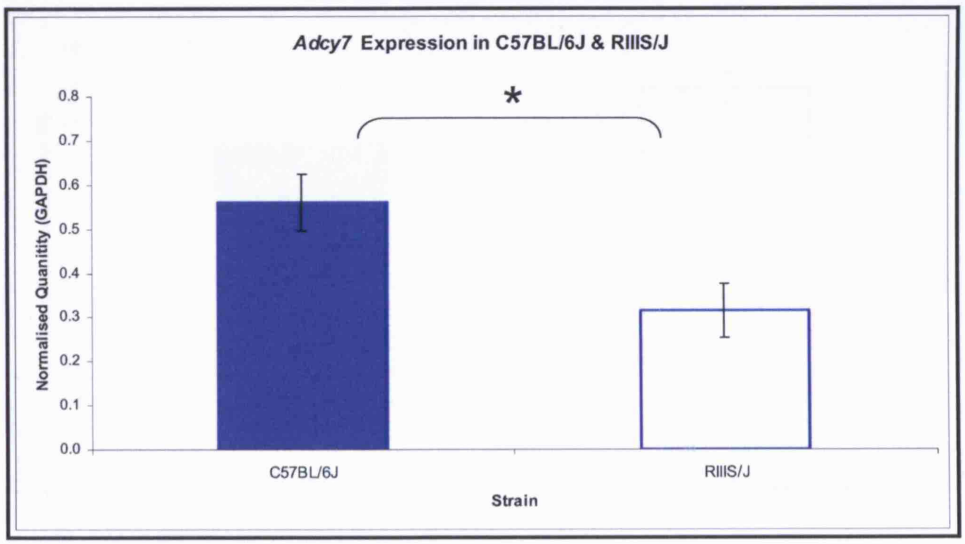

Cyld

No significant difference in *Cyld* expression was identified between SDP groups (p=0.54) (Figure 6.11) or between C57BL/6J and RIIIS/J (p=0.16) (Figure 6.12).

Figure 6.11 *Cyld* mRNA expression grouped by SDP.
Shading of bars refers to Table 6.3. All samples were tested in triplicate. Units are arbitrary and represent quantity of *Cyld* transcript normalised by quantity of GAPDH. N=6 for all strains except CBA where n=4. Error bars represent SEM.

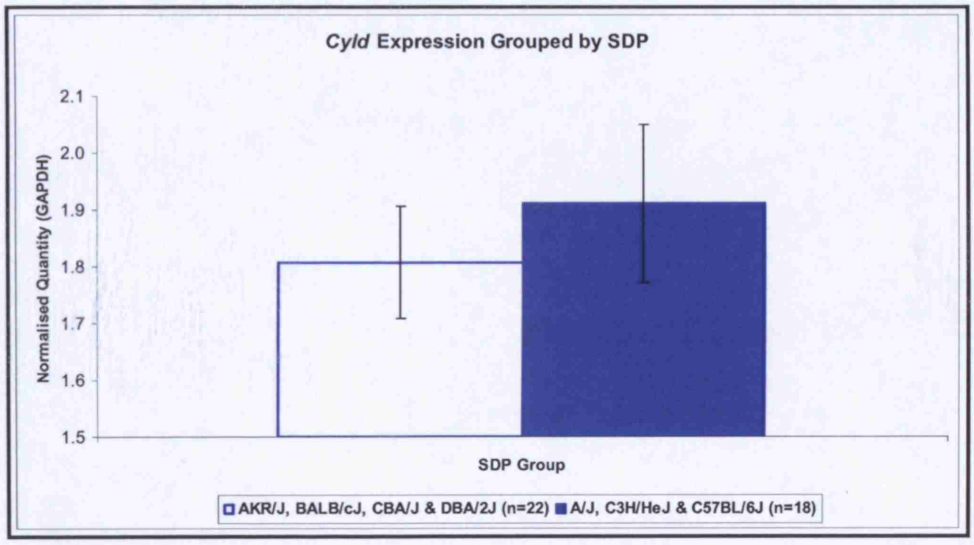

Figure 6.12 *Cyld* mRNA expression in C57BL/6J and RIIIS/J
Shading of bars refers to Table 6.3. All samples were tested in triplicate. Units are arbitrary and represent quantity of *Cyld* transcript normalised by quantity of GAPDH. N=6 for all strains. Error bars represent SEM.

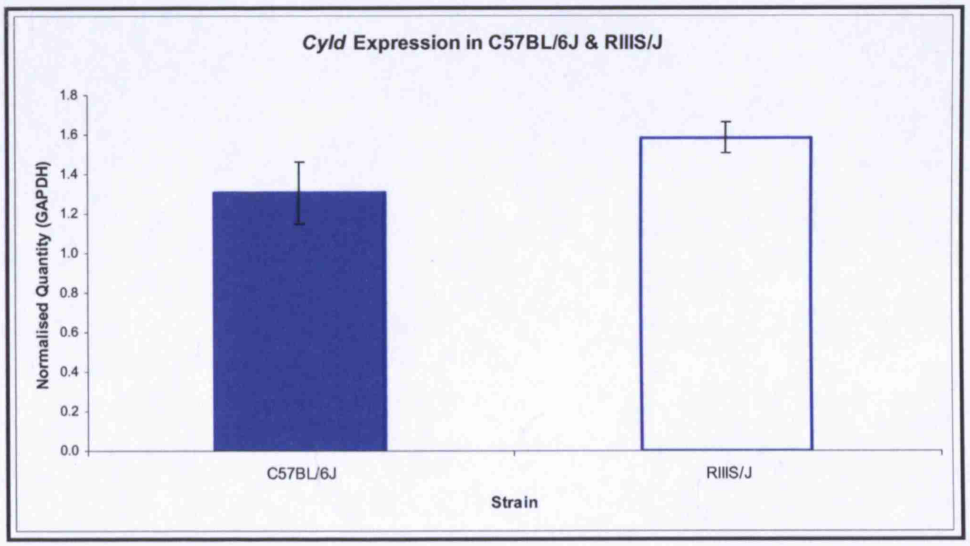

Sall1

No significant difference in *Sall1* expression was observed between SDP groups (p=0.98) (Figure 6.13). However, a significant difference in expression was identified between C57BL/6J and RIIIS/J (p=0.04) (Figure 6.14).

Figure 6.13 *Sall1* mRNA expression grouped by SDP.
Shading of bars refers to Table 6.3. All samples were tested in triplicate. Units are arbitrary and represent quantity of *Sall1* transcript normalised by quantity of GAPDH. N=6 for all strains. Error bars represent SEM.

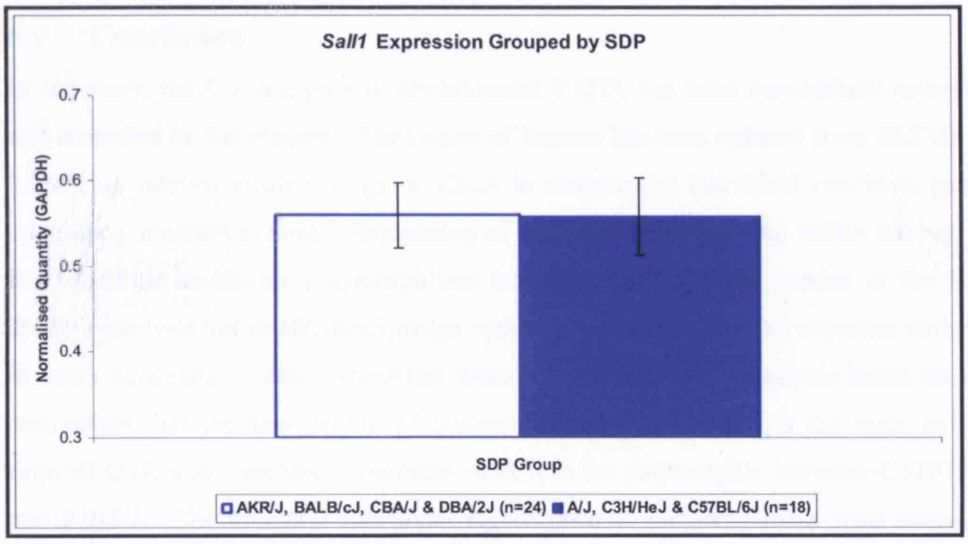

Figure 6.14 *Sall1* mRNA expression in C57BL/6J and RIIIS/J
Shading of bars refers to Table 6.3. All samples were tested in triplicate. Units are arbitrary and represent quantity of *Sall1* transcript normalised by quantity of GAPDH. N=6 for all strains. Error bars represent SEM. * signifies p=0.0356.

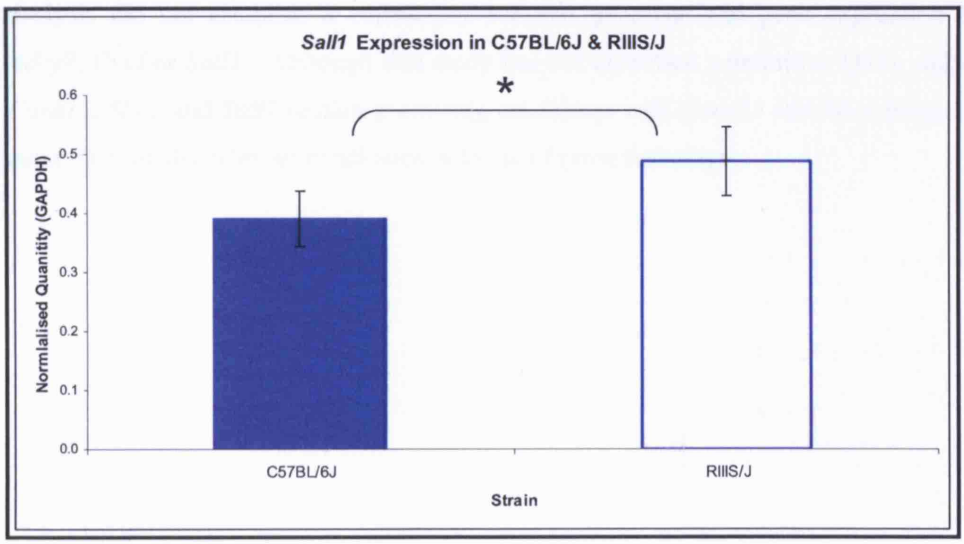

In summary, no correlation was identified between gene expression and genotype according to the SDP established as associated with incubation time (Section 6.7) in *Adcy7*, *Cyld* and *Sall1* suggesting that differential expression of these genes is unlikely to be an important factor controlling incubation time. Marginally significant differences in expression were seen between C57BL/6J and RIIIS/J in *Adcy7* and *Sall1* which are also unlikely to make a significant contribution to the observed variation in incubation time between these strains.

6.9 Conclusion

In summary, the fine mapping of chromosome 8 QTL has been successfully achieved and described in this chapter. The region of interest has been reduced from 20.8Mb to 2.2Mb, an interval small enough in which to characterise individual candidate genes controlling incubation time. Sequencing of ten candidates mapping within the region has identified numerous polymorphisms between the progenitor strains of the HS. HAPPY analysis has established linkage between incubation time and sequence variants in every candidate. Seven candidates were selected for further analysis based on the assumption that the new region of interest identified in the HS is the same as the original QTL and therefore candidates must also be polymorphic between C57BL/6J and RIIIS/J. The potential functional significance of polymorphisms were assessed highlighting numerous 3'UTR variants in putative transcription factor binding sites in *Adcy7*, *Cyld*, *Card15*, *Slic1* and *Sall1*. In addition, a number of nonsynonymous polymorphisms were identified in *Adcy7*, *Card15*, *Slic1* and *Sall1*, some occurring in conserved residues or in known and putative functional domains. mRNA expression analysis did not establish a correlation between genotype and gene expression for *Adcy7*, *Cyld* or *Sall1*. Although this study has not identified a definitive QTG, *Adcy7*, *Card15*, *Slic1* and *Sall1* remain promising candidates with *Card15* and *Slic1* being the most functionally relevant candidates in terms of prion pathology.

7

Fine Mapping Chromosome 9 QTL

7.1 Introduction

As previously described (Section 1.2.5), genome-wide mapping in a Chandler/RML inoculated F2 intercross, generated from 'short' (SJL/J) and 'long' (CAST/Ei) incubation time strains, has identified extensive QTL on chromosomes 9 (Figure 7.1) and 11, named prion incubation determinant-2 (*Pid2*) and -3 (*Pid3*), respectively (Stephenson *et al.*, 2000). This chapter describes the fine mapping of chromosome 9 QTL, spanning approximately 27.9Mb, in order to identify an interval small enough in which to examine individual candidate genes.

Figure 7.1 Chromosome 9 LOD score plot.
Plot represents the Chandler/RML incubation period in a SJL/J x CAST/Ei F2 intercross. The x axes display relative positions of markers along the chromosome in cM. Dotted lines intersecting the y axis in represents a statistical significance threshold of suggestive (2.39), significant (3.97) and highly significant (5.99) linkage. Figure adapted from Stephenson *et al.*, 2000.

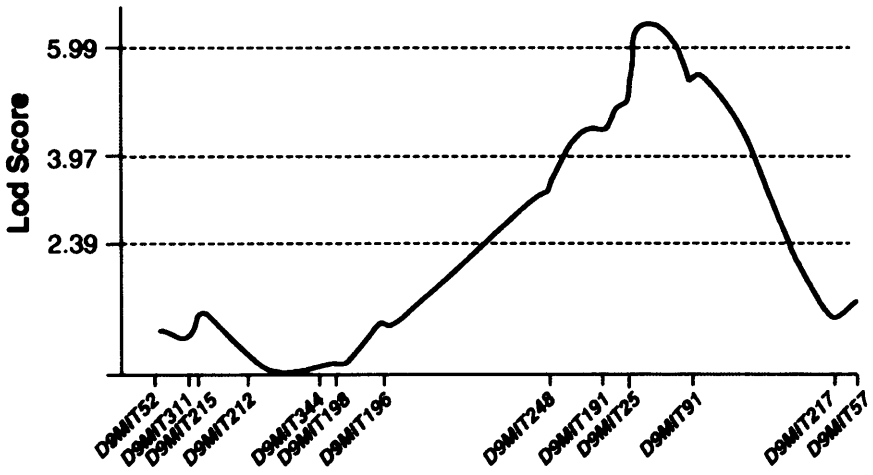

As previously described (Section 5.2), the genetically diverse Northport HS (Section 2.3.1) (Demarest *et al.*, 2001) were employed to fine map the region of interest. A potential limitation of the use of this cross was the absence of the mouse strains used in the original mapping studies to identify chromosome 9 QTL (Stephenson et al., 2000) and it is possible that these loci may be specific and exclusive to SJL/J and CAST/Ei strains. The successful use of the HS in fine mapping chromosome 11 QTL (Chapter 5) supported its further application in resolving chromosome 9 loci, since both were

identified in the same F2 intercross. Furthermore, the potential gains to be made from the use of the HS in reducing regions of interest and enabling the identification of individual candidate genes, outweighed the possible risk that linkage would not be reproduced in these mice.

7.2 HAPPY Linkage Analysis

As previously described (Section 5.2), fluorescently-labelled microsatellite markers mapping within the flanking markers of chromosome 9 QTL, *D9Mit88* and *D9Mit248*, were selected to genotype approximately 400 generation 37 HS mice (Section 2.3.1) from the extreme ~20% of each end of the Chandler/RML incubation time distribution for HAPPY linkage analysis (Section 2.4.4.5) (Mott *et al.*, 2000). Primer sequences and fluorescent labelling details for markers are listed in Appendix 1.3.

Table 7.1 HS progenitor strain allele sizes for chromosome 9 microsatellite markers.
cM=centimorgan and bp=base pairs.

Marker	Position (cM)	Marker Sizes (bp)							
		A	AKR	BALB	C3H	C57	CBA	DBA	LP
D9Mit88	12	202	202	202	202	202	218	202	226
D9Mit297	15	107	107	107	107	101	80	110	110
D9Mit247	17	135	153	135	135	147	149	153	149
D9Mit327	17	129	131	129	129	127	127	131	129
D9Mit285	21	119	127	119	119	123	117	129	125
D9Mit286	23	92	100	92	92	110	92	100	106
D9Mit191	26	99	99	99	99	151	99	99	155
D9Mit97	29	159	149	159	159	149	144	159	132
D9Mit4	29	130	122	130	132	122	122	130	128
D9Mit141	31	101	95	103	101	103	101	101	101
D9Mit102	31	150	154	146	146	146	154	150	146

Two separate regions of significant linkage were successfully identified (Figure 7.2). The most significant interval is defined by the flanking markers *D9Mit327* to *D9Mit286* spanning a combined region of 1.5Mb with a peak occurring between *D9Mit285* to *D9Mit286* (-logP=8.02). This interval is located within the peak of linkage for the reported chromosome 9 QTL (Stephenson et al., 2000) (Figure 7.3) and was chosen for further analysis. A second significant region was also identified within two additional marker intervals spanning a combined region of 7.3Mb between *D9Mit4* and *D9Mit102* with a peak –logP value of 4.69. Both regions represent a marked reduction in size compared to that of the original QTL.

Figure 7.2 Chromosome 9 HAPPY linkage analysis –logP plot.
The x axis represents 10 microsatellite marker intervals across chromosome 9. Dotted line intersecting the y axis indicates the –logP value representing a statistical significance threshold of 4.3.

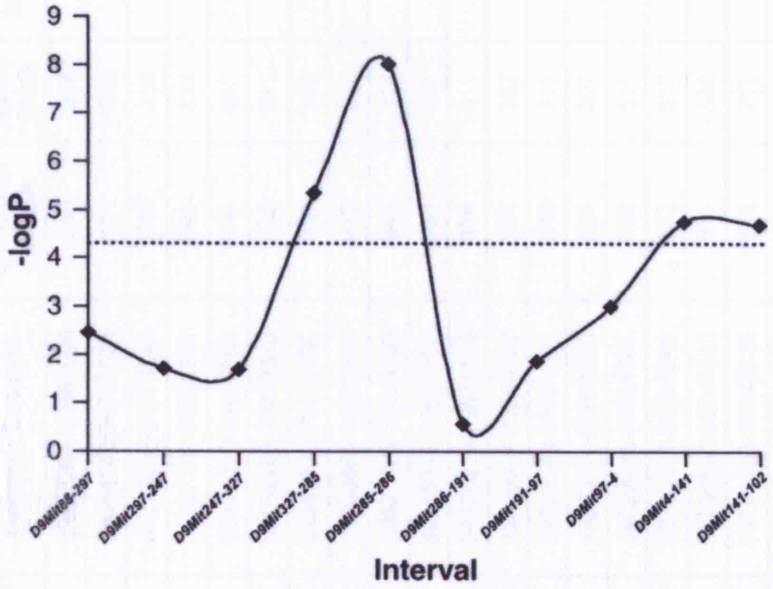

Figure 7.3 Chromosome 9 schematic.
The horizontal red line signifies the chromosome 9 QTL. The peak of linkage within the QTL is indicated by black brackets. Horizontal blue lines signify two new regions of linkage identified in the HS. Flanking markers of each region and their sizes are labelled in corresponding colours.

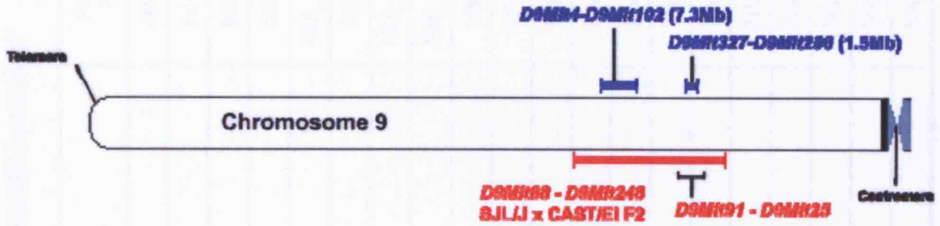

7.3 Candidate Genes

Sequence information for known and predicted candidate genes mapping within the new regions of significant linkage was obtained from sequence annotation databases as previously described (Section 3.2). Due to time constraints only the smallest and most significant interval, *D9Mit327* to *D9Mit286*, was chosen for further investigation in this study. Thirty-one known genes map within this region alongside several less well characterised genes and RefSeq sequences listed in Table 7.2 which provides details of candidate gene accession numbers, genomic location, transcript length, peptide length and number of exons. The function of well characterised genes was assessed to

Table 7.2 Chromosome 9 candidate genes (*D9Mit327-D9Mit286*).

Gene Name (Symbol)	Accession Number	Strand	Genomic Location	Transcript Length	Amino Acids	Exons
AW551984 (*AW551984*)	NM_178737	-1	39337967-39354695	4293	804	20
Olfactory Receptor 148 (*Olfr148*)	NM_146505	1	39364140-39365071	1017	310	1
Olfactory Receptor 960 (*Olfr960*)	NM_146279	1	39373696-39374644	1067	316	1
Olfactory Receptor 961 (*Olfr961*)	NM_146504	1	39397299-39398241	945	314	1
Olfactory Receptor 963 (*Olfr963*)	NM_001011827	1	39419630-39420564	936	311	1
Olfactory Receptor 149 (*Olfr149*)	NM_207138	-1	39452403-39453338	936	311	1
Olfactory Receptor 965 (*Olfr965*)	NM_001011859	1	39469800-39470736	939	312	1
Olfactory Receptor 967 (*Olfr967*)	NM_001011826	1	39500959-39501890	933	310	1
Olfactory Receptor 968 (*Olfr968*)	NM_146612	-1	39522426-39523369	945	314	1
Olfactory Receptor 969 (*Olfr969*)	NM_146826	1	39545948-39546882	936	311	1
Olfactory Receptor 970 (*Olfr970*)	NM_146611	1	39570212-39571146	936	311	1
Olfactory Receptor 971 (*Olfr971*)	NM_146614	1	39590007-39590929	924	307	1
Olfactory Receptor 972 (*Olfr972*)	NM_146610	1	39623848-39624791	945	314	1
Olfactory Receptor 973 (*Olfr973*)	NM_146613	1	39660376-39661298	924	307	1
Olfactory Receptor 974 (*Olfr974*)	NM_147107	1	39692833-39693765	933	310	1
Olfactory Receptor 975 (*Olfr975*)	NM_146828	-1	39700409-39701340	933	310	1
Olfactory Receptor 976 (*Olfr976*)	NM_146367	-1	39706560-39707540	981	326	1
Olfactory Receptor 978 (*Olfr978*)	NM_147105	1	39744383-39745316	936	311	1
Olfactory Receptor 979 (*Olfr979*)	NM_147108	-1	39750863-39751796	936	311	1
Olfactory Receptor 980 (*Olfr980*)	NM_147106	-1	39756586-39757518	933	310	1

Gene Name (Symbol)	Accession Number	Strand	Genomic Location	Transcript Length	Amino Acids	Exons
Olfactory Receptor 981 (*Olfr981*)	NM_146286	1	39772966-39773897	997	310	1
Olfactory Receptor 982 (*Olfr982*)	NM_146854	1	39824868-39825832	966	321	1
Olfactory Receptor 983 (*Olfr983*)	NM_146827	-1	39842588-39843535	948	315	1
Olfactory Receptor 984 (*Olfr984*)	NM_146608	-1	39851116-39852059	945	314	1
Olfactory Receptor 985 (*Olfr985*)	NM_146855	-1	39877597-39878530	936	311	1
AK006538 (*AK006538*)	AK006538	1	39898693-39901445	987	230	4
Olfactory Receptor 986 (*Olfr986*)	NM_146615	1	39937688-39938625	1016	312	1
Zinc Finger Protein 202 (*Zfp202*)	NM_030713	1	39942897-39963762	3454	641	7
Sodium Channel, Voltage-gated Type III, Beta (*Scn3b*)	NM_178227	1	40019788-40042188	4149	215	7
GRAM domain containing 1B (*Gramd1b*)	NM_172768	-1	40048478-40206335	2814	878	20
Adipocyte-Specific Adhesion Molecule (*9030425E11Rik*)	NM_133733	1	40437063-40536231	4015	373	7
Heat Shock Protein 8 (*Hspa8*)	NM_031165	1	40552344-40556268	2102	646	9
AK038159 (*AK038159*)	AK038159	1	40572591-40572944	354	117	1
Brain Specific Homeobox (*Bsx*)	NM_178245	1	40625196-40629041	875	232	3
RIKEN cDNA 4931429I11 gene (*4931429I11Rik*)	NM_001081121	-1	40645918-40715181	3068	770	9
Cytotoxic and Regulatory T Cell Molecule (*Crtam*)	NM_019465	-1	40723865-40755655	1884	388	10
RIKEN cDNA 2810457I06 gene (*2810457I06Rik*)	NM_176860	-1	40764710-40908563	3243	638	14

highlight those which may be potentially relevant in prion pathogenesis. However, as the mechanisms of prion disease have not been fully characterised candidate genes with potentially unrelated functions may also be important.

Olfactory receptors

Twenty-five olfaction receptors map within the region of interest. Olfaction is essential for the survival of animals since it aids the location of food, the identification of mates and offspring and the avoidance of danger. Olfactory receptors interact with a multitude of odorant ligands to initiate a cascade of signal transduction events leading to smell perception (Firestein, 2001). Odorant receptors are the largest mammalian gene family, a recent study identifying 1037 functional genes and 354 pseudogenes distributed in 69 genomic clusters in mice (Niimura and Nei, 2005).

Zinc Finger Protein 202 (Zfp202)

Zinc finger proteins have a role in transcriptional regulation. Human ZNF202 is a transcriptional repressor located within an hypoalphalipoproteinemia susceptibility locus on chromosome 11q23 that binds elements found predominantly in genes involved in HDL metabolism (Porsch-Ozcurumez *et al.*, 2001) and has also been implicated as a candidate gene involved in ischemic heart disease (Stene *et al.*, 2006).

Sodium Channel, Voltage-gated Type III, Beta (Scn3b)

p53 is a transcription factor and tumour suppressor which induces growth arrest and/or apoptosis in response to cellular stress and alterations in this gene have been implicated in human carcinogenesis (Hollstein *et al.*, 1991). SCN3B is upregulated in mouse and human in response to p53-dependent DNA damage suggesting a role for this sodium channel subunit in p53-dependent apoptotic pathways (Adachi *et al.*, 2004).

GRAM domain containing 1B (Gramd1b)

GRAMD1B contains a ~70 amino acid β-sheet GRAM domain which is thought to be involved in intracellular protein-binding or lipid binding signalling in membrane associated processes (Doerks *et al.*, 2000). This domain was originally identified on the basis of homology from bioinformatics between three proteins, namely glucosyltransferases, Rab-like GTPase activators and myotubularins.

Heat Shock Protein 8 (Hspa8)

HSPA8 is a 70kDa heat shock cognate protein which participate as 'molecular chaperones' facilitating protein synthesis, folding and higher ordered protein assembly (Ellis and van der Vies, 1991). A two-fold increase in a *Hsp70* gene, namely *Hsp73*, has been reported in the later stages of disease progression in scrapie-infected mouse brain (Kenward *et al.*, 1994; Kenward *et al.*, 1996) and a high number of lysosomes enriched with PrP and *Hsp73* have been identified in the brains of scrapie-sick mice (Laszlo *et al.*, 1992). Furthermore prominent accumulation of the inducible HSP72 in the cerebellar Purkinje cells of CJD patients has been reported (Kovacs *et al.*, 2001). As previously described (Section 1.1.10), aggresome-like structures associated with apoptosis in the brains of scrapie-infected mice following mild inhibition of the proteasome have been shown to contain HSP70 (Kristiansen *et al.*, 2005). These lines of evidence provide substantial support for the importance of heat shock proteins in prion disease pathology implicating *Hspa8* as the most promising potential candidate in the new region of linkage.

Brain Specific Homeobox (Bsx)

Homeobox (HOX) transcription factors specify and govern development and differentiation in all metazoan (Scott *et al.*, 1989). HOX proteins have a highly conserved 60 amino acid homeodomain which has a sequence specific DNA binding activity that regulates target gene expression (Levine *et al.*, 1984). As it's name denotes, BSX is expressed in specific brain structures in the mouse including the septum, epiphysis, mammillary bodies and arcuate nucleus during development, a pattern which is maintained postnatally (Cremona *et al.*, 2004).

Cytotoxic and Regulatory T Cell Molecule (Crtam)

CRTAM is a member of the immunoglobulin superfamily (Ig-SF) and is expressed by activated T cells (Kennedy *et al.*, 2000). CRTAM has a known role in tumour suppression by mediating the effects of Nectin-like 2 (NECL2), which inhibits tumourigenesis by ensuring that epithelial cells grow in organised layers (Masuda *et al.*, 2002).

The function of *AW551984*, *AK006538*, Adipocyte-Specific Adhesion Molecule (*9030425E11Rik*), *AK038159*, RIKEN cDNA 4931429I11 gene (*4931429I11Rik*) and RIKEN cDNA 2810457I06 gene (*2810457I06Rik*) are unknown as these genes and their

protein products are not well characterised.

7.4 *Hspa8* Sequence Polymorphisms

Due to time constraints a single candidate gene, *Hspa8*, which has putative functional relevance to prion pathology was chosen for sequence analysis. As previously described (Section 3.3), sequence analysis of *Hspa8* was undertaken to identify polymorphisms between the parental strains of the HS and also between SJL/J and CAST/Ei strains used to identify chromosome 9 QTL (Stephenson et al., 2000). Details of PCR primer sequence and conditions for use are listed in Appendix 2.3. Sequence polymorphism data is listed in Table 7.3.

Table 7.3 Haplotype patterns of alleles mapping between *D9Mit327* and *D9Mit286*.
MM=Microsatelitte Marker, E=Exonic, I=Intronic, In=Insertion, D=Deletion, NC=No Change (compared to NCBI, Ensembl and UCSC database sequence), ND=Not Determined and bp=base pair. Shading illustrates polymorphism SDP.

Marker/Polymorphism Description		Position	A	AKR	BALB	C3H	C57	CBA	DBA	LP	SJL	CAST
D9Mit327	**MM**	**39334780**	**129**	**131**	**129**	**129**	**127**	**127**	**131**	**129**	**ND**	**ND**
m*Hspa8* 5'#1	E	40552370	G	G	G	G	T	G	G	G	G	G
m*Hspa8* 5'#2	E	40552377	C	C	C	C	T	C	C	C	C	C
m*Hspa8*x3#1	E	40553810	T	T	T	T	C	T	T	T	T	T
m*Hspa8*x3#3	E	40553945	T	T	T	T	C	T	T	T	T	T
m*Hspa8*x4#2	E	40554132	A	G	A	A	A	G	G	G	A	A
m*Hspa8*xInx7#1	I D	40555522	4bp	4bp	4bp	4bp	NC	4bp	4bp	4bp	4bp	3bp
m*Hspa8*Inx8#1	I In	40555989	1bp	1bp	1bp	1bp	NC	1bp	1bp	1bp	1bp	1bp
D9Mit286	**MM**	**40872548**	**92**	**100**	**92**	**92**	**110**	**92**	**100**	**106**	**ND**	**ND**

Hspa8 spans 3.9kb with a 2102bp mRNA transcript containing 9 exons and a 5' and 3'UTR. In total, seven polymorphisms were identified between the parental strains of the HS (Table 7.3). Two SNPs were identified in the 5'UTR, two synonymous SNPs in exon 3 and one synonymous SNP in exon 4. The 5'UTR polymorphisms were not located in any putative transcription factor binding sites as determined by the TFSEARCH software program (Heinemeyer *et al.*, 1998) (Section 2.1.5). A four base deletion polymorphism was identified in intron 6 and a one base insertion was identified in intron 7. It is difficult to predict the effect of such polymorphisms as they are not located in intronic 5' or 3' splicing signal sequences and are therefore unlikely to effect splicing of *Hspa8* between mouse strains. A heat shock element (HSE) derived from nucleotides 197-217 of the promoter region in addition to an inverted CCAAT box and a TATA box located at nucleotide 223 (Hunt *et al.*, 1999) were also analysed but no polymorphisms identified. A general SDP was seen across *Hspa8* with the C57BL/6J

strain differing from the other parental strains of the HS. A different polymorphism SDP was observed for a SNP identified in exon 4 where A/J, BALB/cJ, C3H/HeJ and C57BL/6J segregated from AKR/J, CBA/J, DBA/2J and LP/J.

7.5 HAPPY Analysis of *Hspa8* Polymorphisms

As previously described (Section 5.5), HAPPY linkage analysis software (Section 2.4.4.5) was used to investigate if any *Hspa8* polymorphisms are potentially associated with incubation time. No polymorphisms reached a level of suggestive (>2.8) or significant (>4.3) linkage (Figure 7.4) suggesting that this candidate is not an important QTG for prion disease incubation time.

Figure 7.4 HAPPY analysis output for polymorphisms identified between *D9Mit327* and *D9Mit286*.
The x axis measures distance along the chromosome between the flanking markers (vertical lines) of the region of significant linkage. The y axis indicates –logP values. Each polymorphism is identified as a black dot on the plot.

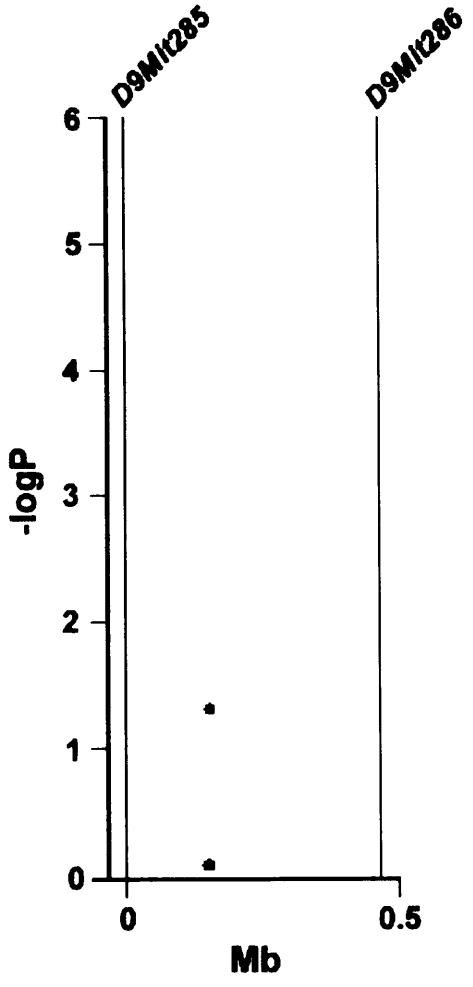

Sequence data for SJL/J and CAST/Ei were compared for the *Hspa8* polymorphisms identified (Table 7.3). With the exception of a three base pair deletion in CAST where a four base pair deletion was identified in all other strains relative to C57BL/6J (m*Hspa8*xInx7#1), no genetic differences were seen between SJL/J and CAST/Ei suggesting that *Hspa8* is not an important incubation time QTG for these strains either.

7.6 Conclusion

In summary, the fine mapping of chromosome 9 QTL has been successfully achieved and described in this chapter. The region of interest has been reduced from 27.9Mb to two intervals spanning 1.5Mb and 7.3Mb which are small enough to characterise individual candidate genes. Time constraints prevented analysis of all candidate genes within the new regions of linkage. Sequence analysis of *Hspa8*, a candidate gene of putative functional relevance to prion pathology and mapping within the smallest and most significant region of linkage, identified seven polymorphisms between the parental strains of the HS. HAPPY analysis did not establish linkage between these polymorphisms and incubation time suggesting that *Hspa8* is not an important QTG. Furthermore, no polymorphisms were observed between SJL/J and CAST/Ei suggesting that this gene is not an important QTG for these strains either. Further sequence analysis of the remaining candidate genes mapping within these regions of interest is required.

8

Discussion

The work described in this thesis aimed to fine map previously identified murine QTL for prion disease incubation time and further characterise candidate genes controlling the phenotype. The mouse is a valuable model of prion disease as it recapitulates key clinical and neuropathological features including the characteristic prolonged incubation time observed in human and animal prion diseases. It is possible to map loci controlling incubation time in mice because it is a quantitative trait and can therefore be used as a phenotype in linkage studies. Characterising the molecular basis of incubation time QTL will potentially uncover new insights into the biology of prion disease. It is hoped that due to the high sequence conservation between mice and humans successful identification of murine genes controlling incubation time within QTL may in turn highlight potential candidates in the human genome.

8.1 Fine Mapping Incubation Time QTL

Prion disease incubation time QTL identified in mice (Lloyd et al., 2001; Lloyd et al., 2002; Manolakou et al., 2001; Moreno et al., 2003; Stephenson et al., 2000) have provided a foundation for further analysis through fine mapping techniques. The ultimate aim of the identification of incubation time QTL and the underlying genes controlling a phenotype is to be able to relate this analysis to the human population and find relevant genes for human prion disease. All work identifying incubation time QTL in mice has used intracerebral inoculation as the preferred method of prion infection whereas some human prion diseases have occurred as a result of alternative routes of infection, such as oral ingestion of prions in the case of kuru and vCJD. The route of transmission is a major factor in the modulation of incubation time and different QTL may be specific to oral and intracerebral infection. In addition, the possibility of a prion strain specific effect is another factor to consider as the mouse-passaged scrapie strain, Chandler/RML, was used in this study but vCJD, for example, is thought to have been caused by exposure to BSE prions. It is possible that QTL are specific to certain prion strains. Furthermore, in the case of vCJD, a species barrier was present in the transmission of disease to humans from exposure to BSE prions, a modulating factor not accounted for in the present study. These factors all present a potential problem for the extrapolation of findings to humans but any advance in the understanding of the

mechanisms of disease and the pathways involved is unquestionably valuable.

The Northport HS

In this study, the genetically diverse Northport HS (Demarest *et al.*, 2001) were used to fine map incubation time QTL on chromosomes 8, 9 and 11 (Lloyd *et al.*, 2001; Manolakou *et al.*, 2001; Stephenson *et al.*, 2000). This high resolution mapping reduced extensive regions of interest into smaller intervals for further characterisation. The HS were chosen as the preferred strategy over the use of other methods such as advanced intercrosses because as an outbred stock they are more genetically diverse and feature more recombination breakpoints. Other alternatives such as congenic mice are also less diverse and may not significantly reduce the regions of interest for analysis.

The Wellcome Trust Centre for Human Genetics has recently utilised the Northport HS in a whole genome genetic association study identifying the molecular basis of naturally occurring genetic variants controlling multiple phenotypes of importance to human health (Solberg *et al.*, 2006). Over 100 phenotypes relating to disease were collected in 2000 HS animals. Anxiety, type II diabetes and asthma were specifically targeted alongside mouse haematology and immunology profiles. A high resolution genetic map of the SNP data collected has been constructed for the progenitor strains of the HS and could be used as an essential resource for the mapping of prion disease incubation time QTL not included in this study, once they have been fine mapped using the HS. The database could also be used to back up the SNP data described here and may represent a potential avenue for the further analysis of the fine mapped chromosome 9 QTL.

This high-throughput phenotyping method allowed the investigation of relationships between a range of physiologic and behavioural parameters, detecting genetic epistatic effects that are so often invisible in single gene-based approaches. A similar genome wide approach using the Northport HS could have been utilised in identifying incubation time QTL, especially given that an assumption has been made that the regions of significant linkage identified in the HS correspond to those identified in the original mapping studies. It is possible that these regions may in fact not represent the same QTL and a genome wide approach in the HS may identify several additional loci. However, this method would have been very costly both in financial terms and the length of time required to carry out such a study. As incubation time QTL have already been identified on chromosomes 8, 9 and 11 (Lloyd et al., 2001; Manolakou et al.,

2001; Stephenson et al., 2000) there was no need for an analysis of the whole mouse genome. Instead the previously identified regions of linkage provided more focused starting points for fine mapping with the HS.

The Northport HS parental strains are a panel of unrelated classical inbred strains with a common ancestry (Beck et al., 2000) which provides potential advantages and disadvantages. A potential limitation of the use of this cross was the absence of the mouse strains used in original mapping studies from the panel of strains generating the HS. This posed the possible risk that if the original QTL were mouse strain specific they would not be relevant for the progenitor strains of the HS and linkage would not be reproducible. On the other hand the ancestry of the HS implies that they may potentially share alleles with the strains used in original mapping efforts. Classical inbred strains derive their genetic background from a combination of *M m. musculus*, *M. m castaneus* and *M m. domesticus* subspecies and the hybrid *M m. molossimus* (Frazer et al., 2007; Wade and Daly, 2005; Wade et al., 2002; Yang et al., 2007). The genetic background of SJL, NZW, CAST and RIII substrains are also derived from these subspecies. This may explain the successful reproduction of linkage on chromosome 8, 9 and 11 and furthermore indicate that the new regions of linkage may be the same as the previously identified QTL.

SNP Identification Strategy

This study aimed to identify the naturally occurring genetic variation between mouse strains which controls incubation time. Such naturally occurring sequence variants are unlikely to have major functional implications and alternatively have more subtle effects in contributing towards the phenotype. For instance, they may confer slight changes in protein structure, gene regulation or in the efficiency of protein enzymatic and/or binding activity. These small genetic differences between mouse strains may be causing minor physiological changes which have a cumulative effect in controlling susceptibility to prion disease therefore influencing observed incubation times.

Analysis of sequence in candidate genes was carried out in genomic regions of potential functional significance such as coding regions, splice sites and regulatory regions such as transcription factor binding sites and therefore it is possible that relevant loci residing in introns may have been overlooked. This somewhat limiting method of SNP discovery was chosen because a complete analysis of the fine mapped regions of

linkage would have required the high consumption of resources, such as time, at great expense. In addition, polymorphisms having potential functional effects at the protein level or influencing gene expression make potentially more tractable candidates for further analysis in cell and animal models. Sequence variants of this nature directly indicate which gene may be the most likely candidate and what type of subsequent experiments are needed to confirm its candidacy. It is far more difficult to ascertain the functional significance of an intronic polymorphism, which may be situated far from any known genes and potentially involved in the regulation of genes in even more remote regions of the genome, than to investigate a nonsynonymous polymorphism affecting protein structure and/or function. However, variants in complex diseases are often detected in non-coding DNA (Yalcin *et al.*, 2004a; Yalcin *et al.*, 2004b) and potential QTN may well be located within regulatory regions remote from their cognate transcriptional units (Nobrega *et al.*, 2003).

The anticipation of this study was that conserved blocks of SDPs would be identified within the HS progenitors which could be subsequently associated with incubation time. Therefore, instead of requiring a complete analysis of all sequence residing in regions of interest it was hoped that haplotype patterns could be identified based on the limited sequencing strategy employed. Candidate gene expression analysis was then used as a tool to support this hypothesis. This method was more likely to identify a QTG rather than a QTN but once this assessment is made further analysis may involve complete elucidation of all existing sequence variants and the identification of important QTN. This method has recently been successfully used to identify potential QTN for anxiety in mice (Yalcin *et al.*, 2005).

Gene expression analysis was carried out using whole brain samples. Many genes are expressed exclusively in certain regions of the brain and these expression patterns may underlie the specific function of a gene. Therefore the method used in this study is perhaps too crude. An analysis exploring expression differences between anatomical regions might have been more sensitive and more useful in identifying potential modifier genes for prion disease incubation time. For example, the identification of high candidate gene expression in areas of the brain known to be most affected by spongiform change or PrP^{Sc} deposition might indicate an involvement of a candidate in prion pathogenesis. To aid this analysis publicly available gene expression databases could have been employed to provide information about known patterns of expression

for candidates analysed in this study.

8.2 Chromosome 11 Candidate Genes

An initial approach undertaken to identify genes underlying incubation time QTL involved the selection of candidates based upon their functional relevance to prion disease and this methodology was chosen for the extensive and overlapping QTL identified on chromosome 11 (Lloyd *et al.*, 2001; Stephenson *et al.*, 2000). The approximate size of the combined regions of interest is 86.5Mb within which an estimated 865 genes are located, based upon an average of 10 genes per 1Mb for the mouse genome (Flint et al., 2005). Six candidate genes were chosen for analysis. By adhering more strictly to this pseudo-random candidate selection strategy many more functionally related genes could have been included in this analysis. However, this process would have been expensive, time consuming and inefficient because of the number of possible candidates for analysis and so those deemed the most functionally relevant were concentrated upon. This enabled as much of a focused candidate gene approach as possible in such expansive regions of linkage but ran the risk of overlooking other more important genes and had the potential to be very limiting in the successful elucidation of candidates. The mechanisms of prion disease and the biochemical pathways involved are not yet fully understood so selecting individual genes for analysis based exclusively upon their functional relevance to the processes related to the normal physiology of the prion protein or those of prion disease may not provide an adequate assessment and neglect more crucial candidates. Therefore, although this strategy provided a justifiable starting point for the analysis of chromosome 11 QTL, fine mapping techniques, such as the later use of the Northport HS, were required to resolve the regions of interest into smaller intervals, essential for a more efficient identification of candidate genes.

The Candidates

The six candidates chosen for analysis included VTN which was selected based upon it reported interaction with the cellular prion protein (Hajj *et al.*, 2007), MPO because of its suggested involvement in AD pathology (Crawford *et al.*, 2001; Green *et al.*, 2004; Reynolds *et al.*, 1999), NGFR for its mediation of prion protein-related neuronal death (Della-Bianca *et al.*, 2001), CDK5RAP3 as a regulator of CDK5, implicated in neurodegeneration (Bu et al., 2002; Nguyen et al., 2001; Smith et al., 2003), GFAP due to its increased expression following astrogliosis in prion disease (Duguid et al., 1988;

Manuelidis et al., 1987) and finally MAPT because of its involvement in neurodegenerative diseases such as AD (Goedert et al., 1988). *Vtn*, *Ngfr* and *Mapt* are perhaps the most interesting candidates from the group as the protein products of the first two genes are known to actually interact with the prion protein (Hajj et al., 2007) and mediate its effects in disease (Della-Bianca et al., 2001) and phosphorylated immunoreactive MAPT structures have been reported in mouse models of vCJD and also in the brains of human vCJD patients (Giaccone *et al.*, 2007). In addition, *Vtn* maps closest to the peaks of linkage, within 3cM, identified in original mapping studies (Lloyd et al., 2001; Stephenson et al., 2000). The remaining candidates are also interesting in terms of their presence at the physical sites of prion pathology and also through their links to other diseases which may uncover common pathways involved in neurodegeneration.

Sequence Variants

Following sequence analysis of chromosome 11 candidates in the 'short' (SJL/J, NZW/OlaHsd) and 'long' (CAST/Ei) incubation time strains used to identify incubation time QTL (Lloyd et al., 2001; Stephenson et al., 2000) polymorphisms were identified in each gene, the majority of alleles segregating between 'short' and 'long' incubation time strains. This may indicate shared QTL which is supported by the considerable overlap observed between the regions of interest (Lloyd et al., 2001; Stephenson et al., 2000). The pattern of segregation of alleles mirrors the phenotypic pattern observed in 'short' and 'long' incubation time strains and may be due to the shared ancestry of SJL/J and NZW/OlaHsd and/or be a possible consequence of CAST/Ei being common to both F2 intercrosses (Lloyd et al., 2001; Stephenson et al., 2000).

Where nonsynonymous polymorphisms were identified between mouse strains, homolog protein sequences were compared to assess whether substitutions were occurring in conserved residues or functional domain regions and therefore might be having an effect on protein structure and function. Several nonsynonymous polymorphisms were identified between 'short' and 'long' incubation time strains in *Mpo*, *Gfap* and *Mapt* which have potential functional implications for protein structure and function.

MPO expression is increased in AD and is predominantly localised with amyloid plaques (Reynolds *et al.*, 1999). MPO catalyses the reaction between hydrogen

peroxide and chloride to yield hypochlorous acid (HOCl) which is a strong oxidant toxic to micro-organisms and cells and this leads to the further generation of additional highly reactive radicals (Daugherty *et al.*, 1994). The contribution of MPO towards AD pathology is thought to be through direct cytotoxic effects on neurons following the generation of these oxidising species. Lipid peroxidation and oxidative damage alongside the appearance of senile plaques are early pathological signs of AD (Sayre *et al.*, 1997; Yan *et al.*, 1994) and it has been suggested that MPO-generated radicals promote the precipitation of beta-amyloid, or the coaggregation of ApoE and beta-amyloid (Strittmatter *et al.*, 1993). Amyloid plaque deposits are also a feature of prion disease and PrP^{Sc} is known to accumulate within these plaques. Therefore, MPO may be contributing towards prion pathology by the same mechanisms suggested for AD. A nonsynonymous polymorphism in *Mpo* (Q280P), causing a residue physicochemical change from hydrophilicity to hydrophobicity, was identified in a highly conserved heavy chain subunit domain which carry a covalently bound heme prosthetic group (Andrews and Krinsky, 1981). The substitution has implications for differences in protein tertiary structure between mouse strains and therefore implications for enzymatic activity, possibly attenuating or exacerbating pathology during disease and subsequently affecting incubation time.

A nonsynonymous polymorphism occurring in *Gfap* (F141L) is located in the large rod-like domain of several α-helices in GFAP which are known to be extensively conserved and show significant homology among all intermediate filaments (Geisler *et al.*, 1982; Geisler and Weber, 1982; Steinert *et al.*, 1983). As previously described (Section 3.2), the hydrophobic backbone of these helices causes aggregation of GFAP monomers into coiled coils which polymerize into filaments. Polymorphisms disrupting this high level of conservation may have implications for the normal cytoskeletal scaffolding within the cell which is vital for maintaining cellular shape. Changes in cellular shape may be potentially detrimental to normal function. No change in residue physicochemical property is observed and so the implications of this polymorphism are unclear. However, even minor changes in such a conserved domain may cause subtle effect on protein structure and/or function.

A nonsynonymous polymorphism in *Mapt* (S50A), causing a change in polarity in a conserved residue, occurs in the variable N-terminal domain of the protein, which has a putative role in microtubule bundling and antigen or ligand binding (Himmler *et al.*,

1989; Kanai *et al.*, 1992). It has recently been shown that an N-terminal fragment, specifically amino acids 18-42, is responsible for inhibiting full-length *Tau* polymerisation *in vitro* via an interaction with C-terminal sequences suggesting a putative role for the N-terminus in stabilising a soluble conformation of *Tau* (Horowitz *et al.*, 2006). Codon 50 resides just outside of this region but there may still be implications for controlling the stability of *Tau*. This stabilizing effect has yet to be tested *in vivo*. A conformation change of *Tau* into a filamentous state is common to the pathology of AD (Goedert et al., 1988), frontotemporal dementia (FTD) (Lee *et al.*, 2001) and is also a feature of vCJD (Giaccone *et al.*, 2007) and therefore, polymorphisms affecting stabilization may contribute towards differences in pathology between mouse strains influencing observed incubation times.

An extension of this analysis could have included investigating the gentoypte of additional 'short' and 'long' incubation time strains (Table 1.1) to determine whether the identified nonsynonymous polymorphisms correlated with phenotype.

Vtn mRNA Expression

Nonsynonymous polymorphisms identified in *Vtn* were identified outside the established critical binding site for PrP^C (Della-Bianca et al., 2001) and although no polymorphisms were identified in characterised regulatory regions of *Vtn* (Miyamoto et al., 1998; Seiffert et al., 1996), gene expression analysis identified a significant difference between SJL/OlaHsd and CAST/Ei strains. The genetic variants responsible for the difference in mRNA expression levels are separate to those identified in this study because SJL/OlaHsd and NZW/OlaHsd share polymorphism alleles but not the same expression profile when compared to CAST/Ei. *Vtn* is therefore a potential QTG for the SJL/J and CAST/Ei F2 intercross (Stephenson et al., 2000) but not for the NZW/OlaHsd and CAST/Ei cross (Lloyd et al., 2001) in which other loci are responsible for observed phenotypic variation. It is possible that multiple small effect QTL and therefore QTG and/or QTN, underlie the extensive and overlapping regions of linkage on chromosome 11 and these may be exclusive to each F2 intercross. Further support for a role for *Vtn* in prion pathogenesis is the finding that mRNA expression in Chandler/RML infected mice is undetectable suggesting that it may be significantly downregulated in disease. It is unclear how VTN may be involved in prion pathogenesis since its central role is in neuron proliferation and differentiation in the CNS during development (Martinez-Morales *et al.*, 1995; Seiffert *et al.*, 1995).

However, its interaction with PrP^C has highlighted a potential role for this gene in prion disease.

Mapt mRNA expression

A significant difference in *Mapt* mRNA expression was identified between normal and Chandler/RML infected CAST/Ei mice suggesting that *Mapt* is significantly downregulated in prion disease in this strain. It is possible that the reduced expression of *Mapt* in the disease state in CAST/Ei mice confers a protective effect, prolonging incubation time in this strain. In line with this theory, no downregulation of *Mapt* was seen in the short incubation time strains and therefore it may be present in levels substantial enough to contribute to pathology and decreased survival in these mice.

In conclusion, following the analysis of six chromosome 11 genes, potentially functionally relevant to prion pathology, there is evidence to support the candidacy and further analysis of MPO, GFAP, MAPT and VTN in cell and/or mouse models. *Mapt* and *Vtn* are perhaps the most promising of these candidates considering the potential functional implications of the nonsynonymous polymorphism in *Mapt* and the differential expression observed for *Vtn*. The validity of the approach of selecting genes for analysis based only upon their functional relevance to prion disease has been verified here by the conclusion that the majority of genes selected remain potential candidates worth further investigation. It could also be argued that this method of analysis is not stringent enough as it has not substantially reduced the candidate gene list for further analysis. In the absence of a complete picture of the mechanisms of disease it may be possible to make a case for many of the numerous candidate genes residing in the broad QTL identified in the original mapping studies, especially those who are known to have some related function. Therefore a more rigourous process of elimination is required in order to isolate the most important candidates.

8.3 Monocyte Chemoattractant Protein 1

Following a recent study detailing a significant delay in the late-stage clinical signs of disease and an increased survival rate in *Mcp1* knockout mice, challenged intracerebrally with the ME7 prion strain (Felton *et al.*, 2005), the role of this chemokine was investigated in the Chandler/RML murine model of prion disease. As previously described (Section 4.1), *Mcp1* maps within chromosome 11 incubation time QTL, in close proximity to peaks of linkage, identified in F2 intercrosses challenged

with the Chandler/RML prion strain (Lloyd et al., 2001; Stephenson et al., 2000) strongly implicating it as a potential QTG for these regions. Chandler/RML and ME7 prion strains are both *Prnp*^{a} (PrP Leu-108, Thr-189) mouse-adapted scrapie strains which produce similar clinical phenotypes in inbred mice suggesting that the findings of Felton *et al.,* may be successfully reproduced in the Chandler/RML murine model of prion disease.

MCP1 is a chemokine expressed by fibroblasts following induction with PDGF (Gu *et al.*, 1999; Rollins *et al.*, 1988). It drives the recruitment of monocytes to the brain parenchyma and activates resident microglia during an inflammatory response (Gu *et al.*, 1997; Gu *et al.*, 1999). MCP1 has potent actions in the CNS and is primarily thought to be responsible for exacerbating neuronal injury and/or death by driving microglial priming and activation. Ablation of *Mcp1* in a murine model of stroke has been shown to have a neuroprotective effect by limiting infarct size following reduced production of the pro-inflammatory cytokine, interleukin-1β (Hughes *et al.*, 2002). *Mcp1* has also been implicated in another chronic neurodegenerative disease, experimental allergic encephalomyeltis (EAE), an animal model of multiple sclerosis (Teuscher *et al.*, 1999). Nonsynonymous sequence polymorphisms in *Mcp1* are promising candidates for a locus (*eae7*) controlling susceptibility and the severity of clinical signs of EAE.

The Atypical Inflammatory Response & Microglial Activation in Prion Disease

An atypical inflammatory response is seen in the CNS in prion disease which is thought to cause accelerated neuronal death (Perry *et al.*, 2002). This response precedes overt neuronal death and the onset of severe clinical signs of disease by several weeks and is dominated by microglial activation (Giese et al., 1998), a key feature in murine models of prion disease, BSE and CJD (Baker *et al.*, 1999; Betmouni *et al.*, 1996; Manuelidis *et al.*, 1997) A large number of microglia are present throughout disease in the brains of scrapie infected mice (Williams *et al.*, 1994) and microglial activation parallels the temporal and spatial pattern of PrP^{Sc} deposition (Giese et al., 1998). It has been suggested that microglia may have a direct role in cell death in prion disease or by a more indirect route by enhancing gliosis (Brown, 2001). Migroglial activation in prion disease supports the hypothesis that MCP1 may have an important role to play in the atypical inflammatory response in prion pathogenesis. Furthermore, both pro- and anti-inflammatory molecules have previously been implicated in the control of incubation

time (Felton et al., 2005; Schultz *et al.*, 2004; Thackray *et al.*, 2004). In the ME7 model of prion disease it has been suggested that MCP1 is not necessary for microglial priming but may stimulate their further activation thus exacerbating neuronal damage (Felton et al., 2005).

Mcp1 Sequence Variants

Sequence analysis of *Mcp1* in 'short' and 'long' incubation time strains used to map chromosome 11 QTL (Lloyd et al., 2001; Stephenson et al., 2000) identified ten exonic polymorphisms, five of which segregated between mouse strains in a pattern consistent with the observed phenotype and providing support for the identification of a potential QTG. Three nonsynonymous polymorphisms (m*Mcp1*x1#1, m*Mcp1*x2#3 and m*Mcp1*x3#3) were identified, the first mirroring the phenotypic pattern of the three mouse strains and suggesting a QTN important for both F2 intercrosses and the alleles of two others segregating in a manner which implied separate QTN for specific F2 intercrosses. Three different haplotypes represented the mouse strains and it is possible that these potential QTN have separate or combined contributions in controlling incubation time. Two amino acid substitutions are located in the N-terminal regions of MCP1, important for chemoattractant activity and receptor binding (Baggiolini et al., 1997; Ernst et al., 1994; Gu et al., 1999) and therefore may have implications for protein structure and function.

Quantitative Complementation

The overall candidacy of *Mcp1* as a QTG was investigated using a quantitative complementation strategy. In contrast to the observations of Felton *et al.*, following intracerebral challenge with the Chandler/RML prion strain, *Mcp1* knockout mice did not show a delay in the onset of clinical signs of disease nor did they have increased survival times. Furthermore, a statistically significant small decrease in incubation time was observed between knockout and wild-type groups. The effect of *Mcp1* in this model is dominant and only observable in a full knockout which is inconsistent with the additive model of inheritance observed for linked markers on chromosome 11 (Lloyd et al., 2001) suggesting that *Mcp1* is not an important QTG. It was concluded that *Mcp1* has no effect on the incubation time phenotype nor does it contribute to the QTL following the further observation that no significant differences were recorded between the 'short' and 'long' incubation time wild-type and knockout crosses.

Mcp1 Expression

As observed by Felton *et al.*, *Mcp1* expression in uninfected mice was very low but significantly increased in terminal disease. The increased level of expression observed in CAST/Ei compared to the 'short' incubation time strains (SJL/J and NZW/OlaHsd) did not fit with the proposed model of MCP1 action as higher levels of *Mcp1* expression would be expected to reduce incubation time, not increase it. It is possible that modifiers in the CAST/Ei strain may act to prolong survival in prion disease in spite of an increased expression of MCP1, overriding the proposed shortening effect on incubation time. The analysis of Mcp1 mRNA expression in CAST/Ei at a number of time points following incoluation would decifer the exact expression pattern of this gene and determine whether an increase in *Mcp1* expression is seen at the point of transition to terminal disease.

Clinical Profile of Disease

A further difference between the findings of this study and that of Felton *et al.*, was that the clinical course of disease in the two models differed. All *Mcp1* knockout mice displayed the full range of clinical signs and symptoms of disease following challenge with the Chandler/RML prion strain whereas these symptoms were not observed in all of the knockout mice in the ME7 study. The ME7 infected *Mcp1* knockout mice were sacrificed at a determined humane experimental endpoint following a $\geq$15% loss of body weight (Felton et al., 2005) and therefore it is possible that this occurred before the presentation of clinical symptoms of disease. It is noteworthy that the end-point criteria used may have led to an underestimation of absolute measures of survival in this study.

Strain Differences Between ME7 & Chandler/RML

A plausible explanation for the differences observed for *Mcp1* between the two murine models of prion disease is the use of the different prion strains ME7 and Chandler/RML. As previously discussed (Section 1.1.8) different prion strains produce characteristic incubation times and neuropathology in defined inbred lines of mice (Bruce et al., 1994; Bruce, 2003; Bruce et al., 1991; Collinge et al., 1996b). For example, in the C57 strain Chandler/RML produces an incubation time of 137 days (Kingsbury *et al.*, 1983) whereas the ME7 incubation time in this strain is more prolonged at 158±2 days (Dickinson and Mackay, 1964). In addition, the Chandler/RML incubation time in the RIII strain is 136±3 days (Westaway *et al.*, 1987) whereas with ME7 it is increased at 146±2 days (Dickinson and Mackay, 1964).

Neuropathologically, strains of scrapie are also known to differ markedly in the severity and vacuolar degeneration they produce in the brain and the degree of vacuolation or 'lesion profile' has been used as an established method of strain discrimination (Fraser and Dickinson, 1968). Following intracerebral inoculation with ME7 or Chandler/RML in mice, vacuolar lesions are seen to be widespread throughout the brain (Bruce *et al.*, 1989; Chandler, 1961) with ME7 producing particularly marked vacuolation in the hippocampal, septal and thalamic neuropil (Bruce et al., 1991; Cunningham *et al.*, 2005; Jeffrey *et al.*, 2000; Williams *et al.*, 1994). Spongiosis in Chandler/RML infected mice has been reported to be most intense in the cortex and hippocampus and to a lesser extent in the thalamus (Lloyd *et al.*, 2004). Differences in the pattern of vacuolation between the ME7 and Chandler/RML indicate that these prion strains target different areas of the brain. *Mcp1* may be expressed at higher levels or have more potent effects in certain brain regions and this may therefore produce differences in disease progression and the observed clinical and incubation time phenotype produced in response to each strain.

Further evidence of differences between the two prion strains has come from *in vitro* experiments which show that selected sublines of murine neuroblastoma-derived N2a cells are susceptible to the Chandler/RML prion strain but not to other strains including ME7 (Bosque and Prusiner, 2000; Klohn *et al.*, 2003). Furthermore, recent work has confirmed that Chandler/RML and ME7 PrP^{Sc} show distinct biochemical and physicochemical properties, differing in their glycoform profile and levels of PK-sensitive and PK-resistant isoforms (Thackray *et al.*, 2007). In addition, the PK-resistant core of ME7 PrP^{Sc} is conformationally more stable following degradation with guanidine hydrochloride and sarkosyl. As previously described (Section 1.1.8), it is currently thought that the basis of prion strain specificity lies in the structural variation of PrP^{Sc} (Bessen and Marsh, 1992; Bessen and Marsh, 1994; Collinge et al., 1996b; Hill and Collinge, 2001; Telling et al., 1996).

Both Chandler/RML and ME7 prion strains are $Prnp^{a}$ mouse-adapted scrapie strains but they have been independently derived. Chandler/RML was originally derived from brain samples taken from scrapie infected goat and subsequently passsaged in sheep and CD-1 Swiss mice (Chandler, 1961) whereas ME7 was derived from the spleens of scrapie infected Suffolk sheep, first passaged in Swiss white mice and then passaged in C57BL mice (Dickinson *et al.*, 1969; Zlotnik and Rennie, 1963). The highly variable

nature of naturally occurring scrapie is well established with multiple strains in existence (Bruce *et al.*, 2002; Bruce et al., 1991). Therefore, strain differences between ME7 and Chandler/RML are potentially responsible for the disparity observed in *Mcp1* knockout mice between these two models of prion disease.

Potential Limitations

A potential limitation of the study carried out by Felton *et al.*, and one perhaps providing further explanation for the inability of the current study to reproduce the results of the ME7 model, is the potential presence of discrepancies between the genetic background of the *Mcp1* knockout mice and the wild-type C57BL6 mice used as controls. In both studies the *Mcp1* knockout mice under observation had been generated upon the background of C57BL/6J mice from the Jackson Laboratories as described in earlier studies (Hughes et al., 2002; Lu *et al.*, 1998) and therefore C57BL6 mice from the same source are the rational choice for the control group. However, Felton *et al.*, obtained C57BL/6J mice derived from a different breeding colony, C57BL/6JOlaHsd from Harlan (UK), introducing the possibility of variation, however slight, between the genetic background of the knockout and control animals which may be partially be responsible for the observed phenotypic variation between these strains. Commercial animal suppliers propagate their stocks with constant brother-sister matings and C57BL/6J mice sold by a variety of suppliers can all be traced back to common founder animals. However, over time each independently-maintained line will slowly drift apart genetically from its ancestors and distant cousins preventing accurate comparisons (Silver, 1995). For example, Chandler/RML incubation times for C57BL/6J mice and an independently maintained substrain, C57BL/6JOlaHsd, are significantly different at 166±4 days and 134±3 days respectively (unpublished data). Incubation time and neuropathology following challenge with different prion strains is modulated by host genetic background (Bruce, 1993) so any potential variation between the *Mcp1* knockout and the control group may implicate additional genetic loci contributing towards phenotype. Futhermore, the Harlan C57BL/6J substrain has been shown to carry a chromosomal deletion of the α-synuclein locus (Specht and Schoepfer, 2001). α-synuclein is a pre-synaptic protein which has a role in several neurodegenerative diseases classified as synucleinopathies and is a major component of Lewy bodies in Parkinson's disease (Spillantini *et al.*, 1997). α-synuclein-immunoreactive deposits have been identified in the CNS of various prion diseases and it has been shown to accumulate close to PrP^{Sc} plaques (Haik *et al.*, 2002). These

findings suggest that the absence of α-synuclein in Harlan C57BL/6J mice may have a protective effect in prion disease and may potentially increase the incubation time of these mice. This substantiated genetic difference between the control groups of the ME7 and Chandler/RML model make a direct comparison between the two studies difficult.

In conclusion, the contrasting outcomes of these studies demonstrates the strain specific involvement of individual molecules in prion disease and the role of MCP1 appears to be exclusive to the specific pathogenesis of the ME7 strain. Several lines of evidence differentiate the ME7 and Chandler/RML strains and may underpin the observed dissimilarities in incubation time between these murine models of prion disease. It is therefore difficult and precarious to extrapolate from these findings the role of MCP1 in human prion disease whilst such complex mechanisms of strain specific effects remain unclear.

8.4 Fine Mapping Chromosome 11 QTL

Following an initial analysis of several functionally relevant candidate genes mapping within chromosome 11 QTL (Lloyd et al., 2001; Stephenson et al., 2000), fine mapping of these extensive regions was carried out using the Northport HS to resolve regions of interest into smaller intervals and reduce the number of candidate genes for analysis. Fine mapping of chromosome 11 QTL was successfully achieved despite the absence of the strains use in the original mapping studies from the panel of parental strains used to generate the HS and so potential limitations associated with the use of the HS were not realised. As previously described, one explanation for this may be the shared ancestry of the 'short' and 'long' incubation time strains and the progenitor strains of the HS. The original 86.5Mb region of linkage was greatly reduced to a new and much smaller interval of 708kb mapping within the flanking microsatellite markers *D11Mit67* and *D11Mit145* containing seventeen candidate genes. This represents a substantial reduction from the estimated 856 genes mapping within combined chromosome 11 QTL (Lloyd et al., 2001; Stephenson et al., 2000). Genes located in these reduced intervals that had an obvious functional relevance to prion disease were highlighted as potentially interesting candidates but equal attention was paid in the assessment of others also mapping within the region of interest and therefore analysis was unbiased. An association between candidate genes with, as yet, unknown functions relating to prion biology and incubation time may uncover new pathways in disease.

Sp6

Sequence analysis of candidates identified numerous polymorphisms between the founder strains of the HS and also between SJL/J, NZW/OlaHsd and CAST/Ei. HAPPY analysis of these polymorphisms reduced the candidate gene list to a single gene by identifying nine sequence variants that reached a significant level of linkage in *Sp6* and were also established as being associated with incubation time. It is possible that multiple QTL underlie the extensive regions of linkage on chromosome 11 identified in two-way crosses (Lloyd et al., 2001; Stephenson et al., 2000) although it is difficult to ascertain this with such a low resolution method of QTL detection. However, fine mapping with the HS has highlighted more specific regions on chromosome 11 and has suggested the involvement of a single QTG. Although two-way crosses are low resolution techniques the genetically divergent nature of the wild-derived CAST/Ei strain may have uncovered more QTL than in the HS whose progenitor strains have a higher level of shared ancestry and may not represent such a maximisation of genetic diversity.

As previously described (Section 5.3), *Sp6* is a member of the Specificity Protein/Krüppel-like Factor (SP/KLF) transcription factor family and gives rise to two transcripts, *Sp6* and epiprofin, which are treated as synonyms in current sequence databases (Hertveldt *et al.*, 2007). Six of the significant SNPs identified in *Sp6* were polymorphic between SJL/J and CAST/Ei suggesting that this candidate may be an important QTG for the SJL/J and CAST/Ei F2 intercross QTL but not that of NZW/OlaHsd and CAST/Ei which were not polymorphic in any of the nine significant SNPs. A correlation between genotype and gene expression was identified for *Sp6* according to the significant SDP identified in the parental strains of the HS. This suggests that differential regulation of *Sp6* mRNA may be responsible for control of incubation time. Further evidence to support the identification of a shared QTG between the HS and SJL/J and CAST/Ei strains is the observation that *Sp6* expression also differed significantly between these 'short' and 'long' incubation time strains. A potential caveat of the assumption that *Sp6* is a shared QTG for SJL/J, CAST/Ei and the HS is that since SJL/J and CAST/Ei are derived from genetically divergent subspecies of mouse, it is expected that they would be very polymorphic across their genomes and in addition show significant expression differences for many genes. The polymorphic nature of these strains in *Sp6* does not necessarily confirm the identification of a shared

QTG for incubation time and further analysis of *Sp6*'s contribution in SJL/J and CAST/Ei strains would be required via avenues of further work described later.

Following challenge with the Chandler/RML prion strain the expression of *Sp6* in CAST/Ei was significantly increased but this was not seen in the 'short' incubation time strains. It may be that *Sp6* SNPs change the gene's functional properties and in the case of CAST/Ei confers some protection against prion pathology through increased expression, underpinning the increased incubation time of this strain.

Sp6 3'UTR Polymorphisms

Following an assessment of the potential functional significance of *Sp6* polymorphisms, a 3'-UTR *Sp6* SNP was also located in a putative binding site for Heat Shock Transcription Factor 1 (*Hstf1*) and 2 (*Hstf2*) which are transcriptional activators responsible for the inducible expression of heat shock genes (Abravaya *et al.*, 1991). *Hstf1* in particular has been shown to be the major factor induced during heat stress (Sarge *et al.*, 1993). Increased expression and accumulation of heat shock proteins have been observed in the brains of scrapie-sick mice and CJD patients (Kenward *et al.*, 1994; Kenward *et al.*, 1996; Kovacs *et al.*, 2001; Laszlo *et al.*, 1992; Tatzelt *et al.*, 1998). Aggresomes have been implicated in prion disease neurotoxicity through their clearance of toxic cytoplasmic misfolded aggregates (Garcia-Mata *et al.*, 2002; Kawaguchi *et al.*, 2003) and have been show to contain heat shock proteins alongside PrP^{Sc} (Kristiansen *et al.*, 2005). It is not clear whether *Sp6* is a key regulator of heat shock proteins but the *Sp6* SNP residing in this putative binding site for *Hstf1* and *Hstf2* may cause differential expression of heat shock proteins between mouse strains which may in turn be important in the response to prion infection influencing pathology and incubation time.

A putative relationship between *Sp6* and *Prnp* was investigated in this study but the expression profile for each did not substantially match. Nor did *Prnp* expression correlate with the *Sp6* SDP associated with incubation time. Further analysis of this potential candidate gene is required to fully understand its putative role in controlling incubation time. This may include an *in silico* assessment of the location of *Sp6* binding sites throughout the genome to draw conclusions about the type of genes whose expression *Sp6* may be controlling.

Further Work & Limitations

It is possible that SNPs in *Sp6* are not the only potential QTN involved in incubation time as other QTN may have been overlooked as a result of the limiting SNP discovery method employed which does not assess intronic regions. A more complete analysis of sequence surrounding *Sp6* and also in additional candidates, *Npepps*, *Mrpl45*, *AK*, *P140*, *HypPro*, *Mllt6* and *Psmb3*, whose –logP values reached a suggestive level of significance may uncover additional potential QTN. Furthermore, a region of suggestive linkage between the flanking markers *D11Mit36* and *D11Mit54* was also identified by fine mapping in the HS in addition to the significant region focused on in this study and is a further avenue for analysis on chromosome 11.

Confidence intervals have not been assigned to the HAPPY analysis software and therefore the exact boundaries of significance were not defined. It was therefore prudent to consider genes mapping close to the flanking marker of defined significant chromosomal intervals. This cautionary measure was applied to analysis on chromosome 11 where a gene family member of *Sp6* was identified close to the marker boundary of the region of significant linkage. However, analysis of this gene, *Sp2*, did not suggest association with incubation time.

8.5 Fine Mapping Chromosome 8 QTL

Fine mapping of chromosome 8 QTL in the HS has successfully and substantially reduced the region of interest from 20.8Mb to a minimal interval spanning 2.2Mb between the microsatelitte markers *D8Mit57* and *D8Mit197*. Numerous polymorphisms were identified in ten candidate genes mapping within the new region and HAPPY analysis predicted that sequence variants from each candidate showed a suggestive level of linkage to incubation time. Thus, the resulting candidate list included every gene mapping within the new region of interest and a further attempt was made to reduce the number for analysis.

Based upon an assumption that the new region of linkage identified in the HS is the same as the previously identified QTL (Manolakou et al., 2001), the candidate list was reduced to seven genes by discounting sequence variants which were not polymorphic between C57BL/6J and RIIIS/J. The candidate genes *Zfp423*, *HypPro* and *Heatr3* were removed from analysis along with several polymorphisms in other genes. While this was an effective way of reducing the number of candidates for further analysis, a

potential limitation of this strategy is that the two regions of interest may in fact be independent QTL due to the use of different prion strains to identify each. The HS were inoculated with Chandler/RML and the C57 x RIII backcross population with BSE. The use of BSE prions also introduces the factor of a species barrier which is a major modulator of incubation time (Bruce et al., 1994) and therefore potentially adds another level of complexity implicating further separate QTL. However, the majority of sequence variants identified in chromosome 8 candidates were polymorphic between RIIIS/J and C57BL/6J suggesting the identification of shared QTL originating from the presence of mutual ancestral alleles.

Another potential reason why the QTL may be separate is the disparity of mouse strains used in each cross. It is possible that each QTL may be mouse strain specific. The RIII mouse strain is not featured in the HS but the presence of the C57BL/6J strain in the panel of parental strains generating the Northport HS suggested that the use of this cross to fine map chromosome 8 QTL would be plausible since the original region of interest was identified in a cross utilising a C57 substrain. The potential existence of common alleles between the two crosses suggested that linkage would be reproducible but the exact genetic and phenotypic differences between the C57BL/6J and C57BL/Fa/Dk substrains have not been quantified presenting a possible limitation. A recent study has demonstrated significant differences in behaviour between C57BL substrains derived from common ancestors (Deacon *et al.*, 2007) and so the substitution of one C57BL substrain for another as a direct counterpart for comparison should be approached with caution.

Functional Significance of Sequence Variants

Polymorphisms in the seven remaining candidate genes corresponding to the most common and significant SDP, as determined by HAPPY, were further analysed for their potential functional implications. Numerous 3'UTR polymorphisms were found in several candidates and located within putative transcriptional factor binding sites. It is difficult to ascribe the functional significance of these as no transcription factors appeared to be directly relevant to known pathways involved in prion pathogenesis. They may however have broader roles in controlling gene expression and be important in pathways yet to be implicated in prion disease.

A nonsynonymous polymorphism identified in *Adcy7* is located in a region of the

corresponding protein product predicted to form one of 12 membrane-associated helices (Watson et al., 1994). It is difficult to ascertain the significance of this change as the residue involved is only semi-conserved and the amino acid change seen between mouse strains is negligible in terms of physicochemical properties. A nonsynonymous polymorphism in *Sall1* was located in a highly conserved amino acid residue of the protein which may have potential implications for function and structure. However the residue in question is located outside of known functional domains, such as its characterised zinc finger motifs (Nishinakamura et al., 2001), and therefore it is unclear how significant the effect would be.

Nonsynonymous polymorphisms identified in *Slic1* and *Card15*, although not located in highly conserved residues, may have potential functional implications for protein structure and function because they are located in functional domain regions. The nonsynonymous changes in these genes may also be potentially more interesting than those in other candidates due to the functional relevance of *Slic1* and *Card15* to prion disease.

SLIC1 is thought to be member of the sorting nexin family which are peripheral membrane proteins regulating membrane traffic (Haft *et al.*, 1998; Kurten *et al.*, 1996; Ponting, 1996; Worby and Dixon, 2002) and are defined by the presence of a ~100 amino acid phospholipid-binding motif SNX phox homology (PX) domain (SNX-PX). The nonsynonymous polymorphism (A136T), which causes a change in residue polarity, is located within this PX domain, a lipid-binding module that aids the association of their host protein with membrane enriched phosphoinositides (Ponting, 1996). The PX domain is thought to target SNXs to endosomes by binding to phosphatidylinositol 3-monophosphate (PtdIns3P) in the membranes of sorting endosomes to control endosomal sorting events (Cozier *et al.*, 2002; Petiot *et al.*, 2003). Therefore, a residue change in this SNX-PX domain may affect the efficiency of *SLIC1* to bind to endosomes. The putative function of this gene is interesting because, as previously described (Section 1.1.5), the cellular prion protein is located at the surface of neuronal cells in detergent-insoluble lipid rafts (Stahl *et al.*, 1987), and is regularly recycled in endosomes (Shyng *et al.*, 1993; Sunyach *et al.*, 2003). Furthermore, the conversion of PrP^{C} to PrP^{Sc} is thought to occur at the cell membrane or in the endosome/lysosome system, and PrP^{Sc} is known to accumulate in the endosomes and lysosomes of brain cells (Caughey *et al.*, 1991; Laszlo et al., 1992; McKinley *et al.*,

1991). Therefore it is possible that SLIC1 may be involved in the recycling of normal PrP^C and/or conversion of this protein into the misfolded disease associated form. Physicochemical residue property differences between mouse strains may underlie differences in the activity of this protein in prion pathology and in turn affect incubation time.

Alterations in gene expression in mice challenged with different strains of scrapie has been reported in several genes that encode proteins which localise to endosome/lysosomes systems (Skinner et al., 2006) suggesting a potential molecular basis for the differences observed in clinical and neuropathological phenotypes. In addition, endosomal and lysosomal activity correlates well with the severity of neuropathological changes observed in human sporadic CJD brains (Kovacs *et al.*, 2007). Defects in the endosomal-lysosomal pathway have also been implicated in a number of neurodegenerative diseases such as AD, FTD and ALS (Nixon, 2005; Parkinson *et al.*, 2006; Skibinski *et al.*, 2005).

A nonsynonymous polymorphism in *Card15* (L415C) is located in a semi-conserved residue within the NOD binding domain of its gene product NOD2. This amino acid substitution has potential implications for protein structure and function due to the possible disruption of a disulfide bond as a result of the substitution of cysteine for a leucine residue. The effect of codon changes on protein binding activity in this domain have been examined using mutational analysis in humans but changes at this particular residue were not investigated (Tanabe *et al.*, 2004). NOD2 is expressed in the cytoplasmic region of antigen-presenting cells (APCs) and in intestinal epithelial cells (Gutierrez *et al.*, 2002; Hisamatsu *et al.*, 2003) and is thought to be involved in enteric bacteria-host interactions. Activation of NOD2 through its carboxy-terminal recognition LRR domain leads to self-oligomerisation and subsequent activation of the NF-κB transcription pathway (Abbott *et al.*, 2004; Inohara *et al.*, 2003; Ogura *et al.*, 2001b) which is involved in the initiation of apoptosis, a process central to prion pathology (Cronier et al., 2004; Hetz et al., 2003).

In other NOD domain containing proteins such as apoptotic protease activating factor 1 (Apaf-1) and its nematode homologue Ced-4, which are regulators of p53-dependent programmed cell death, protein oligomerisation mediated by the NOD domain is critical for caspase activation and functional activity (Hu *et al.*, 1998; Inohara and Nunez, 2001;

Yang *et al.*, 1998). Therefore, amino acid changes in this domain may affect the efficiency of self-oligomerisation between mouse strains and affect the subsequent activation of signalling pathways and the induction of apoptosis. There is evidence to support a role for the NF-κB transcription pathway in prion disease and it is possible that sequence variants in *Card15* may contribute in varying degrees towards NF-κB-induced apoptosis. Enhanced NF-κB activity has been described in the brain of scrapie infected mice (Kim *et al.*, 1999) and the synthetic peptide of the prion protein PrP 106-126 has been shown to activate NF-κB in microglial cells (Fabrizi *et al.*, 2001).

Candidate Gene Expression

No correlation between genotype and gene expression was observed for chromosome 8 candidates and only marginal differences in *Adcy7* and *Sall1* expression were identified between C57BL/6J and RIIIS/J strains.

In conclusion, following the analysis of ten candidate genes in the new chromosome 8 region of linkage *Adcy7*, *Card15*, *Slic1* and *Sall1* have been highlighted as potential candidates controlling incubation time which are worth pursuing further. *Card15* and *Slic1* are perhaps the most interesting candidates based on their known and suggested functional relevance to prion disease and the identification of coding polymorphisms in the known and putative functional domains of these genes. The most significant region of linkage identified between *D8Mit81* and *D8Mit197* which is characterised as a gene desert remains a potential avenue for analysis following further characterisation. Regulatory sequence variants in this intergenic region may be controlling the expression of candidate genes elsewhere in the genome which are important modifiers of prion disease incubation time.

8.6 Fine Mapping Chromosome 9 QTL

Fine mapping of extensive chromosome 9 QTL, spanning a 27.9Mb region (Stephenson et al., 2000), with the Northport HS identified a highly significant region of linkage for prion disease incubation time spanning a 1.5Mb interval which is defined by the microsatelitte markers *D9Mit327* and *D9Mit286*. This finding represents a substantial reduction in the size of the region for analysis and the number of genes contained within. As with the fine mapping of chromosome 11 QTL a potential limitation of the use of the HS to fine map chromosome 9 QTL was the absence of the strains used in the original mapping studies from the panel of HS progenitor strains. Therefore if the

original QTL was specific to SJL/J and CAST/Ei strains there was a risk that linkage would not be reproducible in the HS. However this limitation was not realised, possibly due to shared ancestry of SJL and the classical inbred strains generating the HS.

Unfortunately, due to time constraints, analysis of candidate genes within this region was not carried out to completion. Following a review of the thirty-one known genes and several less well characterised genes and RefSeq sequences mapping within this region the most functionally relevant candidate, *Hspa8*, was chosen for further analysis based upon the knowledge that heat shock proteins play a major role in prion pathogenesis (Kenward et al., 1994; Kenward et al., 1996; Kovacs et al., 2001; Laszlo et al., 1992; Tatzelt et al., 1998). As previously discussed, there are potential limitations to the strategy of selecting candidates based upon their functional relevance to prion disease because not all of the mechanisms of disease are fully understood and therefore more important candidates with supposed unrelated functions may be overlooked.

HAPPY analysis of *Hsap8* sequence variants identified between the strains of the HS did not associate them with incubation time and furthermore they were not seen to be polymorphic between the strains identifying the original QTL discounting this gene as a QTG in both the HS and the SJL/J x CAST/Ei F2 intercross (Stephenson et al., 2000). Further assessment of *Hspa8* may have included investigating its mRNA expression levels. Differential expression would imply regulatory polymorphisms between mouse strains which may correlate with the observed variation in incubation time and these polymorphisms may be residing in intronic regions not assessed by the method of sequence analysis employed here.

Further sequence analysis of other candidates within this highly significant region of linkage may uncover important genes controlling incubation time. The remaining candidates in this regions include several olfaction receptors, a zinc finger protein (*Znf202*), a sodium channel subunit (*Scn3b*), a GRAM domain-containing protein (*Gramd1b*), a homoebox transcription factor (*Bsx*) and a member of the immunoglobulin superfamily (*Crtam*). Perhaps the most interesting of these is *Scn3b* which has been proposed to have a role in p53-dependent apoptotic pathways in mouse and human (Adachi *et al.*, 2004) as programmed cell death is a central feature of prion pathogenesis (Cronier et al., 2004; Hetz et al., 2003). This new region of interest identified on chromosome 9 is the most significant region to be identified using the HS

and represents an interesting avenue for further work.

A second interval of significant linkage was also identified spanning 7.3Mb between the flanking microsatellite markers *D9Mit4* and *D9Mit102*. This region contained several functionally relevant genes having roles in protein degradation and cellular stress response mechanisms. These candidates include Heat Shock Protein, DNAJ-like 4 (*Dnaja4*), Cullin5 (*Cul5*), two putative Ubiquitin-Conjugating Enzymes, E2Q2 (*Ube2q2*) and E2S (*Ube2s*) and Proteasome (prosome, macropain) Subunit, Alpha 4 (*Psma4*).

The heat shock protein, *Dnaja4*, is one of more than 20 homologs of a family of proteins named HSP40/DNAJ, which regulate HSP70/DNAK molecular chaperones through a J domain, consisting of 70 amino acids that interact with HSP70 and stimulate its ATPase activity (Ohtsuka and Hata, 2000). Ubiquitin-mediated protein degradation is known to play a key role in the regulation of a number of cellular processes (Pray *et al.*, 2002). *Cul5* is known to interact with several cellular proteins to form an E3 ubiquitin ligase complex that induces polyubiquitination and proteasomal degradation (Petroski and Deshaies, 2005). The prion protein is known to be ubiquitinated after developing protease resistance in the brain of ME7 scrapie infected mice (Kang *et al.*, 2004). Furthermore, the putative ubiquitin conjugating enzymes mapping within this new region of linkage may be of interest as these enzymes, also known as E2s, perform intermediate steps in the enzymatic cascade interacting with specific E3 ubiquitin ligases (Weissman, 2001). Mouse *Psma4* has been cloned as one of several subunits, including chromosome 11 candidate gene, *Psmb3*, that comprise the mouse 20S proteasome involved in protein degradation (Elenich *et al.*, 1999) and therefore having clear functional relevance to prion pathology.

This additional region of linkage is another potential source of important candidate genes controlling incubation time and requires further analysis.

8.7 Verification of Candidate Genes and Future Work

Several potential candidate genes for prion disease incubation time have been identified by this study. Verification of the exact contributions of each in controlling the phenotype is required and further work may include the use of cell and/or mouse models.

The scrapie cell assay (SCA) provides a useful and efficient *in vitro* alternative to mouse bioassays which are more prolonged and costly (Klohn et al., 2003). The assay involves the infection of neuroblastoma N2a sublines which are highly susceptible to mouse prions and subsequent visualisation of individual PrP^{Sc} positive cells using an enzyme-linked immunospot (ELISPOT) plate. RNA interference (RNAi) could be utilised in the SCA to assess the effects of stable or transient knockdown of candidate gene mRNA expression, on the generation of detectable PrP^{Sc}. This post-transcriptional gene silencing method involves introducing a double stranded RNA which targets an endogenous mRNA for degradation (Montgomery *et al.*, 1998). Analysis of differences in prion susceptibility and propagation could be investigated following downregulation of putative candidate genes in prion infected cell lines.

Following assessment in a cell model, the contribution of a candidate gene to the incubation time phenotype may be tested in mouse models by generating knockout mice for the gene in question and comparing these mice with wild-type controls following challenge with prions. The overall candidacy of a candidate gene may also be tested using a quantitative complementation strategy, as described for *Mcp1*. Transgenic mice which overexpress a candidate gene are another source of comparison against control animals. Following verification of a candidate gene's involvement in controlling the phenotype, subsequent analysis of the contribution of individual polymorphisms may be assessed by generating targeted mutations in transgenic mice. The most tractable polymorphisms may be those producing amino acid substitutions compared to those polymorphisms whose potential functional implications are less obvious.

Mouse SNP database information could be used to reinforce the number of polymorphisms identified in this study and fill in gaps such as intronic regions to provide a more complete analysis. Following fine mapping with the HS of additional incubation time QTL, not included in this study, SNP information for the progenitor strains of the HS, providing it is available, would preclude the need for *de novo* sequencing of these additional regions. A limitation of the SNP databases is that they may not be comprehensive enough, for example they may not include specific mouse strains or the sequence data may not be complete for all strains in all regions of interest.

The ultimate aim of identifying candidate genes for incubation time in mice is to relate these to human disease. Human association studies could be used to verify the

contribution of a candidate gene to disease susceptibility. If there are known SNPs in the corresponding human homolog of a putative candidate gene they could be analysed to investigate an association with disease or used as tagging SNPs to assess an association of haplotype with disease. Successful association of candidates with disease is often confounded in human studies by the small sizes of samples available which has certainly been the case for association studies using vCJD samples, as previously discussed in Section 1.2.1. However, it may be possible to identify association where candidate genes have a large effect on the phenotype. Sample sets available for sporadic CJD are somewhat larger and may provide a more powerful analysis tool for verifying potential candidate genes.

8.8 Conclusion

In conclusion, the work described in this thesis represents an advancement in the identification of candidate genes controlling prion disease incubation time in mice. Extensive QTL on chromosome 8, 9 and 11 have been successfully reduced in size by fine mapping in the HS to allow a more focused candidate gene approach in regions of interest. Sequence analysis of candidates identified numerous polymorphisms between the founder strains of the HS and also between 'short' and 'long' incubation time strains used to originally identify QTL. These sequence variants may provide the molecular basis for the control of incubation time. The number of potential candidates was further reduced by assessing the association of polymorphisms with incubation time and investigating correlations between gene expression and genotype. The potential functional significance of sequence variants was also considered. A number of genes were identified as being worth further investigation on Chromosome 11 including *Mpo*, *Gfap*, *Mapt* and *Vtn*. Following fine mapping of chromosome 11 QTL, a single gene, *Sp6*, was identified as the most promising candidate for the identified regions of interest. The candidacy of another, *Mcp1*, assessed by quantitative complementation in the Chandler/RML murine model of prion disease, has highlighted the prion strain specific involvement of individual genes. A further four genes, *Adcy7*, *Sall1*, *Card15* and *Slic1*, were assessed to be the most promising and functionally relevant candidates for chromosome 8. A highly significant region of linkage has also been identified on chromosome 9 and remains a potentially interesting avenue for further investigation. Further analysis of candidate genes *in vitro* and *in vivo* models will determine the exact implications of each in controlling incubation time. These candidates may also be important in controlling susceptibility to prion disease in humans and their physiological functions may highlight important biochemical pathways for therapeutic strategies.

9

References

Abbott, D.W., Wilkins, A., Asara, J.M. and Cantley, L.C. (2004) The Crohn's disease protein, NOD2, requires RIP2 in order to induce ubiquitinylation of a novel site on NEMO. *Curr Biol*, **14**, 2217-2227.

Abravaya, K., Phillips, B. and Morimoto, R.I. (1991) Heat shock-induced interactions of heat shock transcription factor and the human hsp70 promoter examined by in vivo footprinting. *Mol Cell Biol*, **11**, 586-592.

Adachi, K., Toyota, M., Sasaki, Y., Yamashita, T., Ishida, S., Ohe-Toyota, M., Maruyama, R., Hinoda, Y., Saito, T., Imai, K., Kudo, R. and Tokino, T. (2004) Identification of SCN3B as a novel p53-inducible proapoptotic gene. *Oncogene*, **23**, 7791-7798.

Aguzzi, A. and Heikenwalder, M. (2005) Prions, cytokines, and chemokines: a meeting in lymphoid organs. *Immunity*, **22**, 145-154.

Alcaraz, W.A., Gold, D.A., Raponi, E., Gent, P.M., Concepcion, D. and Hamilton, B.A. (2006) Zfp423 controls proliferation and differentiation of neural precursors in cerebellar vermis formation. *Proc Natl Acad Sci U S A*, **103**, 19424-19429.

Alper, T., Cramp, W.A., Haig, D.A. and Clarke, M.C. (1967) Does the agent of scrapie replicate without nucleic acid? *Nature*, **214**, 764-766.

Alpers, M. and Rail, L. (1971) Kuru and Creutzfeldt-Jakob disease: clinical and aetiological aspects. *Proc Aust Assoc Neurol*, **8**, 7-15.

Anderson, L., Rossi, D., Linehan, J., Brandner, S. and Weissmann, C. (2004) Transgene-driven expression of the Doppel protein in Purkinje cells causes Purkinje cell degeneration and motor impairment. *Proc Natl Acad Sci U S A*, **101**, 3644-3649.

Andersson, E., Hellman, L., Gullberg, U. and Olsson, I. (1998) The role of the propeptide for processing and sorting of human myeloperoxidase. *J Biol Chem*, **273**, 4747-4753.

Andrade, M.A. and Bork, P. (1995) HEAT repeats in the Huntington's disease protein. *Nat Genet*, **11**, 115-116.

Andrews, N.C., Erdjument-Bromage, H., Davidson, M.B., Tempst, P. and Orkin, S.H. (1993) Erythroid transcription factor NF-E2 is a haematopoietic-specific basic-leucine zipper protein. *Nature*, **362**, 722-728.

Andrews, P.C. and Krinsky, N.I. (1981) The reductive cleavage of myeloperoxidase in half, producing enzymically active hemi-myeloperoxidase. *J Biol Chem*, **256**, 4211-4218.

Arrasate, M., Mitra, S., Schweitzer, E.S., Segal, M.R. and Finkbeiner, S. (2004) Inclusion body formation reduces levels of mutant huntingtin and the risk of neuronal death. *Nature*, **431**, 805-810.

Asante, E.A., Linehan, J.M., Desbruslais, M., Joiner, S., Gowland, I., Wood, A.L., Welch, J., Hill, A.F., Lloyd, S.E., Wadsworth, J.D. and Collinge, J. (2002) BSE prions propagate as either variant CJD-like or sporadic CJD-like prion strains in transgenic mice expressing human prion protein. *Embo J*, **21**, 6358-6366.

Austin, C.P., Battey, J.F., Bradley, A., Bucan, M., Capecchi, M., Collins, F.S., Dove, W.F., Duyk, G., Dymecki, S., Eppig, J.T., Grieder, F.B., Heintz, N., Hicks, G., Insel, T.R., Joyner, A., Koller, B.H., Lloyd, K.C., Magnuson, T., Moore, M.W., Nagy, A., Pollock, J.D., Roses, A.D., Sands, A.T., Seed, B., Skarnes, W.C., Snoddy, J., Soriano, P., Stewart, D.J., Stewart, F., Stillman, B., Varmus, H., Varticovski, L., Verma, I.M., Vogt, T.F., von Melchner, H., Witkowski, J., Woychik, R.P., Wurst, W., Yancopoulos, G.D., Young, S.G. and Zambrowicz, B. (2004) The knockout mouse project. *Nat Genet*, **36**, 921-924.

Baggiolini, M., Dewald, B. and Moser, B. (1997) Human chemokines: an update. *Annu Rev Immunol*, **15**, 675-705.

Baker, C.A., Lu, Z.Y., Zaitsev, I. and Manuelidis, L. (1999) Microglial activation varies in different models of Creutzfeldt-Jakob disease. *J Virol*, **73**, 5089-5097.

Baker, H.E., Poulter, M., Crow, T.J., Frith, C.D., Lofthouse, R. and Ridley, R.M. (1991) Aminoacid polymorphism in human prion protein and age at death in inherited prion disease. *Lancet*, **337**, 1286.

Bamshad, M., Lin, R.C., Law, D.J., Watkins, W.C., Krakowiak, P.A., Moore, M.E., Franceschini, P., Lala, R., Holmes, L.B., Gebuhr, T.C., Bruneau, B.G., Schinzel, A., Seidman, J.G., Seidman, C.E. and Jorde, L.B. (1997) Mutations in human TBX3 alter limb, apocrine and genital development in ulnar-mammary syndrome. *Nat Genet*, **16**, 311-315.

Banks, A.S., Li, J., McKeag, L., Hribal, M.L., Kashiwada, M., Accili, D. and Rothman, P.B. (2005) Deletion of SOCS7 leads to enhanced insulin action and enlarged islets of Langerhans. *J Clin Invest*, **115**, 2462-2471.

Barron, R.M., Baybutt, H., Tuzi, N.L., McCormack, J., King, D., Moore, R.C., Melton, D.W. and Manson, J.C. (2005) Polymorphisms at codons 108 and 189 in murine PrP play distinct roles in the control of scrapie incubation time. *J Gen Virol*, **86**, 859-868.

Basler, K., Oesch, B., Scott, M., Westaway, D., Walchli, M., Groth, D.F., McKinley, M.P., Prusiner, S.B. and Weissmann, C. (1986) Scrapie and cellular PrP isoforms are encoded by the same chromosomal gene. *Cell*, **46**, 417-428.

Beck, J.A., Lloyd, S., Hafezparast, M., Lennon-Pierce, M., Eppig, J.T., Festing, M.F. and Fisher, E.M. (2000) Genealogies of mouse inbred strains. *Nat Genet*, **24**, 23-25.

Behrens, A., Genoud, N., Naumann, H., Rulicke, T., Janett, F., Heppner, F.L., Ledermann, B. and Aguzzi, A. (2002) Absence of the prion protein homologue Doppel causes male sterility. *Embo J*, **21**, 3652-3658.

Bessen, R.A. and Marsh, R.F. (1992) Biochemical and physical properties of the prion protein from two strains of the transmissible mink encephalopathy agent. *J Virol*, **66**, 2096-2101.

Bessen, R.A. and Marsh, R.F. (1994) Distinct PrP properties suggest the molecular basis of strain variation in transmissible mink encephalopathy. *J Virol*, **68**, 7859-7868.

Betmouni, S., Perry, V.H. and Gordon, J.L. (1996) Evidence for an early inflammatory response in the central nervous system of mice with scrapie. *Neuroscience*, **74**, 1-5.

Bieschke, J., Weber, P., Sarafoff, N., Beekes, M., Giese, A. and Kretzschmar, H. (2004) Autocatalytic self-propagation of misfolded prion protein. *Proc Natl Acad Sci U S A*, **101**, 12207-12211.

Bignami, A., Eng, L.F., Dahl, D. and Uyeda, C.T. (1972) Localization of the glial fibrillary acidic protein in astrocytes by immunofluorescence. *Brain Res*, **43**, 429-435.

Bignell, G.R., Warren, W., Seal, S., Takahashi, M., Rapley, E., Barfoot, R., Green, H., Brown, C., Biggs, P.J., Lakhani, S.R., Jones, C., Hansen, J., Blair, E., Hofmann, B., Siebert, R., Turner, G., Evans, D.G., Schrander-Stumpel, C., Beemer, F.A., van Den Ouweland, A., Halley, D., Delpech, B., Cleveland, M.G., Leigh, I., Leisti, J. and Rasmussen, S. (2000) Identification of the familial cylindromatosis tumour-suppressor gene. *Nat Genet*, **25**, 160-165.

Binder, L.I., Frankfurter, A. and Rebhun, L.I. (1985) The distribution of tau in the mammalian central nervous system. *J Cell Biol*, **101**, 1371-1378.

Birkenmeier, E.H., Gwynn, B., Howard, S., Jerry, J., Gordon, J.I., Landschulz, W.H. and McKnight, S.L. (1989) Tissue-specific expression, developmental regulation, and genetic mapping of the gene encoding CCAAT/enhancer binding protein. *Genes Dev*, **3**, 1146-1156.

Bonizzi, G. and Karin, M. (2004) The two NF-kappaB activation pathways and their role in innate and adaptive immunity. *Trends Immunol*, **25**, 280-288.

Bosque, P.J. and Prusiner, S.B. (2000) Cultured cell sublines highly susceptible to prion infection. *J Virol*, **74**, 4377-4386.

Bouwmeester, T., Bauch, A., Ruffner, H., Angrand, P.O., Bergamini, G., Croughton, K., Cruciat, C., Eberhard, D., Gagneur, J., Ghidelli, S., Hopf, C., Huhse, B., Mangano, R., Michon, A.M., Schirle, M., Schlegl, J., Schwab, M., Stein, M.A., Bauer, A., Casari, G., Drewes, G., Gavin, A.C., Jackson, D.B., Joberty, G., Neubauer, G., Rick, J., Kuster, B. and Superti-Furga, G. (2004) A physical and functional map of the human TNF-alpha/NF-kappa B signal transduction pathway. *Nat Cell Biol*, **6**, 97-105.

Brandner, S., Isenmann, S., Raeber, A., Fischer, M., Sailer, A., Kobayashi, Y., Marino, S., Weissmann, C. and Aguzzi, A. (1996) Normal host prion protein necessary for scrapie-induced neurotoxicity. *Nature*, **379**, 339-343.

Brown, D.R. (2001) Microglia and prion disease. *Microsc Res Tech*, **54**, 71-80.

Brown, D.R. (2003) Prion protein expression modulates neuronal copper content. *J Neurochem*, **87**, 377-385.

Brown, D.R., Wong, B.S., Hafiz, F., Clive, C., Haswell, S.J. and Jones, I.M. (1999) Normal prion protein has an activity like that of superoxide dismutase. *Biochem J*, **344 Pt 1**, 1-5.

Bruce, M., Chree, A., McConnell, I., Foster, J., Pearson, G. and Fraser, H. (1994) Transmission of bovine spongiform encephalopathy and scrapie to mice: strain variation and the species barrier. *Philos Trans R Soc Lond B Biol Sci*, **343**, 405-411.

Bruce, M.E. (1993) Scrapie strain variation and mutation. *Br Med Bull*, **49**, 822-838.

Bruce, M.E. (2003) TSE strain variation. *Br Med Bull*, **66**, 99-108.

Bruce, M.E., Boyle, A., Cousens, S., McConnell, I., Foster, J., Goldmann, W. and Fraser, H. (2002) Strain characterization of natural sheep scrapie and comparison with BSE. *J Gen Virol*, **83**, 695-704.

Bruce, M.E., McBride, P.A. and Farquhar, C.F. (1989) Precise targeting of the pathology of the sialoglycoprotein, PrP, and vacuolar degeneration in mouse scrapie. *Neurosci Lett*, **102**, 1-6.

Bruce, M.E., McConnell, I., Fraser, H. and Dickinson, A.G. (1991) The disease characteristics of different strains of scrapie in Sinc congenic mouse lines: implications for the nature of the agent and host control of pathogenesis. *J Gen Virol*, **72 (Pt 3)**, 595-603.

Bruce, M.E., Will, R.G., Ironside, J.W., McConnell, I., Drummond, D., Suttie, A., McCardle, L., Chree, A., Hope, J., Birkett, C., Cousens, S., Fraser, H. and Bostock, C.J. (1997) Transmissions to mice indicate that 'new variant' CJD is caused by the BSE agent. *Nature*, **389**, 498-501.

Bu, B., Li, J., Davies, P. and Vincent, I. (2002) Deregulation of cdk5, hyperphosphorylation, and cytoskeletal pathology in the Niemann-Pick type C murine model. *J Neurosci*, **22**, 6515-6525.

Bucciantini, M., Giannoni, E., Chiti, F., Baroni, F., Formigli, L., Zurdo, J., Taddei, N., Ramponi, G., Dobson, C.M. and Stefani, M. (2002) Inherent toxicity of aggregates implies a common mechanism for protein misfolding diseases. *Nature*, **416**, 507-511.

Bueler, H., Aguzzi, A., Sailer, A., Greiner, R.A., Autenried, P., Aguet, M. and Weissmann, C. (1993) Mice devoid of PrP are resistant to scrapie. *Cell*, **73**, 1339-1347.

Bueler, H., Fischer, M., Lang, Y., Bluethmann, H., Lipp, H.P., DeArmond, S.J., Prusiner, S.B., Aguet, M. and Weissmann, C. (1992) Normal development and behaviour of mice lacking the neuronal cell-surface PrP protein. *Nature*, **356**, 577-582.

Carlson, G.A., Ebeling, C., Torchia, M., Westaway, D. and Prusiner, S.B. (1993) Delimiting the location of the scrapie prion incubation time gene on chromosome 2 of the mouse. *Genetics*, **133**, 979-988.

Carlson, G.A., Goodman, P.A., Lovett, M., Taylor, B.A., Marshall, S.T., Peterson-Torchia, M., Westaway, D. and Prusiner, S.B. (1988a) Genetics and polymorphism of the mouse prion gene complex: control of scrapie incubation time. *Mol Cell Biol*, **8**, 5528-5540.

Carlson, G.A., Kingsbury, D.T., Goodman, P.A., Coleman, S., Marshall, S.T., DeArmond, S., Westaway, D. and Prusiner, S.B. (1986) Linkage of prion protein and scrapie incubation time genes. *Cell*, **46**, 503-511.

Carlson, G.A., Westaway, D., Goodman, P.A., Peterson, M., Marshall, S.T. and Prusiner, S.B. (1988b) Genetic control of prion incubation period in mice. *Ciba Found Symp*, **135**, 84-99.

Carp, R.I., Moretz, R.C., Natelli, M. and Dickinson, A.G. (1987) Genetic control of scrapie: incubation period and plaque formation in I mice. *J Gen Virol*, **68 (Pt 2)**, 401-407.

Castilla, J., Saa, P., Hetz, C. and Soto, C. (2005) In vitro generation of infectious scrapie prions. *Cell*, **121**, 195-206.

Caughey, B., Race, R.E. and Chesebro, B. (1988) Detection of prion protein mRNA in normal and scrapie-infected tissues and cell lines. *J Gen Virol*, **69 (Pt 3)**, 711-716.

Caughey, B., Raymond, G.J., Ernst, D. and Race, R.E. (1991) N-terminal truncation of the scrapie-associated form of PrP by lysosomal protease(s): implications regarding the site of conversion of PrP to the protease-resistant state. *J Virol*, **65**, 6597-6603.

Cervenakova, L., Goldfarb, L.G., Garruto, R., Lee, H.S., Gajdusek, D.C. and Brown, P. (1998) Phenotype-genotype studies in kuru: implications for new variant Creutzfeldt-Jakob disease. *Proc Natl Acad Sci U S A*, **95**, 13239-13241.

Chandler, R.L. (1961) Encephalopathy in mice produced by inoculation with scrapie brain material. *Lancet*, **1**, 1378-1379.

Chia, R., Achilli, F., Festing, M.F. and Fisher, E.M. (2005) The origins and uses of mouse outbred stocks. *Nat Genet*, **37**, 1181-1186.

Churchill, G.A., Airey, D.C., Allayee, H., Angel, J.M., Attie, A.D., Beatty, J., Beavis, W.D., Belknap, J.K., Bennett, B., Berrettini, W., Bleich, A., Bogue, M., Broman, K.W., Buck, K.J., Buckler, E., Burmeister, M., Chesler, E.J., Cheverud, J.M., Clapcote, S., Cook, M.N., Cox, R.D., Crabbe, J.C., Crusio, W.E., Darvasi, A., Deschepper, C.F., Doerge, R.W., Farber, C.R., Forejt, J., Gaile, D., Garlow, S.J., Geiger, H., Gershenfeld, H., Gordon, T., Gu, J., Gu, W., de Haan, G., Hayes, N.L., Heller, C., Himmelbauer, H., Hitzemann, R., Hunter, K., Hsu, H.C., Iraqi, F.A., Ivandic, B., Jacob, H.J., Jansen, R.C., Jepsen, K.J., Johnson, D.K., Johnson, T.E., Kempermann, G., Kendziorski, C., Kotb, M., Kooy, R.F., Llamas, B., Lammert, F., Lassalle, J.M., Lowenstein, P.R., Lu, L., Lusis, A., Manly, K.F., Marcucio, R., Matthews, D., Medrano, J.F., Miller, D.R., Mittleman, G., Mock, B.A., Mogil, J.S., Montagutelli, X., Morahan, G., Morris, D.G., Mott, R., Nadeau, J.H., Nagase, H., Nowakowski, R.S., O'Hara, B.F., Osadchuk, A.V., Page, G.P., Paigen, B., Paigen, K., Palmer, A.A., Pan, H.J., Peltonen-Palotie, L., Peirce, J., Pomp, D., Pravenec, M., Prows, D.R., Qi, Z., Reeves, R.H., Roder, J., Rosen, G.D., Schadt, E.E., Schalkwyk, L.C., Seltzer, Z., Shimomura, K., Shou, S., Sillanpaa, M.J., Siracusa, L.D., Snoeck, H.W., Spearow, J.L., Svenson, K., Tarantino, L.M., Threadgill, D., Toth, L.A., Valdar, W., de Villena, F.P., Warden, C., Whatley, S., Williams, R.W., Wiltshire, T., Yi, N., Zhang, D., Zhang, M. and Zou, F. (2004) The Collaborative Cross, a community resource for the genetic analysis of complex traits. *Nat Genet*, **36**, 1133-1137.

Cohen, B.A., Mitra, R.D., Hughes, J.D. and Church, G.M. (2000) A computational analysis of whole-genome expression data reveals chromosomal domains of gene expression. *Nat Genet*, **26**, 183-186.

Colling, S.B., Collinge, J. and Jefferys, J.G. (1996) Hippocampal slices from prion protein null mice: disrupted Ca(2+)-activated K+ currents. *Neurosci Lett*, **209**, 49-52.

Collinge, J. (1997) Human prion diseases and bovine spongiform encephalopathy (BSE). *Hum Mol Genet*, **6**, 1699-1705.

Collinge, J. (1999) Variant Creutzfeldt-Jakob disease. *Lancet*, **354**, 317-323.

Collinge, J. (2001) Prion diseases of humans and animals: their causes and molecular basis. *Annu Rev Neurosci*, **24**, 519-550.

Collinge, J. (2005) Molecular neurology of prion disease. *J Neurol Neurosurg Psychiatry*, **76**, 906-919.

Collinge, J., Beck, J., Campbell, T., Estibeiro, K. and Will, R.G. (1996a) Prion protein gene analysis in new variant cases of Creutzfeldt-Jakob disease. *Lancet*, **348**, 56.

Collinge, J., Brown, J., Hardy, J., Mullan, M., Rossor, M.N., Baker, H., Crow, T.J., Lofthouse, R., Poulter, M., Ridley, R. and et al. (1992) Inherited prion disease with 144 base pair gene insertion. 2. Clinical and pathological features. *Brain*, **115 (Pt 3)**, 687-710.

Collinge, J. and Clarke, A.R. (2007) A general model of prion strains and their pathogenicity. *Science*, **318**, 930-936.

Collinge, J., Palmer, M.S. and Dryden, A.J. (1991) Genetic predisposition to iatrogenic Creutzfeldt-Jakob disease. *Lancet*, **337**, 1441-1442.

Collinge, J., Palmer, M.S., Sidle, K.C., Gowland, I., Medori, R., Ironside, J. and Lantos, P. (1995) Transmission of fatal familial insomnia to laboratory animals. *Lancet*, **346**, 569-570.

Collinge, J., Sidle, K.C., Meads, J., Ironside, J. and Hill, A.F. (1996b) Molecular analysis of prion strain variation and the aetiology of 'new variant' CJD. *Nature*, **383**, 685-690.

Collinge, J., Whitfield, J., McKintosh, E., Beck, J., Mead, S., Thomas, D.J. and Alpers, M.P. (2006) Kuru in the 21st century--an acquired human prion disease with very long incubation periods. *Lancet*, **367**, 2068-2074.

Collinge, J., Whittington, M.A., Sidle, K.C., Smith, C.J., Palmer, M.S., Clarke, A.R. and Jefferys, J.G. (1994) Prion protein is necessary for normal synaptic function. *Nature*, **370**, 295-297.

Cozier, G.E., Carlton, J., McGregor, A.H., Gleeson, P.A., Teasdale, R.D., Mellor, H. and Cullen, P.J. (2002) The phox homology (PX) domain-dependent, 3-phosphoinositide-mediated association of sorting nexin-1 with an early sorting endosomal compartment is required for its ability to regulate epidermal growth factor receptor degradation. *J Biol Chem*, **277**, 48730-48736.

Crawford, F.C., Freeman, M.J., Schinka, J.A., Morris, M.D., Abdullah, L.I., Richards, D., Sevush, S., Duara, R. and Mullan, M.J. (2001) Association between Alzheimer's disease and a functional polymorphism in the Myeloperoxidase gene. *Exp Neurol*, **167**, 456-459.

Cremona, M., Colombo, E., Andreazzoli, M., Cossu, G. and Broccoli, V. (2004) Bsx, an evolutionary conserved Brain Specific homeoboX gene expressed in the septum, epiphysis, mammillary bodies and arcuate nucleus. *Gene Expr Patterns*, **4**, 47-51.

Croes, E.A., Alizadeh, B.Z., Bertoli-Avella, A.M., Rademaker, T., Vergeer-Drop, J., Dermaut, B., Houwing-Duistermaat, J.J., Wientjens, D.P., Hofman, A., Van Broeckhoven, C. and van Duijn, C.M. (2004) Polymorphisms in the prion protein gene and in the doppel gene increase susceptibility for Creutzfeldt-Jakob disease. *Eur J Hum Genet*, **12**, 389-394.

Cronier, S , Laude, H. and Peyrin, J.M. (2004) Prions can infect primary cultured neurons and astrocytes and promote neuronal cell death. *Proc Natl Acad Sci U S A*, **101**, 12271-12276.

Cunningham, C., Deacon, R.M., Chan, K., Boche, D., Rawlins, J.N. and Perry, V.H. (2005) Neuropathologically distinct prion strains give rise to similar temporal profiles of behavioral deficits. *Neurobiol Dis*, **18**, 258-269.

Cuppen, E. (2005) Haplotype-based genetics in mice and rats. *Trends Genet*, **21**, 318-322.

Darvasi, A. (1998) Experimental strategies for the genetic dissection of complex traits in animal models. *Nat Genet*, **18**, 19-24.

Darvasi, A. and Soller, M. (1995) Advanced intercross lines, an experimental population for fine genetic mapping. *Genetics*, **141**, 1199-1207.

Darvasi, A. and Soller, M. (1997) A simple method to calculate resolving power and confidence interval of QTL map location. *Behav Genet*, **27**, 125-132.

Daugherty, A., Dunn, J.L., Rateri, D.L. and Heinecke, J.W. (1994) Myeloperoxidase, a catalyst for lipoprotein oxidation, is expressed in human atherosclerotic lesions. *J Clin Invest*, **94**, 437-444.

de Jong, R., van der Heijden, J. and Meijlink, F. (1993) DNA-binding specificity of the S8 homeodomain. *Nucleic Acids Res*, **21**, 4711-4720.

de la Baume, S., Yi, C.C., Schwartz, J.C., Chaillet, P., Marcais-Collado, H. and Costentin, J. (1983) Participation of both 'enkephalinase' and aminopeptidase activities in the metabolism of endogenous enkephalins. *Neuroscience*, **8**, 143-151.

Deacon, R.M., Thomas, C.L., Rawlins, J.N. and Morley, B.J. (2007) A comparison of the behavior of C57BL/6 and C57BL/10 mice. *Behav Brain Res*, **179**, 239-247.

DeArmond, S.J., Sanchez, H., Yehiely, F., Qiu, Y., Ninchak-Casey, A., Daggett, V., Camerino, A.P., Cayetano, J., Rogers, M., Groth, D., Torchia, M., Tremblay, P., Scott, M.R., Cohen, F.E. and Prusiner, S.B. (1997) Selective neuronal targeting in prion disease. *Neuron*, **19**, 1337-1348.

Della-Bianca, V., Rossi, F., Armato, U., Dal-Pra, I., Costantini, C., Perini, G., Politi, V. and Della Valle, G. (2001) Neurotrophin p75 receptor is involved in neuronal damage by prion peptide-(106-126). *J Biol Chem*, **276**, 38929-38933.

Demarest, K., Koyner, J., McCaughran, J., Jr., Cipp, L. and Hitzemann, R. (2001) Further characterization and high-resolution mapping of quantitative trait loci for ethanol-induced locomotor activity. *Behav Genet*, **31**, 79-91.

Denny, P., Swift, S., Brand, N., Dabhade, N., Barton, P. and Ashworth, A. (1992) A conserved family of genes related to the testis determining gene, SRY. *Nucleic Acids Res*, **20**, 2887.

Di Stefano, P., Cabodi, S., Boeri Erba, E., Margaria, V., Bergatto, E., Giuffrida, M.G., Silengo, L., Tarone, G., Turco, E. and Defilippi, P. (2004) P130Cas-associated protein

(p140Cap) as a new tyrosine-phosphorylated protein involved in cell spreading. *Mol Biol Cell*, **15**, 787-800.

Dickinson, A.G. (1976) Scrapie in sheep and goats. *Front Biol*, **44**, 209-241.

Dickinson, A.G. and Mackay, J.M. (1964) Genetical Control of the Incubation Period in Mice of the Neurological Disease, Scrapie. *Heredity*, **19**, 279-288.

Dickinson, A.G. and Meikle, V.M. (1971) Host-genotype and agent effects in scrapie incubation: change in allelic interaction with different strains of agent. *Mol Gen Genet*, **112**, 73-79.

Dickinson, A.G., Meikle, V.M. and Fraser, H. (1968) Identification of a gene which controls the incubation period of some strains of scrapie agent in mice. *J Comp Pathol*, **78**, 293-299.

Dickinson, A.G., Meikle, V.M. and Fraser, H. (1969) Genetical control of the concentration of ME7 scrapie agent in the brain of mice. *J Comp Pathol*, **79**, 15-22.

Doerks, T., Strauss, M., Brendel, M. and Bork, P. (2000) GRAM, a novel domain in glucosyltransferases, myotubularins and other putative membrane-associated proteins. *Trends Biochem Sci*, **25**, 483-485.

Du, Y., Bales, K.R., Dodel, R.C., Liu, X., Glinn, M.A., Horn, J.W., Little, S.P. and Paul, S.M. (1998) Alpha2-macroglobulin attenuates beta-amyloid peptide 1-40 fibril formation and associated neurotoxicity of cultured fetal rat cortical neurons. *J Neurochem*, **70**, 1182-1188.

Duguid, J.R., Rohwer, R.G. and Seed, B. (1988) Isolation of cDNAs of scrapie-modulated RNAs by subtractive hybridization of a cDNA library. *Proc Natl Acad Sci U S A*, **85**, 5738-5742.

Elenich, L.A., Nandi, D., Kent, A.E., McCluskey, T.S., Cruz, M., Iyer, M.N., Woodward, E.C., Conn, C.W., Ochoa, A.L., Ginsburg, D.B. and Monaco, J.J. (1999) The complete primary structure of mouse 20S proteasomes. *Immunogenetics*, **49**, 835-842.

Ellis, R.J. and van der Vies, S.M. (1991) Molecular chaperones. *Annu Rev Biochem*, **60**, 321-347.

Ennulat, D.J., Liem, R.K., Hashim, G.A. and Shelanski, M.L. (1989) Two separate 18-amino acid domains of tau promote the polymerization of tubulin. *J Biol Chem*, **264**, 5327-5330.

Ernst, C.A., Zhang, Y.J., Hancock, P.R., Rutledge, B.J., Corless, C.L. and Rollins, B.J. (1994) Biochemical and biologic characterization of murine monocyte chemoattractant protein-1. Identification of two functional domains. *J Immunol*, **152**, 3541-3549.

Etienne-Manneville, S. and Hall, A. (2002) Rho GTPases in cell biology. *Nature*, **420**, 629-635.

Ettaiche, M., Pichot, R., Vincent, J.P. and Chabry, J. (2000) In vivo cytotoxicity of the prion protein fragment 106-126. *J Biol Chem*, **275**, 36487-36490.

Ewart-Toland, A., Briassouli, P., de Koning, J.P., Mao, J.H., Yuan, J., Chan, F., MacCarthy-Morrogh, L., Ponder, B.A., Nagase, H., Burn, J., Ball, S., Almeida, M., Linardopoulos, S. and Balmain, A. (2003) Identification of Stk6/STK15 as a candidate low-penetrance tumor-susceptibility gene in mouse and human. *Nat Genet*, **34**, 403-412.

Fabrizi, C., Silei, V., Menegazzi, M., Salmona, M., Bugiani, O., Tagliavini, F., Suzuki, H. and Lauro, G.M. (2001) The stimulation of inducible nitric-oxide synthase by the prion protein fragment 106--126 in human microglia is tumor necrosis factor-alpha-dependent and involves p38 mitogen-activated protein kinase. *J Biol Chem*, **276**, 25692-25696.

Felton, L.M., Cunningham, C., Rankine, E.L., Waters, S., Boche, D. and Perry, V.H. (2005) MCP-1 and murine prion disease: separation of early behavioural dysfunction from overt clinical disease. *Neurobiol Dis*, **20**, 283-295.

Ferris, S.D., Sage, R.D., Prager, E.M., Ritte, U. and Wilson, A.C. (1983) Mitochondrial DNA evolution in mice. *Genetics*, **105**, 681-721.

Firestein, S. (2001) How the olfactory system makes sense of scents. *Nature*, **413**, 211-218.

Fischer, M., Rulicke, T., Raeber, A., Sailer, A., Moser, M., Oesch, B., Brandner, S., Aguzzi, A. and Weissmann, C. (1996) Prion protein (PrP) with amino-proximal deletions restoring susceptibility of PrP knockout mice to scrapie. *Embo J*, **15**, 1255-1264.

Flint, J. (2003) Analysis of quantitative trait loci that influence animal behavior. *J Neurobiol*, **54**, 46-77.

Flint, J. and Mott, R. (2001) Finding the molecular basis of quantitative traits: successes and pitfalls. *Nat Rev Genet*, **2**, 437-445.

Flint, J., Valdar, W., Shifman, S. and Mott, R. (2005) Strategies for mapping and cloning quantitative trait genes in rodents. *Nat Rev Genet*, **6**, 271-286.

Forloni, G., Angeretti, N., Chiesa, R., Monzani, E., Salmona, M., Bugiani, O. and Tagliavini, F. (1993) Neurotoxicity of a prion protein fragment. *Nature*, **362**, 543-546.

Fraser, H., Bruce, M.E., Chree, A., McConnell, I. and Wells, G.A. (1992) Transmission of bovine spongiform encephalopathy and scrapie to mice. *J Gen Virol*, **73 (Pt 8)**, 1891-1897.

Fraser, H. and Dickinson, A.G. (1968) The sequential development of the brain lesion of scrapie in three strains of mice. *J Comp Pathol*, **78**, 301-311.

Frazer, K.A., Eskin, E., Kang, H.M., Bogue, M.A., Hinds, D.A., Beilharz, E.J., Gupta, R.V., Montgomery, J., Morenzoni, M.M., Nilsen, G.B., Pethiyagoda, C.L., Stuve, L.L., Johnson, F.M., Daly, M.J., Wade, C.M. and Cox, D.R. (2007) A sequence-based variation map of 8.27 million SNPs in inbred mouse strains. *Nature*.

Frazer, K.A., Wade, C.M., Hinds, D.A., Patil, N., Cox, D.R. and Daly, M.J. (2004) Segmental phylogenetic relationships of inbred mouse strains revealed by fine-scale analysis of sequence variation across 4.6 mb of mouse genome. *Genome Res*, **14**, 1493-1500.

French, L.E., Wohlwend, A., Sappino, A.P., Tschopp, J. and Schifferli, J.A. (1994) Human clusterin gene expression is confined to surviving cells during in vitro programmed cell death. *J Clin Invest*, **93**, 877-884.

Freter, R.R., Alberta, J.A., Lam, K.K. and Stiles, C.D. (1995) A new platelet-derived growth factor-regulated genomic element which binds a serine/threonine phosphoprotein mediates induction of the slow immediate-early gene MCP-1. *Mol Cell Biol*, **15**, 315-325.

Gajdusek, D.C. (1977) Unconventional viruses and the origin and disappearance of kuru. *Science*, **197**, 943-960.

Gajdusek, D.C., Gibbs, C.J. and Alpers, M. (1966) Experimental transmission of a Kuru-like syndrome to chimpanzees. *Nature*, **209**, 794-796.

Gao, L., Tucker, K.L. and Andreadis, A. (2005) Transcriptional regulation of the mouse microtubule-associated protein tau. *Biochim Biophys Acta*, **1681**, 175-181.

Garcia-Mata, R., Gao, Y.S. and Sztul, E. (2002) Hassles with taking out the garbage: aggravating aggresomes. *Traffic*, **3**, 388-396.

Gavier-Widen, D., Stack, M.J., Baron, T., Balachandran, A. and Simmons, M. (2005) Diagnosis of transmissible spongiform encephalopathies in animals: a review. *J Vet Diagn Invest*, **17**, 509-527.

Geisler, N., Plessmann, U. and Weber, K. (1982) Related amino acid sequences in neurofilaments and non-neural intermediate filaments. *Nature*, **296**, 448-450.

Geisler, N. and Weber, K. (1982) The amino acid sequence of chicken muscle desmin provides a common structural model for intermediate filament proteins. *Embo J*, **1**, 1649-1656.

Georgopoulos, K., Bigby, M., Wang, J.H., Molnar, A., Wu, P., Winandy, S. and Sharpe, A. (1994) The Ikaros gene is required for the development of all lymphoid lineages. *Cell*, **79**, 143-156.

Giaccone, G., Mangieri, M., Capobianco, R., Limido, L., Hauw, J.J., Haik, S., Fociani, P., Bugiani, O. and Tagliavini, F. (2007) Tauopathy in human and experimental variant Creutzfeldt-Jakob disease. *Neurobiol Aging*.

Gibbs, C.J., Jr., Gajdusek, D.C., Asher, D.M., Alpers, M.P., Beck, E., Daniel, P.M. and Matthews, W.B. (1968) Creutzfeldt-Jakob disease (spongiform encephalopathy): transmission to the chimpanzee. *Science*, **161**, 388-389.

Gibbs, C.J., Jr., Joy, A., Heffner, R., Franko, M., Miyazaki, M., Asher, D.M., Parisi, J.E., Brown, P.W. and Gajdusek, D.C. (1985) Clinical and pathological features and laboratory confirmation of Creutzfeldt-Jakob disease in a recipient of pituitary-derived human growth hormone. *N Engl J Med*, **313**, 734-738.

Giese, A., Brown, D.R., Groschup, M.H., Feldmann, C., Haist, I. and Kretzschmar, H.A. (1998) Role of microglia in neuronal cell death in prion disease. *Brain Pathol*, **8**, 449-457.

Gilmore, E.C., Ohshima, T., Goffinet, A.M., Kulkarni, A.B. and Herrup, K. (1998) Cyclin-dependent kinase 5-deficient mice demonstrate novel developmental arrest in cerebral cortex. *J Neurosci*, **18**, 6370-6377.

Goedert, M., Wischik, C.M., Crowther, R.A., Walker, J.E. and Klug, A. (1988) Cloning and sequencing of the cDNA encoding a core protein of the paired helical filament of Alzheimer disease: identification as the microtubule-associated protein tau. *Proc Natl Acad Sci U S A*, **85**, 4051-4055.

Gordon, W.S. (1946) Advances in veterinary research: louping ill, tick-borne fever and scrapie. *Veterinary Record*, **58**, 516-525.

Gorlich, D., Prehn, S., Laskey, R.A. and Hartmann, E. (1994) Isolation of a protein that is essential for the first step of nuclear protein import. *Cell*, **79**, 767-778.

Graner, E., Mercadante, A.F., Zanata, S.M., Forlenza, O.V., Cabral, A.L., Veiga, S.S., Juliano, M.A., Roesler, R., Walz, R., Minetti, A., Izquierdo, I., Martins, V.R. and Brentani, R.R. (2000) Cellular prion protein binds laminin and mediates neuritogenesis. *Brain Res Mol Brain Res*, **76**, 85-92.

Green, P.S., Mendez, A.J., Jacob, J.S., Crowley, J.R., Growdon, W., Hyman, B.T. and Heinecke, J.W. (2004) Neuronal expression of myeloperoxidase is increased in Alzheimer's disease. *J Neurochem*, **90**, 724-733.

Griffith, J.S. (1967) Self-replication and scrapie. *Nature*, **215**, 1043-1044.

Grupe, A., Germer, S., Usuka, J., Aud, D., Belknap, J.K., Klein, R.F., Ahluwalia, M.K., Higuchi, R. and Peltz, G. (2001) In silico mapping of complex disease-related traits in mice. *Science*, **292**, 1915-1918.

Gu, L., Rutledge, B., Fiorillo, J., Ernst, C., Grewal, I., Flavell, R., Gladue, R. and Rollins, B. (1997) In vivo properties of monocyte chemoattractant protein-1. *J Leukoc Biol*, **62**, 577-580.

Gu, L., Tseng, S.C. and Rollins, B.J. (1999) Monocyte chemoattractant protein-1. *Chem Immunol*, **72**, 7-29.

Guo, W.J., Datta, S., Band, V. and Dimri, G.P. (2007) Mel-18, a polycomb group protein, regulates cell proliferation and senescence via transcriptional repression of Bmi-1 and c-Myc oncoproteins. *Mol Biol Cell*, **18**, 536-546.

Gutierrez, O., Pipaon, C., Inohara, N., Fontalba, A., Ogura, Y., Prosper, F., Nunez, G. and Fernandez-Luna, J.L. (2002) Induction of Nod2 in myelomonocytic and intestinal epithelial cells via nuclear factor-kappa B activation. *J Biol Chem*, **277**, 41701-41705.

Hadlow, W.J. (1959) Scrapie and kuru. . *Lancet 2*, 289-290.

Haft, C.R., de la Luz Sierra, M., Barr, V.A., Haft, D.H. and Taylor, S.I. (1998) Identification of a family of sorting nexin molecules and characterization of their association with receptors. *Mol Cell Biol*, **18**, 7278-7287.

Hagen, G., Muller, S., Beato, M. and Suske, G. (1992) Cloning by recognition site screening of two novel GT box binding proteins: a family of Sp1 related genes. *Nucleic Acids Res*, **20**, 5519-5525.

Haik, S., Privat, N., Adjou, K.T., Sazdovitch, V., Dormont, D., Duyckaerts, C. and Hauw, J.J. (2002) Alpha-synuclein-immunoreactive deposits in human and animal prion diseases. *Acta Neuropathol*, **103**, 516-520.

Hajj, G.N., Lopes, M.H., Mercadante, A.F., Veiga, S.S., da Silveira, R.B., Santos, T.G., Ribeiro, K.C., Juliano, M.A., Jacchieri, S.G., Zanata, S.M. and Martins, V.R. (2007) Cellular prion protein interaction with vitronectin supports axonal growth and is compensated by integrins. *J Cell Sci*, **120**, 1915-1926.

Hampe, J., Frenzel, H., Mirza, M.M., Croucher, P.J., Cuthbert, A., Mascheretti, S., Huse, K., Platzer, M., Bridger, S., Meyer, B., Nurnberg, P., Stokkers, P., Krawczak, M., Mathew, C.G., Curran, M. and Schreiber, S. (2002) Evidence for a NOD2-independent susceptibility locus for inflammatory bowel disease on chromosome 16p. *Proc Natl Acad Sci U S A*, **99**, 321-326.

Harris, D.A., Huber, M.T., van Dijken, P., Shyng, S.L., Chait, B.T. and Wang, R. (1993) Processing of a cellular prion protein: identification of N- and C-terminal cleavage sites. *Biochemistry*, **32**, 1009-1016.

Healy, A.M., Weavers, E., McElroy, M., Gomez-Parada, M., Collins, J.D., O'Doherty, E., Sweeney, T. and Doherty, M.L. (2003) The clinical neurology of scrapie in Irish sheep. *J Vet Intern Med*, **17**, 908-916.

Heikenwalder, M., Zeller, N., Seeger, H., Prinz, M., Klohn, P.C., Schwarz, P., Ruddle, N.H., Weissmann, C. and Aguzzi, A. (2005) Chronic lymphocytic inflammation specifies the organ tropism of prions. *Science*, **307**, 1107-1110.

Heinemeyer, T., Chen, X., Karas, H., Kel, A.E., Kel, O.V., Liebich, I., Meinhardt, T., Reuter, I., Schacherer, F. and Wingender, E. (1999) Expanding the TRANSFAC database towards an expert system of regulatory molecular mechanisms. *Nucleic Acids Res*, **27**, 318-322.

Heinemeyer, T., Wingender, E., Reuter, I., Hermjakob, H., Kel, A.E., Kel, O.V., Ignatieva, E.V., Ananko, E.A., Podkolodnaya, O.A., Kolpakov, F.A., Podkolodny, N.L. and Kolchanov, N.A. (1998) Databases on transcriptional regulation: TRANSFAC, TRRD and COMPEL. *Nucleic Acids Res*, **26**, 362-367.

Hertveldt, V., De Mees, C., Scohy, S., Van Vooren, P., Szpirer, J. and Szpirer, C. (2007) The Sp6 locus uses several promoters and generates sense and antisense transcripts. *Biochimie*.

Hetz, C., Russelakis-Carneiro, M., Maundrell, K., Castilla, J. and Soto, C. (2003) Caspase-12 and endoplasmic reticulum stress mediate neurotoxicity of pathological prion protein. *Embo J*, **22**, 5435-5445.

Hill, A.F., Antoniou, M. and Collinge, J. (1999a) Protease-resistant prion protein produced in vitro lacks detectable infectivity. *J Gen Virol*, **80 (Pt 1)**, 11-14.

Hill, A.F., Butterworth, R.J., Joiner, S., Jackson, G., Rossor, M.N., Thomas, D.J., Frosh, A., Tolley, N., Bell, J.E., Spencer, M., King, A., Al-Sarraj, S., Ironside, J.W., Lantos, P.L. and Collinge, J. (1999b) Investigation of variant Creutzfeldt-Jakob disease and other human prion diseases with tonsil biopsy samples. *Lancet*, **353**, 183-189.

Hill, A.F. and Collinge, J. (2001) Strain variations and species barriers. *Contrib Microbiol*, **7**, 48-57.

Hill, A.F. and Collinge, J. (2003) Subclinical prion infection. *Trends Microbiol*, **11**, 578-584.

Hill, A.F., Desbruslais, M., Joiner, S., Sidle, K.C., Gowland, I., Collinge, J., Doey, L.J. and Lantos, P. (1997) The same prion strain causes vCJD and BSE. *Nature*, **389**, 448-450, 526.

Hill, A.F., Joiner, S., Wadsworth, J.D., Sidle, K.C., Bell, J.E., Budka, H., Ironside, J.W. and Collinge, J. (2003) Molecular classification of sporadic Creutzfeldt-Jakob disease. *Brain*, **126**, 1333-1346.

Himmler, A., Drechsel, D., Kirschner, M.W. and Martin, D.W., Jr. (1989) Tau consists of a set of proteins with repeated C-terminal microtubule-binding domains and variable N-terminal domains. *Mol Cell Biol*, **9**, 1381-1388.

Hisamatsu, T., Suzuki, M., Reinecker, H.C., Nadeau, W.J., McCormick, B.A. and Podolsky, D.K. (2003) CARD15/NOD2 functions as an antibacterial factor in human intestinal epithelial cells. *Gastroenterology*, **124**, 993-1000.

Hitzemann, R., Demarest, K., Koyner, J., Cipp, L., Patel, N., Rasmussen, E. and McCaughran, J., Jr. (2000) Effect of genetic cross on the detection of quantitative trait loci and a novel approach to mapping QTLs. *Pharmacol Biochem Behav*, **67**, 767-772.

Hitzemann, R., Malmanger, B., Cooper, S., Coulombe, S., Reed, C., Demarest, K., Koyner, J., Cipp, L., Flint, J., Talbot, C., Rademacher, B., Buck, K. and McCaughran, J., Jr. (2002) Multiple cross mapping (MCM) markedly improves the localization of a QTL for ethanol-induced activation. *Genes Brain Behav*, **1**, 214-222.

Hollstein, M., Sidransky, D., Vogelstein, B. and Harris, C.C. (1991) p53 mutations in human cancers. *Science*, **253**, 49-53.

Horowitz, P.M., LaPointe, N., Guillozet-Bongaarts, A.L., Berry, R.W. and Binder, L.I. (2006) N-terminal fragments of tau inhibit full-length tau polymerization in vitro. *Biochemistry*, **45**, 12859-12866.

Hsiao, K., Baker, H.F., Crow, T.J., Poulter, M., Owen, F., Terwilliger, J.D., Westaway, D., Ott, J. and Prusiner, S.B. (1989) Linkage of a prion protein missense variant to Gerstmann-Straussler syndrome. *Nature*, **338**, 342-345.

Hu, Y., Benedict, M.A., Wu, D., Inohara, N. and Nunez, G. (1998) Bcl-XL interacts with Apaf-1 and inhibits Apaf-1-dependent caspase-9 activation. *Proc Natl Acad Sci U S A*, **95**, 4386-4391.

Huber, R., Deboer, T. and Tobler, I. (2002) Sleep deprivation in prion protein deficient mice sleep deprivation in prion protein deficient mice and control mice: genotype dependent regional rebound. *Neuroreport*, **13**, 1-4.

Hughes, P.M., Allegrini, P.R., Rudin, M., Perry, V.H., Mir, A.K. and Wiessner, C. (2002) Monocyte chemoattractant protein-1 deficiency is protective in a murine stroke model. *J Cereb Blood Flow Metab*, **22**, 308-317.

Hugot, J.P., Chamaillard, M., Zouali, H., Lesage, S., Cezard, J.P., Belaiche, J., Almer, S., Tysk, C., O'Morain, C.A., Gassull, M., Binder, V., Finkel, Y., Cortot, A., Modigliani, R., Laurent-Puig, P., Gower-Rousseau, C., Macry, J., Colombel, J.F., Sahbatou, M. and Thomas, G. (2001) Association of NOD2 leucine-rich repeat variants with susceptibility to Crohn's disease. *Nature*, **411**, 599-603.

Huillard d'Aignaux, J., Costagliola, D., Maccario, J., Billette de Villemeur, T., Brandel, J.P., Deslys, J.P., Hauw, J.J., Chaussain, J.L., Agid, Y., Dormont, D. and Alperovitch, A. (1999) Incubation period of Creutzfeldt-Jakob disease in human growth hormone recipients in France. *Neurology*, **53**, 1197-1201.

Hunt, C.R., Parsian, A.J., Goswami, P.C. and Kozak, C.A. (1999) Characterization and expression of the mouse Hsc70 gene. *Biochim Biophys Acta*, **1444**, 315-325.

Hunter, N., Dann, J.C., Bennett, A.D., Somerville, R.A., McConnell, I. and Hope, J. (1992) Are Sinc and the PrP gene congruent? Evidence from PrP gene analysis in Sinc congenic mice. *J Gen Virol*, **73 (Pt 10)**, 2751-2755.

Hunter. N., Hope, J., McConnell, I. and Dickinson, A.G. (1987) Linkage of the scrapie-associated fibril protein (PrP) gene and Sinc using congenic mice and restriction fragment length polymorphism analysis. *J Gen Virol*, **68 (Pt 10)**, 2711-2716.

Hutter, G., Heppner, F.L. and Aguzzi, A. (2003) No superoxide dismutase activity of cellular prion protein in vivo. *Biol Chem*, **384**, 1279-1285.

Imamoto, N., Tachibana, T., Matsubae, M. and Yoneda, Y. (1995) A karyophilic protein forms a stable complex with cytoplasmic components prior to nuclear pore binding. *J Biol Chem*, **270**, 8559-8565.

Inohara, N., Koseki, T., del Peso, L., Hu, Y., Yee, C., Chen, S., Carrio, R., Merino, J., Liu, D., Ni, J. and Nunez, G. (1999) Nod1, an Apaf-1-like activator of caspase-9 and nuclear factor-kappaB. *J Biol Chem*, **274**, 14560-14567.

Inohara, N. and Nunez, G. (2001) The NOD: a signaling module that regulates apoptosis and host defense against pathogens. *Oncogene*, **20**, 6473-6481.

Inohara, N., Ogura, Y., Fontalba, A., Gutierrez, O., Pons, F., Crespo, J., Fukase, K., Inamura, S., Kusumoto, S., Hashimoto, M., Foster, S.J., Moran, A.P., Fernandez-Luna, J.L. and Nunez, G. (2003) Host recognition of bacterial muramyl dipeptide mediated through NOD2. Implications for Crohn's disease. *J Biol Chem*, **278**, 5509-5512.

Jackson, G.S., Beck, J.A., Navarrete, C., Brown, J., Sutton, P.M., Contreras, M. and Collinge, J. (2001a) HLA-DQ7 antigen and resistance to variant CJD. *Nature*, **414**, 269-270.

Jackson, G.S., Murray, I., Hosszu, L.L., Gibbs, N., Waltho, J.P., Clarke, A.R. and Collinge, J. (2001b) Location and properties of metal-binding sites on the human prion protein. *Proc Natl Acad Sci U S A*, **98**, 8531-8535.

Jantzen, H.M., Admon, A., Bell, S.P. and Tjian, R. (1990) Nucleolar transcription factor hUBF contains a DNA-binding motif with homology to HMG proteins. *Nature*, **344**, 830-836.

Jarrett, J.T. and Lansbury, P.T., Jr. (1993) Seeding "one-dimensional crystallization" of amyloid: a pathogenic mechanism in Alzheimer's disease and scrapie? *Cell*, **73**, 1055-1058.

Jeanmougin, F., Wurtz, J.M., Le Douarin, B., Chambon, P. and Losson, R. (1997) The bromodomain revisited. *Trends Biochem Sci*, **22**, 151-153.

Jeffrey, M., Halliday, W.G., Bell, J., Johnston, A.R., MacLeod, N.K., Ingham, C., Sayers, A.R., Brown, D.A. and Fraser, J.R. (2000) Synapse loss associated with abnormal PrP precedes neuronal degeneration in the scrapie-infected murine hippocampus. *Neuropathol Appl Neurobiol*, **26**, 41-54.

Kadonaga, J.T., Courey, A.J., Ladika, J. and Tjian, R. (1988) Distinct regions of Sp1 modulate DNA binding and transcriptional activation. *Science*, **242**, 1566-1570.

Kadonaga, J.T. and Tjian, R. (1986) Affinity purification of sequence-specific DNA binding proteins. *Proc Natl Acad Sci U S A*, **83**, 5889-5893.

Kanai, Y., Chen, J. and Hirokawa, N. (1992) Microtubule bundling by tau proteins in vivo: analysis of functional domains. *Embo J*, **11**, 3953-3961.

Kang, S.C., Brown, D.R., Whiteman, M., Li, R., Pan, T., Perry, G., Wisniewski, T., Sy, M.S. and Wong, B.S. (2004) Prion protein is ubiquitinated after developing protease resistance in the brains of scrapie-infected mice. *J Pathol*, **203**, 603-608.

Kanning, K.C., Hudson, M., Amieux, P.S., Wiley, J.C., Bothwell, M. and Schecterson, L.C. (2003) Proteolytic processing of the p75 neurotrophin receptor and two homologs generates C-terminal fragments with signaling capability. *J Neurosci*, **23**, 5425-5436.

Kanno, M., Hasegawa, M., Ishida, A., Isono, K. and Taniguchi, M. (1995) mel-18, a Polycomb group-related mammalian gene, encodes a transcriptional negative regulator with tumor suppressive activity. *Embo J*, **14**, 5672-5678.

Karsten, S.L., Sang, T.K., Gehman, L.T., Chatterjee, S., Liu, J., Lawless, G.M., Sengupta, S., Berry, R.W., Pomakian, J., Oh, H.S., Schulz, C., Hui, K.S., Wiedau-Pazos, M., Vinters, H.V., Binder, L.I., Geschwind, D.H. and Jackson, G.R. (2006) A genomic screen for modifiers of tauopathy identifies puromycin-sensitive aminopeptidase as an inhibitor of tau-induced neurodegeneration. *Neuron*, **51**, 549-560.

Kawaguchi, Y., Kovacs, J.J., McLaurin, A., Vance, J.M., Ito, A. and Yao, T.P. (2003) The deacetylase HDAC6 regulates aggresome formation and cell viability in response to misfolded protein stress. *Cell*, **115**, 727-738.

Kawai, J., Shinagawa, A., Shibata, K., Yoshino, M., Itoh, M., Ishii, Y., Arakawa, T., Hara, A., Fukunishi, Y., Konno, H., Adachi, J., Fukuda, S., Aizawa, K., Izawa, M., Nishi, K., Kiyosawa, H., Kondo, S., Yamanaka, I., Saito, T., Okazaki, Y., Gojobori, T., Bono, H., Kasukawa, T., Saito, R., Kadota, K., Matsuda, H., Ashburner, M., Batalov, S., Casavant, T., Fleischmann, W., Gaasterland, T., Gissi, C., King, B., Kochiwa, H., Kuehl, P., Lewis, S., Matsuo, Y., Nikaido, I., Pesole, G., Quackenbush, J., Schriml, L.M., Staubli, F., Suzuki, R., Tomita, M., Wagner, L., Washio, T., Sakai, K., Okido, T., Furuno, M., Aono, H., Baldarelli, R., Barsh, G., Blake, J., Boffelli, D., Bojunga, N., Carninci, P., de Bonaldo, M.F., Brownstein, M.J., Bult, C., Fletcher, C., Fujita, M., Gariboldi, M., Gustincich, S., Hill, D., Hofmann, M., Hume, D.A., Kamiya, M., Lee, N.H., Lyons, P., Marchionni, L., Mashima, J., Mazzarelli, J., Mombaerts, P., Nordone, P., Ring, B., Ringwald, M., Rodriguez, I., Sakamoto, N., Sasaki, H., Sato, K., Schonbach, C., Seya, T., Shibata, Y., Storch, K.F., Suzuki, H., Toyo-oka, K., Wang, K.H., Weitz, C., Whittaker, C., Wilming, L., Wynshaw-Boris, A., Yoshida, K., Hasegawa, Y., Kawaji, H., Kohtsuki, S. and Hayashizaki, Y. (2001) Functional annotation of a full-length mouse cDNA collection. *Nature*, **409**, 685-690.

Kayed, R., Head, E., Thompson, J.L., McIntire, T.M., Milton, S.C., Cotman, C.W. and Glabe, C.G. (2003) Common structure of soluble amyloid oligomers implies common mechanism of pathogenesis. *Science*, **300**, 486-489.

Kempster, S., Collins, M.E., Aronow, B.J., Simmons, M., Green, R.B. and Edington, N. (2004) Clusterin shortens the incubation and alters the histopathology of bovine spongiform encephalopathy in mice. *Neuroreport*, **15**, 1735-1738.

Kennedy, J., Vicari, A.P., Saylor, V., Zurawski, S.M., Copeland, N.G., Gilbert, D.J., Jenkins, N.A. and Zlotnik, A. (2000) A molecular analysis of NKT cells: identification of a class-I restricted T cell-associated molecule (CRTAM). *J Leukoc Biol*, **67**, 725-734.

Kenward, N., Hope, J., Landon, M. and Mayer, R.J. (1994) Expression of polyubiquitin and heat-shock protein 70 genes increases in the later stages of disease progression in scrapie-infected mouse brain. *J Neurochem*, **62**, 1870-1877.

Kenward, N., Landon, M., Laszlo, L. and Mayer, R.J. (1996) Heat shock proteins, molecular chaperones and the prion encephalopathies. *Cell Stress Chaperones*, **1**, 18-22.

Keshet, G.I., Ovadia, H., Taraboulos, A. and Gabizon, R. (1999) Scrapie-infected mice and PrP knockout mice share abnormal localization and activity of neuronal nitric oxide synthase. *J Neurochem*, **72**, 1224-1231.

Kim, C.G., Swendeman, S.L., Barnhart, K.M. and Sheffery, M. (1990) Promoter elements and erythroid cell nuclear factors that regulate alpha-globin gene transcription in vitro. *Mol Cell Biol*, **10**, 5958-5966.

Kim, J.I., Ju, W.K., Choi, J.H., Choi, E., Carp, R.I., Wisniewski, H.M. and Kim, Y.S. (1999) Expression of cytokine genes and increased nuclear factor-kappa B activity in the brains of scrapie-infected mice. *Brain Res Mol Brain Res*, **73**, 17-27.

Kim, S., Lee, J., Park, J. and Chung, J. (2003) BP75, bromodomain-containing M(r) 75,000 protein, binds dishevelled-1 and enhances Wnt signaling by inactivating glycogen synthase kinase-3 beta. *Cancer Res*, **63**, 4792-4795.

Kimberlin, R.H., Cole, S. and Walker, C.A. (1987) Temporary and permanent modifications to a single strain of mouse scrapie on transmission to rats and hamsters. *J Gen Virol*, **68 (Pt 7)**, 1875-1881.

Kimberlin, R.H. and Walker, C. (1977) Characteristics of a short incubation model of scrapie in the golden hamster. *J Gen Virol*, **34**, 295-304.

Kimberlin, R.H. and Walker, C.A. (1978a) Evidence that the transmission of one source of scrapie agent to hamsters involves separation of agent strains from a mixture. *J Gen Virol*, **39**, 487-496.

Kimberlin, R.H. and Walker, C.A. (1978b) Pathogenesis of mouse scrapie: effect of route of inoculation on infectivity titres and dose-response curves. *J Comp Pathol*, **88**, 39-47.

King, C.Y. and Diaz-Avalos, R. (2004) Protein-only transmission of three yeast prion strains. *Nature*, **428**, 319-323.

Kingsbury, D.T., Kasper, K.C., Stites, D.P., Watson, J.D., Hogan, R.N. and Prusiner, S.B. (1983) Genetic control of scrapie and Creutzfeldt-Jakob disease in mice. *J Immunol*, **131**, 491-496.

Klebanoff, S.J. (2005) Myeloperoxidase: friend and foe. *J Leukoc Biol*, **77**, 598-625.

Klohn, P.C., Stoltze, L., Flechsig, E., Enari, M. and Weissmann, C. (2003) A quantitative, highly sensitive cell-based infectivity assay for mouse scrapie prions. *Proc Natl Acad Sci U S A*, **100**, 11666-11671.

Kobe, B. and Deisenhofer, J. (1995) Proteins with leucine-rich repeats. *Curr Opin Struct Biol*, **5**, 409-416.

Kobe, B. and Kajava, A.V. (2001) The leucine-rich repeat as a protein recognition motif. *Curr Opin Struct Biol*, **11**, 725-732.

Kocisko, D.A., Come, J.H., Priola, S.A., Chesebro, B., Raymond, G.J., Lansbury, P.T. and Caughey, B. (1994) Cell-free formation of protease-resistant prion protein. *Nature*, **370**, 471-474.

Koopman, P., Munsterberg, A., Capel, B., Vivian, N. and Lovell-Badge, R. (1990) Expression of a candidate sex-determining gene during mouse testis differentiation. *Nature*, **348**, 450-452.

Kovacs, G.G., Gelpi, E., Strobel, T., Ricken, G., Nyengaard, J.R., Bernheimer, H. and Budka, H. (2007) Involvement of the endosomal-lysosomal system correlates with regional pathology in Creutzfeldt-Jakob disease. *J Neuropathol Exp Neurol*, **66**, 628-636.

Kovacs, G.G., Kurucz, I., Budka, H., Adori, C., Muller, F., Acs, P., Kloppel, S., Schatzl, H.M., Mayer, R.J. and Laszlo, L. (2001) Prominent stress response of Purkinje cells in Creutzfeldt-Jakob disease. *Neurobiol Dis*, **8**, 881-889.

Krebs, D.L., Metcalf, D., Merson, T.D., Voss, A.K., Thomas, T., Zhang, J.G., Rakar, S., O'Bryan M, K., Willson, T.A., Viney, E.M., Mielke, L.A., Nicola, N.A., Hilton, D.J. and Alexander, W.S. (2004) Development of hydrocephalus in mice lacking SOCS7. *Proc Natl Acad Sci U S A*, **101**, 15446-15451.

Kristiansen, M., Messenger, M.J., Klohn, P.C., Brandner, S., Wadsworth, J.D., Collinge, J. and Tabrizi, S.J. (2005) Disease-related prion protein forms aggresomes in neuronal cells leading to caspase activation and apoptosis. *J Biol Chem*, **280**, 38851-38861.

Kuhnlein, R.P., Frommer, G., Friedrich, M., Gonzalez-Gaitan, M., Weber, A., Wagner-Bernholz, J.F., Gehring, W.J., Jackle, H. and Schuh, R. (1994) spalt encodes an evolutionarily conserved zinc finger protein of novel structure which provides homeotic gene function in the head and tail region of the Drosophila embryo. *Embo J*, **13**, 168-179.

Kurten, R.C., Cadena, D.L. and Gill, G.N. (1996) Enhanced degradation of EGF receptors by a sorting nexin, SNX1. *Science*, **272**, 1008-1010.

Kuwahara, C., Takeuchi, A.M., Nishimura, T., Haraguchi, K., Kubosaki, A., Matsumoto, Y., Saeki, K., Matsumoto, Y., Yokoyama, T., Itohara, S. and Onodera, T. (1999) Prions prevent neuronal cell-line death. *Nature*, **400**, 225-226.

Lander, E. and Kruglyak, L. (1995) Genetic dissection of complex traits: guidelines for interpreting and reporting linkage results. *Nat Genet*, **11**, 241-247.

Lander, E.S. and Botstein, D. (1989) Mapping mendelian factors underlying quantitative traits using RFLP linkage maps. *Genetics*, **121**, 185-199.

Laplanche, J.L., Lepage, V., Peoc'h, K., Delasnerie-Laupretre, N. and Charron, D. (2003) HLA in French patients with variant Creutzfeldt-Jakob disease. *Lancet*, **361**, 531-532.

Lasmezas, C.I., Deslys, J.P., Demaimay, R., Adjou, K.T., Lamoury, F., Dormont, D., Robain, O., Ironside, J. and Hauw, J.J. (1996) BSE transmission to macaques. *Nature*, **381**, 743-744.

Laszlo, L., Lowe, J., Self, T., Kenward, N., Landon, M., McBride, T., Farquhar, C., McConnell, I., Brown, J., Hope, J. and et al. (1992) Lysosomes as key organelles in the pathogenesis of prion encephalopathies. *J Pathol*, **166**, 333-341.

Lawson, V.A., Priola, S.A., Wehrly, K. and Chesebro, B. (2001) N-terminal truncation of prion protein affects both formation and conformation of abnormal protease-resistant prion protein generated in vitro. *J Biol Chem*, **276**, 35265-35271.

Lee, G., Neve, R.L. and Kosik, K.S. (1989) The microtubule binding domain of tau protein. *Neuron*, **2**, 1615-1624.

Lee, V.M., Goedert, M. and Trojanowski, J.Q. (2001) Neurodegenerative tauopathies. *Annu Rev Neurosci*, **24**, 1121-1159.

Legare, M.E., Bartlett, F.S., 2nd and Frankel, W.N. (2000) A major effect QTL determined by multiple genes in epileptic EL mice. *Genome Res*, **10**, 42-48.

Legname, G., Baskakov, I.V., Nguyen, H.O., Riesner, D., Cohen, F.E., DeArmond, S.J. and Prusiner, S.B. (2004) Synthetic mammalian prions. *Science*, **305**, 673-676.

Legname, G., Nguyen, H.O., Baskakov, I.V., Cohen, F.E., Dearmond, S.J. and Prusiner, S.B. (2005) Strain-specified characteristics of mouse synthetic prions. *Proc Natl Acad Sci U S A*, **102**, 2168-2173.

Leucht, C., Simoneau, S., Rey, C., Vana, K., Rieger, R., Lasmezas, C.I. and Weiss, S. (2003) The 37 kDa/67 kDa laminin receptor is required for PrP(Sc) propagation in scrapie-infected neuronal cells. *EMBO Rep*, **4**, 290-295.

Levine, M., Rubin, G.M. and Tjian, R. (1984) Human DNA sequences homologous to a protein coding region conserved between homeotic genes of Drosophila. *Cell*, **38**, 667-673.

Li, A. and Harris, D.A. (2005) Mammalian prion protein suppresses Bax-induced cell death in yeast. *J Biol Chem*, **280**, 17430-17434.

Li, Q., Ishikawa, T.O., Miyoshi, H., Oshima, M. and Taketo, M.M. (2005) A targeted mutation of Nkd1 impairs mouse spermatogenesis. *J Biol Chem*, **280**, 2831-2839.

Li, Q.Y., Newbury-Ecob, R.A., Terrett, J.A., Wilson, D.I., Curtis, A.R., Yi, C.H., Gebuhr, T., Bullen, P.J., Robson, S.C., Strachan, T., Bonnet, D., Lyonnet, S., Young, I.D., Raeburn, J.A., Buckler, A.J., Law, D.J. and Brook, J.D. (1997) Holt-Oram syndrome is caused by mutations in TBX5, a member of the Brachyury (T) gene family. *Nat Genet*, **15**, 21-29.

Lian, F. and Cockerell, C.J. (2005) Cutaneous appendage tumors: familial cylindromatosis and associated tumors update. *Adv Dermatol*, **21**, 217-234.

Liao, Y.C., Lebo, R.V., Clawson, G.A. and Smuckler, E.A. (1986) Human prion protein cDNA: molecular cloning, chromosomal mapping, and biological implications. *Science*, **233**, 364-367.

Liebman, S.W. and Derkatch, I.L. (1999) The yeast [PSI+] prion: making sense of nonsense. *J Biol Chem*, **274**, 1181-1184.

Linhoff, M.W., Harton, J.A., Cressman, D.E., Martin, B.K. and Ting, J.P. (2001) Two distinct domains within CIITA mediate self-association: involvement of the GTP-binding and leucine-rich repeat domains. *Mol Cell Biol*, **21**, 3001-3011.

Lints, T.J., Parsons, L.M., Hartley, L., Lyons, I. and Harvey, R.P. (1993) Nkx-2.5: a novel murine homeobox gene expressed in early heart progenitor cells and their myogenic descendants. *Development*, **119**, 419-431.

Liu, H., Farr-Jones, S., Ulyanov, N.B., Llinas, M., Marqusee, S., Groth, D., Cohen, F.E., Prusiner, S.B. and James, T.L. (1999) Solution structure of Syrian hamster prion protein rPrP(90-231). *Biochemistry*, **38**, 5362-5377.

Llewelyn, C.A., Hewitt, P.E., Knight, R.S., Amar, K., Cousens, S., Mackenzie, J. and Will, R.G. (2004) Possible transmission of variant Creutzfeldt-Jakob disease by blood transfusion. *Lancet*, **363**, 417-421.

Lloyd, S.E., Onwuazor, O.N., Beck, J.A., Mallinson, G., Farrall, M., Targonski, P., Collinge, J. and Fisher, E.M. (2001) Identification of multiple quantitative trait loci linked to prion disease incubation period in mice. *Proc Natl Acad Sci U S A*, **98**, 6279-6283.

Lloyd, S.E., Thompson, S.R., Beck, J.A., Linehan, J.M., Wadsworth, J.D., Brandner, S., Collinge, J. and Fisher, E.M. (2004) Identification and characterization of a novel mouse prion gene allele. *Mamm Genome*, **15**, 383-389.

Lloyd, S.E., Uphill, J.B., Targonski, P.V., Fisher, E.M. and Collinge, J. (2002) Identification of genetic loci affecting mouse-adapted bovine spongiform encephalopathy incubation time in mice. *Neurogenetics*, **4**, 77-81.

LoPresti, P., Szuchet, S., Papasozomenos, S.C., Zinkowski, R.P. and Binder, L.I. (1995) Functional implications for the microtubule-associated protein tau: localization in oligodendrocytes. *Proc Natl Acad Sci U S A*, **92**, 10369-10373.

Lu, B., Rutledge, B.J., Gu, L., Fiorillo, J., Lukacs, N.W., Kunkel, S.L., North, R., Gerard, C. and Rollins, B.J. (1998) Abnormalities in monocyte recruitment and cytokine expression in monocyte chemoattractant protein 1-deficient mice. *J Exp Med*, **187**, 601-608.

Mackay, T.F. (2001) Quantitative trait loci in Drosophila. *Nat Rev Genet*, **2**, 11-20.

Madore, N., Smith, K.L., Graham, C.H., Jen, A., Brady, K., Hall, S. and Morris, R. (1999) Functionally different GPI proteins are organized in different domains on the neuronal surface. *Embo J*, **18**, 6917-6926.

Makrinou, E., Collinge, J. and Antoniou, M. (2002) Genomic characterization of the human prion protein (PrP) gene locus. *Mamm Genome*, **13**, 696-703.

Mallucci, G., Dickinson, A., Linehan, J., Klohn, P.C., Brandner, S. and Collinge, J. (2003) Depleting neuronal PrP in prion infection prevents disease and reverses spongiosis. *Science*, **302**, 871-874.

Mallucci, G.R., Ratte, S., Asante, E.A., Linehan, J., Gowland, I., Jefferys, J.G. and Collinge, J. (2002) Post-natal knockout of prion protein alters hippocampal CA1 properties, but does not result in neurodegeneration. *Embo J*, **21**, 202-210.

Malmanger, B., Lawler, M., Coulombe, S., Murray, R., Cooper, S., Polyakov, Y., Belknap, J. and Hitzemann, R. (2006) Further studies on using multiple-cross mapping (MCM) to map quantitative trait loci. *Mamm Genome*, **17**, 1193-1204.

Manenti, G., Galbiati, F., Noci, S. and Dragani, T.A. (2003) Outbred CD-1 mice carry the susceptibility allele at the pulmonary adenoma susceptibility 1 (Pas1) locus. *Carcinogenesis*, **24**, 1143-1148.

Mange, A., Milhavet, O., Umlauf, D., Harris, D. and Lehmann, S. (2002) PrP-dependent cell adhesion in N2a neuroblastoma cells. *FEBS Lett*, **514**, 159-162.

Manolakou, K., Beaton, J., McConnell, I., Farquar, C., Manson, J., Hastie, N.D., Bruce, M. and Jackson, I.J. (2001) Genetic and environmental factors modify bovine spongiform encephalopathy incubation period in mice. *Proc Natl Acad Sci U S A*, **98**, 7402-7407.

Manson, J., West, J.D., Thomson, V., McBride, P., Kaufman, M.H. and Hope, J. (1992) The prion protein gene: a role in mouse embryogenesis? *Development*, **115**, 117-122.

Manson, J.C., Clarke, A.R., Hooper, M.L., Aitchison, L., McConnell, I. and Hope, J. (1994) 129/Ola mice carrying a null mutation in PrP that abolishes mRNA production are developmentally normal. *Mol Neurobiol*, **8**, 121-127.

Manuelidis, L., Fritch, W. and Xi, Y.G. (1997) Evolution of a strain of CJD that induces BSE-like plaques. *Science*, **277**, 94-98.

Manuelidis, L., Tesin, D.M., Sklaviadis, T. and Manuelidis, E.E. (1987) Astrocyte gene expression in Creutzfeldt-Jakob disease. *Proc Natl Acad Sci U S A*, **84**, 5937-5941.

Markel, P., Shu, P., Ebeling, C., Carlson, G.A., Nagle, D.L., Smutko, J.S. and Moore, K.J. (1997) Theoretical and empirical issues for marker-assisted breeding of congenic mouse strains. *Nat Genet*, **17**, 280-284.

Martens, N., Wery, M., Wang, P., Braet, F., Gertler, A., Hooghe, R., Vandenhaute, J. and Hooghe-Peters, E.L. (2004) The suppressor of cytokine signaling (SOCS)-7 interacts with the actin cytoskeleton through vinexin. *Exp Cell Res*, **298**, 239-248.

Martinez-Morales, J.R., Marti, E., Frade, J.M. and Rodriguez-Tebar, A. (1995) Developmentally regulated vitronectin influences cell differentiation, neuron survival and process outgrowth in the developing chicken retina. *Neuroscience*, **68**, 245-253.

Masuda, M., Yageta, M., Fukuhara, H., Kuramochi, M., Maruyama, T., Nomoto, A. and Murakami, Y. (2002) The tumor suppressor protein TSLC1 is involved in cell-cell adhesion. *J Biol Chem*, **277**, 31014-31019.

McCormack, J.E., Baybutt, H.N., Everington, D., Will, R.G., Ironside, J.W. and Manson, J.C. (2002) PRNP contains both intronic and upstream regulatory regions that may influence susceptibility to Creutzfeldt-Jakob Disease. *Gene*, **288**, 139-146.

McKinley, M.P., Bolton, D.C. and Prusiner, S.B. (1983) A protease-resistant protein is a structural component of the scrapie prion. *Cell*, **35**, 57-62.

McKinley, M.P., Taraboulos, A., Kenaga, L., Serban, D., Stieber, A., DeArmond, S.J., Prusiner, S.B. and Gonatas, N. (1991) Ultrastructural localization of scrapie prion proteins in cytoplasmic vesicles of infected cultured cells. *Lab Invest*, **65**, 622-630.

McPeek, M.S. (2000) From mouse to human: fine mapping of quantitative trait loci in a model organism. *Proc Natl Acad Sci U S A*, **97**, 12389-12390.

Mead, S (2006) Prion disease genetics. *Eur J Hum Genet*, **14**, 273-281.

Mead, S., Beck, J., Dickinson, A., Fisher, E.M. and Collinge, J. (2000) Examination of the human prion protein-like gene doppel for genetic susceptibility to sporadic and variant Creutzfeldt-Jakob disease. *Neurosci Lett*, **290**, 117-120.

Mead, S., Mahal, S.P., Beck, J., Campbell, T., Farrall, M., Fisher, E. and Collinge, J. (2001) Sporadic--but not variant--Creutzfeldt-Jakob disease is associated with polymorphisms upstream of PRNP exon 1. *Am J Hum Genet*, **69**, 1225-1235.

Mead, S., Stumpf, M.P., Whitfield, J., Beck, J.A., Poulter, M., Campbell, T., Uphill, J.B., Goldstein, D., Alpers, M., Fisher, E.M. and Collinge, J. (2003) Balancing selection at the prion protein gene consistent with prehistoric kurulike epidemics. *Science*, **300**, 640-643.

Mears, J.A., Sharma, M.R., Gutell, R.R., McCook, A.S., Richardson, P.E., Caulfield, T.R., Agrawal, R.K. and Harvey, S.C. (2006) A structural model for the large subunit of the mammalian mitochondrial ribosome. *J Mol Biol*, **358**, 193-212.

Meyer, R.K., McKinley, M.P., Bowman, K.A., Braunfeld, M.B., Barry, R.A. and Prusiner, S.B. (1986) Separation and properties of cellular and scrapie prion proteins. *Proc Natl Acad Sci U S A*, **83**, 2310-2314.

Milhavet, O., McMahon, H.E., Rachidi, W., Nishida, N., Katamine, S., Mange, A., Arlotto, M., Casanova, D., Riondel, J., Favier, A. and Lehmann, S. (2000) Prion infection impairs the cellular response to oxidative stress. *Proc Natl Acad Sci U S A*, **97**, 13937-13942.

Mitterbauer-Hohendanner, G. and Mannhalter, C. (2004) The biological and clinical significance of MLL abnormalities in haematological malignancies. *Eur J Clin Invest*, **34 Suppl 2**, 12-24.

Miyamoto, Y., Hara, K., Matsumoto, Y. and Hayashi, M. (1998) TATA-less mouse vitronectin gene promoter: characterization of the transcriptional regulatory elements and a nuclear protein binding site on the promoter. *Cell Struct Funct*, **23**, 23-32.

Molnar, A. and Georgopoulos, K. (1994) The Ikaros gene encodes a family of functionally diverse zinc finger DNA-binding proteins. *Mol Cell Biol*, **14**, 8292-8303.

Montgomery, M.K., Xu, S. and Fire, A. (1998) RNA as a target of double-stranded RNA-mediated genetic interference in Caenorhabditis elegans. *Proc Natl Acad Sci U S A*, **95**, 15502-15507.

Moore, R.A., Vorberg, I. and Priola, S.A. (2005) Species barriers in prion diseases--brief review. *Arch Virol Suppl*, 187-202.

Moore, R.C., Hope, J., McBride, P.A., McConnell, I., Selfridge, J., Melton, D.W. and Manson, J.C. (1998) Mice with gene targetted prion protein alterations show that Prnp, Sinc and Prni are congruent. *Nat Genet*, **18**, 118-125.

Moore, R.C., Lee, I.Y., Silverman, G.L., Harrison, P.M., Strome, R., Heinrich, C., Karunaratne, A., Pasternak, S.H., Chishti, M.A., Liang, Y., Mastrangelo, P., Wang, K., Smit, A.F.,

Katamine, S., Carlson, G.A., Cohen, F.E., Prusiner, S.B., Melton, D.W., Tremblay, P., Hood, L.E. and Westaway, D. (1999) Ataxia in prion protein (PrP)-deficient mice is associated with upregulation of the novel PrP-like protein doppel. *J Mol Biol*, **292**, 797-817.

Moore, R.C., Mastrangelo, P., Bouzamondo, E., Heinrich, C., Legname, G., Prusiner, S.B., Hood, L., Westaway, D., DeArmond, S.J. and Tremblay, P. (2001) Doppel-induced cerebellar degeneration in transgenic mice. *Proc Natl Acad Sci U S A*, **98**, 15288-15293.

Moreno, C.R., Lantier, F., Lantier, I., Sarradin, P. and Elsen, J.M. (2003) Detection of new quantitative trait Loci for susceptibility to transmissible spongiform encephalopathies in mice. *Genetics*, **165**, 2085-2091.

Mott, R. and Flint, J. (2002) Simultaneous detection and fine mapping of quantitative trait loci in mice using heterogeneous stocks. *Genetics*, **160**, 1609-1618.

Mott, R., Talbot, C.J., Turri, M.G., Collins, A.C. and Flint, J. (2000) A method for fine mapping quantitative trait loci in outbred animal stocks. *Proc Natl Acad Sci U S A*, **97**, 12649-12654.

Mutai, H., Toyoshima, Y., Sun, W., Hattori, N., Tanaka, S. and Shiota, K. (2000) PAL31, a novel nuclear protein, expressed in the developing brain. *Biochem Biophys Res Commun*, **274**, 427-433.

Nagase, H., Bryson, S., Cordell, H., Kemp, C.J., Fee, F. and Balmain, A. (1995) Distinct genetic loci control development of benign and malignant skin tumours in mice. *Nat Genet*, **10**, 424-429.

Nagase, H., Mao, J.H. and Balmain, A. (1999) A subset of skin tumor modifier loci determines survival time of tumor-bearing mice. *Proc Natl Acad Sci U S A*, **96**, 15032-15037.

Nagata, S. (1997) Apoptosis by death factor. *Cell*, **88**, 355-365.

Nakamura, T., Unda, F., de-Vega, S., Vilaxa, A., Fukumoto, S., Yamada, K.M. and Yamada, Y. (2004) The Kruppel-like factor epiprofin is expressed by epithelium of developing teeth, hair follicles, and limb buds and promotes cell proliferation. *J Biol Chem*, **279**, 626-634.

Nauseef, W.M., Olsson, I. and Arnljots, K. (1988) Biosynthesis and processing of myeloperoxidase--a marker for myeloid cell differentiation. *Eur J Haematol*, **40**, 97-110.

Nguyen, M.D., Lariviere, R.C. and Julien, J.P. (2001) Deregulation of Cdk5 in a mouse model of ALS: toxicity alleviated by perikaryal neurofilament inclusions. *Neuron*, **30**, 135-147.

Niimura, Y. and Nei, M. (2005) Comparative evolutionary analysis of olfactory receptor gene clusters between humans and mice. *Gene*, **346**, 13-21.

Nishinakamura, R., Matsumoto, Y., Nakao, K., Nakamura, K., Sato, A., Copeland, N.G., Gilbert, D.J., Jenkins, N.A., Scully, S., Lacey, D.L., Katsuki, M., Asashima, M. and Yokota, T. (2001) Murine homolog of SALL1 is essential for ureteric bud invasion in kidney development. *Development*, **128**, 3105-3115.

Nixon, R.A. (2005) Endosome function and dysfunction in Alzheimer's disease and other neurodegenerative diseases. *Neurobiol Aging*, **26**, 373-382.

Nobrega, M.A., Ovcharenko, I., Afzal, V. and Rubin, E.M. (2003) Scanning human gene deserts for long-range enhancers. *Science*, **302**, 413.

Oesch, B., Westaway, D., Walchli, M., McKinley, M.P., Kent, S.B., Aebersold, R., Barry, R.A., Tempst, P., Teplow, D.B., Hood, L.E. and et al. (1985) A cellular gene encodes scrapie PrP 27-30 protein. *Cell*, **40**, 735-746.

Ogura, Y., Bonen, D.K., Inohara, N., Nicolae, D.L., Chen, F.F., Ramos, R., Britton, H., Moran, T., Karaliuskas, R., Duerr, R.H., Achkar, J.P., Brant, S.R., Bayless, T.M., Kirschner, B.S., Hanauer, S.B., Nunez, G. and Cho, J.H. (2001a) A frameshift mutation in NOD2 associated with susceptibility to Crohn's disease. *Nature*, **411**, 603-606.

Ogura, Y., Inohara, N., Benito, A., Chen, F.F., Yamaoka, S. and Nunez, G. (2001b) Nod2, a Nod1/Apaf-1 family member that is restricted to monocytes and activates NF-kappaB. *J Biol Chem*, **276**, 4812-4818.

Ohtsuka, K. and Hata, M. (2000) Mammalian HSP40/DNAJ homologs: cloning of novel cDNAs and a proposal for their classification and nomenclature. *Cell Stress Chaperones*, **5**, 98-112.

Orkin, S.H. (1992) GATA-binding transcription factors in hematopoietic cells. *Blood*, **80**, 575-581.

Owen, F., Poulter, M., Collinge, J. and Crow, T.J. (1990) Codon 129 changes in the prion protein gene in Caucasians. *Am J Hum Genet*, **46**, 1215-1216.

Palmer, M.S., Dryden, A.J., Hughes, J.T. and Collinge, J. (1991) Homozygous prion protein genotype predisposes to sporadic Creutzfeldt-Jakob disease. *Nature*, **352**, 340-342.

Pan, K.M., Baldwin, M., Nguyen, J., Gasset, M., Serban, A., Groth, D., Mehlhorn, I., Huang, Z., Fletterick, R.J., Cohen, F.E. and et al. (1993) Conversion of alpha-helices into beta-sheets features in the formation of the scrapie prion proteins. *Proc Natl Acad Sci U S A*, **90**, 10962-10966.

Parchi, P., Castellani, R., Capellari, S., Ghetti, B., Young, K., Chen, S.G., Farlow, M., Dickson, D.W., Sima, A.A., Trojanowski, J.Q., Petersen, R.B. and Gambetti, P. (1996) Molecular basis of phenotypic variability in sporadic Creutzfeldt-Jakob disease. *Ann Neurol*, **39**, 767-778.

Parkinson, N., Ince, P.G., Smith, M.O., Highley, R., Skibinski, G., Andersen, P.M., Morrison, K.E., Pall, H.S., Hardiman, O., Collinge, J., Shaw, P.J. and Fisher, E.M. (2006) ALS phenotypes with mutations in CHMP2B (charged multivesicular body protein 2B). *Neurology*, **67**, 1074-1077.

Pattison, I.H. and Jones, K.M. (1967) The possible nature of the transmissible agent of scrapie. *Vet Rec*, **80**, 2-9.

Peden, A.H., Head. M.W., Ritchie, D.L., Bell, J.E. and Ironside, J.W. (2004) Preclinical vCJD after blood transfusion in a PRNP codon 129 heterozygous patient. *Lancet*, **364**, 527-529.

Peng, C., Zhou, J., Liu, H.Y., Zhou, M., Wang, L.L., Zhang, Q.H., Yang, Y.X., Xiong, W., Shen, S.R., Li, X.L. and Li, G.Y. (2006) The transcriptional regulation role of BRD7 by binding to acetylated histone through bromodomain. *J Cell Biochem*, **97**, 882-892.

Peoc'h, K., Guerin, C., Brandel, J.P., Launay, J.M. and Laplanche, J.L. (2000) First report of polymorphisms in the prion-like protein gene (PRND): implications for human prion diseases. *Neurosci Lett*, **286**, 144-148.

Pepys, M.B., Bybee, A., Booth, D.R., Bishop, M.T., Will, R.G., Little, A.M., Prokupek, B. and Madrigal, J.A. (2003) MHC typing in variant Creutzfeldt-Jakob disease. *Lancet*, **361**, 487-489.

Perry, V.H., Cunningham, C. and Boche, D. (2002) Atypical inflammation in the central nervous system in prion disease. *Curr Opin Neurol*, **15**, 349-354.

Petiot, A., Faure, J., Stenmark, H. and Gruenberg, J. (2003) PI3P signaling regulates receptor sorting but not transport in the endosomal pathway. *J Cell Biol*, **162**, 971-979.

Petroski, M.D. and Deshaies, R.J. (2005) Function and regulation of cullin-RING ubiquitin ligases. *Nat Rev Mol Cell Biol*, **6**, 9-20.

Pevny, L., Lin, C.S., D'Agati, V., Simon, M.C., Orkin, S.H. and Costantini, F. (1995) Development of hematopoietic cells lacking transcription factor GATA-1. *Development*, **121**, 163-172.

Pletcher, M.T., McClurg, P., Batalov, S., Su, A.I., Barnes, S.W., Lagler, E., Korstanje, R., Wang, X., Nusskern, D., Bogue, M.A., Mural, R.J., Paigen, B. and Wiltshire, T. (2004) Use of a dense single nucleotide polymorphism map for in silico mapping in the mouse. *PLoS Biol*, **2**, e393.

Podolin, P.L., Denny, P., Armitage, N., Lord, C.J., Hill, N.J., Levy, E.R., Peterson, L.B., Todd, J.A., Wicker, L.S. and Lyons, P.A. (1998) Localization of two insulin-dependent diabetes (Idd) genes to the Idd10 region on mouse chromosome 3. *Mamm Genome*, **9**, 283-286.

Ponting, C.P. (1996) Novel domains in NADPH oxidase subunits, sorting nexins, and PtdIns 3-kinases: binding partners of SH3 domains? *Protein Sci*, **5**, 2353-2357.

Porsch-Ozcurumez, M., Langmann, T., Heimerl, S., Borsukova, H., Kaminski, W.E., Drobnik, W., Honer, C., Schumacher, C. and Schmitz, G. (2001) The zinc finger protein 202 (ZNF202) is a transcriptional repressor of ATP binding cassette transporter A1 (ABCA1) and ABCG1 gene expression and a modulator of cellular lipid efflux. *J Biol Chem*, **276**, 12427-12433.

Pray, T.R., Parlati, F., Huang, J., Wong, B.R., Payan, D.G., Bennett, M.K., Issakani, S.D., Molineaux, S. and Demo, S.D. (2002) Cell cycle regulatory E3 ubiquitin ligases as anticancer targets. *Drug Resist Updat*, **5**, 249-258.

Preissner, K.T. (1991) Structure and biological role of vitronectin. *Annu Rev Cell Biol*, **7**, 275-310.

Prestridge, D.S. (1995) Predicting Pol II promoter sequences using transcription factor binding sites. *J Mol Biol*, **249**, 923-932.

Prusiner, S.B. (1982) Novel proteinaceous infectious particles cause scrapie. *Science*, **216**, 136-144.

Prusiner, S.B. (1989) Scrapie prions. *Annu Rev Microbiol*, **43**, 345-374.

Prusiner, S.B. (1991) Molecular biology of prion diseases. *Science*, **252**, 1515-1522.

Prusiner, S.B. (1997) Prion diseases and the BSE crisis. *Science*, **278**, 245-251.

Prusiner, S.B. (1998) Prions. *Proc Natl Acad Sci U S A*, **95**, 13363-13383.

Prusiner, S.B., Bolton, D.C., Groth, D.F., Bowman, K.A., Cochran, S.P. and McKinley, M.P. (1982) Further purification and characterization of scrapie prions. *Biochemistry*, **21**, 6942-6950.

Prusiner, S.B., Scott, M., Foster, D., Pan, K.M., Groth, D., Mirenda, C., Torchia, M., Yang, S.L., Serban, D., Carlson, G.A. and et al. (1990) Transgenetic studies implicate interactions between homologous PrP isoforms in scrapie prion replication. *Cell*, **63**, 673-686.

Puckett, C., Concannon, P., Casey, C. and Hood, L. (1991) Genomic structure of the human prion protein gene. *Am J Hum Genet*, **49**, 320-329.

Race, R.E., Graham, K., Ernst, D., Caughey, B. and Chesebro, B. (1990) Analysis of linkage between scrapie incubation period and the prion protein gene in mice. *J Gen Virol*, **71 (Pt 2)**, 493-497.

Rane, N.S., Yonkovich, J.L. and Hegde, R.S. (2004) Protection from cytosolic prion protein toxicity by modulation of protein translocation. *Embo J*, **23**, 4550-4559.

Reynolds, W.F., Rhees, J., Maciejewski, D., Paladino, T., Sieburg, H., Maki, R.A. and Masliah, E. (1999) Myeloperoxidase polymorphism is associated with gender specific risk for Alzheimer's disease. *Exp Neurol*, **155**, 31-41.

Rieger, R., Edenhofer, F., Lasmezas, C.I. and Weiss, S. (1997) The human 37-kDa laminin receptor precursor interacts with the prion protein in eukaryotic cells. *Nat Med*, **3**, 1383-1388.

Riek, R., Hornemann, S., Wider, G., Billeter, M., Glockshuber, R. and Wuthrich, K. (1996) NMR structure of the mouse prion protein domain PrP(121-321). *Nature*, **382**, 180-182.

Riek, R., Wider, G., Billeter, M., Hornemann, S., Glockshuber, R. and Wuthrich, K. (1998) Prion protein NMR structure and familial human spongiform encephalopathies. *Proc Natl Acad Sci U S A*, **95**, 11667-11672.

Rikke, B.A. and Johnson, T.E. (1998) Towards the cloning of genes underlying murine QTLs. *Mamm Genome*, **9**, 963-968.

Rollins, B.J., Morrison, E.D. and Stiles, C.D. (1988) Cloning and expression of JE, a gene inducible by platelet-derived growth factor and whose product has cytokine-like properties. *Proc Natl Acad Sci U S A*, **85**, 3738-3742.

Rosenfeld, M.G. (1991) POU-domain transcription factors: pou-er-ful developmental regulators. *Genes Dev*, **5**, 897-907.

Roucou, X., Guo, Q., Zhang, Y., Goodyer, C.G. and LeBlanc, A.C. (2003) Cytosolic prion protein is not toxic and protects against Bax-mediated cell death in human primary neurons. *J Biol Chem*, **278**, 40877-40881.

Rozen, S. and Skaletsky, H. (2000) Primer3 on the WWW for general users and for biologist programmers. *Methods Mol Biol*, **132**, 365-386.

Rudd, P.M., Wormald, M.R., Wing, D.R., Prusiner, S.B. and Dwek, R.A. (2001) Prion glycoprotein: structure, dynamics, and roles for the sugars. *Biochemistry*, **40**, 3759-3766.

Saborio, G.P., Permanne, B. and Soto, C. (2001) Sensitive detection of pathological prion protein by cyclic amplification of protein misfolding. *Nature*, **411**, 810-813.

Safar, J., Wille, H., Itri, V., Groth, D., Serban, H., Torchia, M., Cohen, F.E. and Prusiner, S.B. (1998) Eight prion strains have PrP(Sc) molecules with different conformations. *Nat Med*, **4**, 1157-1165.

Sailer, A., Bueler, H., Fischer, M., Aguzzi, A. and Weissmann, C. (1994) No propagation of prions in mice devoid of PrP. *Cell*, **77**, 967-968.

Sakaguchi, S., Katamine, S., Nishida, N., Moriuchi, R., Shigematsu, K., Sugimoto, T., Nakatani, A., Kataoka, Y., Houtani, T., Shirabe, S., Okada, H., Hasegawa, S., Miyamoto, T. and Noda, T. (1996) Loss of cerebellar Purkinje cells in aged mice homozygous for a disrupted PrP gene. *Nature*, **380**, 528-531.

Salmona, M., Capobianco, R., Colombo, L., De Luigi, A., Rossi, G., Mangieri, M., Giaccone, G., Quaglio, E., Chiesa, R., Donati, M.B., Tagliavini, F. and Forloni, G. (2005) Role of plasminogen in propagation of scrapie. *J Virol*, **79**, 11225-11230.

Sarge, K.D., Murphy, S.P. and Morimoto, R.I. (1993) Activation of heat shock gene transcription by heat shock factor 1 involves oligomerization, acquisition of DNA-binding activity, and nuclear localization and can occur in the absence of stress. *Mol Cell Biol*, **13**, 1392-1407.

Sasaki, K., Doh-ura, K., Ironside, J., Mabbott, N. and Iwaki, T. (2006) Clusterin expression in follicular dendritic cells associated with prion protein accumulation. *J Pathol*, **209**, 484-491.

Sayre, L.M., Zelasko, D.A., Harris, P.L., Perry, G., Salomon, R.G. and Smith, M.A. (1997) 4-Hydroxynonenal-derived advanced lipid peroxidation end products are increased in Alzheimer's disease. *J Neurochem*, **68**, 2092-2097.

Schmitt-Ulms, G., Legname, G., Baldwin, M.A., Ball, H.L., Bradon, N., Bosque, P.J., Crossin, K.L., Edelman, G.M., DeArmond, S.J., Cohen, F.E. and Prusiner, S.B. (2001) Binding of neural cell adhesion molecules (N-CAMs) to the cellular prion protein. *J Mol Biol*, **314**, 1209-1225.

Schroder, B., Franz, B., Hempfling, P., Selbert, M., Jurgens, T., Kretzschmar, H.A., Bodemer, M., Poser, S. and Zerr, I. (2001) Polymorphisms within the prion-like protein gene (Prnd) and their implications in human prion diseases, Alzheimer's disease and other neurological disorders. *Hum Genet*, **109**, 319-325.

Schultz, J., Schwarz, A., Neidhold, S., Burwinkel, M., Riemer, C., Simon, D., Kopf, M., Otto, M. and Baier, M. (2004) Role of interleukin-1 in prion disease-associated astrocyte activation. *Am J Pathol*, **165**, 671-678.

Scohy, S., Gabant, P., Van Reeth, T., Hertveldt, V., Dreze, P.L., Van Vooren, P., Riviere, M., Szpirer, J. and Szpirer, C. (2000) Identification of KLF13 and KLF14 (SP6), novel members of the SP/XKLF transcription factor family. *Genomics*, **70**, 93-101.

Scohy, S., Van Vooren, P., Szpirer, C. and Szpirer, J. (1998) Assignment1 of Sp genes to rat chromosome bands 7q36 (Sp1), 10q31-->q32.1 (Sp2), 3q24-->q31 (Sp3) and 6q33 (Sp4) and of the SP2 gene to human chromosome bands 17q21.3-->q22 by in situ hybridization. *Cytogenet Cell Genet*, **81**, 273-274.

Scott, M.P., Tamkun, J.W. and Hartzell, G.W., 3rd. (1989) The structure and function of the homeodomain. *Biochim Biophys Acta*, **989**, 25-48.

Seiffert, D., Curriden, S.A., Jenne, D., Binder, B.R. and Loskutoff, D.J. (1996) Differential regulation of vitronectin in mice and humans in vitro. *J Biol Chem*, **271**, 5474-5480.

Seiffert, D., Iruela-Arispe, M.L., Sage, E.H. and Loskutoff, D.J. (1995) Distribution of vitronectin mRNA during murine development. *Dev Dyn*, **203**, 71-79.

Sengupta, S., Horowitz, P.M., Karsten, S.L., Jackson, G.R., Geschwind, D.H., Fu, Y., Berry, R.W. and Binder, L.I. (2006) Degradation of tau protein by puromycin-sensitive aminopeptidase in vitro. *Biochemistry*, **45**, 15111-15119.

Shibuya, S., Higuchi, J., Shin, R.W., Tateishi, J. and Kitamoto, T. (1998) Codon 219 Lys allele of PRNP is not found in sporadic Creutzfeldt-Jakob disease. *Ann Neurol*, **43**, 826-828.

Shifman, S., Bell, J.T., Copley, R.R., Taylor, M.S., Williams, R.W., Mott, R. and Flint, J. (2006) A high-resolution single nucleotide polymorphism genetic map of the mouse genome. *PLoS Biol*, **4**, e395.

Shyng, S.L., Huber, M.T. and Harris, D.A. (1993) A prion protein cycles between the cell surface and an endocytic compartment in cultured neuroblastoma cells. *J Biol Chem*, **268**, 15922-15928.

Silver, L. (1995) Mouse Genetics. *Oxford University Press.*

Skibinski, G., Parkinson, N.J., Brown, J.M., Chakrabarti, L., Lloyd, S.L., Hummerich, H., Nielsen, J.E., Hodges, J.R., Spillantini, M.G., Thusgaard, T., Brandner, S., Brun, A., Rossor, M.N., Gade, A., Johannsen, P., Sorensen, S.A., Gydesen, S., Fisher, E.M. and Collinge, J. (2005) Mutations in the endosomal ESCRTIII-complex subunit CHMP2B in frontotemporal dementia. *Nat Genet*, **37**, 806-808.

Skinner, P.J., Abbassi, H., Chesebro, B., Race, R.E., Reilly, C. and Haase, A.T. (2006) Gene expression alterations in brains of mice infected with three strains of scrapie. *BMC Genomics*, **7**, 114.

Smit, A., Hubley, R. and Green, P. (1996-2004) RepeatMasker Open-3.0. *http://www.repeatmasker.org*.

Smith, J. (1999) T-box genes:what they do and how they do it. *Trends Genet*, **15**, 154-158.

Smith, M.A., Hirai, K., Hsiao, K., Pappolla, M.A., Harris, P.L., Siedlak, S.L., Tabaton, M. and Perry, G. (1998) Amyloid-beta deposition in Alzheimer transgenic mice is associated with oxidative stress. *J Neurochem*, **70**, 2212-2215.

Smith, P.D., Crocker, S.J., Jackson-Lewis, V., Jordan-Sciutto, K.L., Hayley, S., Mount, M.P., O'Hare, M.J., Callaghan, S., Slack, R.S., Przedborski, S., Anisman, H. and Park, D.S. (2003) Cyclin-dependent kinase 5 is a mediator of dopaminergic neuron loss in a mouse model of Parkinson's disease. *Proc Natl Acad Sci U S A*, **100**, 13650-13655.

Solberg, L.C., Valdar, W., Gauguier, D., Nunez, G., Taylor, A., Burnett, S., Arboledas-Hita, C., Hernandez-Pliego, P., Davidson, S., Burns, P., Bhattacharya, S., Hough, T., Higgs, D., Klenerman, P., Cookson, W.O., Zhang, Y., Deacon, R.M., Rawlins, J.N., Mott, R. and Flint, J. (2006) A protocol for high-throughput phenotyping, suitable for quantitative trait analysis in mice. *Mamm Genome*, **17**, 129-146.

Sparkes, R.S., Simon, M., Cohn, V.H., Fournier, R.E., Lem, J., Klisak, I., Heinzmann, C., Blatt, C., Lucero, M., Mohandas, T. and et al. (1986) Assignment of the human and mouse prion protein genes to homologous chromosomes. *Proc Natl Acad Sci U S A*, **83**, 7358-7362.

Specht, C.G. and Schoepfer, R. (2001) Deletion of the alpha-synuclein locus in a subpopulation of C57BL/6J inbred mice. *BMC Neurosci*, **2**, 11.

Spillantini, M.G., Schmidt, M.L., Lee, V.M., Trojanowski, J.Q., Jakes, R. and Goedert, M. (1997) Alpha-synuclein in Lewy bodies. *Nature*, **388**, 839-840.

Stahl, N., Baldwin, M.A., Teplow, D.B., Hood, L., Gibson, B.W., Burlingame, A.L. and Prusiner, S.B. (1993) Structural studies of the scrapie prion protein using mass spectrometry and amino acid sequencing. *Biochemistry*, **32**, 1991-2002.

Stahl, N., Borchelt, D.R., Hsiao, K. and Prusiner, S.B. (1987) Scrapie prion protein contains a phosphatidylinositol glycolipid. *Cell*, **51**, 229-240.

Stahl, N. and Prusiner, S.B. (1991) Prions and prion proteins. *Faseb J*, **5**, 2799-2807.

Steinert, P.M., Rice, R.H., Roop, D.R., Trus, B.L. and Steven, A.C. (1983) Complete amino acid sequence of a mouse epidermal keratin subunit and implications for the structure of intermediate filaments. *Nature*, **302**, 794-800.

Steinmetz, L.M., Sinha, H., Richards, D.R., Spiegelman, J.I., Oefner, P.J., McCusker, J.H. and Davis, R.W. (2002) Dissecting the architecture of a quantitative trait locus in yeast. *Nature*, **416**, 326-330.

Stene, M.C., Frikke-Schmidt, R., Nordestgaard, B.G., Steffensen, R., Schnohr, P. and Tybjaerg-Hansen, A. (2006) Zinc Finger Protein 202: a new candidate gene for ischemic heart disease: The Copenhagen City Heart Study. *Atherosclerosis*, **188**, 43-50.

Stephenson, D.A., Chiotti, K., Ebeling, C., Groth, D., DeArmond, S.J., Prusiner, S.B. and Carlson, G.A. (2000) Quantitative trait loci affecting prion incubation time in mice. *Genomics*, **69**, 47-53.

Strittmatter, W.J., Weisgraber, K.H., Huang, D.Y., Dong, L.M., Salvesen, G.S., Pericak-Vance, M., Schmechel, D., Saunders, A.M., Goldgaber, D. and Roses, A.D. (1993) Binding of human apolipoprotein E to synthetic amyloid beta peptide: isoform-specific effects and implications for late-onset Alzheimer disease. *Proc Natl Acad Sci U S A*, **90**, 8098-8102.

Strober, W., Murray, P.J., Kitani, A. and Watanabe, T. (2006) Signalling pathways and molecular interactions of NOD1 and NOD2. *Nat Rev Immunol*, **6**, 9-20.

Sturm, R.A. and Herr, W. (1988) The POU domain is a bipartite DNA-binding structure. *Nature*, **336**, 601-604.

Stylianou, I.M., Christians, J.K., Keightley, P.D., Bunger, L., Clinton, M., Bulfield, G. and Horvat, S. (2004) Genetic complexity of an obesity QTL (Fob3) revealed by detailed genetic mapping. *Mamm Genome*, **15**, 472-481.

Sunyach, C., Jen, A., Deng, J., Fitzgerald, K.T., Frobert, Y., Grassi, J., McCaffrey, M.W. and Morris, R. (2003) The mechanism of internalization of glycosylphosphatidylinositol-anchored prion protein. *Embo J*, **22**, 3591-3601.

Suske, G., Bruford, E. and Philipsen, S. (2005) Mammalian SP/KLF transcription factors: bring in the family. *Genomics*, **85**, 551-556.

Talbot, C.J., Nicod, A., Cherny, S.S., Fulker, D.W., Collins, A.C. and Flint, J. (1999) High-resolution mapping of quantitative trait loci in outbred mice. *Nat Genet*, **21**, 305-308.

Talbot, C.J., Radcliffe, R.A., Fullerton, J., Hitzemann, R., Wehner, J.M. and Flint, J. (2003) Fine scale mapping of a genetic locus for conditioned fear. *Mamm Genome*, **14**, 223-230.

Tanabe, T., Chamaillard, M., Ogura, Y., Zhu, L., Qiu, S., Masumoto, J., Ghosh, P., Moran, A., Predergast, M.M., Tromp, G., Williams, C.J., Inohara, N. and Nunez, G. (2004) Regulatory regions and critical residues of NOD2 involved in muramyl dipeptide recognition. *Embo J*, **23**, 1587-1597.

Tanaka, M., Chien, P., Naber, N., Cooke, R. and Weissman, J.S. (2004) Conformational variations in an infectious protein determine prion strain differences. *Nature*, **428**, 323-328.

Tateishi, J., Brown, P., Kitamoto, T., Hoque, Z.M., Roos, R., Wollman, R., Cervenakova, L. and Gajdusek, D.C. (1995) First experimental transmission of fatal familial insomnia. *Nature*, **376**, 434-435.

Tatzelt, J., Voellmy, R. and Welch, W.J. (1998) Abnormalities in stress proteins in prion diseases. *Cell Mol Neurobiol*, **18**, 721-729.

Taylor, K.L. and Wickner, R.B. (2001) [URE3] and [PSI]: prions of Saccharomyces cerevisiae. *Contrib Microbiol*, **7**, 21-31.

Telling, G.C., Parchi, P., DeArmond, S.J., Cortelli, P., Montagna, P., Gabizon, R., Mastrianni, J., Lugaresi, E., Gambetti, P. and Prusiner, S.B. (1996) Evidence for the conformation of the pathologic isoform of the prion protein enciphering and propagating prion diversity. *Science*, **274**, 2079-2082.

Teuscher, C., Butterfield, R.J., Ma, R.Z., Zachary, J.F., Doerge, R.W. and Blankenhorn, E.P. (1999) Sequence polymorphisms in the chemokines Scya1 (TCA-3), Scya2 (monocyte chemoattractant protein (MCP)-1), and Scya12 (MCP-5) are candidates for eae7, a locus controlling susceptibility to monophasic remitting/nonrelapsing experimental allergic encephalomyelitis. *J Immunol*, **163**, 2262-2266.

Thackray, A.M., Hopkins, L., Klein, M.A. and Bujdoso, R. (2007) Mouse-adapted ovine scrapie prion strains are characterized by different conformers of PrPSc. *J Virol*, **81**, 12119-12127.

Thackray, A.M., McKenzie, A.N., Klein, M.A., Lauder, A. and Bujdoso, R. (2004) Accelerated prion disease in the absence of interleukin-10. *J Virol*, **78**, 13697-13707.

Trompouki, E., Hatzivassiliou, E., Tsichritzis, T., Farmer, H., Ashworth, A. and Mosialos, G. (2003) CYLD is a deubiquitinating enzyme that negatively regulates NF-kappaB activation by TNFR family members. *Nature*, **424**, 793-796.

Tuzi, N.L., Gall, E., Melton, D. and Manson, J.C. (2002) Expression of doppel in the CNS of mice does not modulate transmissible spongiform encephalopathy disease. *J Gen Virol*, **83**, 705-711.

Valdar, W., Flint, J. and Mott, R. (2006a) Simulating the collaborative cross: power of quantitative trait loci detection and mapping resolution in large sets of recombinant inbred strains of mice. *Genetics*, **172**, 1783-1797.

Valdar, W., Solberg, L.C., Gauguier, D., Burnett, S., Klenerman, P., Cookson, W.O., Taylor, M.S., Rawlins, J.N., Mott, R. and Flint, J. (2006b) Genome-wide genetic association of complex traits in heterogeneous stock mice. *Nat Genet*, **38**, 879-887.

Valdar, W.S., Flint, J. and Mott, R. (2003) QTL fine-mapping with recombinant-inbred heterogeneous stocks and in vitro heterogeneous stocks. *Mamm Genome*, **14**, 830-838.

Vey, M., Pilkuhn, S., Wille, H., Nixon, R., DeArmond, S.J., Smart, E.J., Anderson, R.G., Taraboulos, A. and Prusiner, S.B. (1996) Subcellular colocalization of the cellular and scrapie prion proteins in caveolae-like membranous domains. *Proc Natl Acad Sci U S A*, **93**, 14945-14949.

Viles, J.H., Cohen, F.E., Prusiner, S.B., Goodin, D.B., Wright, P.E. and Dyson, H.J. (1999) Copper binding to the prion protein: structural implications of four identical cooperative binding sites. *Proc Natl Acad Sci U S A*, **96**, 2042-2047.

Wade, C.M. and Daly, M.J. (2005) Genetic variation in laboratory mice. *Nat Genet*, **37**, 1175-1180.

Wade, C.M., Kulbokas, E.J., 3rd, Kirby, A.W., Zody, M.C., Mullikin, J.C., Lander, E.S., Lindblad-Toh, K. and Daly, M.J. (2002) The mosaic structure of variation in the laboratory mouse genome. *Nature*, **420**, 574-578.

Wang, X., Korstanje, R., Higgins, D. and Paigen, B. (2004) Haplotype analysis in multiple crosses to identify a QTL gene. *Genome Res*, **14**, 1767-1772.

Wang, X., Le Roy, I., Nicodeme, E., Li, R., Wagner, R., Petros, C., Churchill, G.A., Harris, S., Darvasi, A., Kirilovsky, J., Roubertoux, P.L. and Paigen, B. (2003) Using advanced intercross lines for high-resolution mapping of HDL cholesterol quantitative trait loci. *Genome Res*, **13**, 1654-1664.

Warming, S., Rachel, R.A., Jenkins, N.A. and Copeland, N.G. (2006) Zfp423 is required for normal cerebellar development. *Mol Cell Biol*, **26**, 6913-6922.

Watanabe, T., Kitani, A. and Strober, W. (2005) NOD2 regulation of Toll-like receptor responses and the pathogenesis of Crohn's disease. *Gut*, **54**, 1515-1518.

Watson, P.A., Krupinski, J., Kempinski, A.M. and Frankenfield, C.D. (1994) Molecular cloning and characterization of the type VII isoform of mammalian adenylyl cyclase expressed widely in mouse tissues and in S49 mouse lymphoma cells. *J Biol Chem*, **269**, 28893-28898.

Way, G., Morrice, N., Smythe, C. and O'Sullivan, A.J. (2002) Purification and identification of secernin, a novel cytosolic protein that regulates exocytosis in mast cells. *Mol Biol Cell*, **13**, 3344-3354.

Weissman, A.M. (2001) Themes and variations on ubiquitylation. *Nat Rev Mol Cell Biol*, **2**, 169-178.

Weissmann, C. (1999) Molecular genetics of transmissible spongiform encephalopathies. *J Biol Chem*, **274**, 3-6.

Westaway, D., Cooper, C., Turner, S., Da Costa, M., Carlson, G.A. and Prusiner, S.B. (1994) Structure and polymorphism of the mouse prion protein gene. *Proc Natl Acad Sci U S A*, **91**, 6418-6422.

Westaway, D., Goodman, P.A., Mirenda, C.A., McKinley, M.P., Carlson, G.A. and Prusiner, S.B. (1987) Distinct prion proteins in short and long scrapie incubation period mice. *Cell*, **51**, 651-662.

Westaway, D., Mirenda, C.A., Foster, D., Zebarjadian, Y., Scott, M., Torchia, M., Yang, S.L., Serban, H., DeArmond, S.J., Ebeling, C. and et al. (1991) Paradoxical shortening of scrapie incubation times by expression of prion protein transgenes derived from long incubation period mice. *Neuron*, **7**, 59-68.

Westaway, D. and Prusiner, S.B. (1986) Conservation of the cellular gene encoding the scrapie prion protein. *Nucleic Acids Res*, **14**, 2035-2044.

Wharton, K.A., Jr., Zimmermann, G., Rousset, R. and Scott, M.P. (2001) Vertebrate proteins related to Drosophila Naked Cuticle bind Dishevelled and antagonize Wnt signaling. *Dev Biol*, **234**, 93-106.

Wickner, R.B. (1994) [URE3] as an altered URE2 protein: evidence for a prion analog in Saccharomyces cerevisiae. *Science*, **264**, 566-569.

Wilesmith, J.W., Wells, G.A., Cranwell, M.P. and Ryan, J.B. (1988) Bovine spongiform encephalopathy: epidemiological studies. *Vet Rec*, **123**, 638-644.

Will, R.G., Ironside, J.W., Zeidler, M., Cousens, S.N., Estibeiro, K., Alperovitch, A., Poser, S., Pocchiari, M., Hofman, A. and Smith, P.G. (1996) A new variant of Creutzfeldt-Jakob disease in the UK. *Lancet*, **347**, 921-925.

Williams, A.E., Lawson, L.J., Perry, V.H. and Fraser, H. (1994) Characterization of the microglial response in murine scrapie. *Neuropathol Appl Neurobiol*, **20**, 47-55.

Wiltshire, T., Pletcher, M.T., Batalov, S., Barnes, S.W., Tarantino, L.M., Cooke, M.P., Wu, H., Smylie, K., Santrosyan, A., Copeland, N.G., Jenkins, N.A., Kalush, F., Mural, R.J., Glynne, R.J., Kay, S.A., Adams, M.D. and Fletcher, C.F. (2003) Genome-wide single-nucleotide polymorphism analysis defines haplotype patterns in mouse. *Proc Natl Acad Sci U S A*, **100**, 3380-3385.

Windl, O., Dempster, M., Estibeiro, J.P., Lathe, R., de Silva, R., Esmonde, T., Will, R., Springbett, A., Campbell, T.A., Sidle, K.C., Palmer, M.S. and Collinge, J. (1996) Genetic basis of Creutzfeldt-Jakob disease in the United Kingdom: a systematic analysis of predisposing mutations and allelic variation in the PRNP gene. *Hum Genet*, **98**, 259-264.

Wong, B.S., Pan, T., Liu, T., Li, R., Petersen, R.B., Jones, I.M., Gambetti, P., Brown, D.R. and Sy, M.S. (2000) Prion disease: A loss of antioxidant function? *Biochem Biophys Res Commun*, **275**, 249-252.

Wopfner, F., Weidenhofer, G., Schneider, R., von Brunn, A., Gilch, S., Schwarz, T.F., Werner, T. and Schatzl, H.M. (1999) Analysis of 27 mammalian and 9 avian PrPs reveals high conservation of flexible regions of the prion protein. *J Mol Biol*, **289**, 1163-1178.

Worby, C.A. and Dixon, J.E. (2002) Sorting out the cellular functions of sorting nexins. *Nat Rev Mol Cell Biol*, **3**, 919-931.

Wroe, S.J., Pal, S., Siddique, D., Hyare, H., Macfarlane, R., Joiner, S., Linehan, J.M., Brandner, S., Wadsworth, J.D., Hewitt, P. and Collinge, J. (2006) Clinical presentation and pre-mortem diagnosis of variant Creutzfeldt-Jakob disease associated with blood transfusion: a case report. *Lancet*, **368**, 2061-2067.

Wyatt, J.M., Pearson, G.R., Smerdon, T.N., Gruffydd-Jones, T.J., Wells, G.A. and Wilesmith, J.W. (1991) Naturally occurring scrapie-like spongiform encephalopathy in five domestic cats. *Vet Rec*, **129**, 233-236.

Xiong, M. and Guo, S.W. (1997) Fine-scale mapping of quantitative trait loci using historical recombinations. *Genetics*, **145**, 1201-1218.

Yalcin, B., Flint, J. and Mott, R. (2005) Using progenitor strain information to identify quantitative trait nucleotides in outbred mice. *Genetics*, **171**, 673-681.

Yalcin, B., Fullerton, J., Miller, S., Keays, D.A., Brady, S., Bhomra, A., Jefferson, A., Volpi, E., Copley, R.R., Flint, J. and Mott, R. (2004a) Unexpected complexity in the haplotypes of commonly used inbred strains of laboratory mice. *Proc Natl Acad Sci U S A*, **101**, 9734-9739.

Yalcin, B., Willis-Owen, S.A., Fullerton, J., Meesaq, A., Deacon, R.M., Rawlins, J.N., Copley, R.R., Morris, A.P., Flint, J. and Mott, R. (2004b) Genetic dissection of a behavioral quantitative trait locus shows that Rgs2 modulates anxiety in mice. *Nat Genet*, **36**, 1197-1202.

Yamada, S., Aiba, T., Endo, Y., Hara, M., Kitamoto, T. and Tateishi, J. (1994) Creutzfeldt-Jakob disease transmitted by a cadaveric dura mater graft. *Neurosurgery*, **34**, 740-743; discussion 743-744.

Yan, S.D., Chen, X., Schmidt, A.M., Brett, J., Godman, G., Zou, Y.S., Scott, C.W., Caputo, C., Frappier, T., Smith, M.A. and et al. (1994) Glycated tau protein in Alzheimer disease: a mechanism for induction of oxidant stress. *Proc Natl Acad Sci U S A*, **91**, 7787-7791.

Yang, H., Bell, T.A., Churchill, G.A. and Pardo-Manuel de Villena, F. (2007) On the subspecific origin of the laboratory mouse. *Nat Genet*.

Yang, X., Chang, H.Y. and Baltimore, D. (1998) Essential role of CED-4 oligomerization in CED-3 activation and apoptosis. *Science*, **281**, 1355-1357.

Zahn, R., Liu, A., Luhrs, T., Riek, R., von Schroetter, C., Lopez Garcia, F., Billeter, M., Calzolai, L., Wider, G. and Wuthrich, K. (2000) NMR solution structure of the human prion protein. *Proc Natl Acad Sci U S A*, **97**, 145-150.

Zappia, M., Manna, I., Serra, P., Cittadella, R., Andreoli, V., La Russa, A., Annesi, F., Spadafora, P., Romeo, N., Nicoletti, G., Messina, D., Gambardella, A. and Quattrone, A. (2004) Increased risk for Alzheimer disease with the interaction of MPO and A2M polymorphisms. *Arch Neurol*, **61**, 341-344.

Zeidler, M., Johnstone, E.C., Bamber, R.W., Dickens, C.M., Fisher, C.J., Francis, A.F., Goldbeck, R., Higgo, R., Johnson-Sabine, E.C., Lodge, G.J., McGarry, P., Mitchell, S.,

Tarlo, L., Turner, M., Ryley, P. and Will, R.G. (1997a) New variant Creutzfeldt-Jakob disease: psychiatric features. *Lancet*, **350**, 908-910.

Zeidler, M., Stewart, G., Cousens, S.N., Estibeiro, K. and Will, R.G. (1997b) Codon 129 genotype and new variant CJD. *Lancet*, **350**, 668.

Zhang, W.X. and Yang, S.Y. (2000) Cloning and characterization of a new member of the T-box gene family. *Genomics*, **70**, 41-48.

Ziemin-van der Poel, S., McCabe, N.R., Gill, H.J., Espinosa, R., III, Patel, Y., Harden, A., Rubinelli, P., Smith, S.D., LeBeau, M.M., Rowley, J.D. and et al. (1991) Identification of a gene, MLL, that spans the breakpoint in 11q23 translocations associated with human leukemias. *Proc Natl Acad Sci U S A*, **88**, 10735-10739.

Zlotnik, I. and Rennie, J.C. (1963) Further observations on the experimental transmission of scrapie from sheep and goats to laboratory mice. *J Comp Pathol*, **73**, 150-162.

10
Appendices

Appendix 1 Genotyping Primers

Appendix 1.1 Chromosome 11

Marker	Forward Primer	Reverse Primer	Amp (bp)	Dye
D11Mit260	cactttgcctttatactatatggtgg	catttgtttagttctcagcacca	95	TET
D11Mit5	ttctgtgagcctggaggagt	tacaggactagtttccatttggg	203	TET
D11Mit278	aggtcctcccagatcctctc	tatcaaccactccaggacagg	114	FAM
D11Mit90	tctccagccccttcattatg	tgccaaacacccatgagac	150	FAM
D11Mit320	cccatatagtgaagcaagaaacg	ttatagtgtatgcatccaggtgtg	119	TET
D11Mit194	tagtgtctctatagacatcagtggtcc	atggcaatttaagccactgg	130	HEX
D11Mit40	agccaggaatacttagtcagaacc	tcctgccctgcttgattc	207	HEX
D11Mit36	ccagaacttttgctgcttcc	gtgagccctaggtccagtga	232	HEX
D11Mit326	ctatggcaggcacatgactg	ttaaaagtggtttcaggtgtgtatg	94	TET
D11Mit41	ctgctaaagtggggttaaatgc	cgactgagcaagttgtatttctg	134	HEX
D11Mit212	ctctggtctctctgtatacatgtgc	agcaactggggcatttaatg	146	TET
D11Mit179	tttggcattcacatgtaggtc	ttgctttataatctttctctgtgtg	165	FAM
D11Mit70	ggaagtagctatggaggtggc	tctgacccagagctcaaataca	142	FAM
D11Mit288	agcatgaatttaaaaggcctg	ggctgctagttttcctgatg	124	TET
D11Mit289	ctttggttggttttaaatgttttaa	aaggagaaagcagattcatacaca	122	FAM
D11Mit263	gaaaccattttaaaatatacagttcgg	ccagggttaggtaggtatggc	147	HEX
D11Mit54	aggctggtggctagtgtcc	aagtcttgcgctgcatcttt	144	TET
D11Mit67	aaaaaaaaaaagttcaaggctgg	ggaactcaactcctagaacttctg	134	FAM
D11Mit145	gctagtacttgggctggacg	gctctactcctccctgcctt	150	HEX
D11Mit124	ccgggatgagagacctaaca	ctgtggggtgtggaagactt	117	HEX
D11Mit132	ggtcagaggacaatcttacatgc	gttccaagacaatgagagaccc	117	TET
D11Mit99	ctgtaggtaaaatacacttgccg	ggtggacagacccttctgaa	122	FAM

Appendix 1.2 Chromosome 8

Marker	Forward Primer	Reverse Primer	Amp (bp)	Dye
D8Mit104	gaaagcaaacttctaaaggattatatg	tgcaaattctcaaactgataccc	143	FAM
D8Mit236	cctcacttcaccagcactca	ctccagaacctgagtgtgacc	118	HEX
D8Mit105	tggcaaaattccttctgacc	caagcatatttttaaatgaacctaca	122-127	HEX
D8Mit45	gaacaggaccaataaaatgaaagc	ctaccttaccaaacttcccgg	121	TET
D8Mit57	cccaaatctagcaggttcca	acagctatgctgcttactggc	163	TET
D8Mit81	ccaggcgccaaaagtaactt	acatggctgtaatatgtgctgc	136	FAM
D8Mit197	cagaccaaaaagaaactactaatcca	aaagttgccaaatgattgtgg	116	FAM
D8Mit267	cttgaccataaagagaaaaaaatgc	gaggtacatggtatatttgcctacg	107	HEX
D8Mit109	agccccctgttttgttttg	ccgtaggcatctacccacat	133	TET
D8Mit164	taactgcaaagagggtagtgagc	tcctgtctccacagacatgtg	144	FAM
D8Mit183	tctcaaataactatcaactcttagggg	tctttgaactggctataatcactca	149	FAM
D8Mit85	tagtggatggatatgcattcatg	aacaccctctggcatctttg	123	FAM
D8Mit211	cagaacactgtcctgaaaagtcc	tacccacaaacctgtatttaaattaa	149	TET

Appendix 1.3 Chromosome 9

Marker	Forward Primer	Reverse Primer	Amp (bp)	Dye
D9Mit88	cattatgcaccccagttcct	acatgtgtaagtgaagatgtgtcg	202-203	TET
D9Mit297	tgcctctctcatctctttaaaca	atttgtctctctgtctttgctca	97-104	HEX
D9Mit247	ttttaatggagagggtgaggg	aaggagaccctgggtcagag	149	FAM
D9Mit327	ggtgtctcatgagaagacacatg	cgatcttacgccctcttcag	125	FAM
D9Mit285	caaatacattgctgattatatcagaga	ggactctagatctcatcaggga	125	HEX
D9Mit286	caaaatgtcatattcttgtgtttgg	gtcttcttttacaaatttcccagc	108	HEX
D9Mit191	gtaagtatgcctgcggagga	cagaagaccgcttttcaagg	146	FAM
D9Mit97	tctcactactgcctgccaga	tagatttctcaggcaaggaagc	151	FAM
D9Mit4	tgctgagcaagctatgagga	gacagcccatcacagctaca	122	FAM
D9Mit141	aaccttcacacacatgctatgg	atttaattttcacagcaatttctgc	105	HEX
D9Mit102	gatctgcttgcttaccatgtagg	atgttcttgtgcagcagtgtg	142-144	TET

Appendix 2 PCR/Sequencing Primers

Appendix 2.1 Chromosome 11

Vitronectin (*Vtn*)				
Region	**Forward Primer**	**Reverse Primer**	**Amp (bp)**	**Ta/Cycles**
5'	gctcagagggtgacaacaca	gcccttgcatgactctatgg	496	60/40
Ex1	gctcagagggtgacaacaca	gcccttgcatgactctatgg	496	60/40
Ex2	gtttctctggctgaccaagg	taggaaggctgtcggcttta	473	60/40
Ex3a	tccctcccatagagtcatgc	ggtcccttgatcagtggtgt	464	60/40
Ex3b	ggagcccaagaacaatacca	ctcaatgccccagacatctt	440	60/40
Ex4	agtggagcaacaggaggaga	tgaagccttcggagatgttt	599	60/40
Ex5	tctgtccctcaatcggttct	ggcagagaggaatcatggaat	284	62/42
Ex6	acaatgttgatgcagcgttc	cgatggtgtcacagttccag	429	62/40
Ex7a	cagacaaccttgctggagaa	tctcctcgctggagaacaaa	322	62/40
Ex7b	gaagtctaagcgtagaagc	gtgaacatccaccaagcaga	343	62/40
Ex8	tgcttggtggatgttcactt	tctgtccctcaatcggttct	390	60/40

Myeloperoxidase (*Mpo*)				
Region	**Forward Primer**	**Reverse Primer**	**Amp (bp)**	**Ta/Cycles**
Pro a	cagctctgggtccttctctg	agatggacctatcccaagact	490	64/40
Pro b	ttctcagctttagctccctga	caattctcctcctcccaagc	429	60/40
Ex1	tgttacggatggttgtgagc	agagctgcccagagcataaa	364	60/40
Ex2	ggactaagggattgggggta	ggtgagcaggcagaaagaac	498	62/42
Ex3	catccaggtccatgtccttt	cccatgtgagagggtcactt	450	60/40
Ex4	catgggtccacctaagacca	gacgccatcttcatactctgc	592	60/40
Ex5	gtgtcaagtggctgtgccta	gttgaggccagtgaagaagg	559	60/40
Ex6	cctggagtcaatcgcaatg	tgctgagggagccaagtatt	484	60/40
Ex7	ggggccagagttctcttctg	ctccatccaactcgttaccaa	559	60/40
Ex8	gtgcctaaggtctgctccag	tcgctcctttgagcctttta	497	60/40
Ex9	tgaggtgagttctatttatgtcctt	cgtaggggtcagagagaagc	612	60/40
Ex10	ctctgacccctacgattcca	cttccagatcgtgggatgat	477	60/40
Ex11	gcctgagccaatcatttagg	agatggttcagtgggcaaag	364	60/40
Ex12	gacctgagctctcctgtgct	gcactcacaagtgaatgtcca	500	60/40
Ex13	gttggcagaaacaaggtggt	tgcaccccagaacaatcata	351	60/40

Nerve Growth Factor Receptor (*Ngfr*)				
Region	**Forward Primer**	**Reverse Primer**	**Amp (bp)**	**Ta/Cycles**
Pro	tcggaataagggctaggtaggc	tgcgcgctgagctgagctgc	431	58/42
5'	aaccggaggtgccctgggta	cgttgccagcatctgggacc	564	60/40
Ex1	aaccggaggtgccctgggta	cgttgccagcatctgggacc	564	60/40
Ex2	cccaggtggttctaatagaaagt	tggtacctgtacagaggttggc	353	60/40
Ex3	acatgcccgtgctcaaacacc	gcctaggcccttacgacctc	527	60/40
Ex4	ggaggctcatgatgaagccct	caggtcaaggtcggagcaaac	392	60/40
Ex5	cctcagtcggcagcacagct	ctaccctggtacctgccggt	302	60/40
Ex6	aacacggaagtgagggctcag	agaggccctacacagagatgct	506	60/40
3'a	gaagctgctcaatggtgaca	gtccatggctctggttcatt	599	60/40
3'b	accatctcaggcctttcctt	tgttgggtggcctaggttag	329	60/40
3'c	gctgcacccagaaaacagtg	ctgagatctgggagcaaagg	895	62/40
3'd	cctgttctgttttgcttgct	ctgagatctgggagcaaagg	709	62/40

Cyclin Dependent Kinase 5 Regulatory Associated Protein 3 (*Cdk5rap3*)				
Region	**Forward Primer**	**Reverse Primer**	**Amp (bp)**	**Ta/Cycles**
Pro	cccagtcgtccaacaagaat	cccagtcgtccaacaagaat	635	65/40
Ex1	gagcgtggtcttggattggct	aggacttgaggaggcaggaca	219	65/40
Ex2	tcaagtcctcccgtcctctgt	cggagccagtacagactttcc	342	62/40
Ex3	gtatgtggcacttgaaccagt	aggactctcagaattccacct	385	65/40
Ex4	gaatcgcagatgctggttgg	gttcaccagtgagactgcag	279	60/40
Ex5	gcagccttctctgcaggttt	tcagctggctgtttcagagc	201	60/40
Ex6	atgctagggcatctgtgtgc	aactgagaaagaagcccgcc	337	60/40
Ex7	atctcccaccatgtgtgacc	ggcgtgccatgtgggataat	270	60/40
Ex8	gtgttggtaactcgtggacc	tatgggaagtcaggtcaggg	309	52/40
Ex9	aggcaaactcctctccctct	ctggccttacaactgggaac	248	62/40
Ex10	ttcagggcctctagtctgct	cactgtagctacagatgccc	230	62/40
Ex11	agggctgagaagagtctgtc	gggtactgaaatcagtccgg	250	60/40
Ex12	cctctggactctagctcttc	gccatgtacacaggaaggag	409	65/40
Ex13	gggaattagcttcctgagcc	ggtttctcggtctgtggaag	309	62/40
Ex14	cttccacagaccgagaaacc	ttcctcatggctctgtctcc	256	62/40
3'a	cttccacagaccgagaaacc	ttcctcatggctctgtctcc	256	62/40
3'b	acagcccaggctgatgctact	gctcaaggcctccttggatca	287	62/40

Glial Fibrillary Acidic Protein (*Gfap*)				
Region	**Forward Primer**	**Reverse Primer**	**Amp (bp)**	**Ta/Cycles**
Prox	ctggatctggaactcgccaat	gtggaggagtcattcgagaca	568	65/40
Ex1a	ccttgactctgggtacagtga	cctggtagacatcagccagtt	529	65/40
Ex1b	tgtctcgaatgactcctccac	aaatgcaggagctgagaggct	461	65/40
Ex2	ctccgttgcttacttctgcca	ttgtgggaatcttggcagcac	303	65/40
Ex3	gtgctgccaagattcccacaa	cagttggttcctctatcctcc	284	65/40
Ex4	cgtgtctagcagacagaagtg	atgcctacatggtcctaggca	396	65/40
Ex5	ctgactgaggtcggttttcca	agatcccgtctgtcttagcct	370	65/40
Ex6	aggctaagacagacgggatct	aactcaaggccttagtcctgg	505	65/40
Ex8	cctagctagctagccccatat	cacaccaccagtgaaagacct	322	65/40
3'a	cccaaggctcaatcagtgcta	agtacaccttccctctccact	464	65/40
3b	aatggccactaaggcagtcct	agggtaagatgactgagcgga	478	65/40
3'c	aatggcagaggcactggtaga	ccaccaatcagcctcagagaa	465	65/40
3'd	actagctgttgctctccaagc	aaggtggatttgacaggcagc	467	64/42

Microtubule-Associated Protein Tau (*Mapt*)				
Region	**Forward Primer**	**Reverse Primer**	**Amp (bp)**	**Ta/Cycles**
Pro a	cgtagctggaaggagaactaa	ggagcattcaaacccattagg	247	64/40
Pro b	cttcgctagggtcacagtcaa	ttttcagttcaccctcgctgg	307	64/40
5'	aggcctcgctgcccgcccct	gggtggcaggaggacggcgc	297	62/40
Ex2	ctgaggctctcctactgtga	tgcctgacagagtccagatg	599	50/40
Ex3	ccctgtctcacccacattct	gttgagccaggcatagaagc	484	60/40
Ex4	agctggcttttcttgcatgt	gaggcagtcagactccaagg	303	60/40
Ex5	gtacagagagcatgggttgca	tcaaggtagagcccactgagt	214	62/40
Ex6	accaggctgctctgagtgac	aatggcaggaggtaggtgttg	451	60/40
Ex 7	ctcagcatctgtctccacca	tccaaagaggtaggggacct	571	60/40
Ex8	gcctcagggactttgcagacg	gggagcaagtctggctaggtg	407	65/40
Ex9	cagctctgtcctcctgttcc	acgggttgctctccctactt	481	60/40
Ex10	tggtccatcagcctttgtgct	ggttggcctattctaggaagc	244	58/42
Ex11a	tggtgggtgatacctgacct	ccccacacacacaccataaa	467	60/40
Ex11b	gagccagtggggatgtctta	gcctttgatcttctgccttg	649	52/40
Ex13	gaacgaacgaacgaacgaat	agccacaaaagcaggttagg	482	60/40
Ex14a	ttggttctcttgaaggctgctc	cccacatcccagaataccacc	300	64/40
Ex14b	ctctggcacttctgtagtggg	acccctagtgtagacgagatatt	241	52/40
Ex14c	cctgagtgccatgcctctccc	gctgcctccagctcaacacaag	263	62/42
Ex14d	ctcctaggcctgactccttg	actggggtgtggagactgatt	203	62/42
Ex14e	gccacacttctcccatcttt	atgtcccagcaggttagcac	472	58/40

Monocyte Chemoattractant Protein 1 (*Mcp-1*)				
Region	**Forward Primer**	**Reverse Primer**	**Amp (bp)**	**Ta/Cycles**
Pro	attctccggcccatgagagaa	tgaattggccgctgcaagctt	284	62/40
5'a	cacttatccagggtgatgcta	gtacctgaccatgtgagacta	348	62/40
5'b	cacttatccagggtgatgcta	ccaacccaagcctctgtttga	550	65/40
Ex1a	cacttatccagggtgatgcta	gtacctgaccatgtgagacta	348	62/40
Ex1b	cacttatccagggtgatgcta	ccaacccaagcctctgtttga	550	65/40
Ex2	catcctgctgaaactgccttc	ggatctgagtgtgtgactgac	310	65/40
Ex3a	ccctttctactccacaagctt	agggaaaaatggatccacacc	531	62/40
Ex3b	agcattgtctctatggctgct	aatctggattcacagagaggg	576	62/40
3'	ccctttctactccacaagctt	agggaaaaatggatccacacc	531	62/40

Sp2 Transcription Factor (*Sp2*)				
Region	**Forward Primer**	**Reverse Primer**	**Amp (bp)**	**Ta/Cycles**
Ex2	tggaaaagcagcaacagaggc	aagtgaatctccctgggtgtc	319	58/40
Ex3	actccacctatgctgattcgg	ctagtgtcggcagggataaca	123	64/40
Ex4a	aagctgctgagaagagaggct	cttggatctgagggacttggt	415	64/40
Ex4b	cctggagggcagtttgtgttt	ggaggctcttcttcctagctt	439	64/40
Ex4c	cgctcaacaacctggtgaaca	ctgacgatgatctgcctcagt	498	58/40
Ex5	gtgcacaagtgtgttcttggg	gctcaggattcccatatgctg	502	64/40
Ex6	aggctccatgagtcttcctca	tgaggggttgggttcagagta	409	64/40
Ex7	agaggtaatatgcccgaccct	ctgggtagtgtggatggtgaa	415	64/40
Ex8	tgcagagacaaggccaagttg	ctcctcgacggagtgaaatgt	529	64/40
3'a	gactctgttcctgtgttctcc	ctcggcgtctgacctttcata	431	64/40
3'b	tcaattaagtcctcctgggcc	gaaggtgttctcaggtgagtc	441	64/40
3'c	tcctctctttgctagacgcct	tcagcccagtactgaccaaca	417	64/40

Transacting Transcription Factor 6 (*Sp6*)				
Region	**Forward Primer**	**Reverse Primer**	**Amp (bp)**	**Ta/Cycles**
Pro	ccaggtccagagctataatcc	cacccatcaagcaggagagaa	462	65/40
5'a	gataggacttggcagcatcct	cactccaaagacttcccagag	332	58/40
5'b	tctagtcctcacccagagtca	ggcaactcatagccctgtgaa	393	65/40
Ex1a	gcaatgctaaccgctgtctgt	atcctcccaaagcaggctaa	466	58/40
Ex1b	ccggacatgtcacaccactat	acgctgcatccagactggaat	337	58/40
Ex1c	atacgtcggagaccatcagct	gccttcagatgcgacgtctta	357	58/40
Ex1d	gatgggggcaagaagaagcat	tcatgtgtttggccaggtggt	265	64/40
Ex1e	ccttcgtgtgcaactggcttt	ttcaagcagcctcccatgtag	444	64/40
3'a	aaaggcaaacgtgaggccgaa	ccaaggtgcttttatgtccgg	434	64/40
3'b	agtagagagatggcatgtccc	tggatccctcctctatgccat	400	64/40
3'c	ttaaggggctgtctacctagc	gctgtaatccctctgctagga	430	64/40
3'd	aagagctagccgctcctttca	tcccagaattccttccagtgg	381	64/40
3'e	cccatcccttgctttcctgtt	agaaggttctgggtggagaga	395	64/40
3'f	ggcactctcaggtttgaggta	tattcctacccagatcccagc	358	65/40
3'g	gcagggaatagctgtgtgttg	ttcacaggaggtggggaaaga	477	58/40
3'h	ttgtgtagaaaggcctcctcc	gggttcaaggcctctataagg	376	58/40
3'i	aaaaccagccacctctcactg	gtgacgcttgaccaaagatcc	376	65/40

Secernin 2 (*Scrn2*)				
Region	**Forward Primer**	**Reverse Primer**	**Amp (bp)**	**Ta/Cycles**
Ex1	tgacattgcaggtgtcctgtg	aaagctggctccaagaatccc	257	65/40
Ex2	tcaggcttctcagagtgcaca	gactggaactccgtactcgtt	392	65/40
Ex3	aaagtggctgacaaagggtcc	aagactgcagccgccttagaa	379	65/40
Ex4a	ataccatcatggctgctgggt	aatggtagcctccagaagtgg	371	65/40
Ex4b	ttgctgtgctacgtgggcttt	ccaaggctgtcaggaagaaca	373	65/40
Ex5	cctgtgtggttaggaggtctt	agggactcagcaaacgtgagt	503	65/40
Ex6	ctctttgactttgcggaggtc	gaagtaaccaggaacaggtgc	429	65/40
Ex7	atcccacaaagccctgtgtcc	cagccctttctggtcccaga	394	65/40
Ex8	accttcagctagtcttgggag	ttgtggcttggcactacaggt	459	65/40
3'	accttcagctagtcttgggag	ttgtggcttggcactacaggt	459	65/40

Leucine Rich Repeat Containing 46 (*Lrrc46*)				
Region	**Forward Primer**	**Reverse Primer**	**Amp (bp)**	**Ta/Cycles**
5'	tgatagggccgctatgcgcat	tttggaaacccgaccgacctc	438	58/42
Ex1	tgatagggccgctatgcgcat	tttggaaacccgaccgacctc	438	58/42
Ex2a	tgaacccaaggcgacaaaagg	agtcagtacagctcagcaacc	215	65/40
Ex2b	gagttgacagaacagttgggc	agcaacctggacgtcactgtt	273	64/40
Ex3	cctttccttgagtgagacacg	gcaaggatgagctgttcagct	317	64/40
Ex4	gctgagcataaccatggtggt	ccaagccagttctagtggtgt	226	65/40
Ex5	acacagggagcctaggtactt	agaaggagcttggagccaaga	289	65/40
Ex6	tcttggctccaagctccttct	tgtgaggtgctggatatggga	296	64/40
Ex7	agggatgggcactaaagcaca	ggacggtgtcagtgagattct	308	65/40
Ex8a	cgggaggtttacccaaggata	ttggaggttgtggctgctaga	374	65/40
Ex8b	ccctaaagctacctcctcaac	cggctgccttctggttttgat	295	65/40
3'	ccctaaagctacctcctcaac	cggctgccttctggttttgat	295	65/40

Mitochondrial Ribosomal Protein L10 (*Mrpl10*)				
Region	**Forward Primer**	**Reverse Primer**	**Amp (bp)**	**Ta/Cycles**
5'	actgctgccccacaatcctta	gctgtcgacggtcagagatta	222	65/40
Ex1	actgctgccccacaatcctta	gctgtcgacggtcagagatta	222	65/40
Ex2	tgtgccatgcctaactctgtg	cacacacactctgtctctcag	392	65/40
Ex3	acacctggcatcactgaccat	acccacagtttaggctcttgg	367	65/40
Ex4	ggtacagcctgtgactaaggt	aggtgttgagtggcagtcagt	335	65/40
Ex5	gcacacgtgtgaccctgaatt	ccactccccactccaaattct	454	65/40
3'a	tgtccagctgacttccctgtt	actgggaaaacagcatggggt	453	65/40
3'b	ttgttccaactagggacccga	ttctttccacagcccagcaca	383	65/40
3'c	gcccattgtccttggtttcac	cagccccgtaagcacagtttt	516	65/40
3'd	gcctgagttctggataaggtc	aagatcaggagttcagggctg	582	65/40

T-box 21 (*Tbx21*)				
Region	**Forward Primer**	**Reverse Primer**	**Amp (bp)**	**Ta/Cycles**
5'a	gcgaattcgcgctgtattagc	agaaacgatgctgttggtccg	406	65/40
5'b	gggcttcagtcctcaccaaaa	ggctcgggatagaagaaacga	440	65/40
Ex1a	cccgctccagtgaagtttcat	cttggaccacaacaggtggtt	553	65/40
Ex1b	cggaccaacagcatcgtttct	actcagcaacctgcagcttca	552	65/40
Ex1c	tcgtttcttctatcccgagcc	agaggaaagtcgttgttccgg	486	62/40
Ex2	gctacagcttgacacatgcac	gtggataggctgtagggttca	347	65/40
Ex3a	tctcacggtccactcagaaga	caccttttgtctagtctggtgc	446	65/40
Ex3b	ctgtcctctcccttgcatctt	gagacgagactccaacagtac	315	62/40
Ex4	gagtgcatctagagatgaggc	cagggcatgttgagcactgaa	480	65/40
Ex5	gagtgcatctagagatgaggc	cagggcatgttgagcactgaa	480	65/40
Ex6a	gggtctggggaccatcatatt	atcatatccttgggctggcct	459	64/40
Ex6b	gggaattgaactcaggacctc	agccagtaaggctgtgagatc	279	65/40
Ex6c	tggacccaactgtcaactgct	tagtgtctccttcgcctagtc	452	65/40
Ex6d	tcaatacccgcccaagatgag	gcttcctctccaaccaatcac	402	65/40
3'a	gactaggcgaaggagacacta	aagttactgactggacagggg	510	65/40
3'b	gataaggaaaccgaaggccag	agtccctctgggtccaaaact	338	62/40
3'c	ggttccatggagaacggagaa	catgaaccatcagctggagtg	526	65/40
3'd	actacagtcacgaacctggtg	catccagacaccactctctac	448	64/40
3'e	agagaagactcaggtgactgc	ccctaagtggggtcactttag	384	64/40

TBK1 Binding Protein 1 (*Tbkbp1*)				
Region	**Forward Primer**	**Reverse Primer**	**Amp (bp)**	**Ta/Cycles**
5'	ttcctgaactctgggatcctg	aggagagacctgtggacagat	247	65/40
Ex1	ggttcctcagaccagcatgga	attggctgcaggagcagagct	475	65/40
Ex2	tttggagtggtgggtcccatt	gaagctgatttagggaaggcg	352	65/40
Ex3	attgggaatagggttggggag	cacacactcatcgggttggaa	292	65/40
Ex4	tgctccagtctggagagtgat	aggtgcccagtcacactgaaa	367	65/40
Ex5	ctgcccataccggtttcactt	ccaagagctaggaagagaggt	539	65/40
Ex6	ctgcccataccggtttcactt	ccaagagctaggaagagaggt	539	65/40
Ex7	tgaacgctgtatggccgaaca	gagggcttacaatggcaatgc	304	65/40
Ex8	gacgctggccgagcgtgtcta	gaggtgcgaccccagagagag	484	65/40
Ex9	ctccttgataggagtcctagg	cccacgagattcatgcagcat	294	62/40

Karyopherin (Importin) Beta 1 (*Kpnb1*)				
Region	**Forward Primer**	**Reverse Primer**	**Amp (bp)**	**Ta/Cycles**
5'	ccggtgaatgggcttgtggtg	cacgcaccagattctccacgg	349	62/40
Ex1	ccggtgaatgggcttgtggtg	cacgcaccagattctccacgg	349	62/40
Ex3a	tcaatgttgagtctaggcagg	ggtctcagaaatctgtcatgc	439	64/40
Ex3b	cccagtttcctgagatacctt	caaacacccatttccacacca	459	64/40
Ex4	gaagtggttgttggtgggtga	gctcccagtcttgtgatagag	381	64/40
Ex5	gtaggctctcttcagtagctg	ggagatgagcacattctgacc	336	62/40
Ex6	gatgcctttcttgtggagtct	ccctaaatctccaaatggctg	214	62/40
Ex7a	cgttactcagaggtgccttta	gccttaacacccatactcaag	312	62/40
Ex7b	ggggcagactgaatatacaag	tggtgtgaaacactgtctcac	403	62/40
Ex8	ttttagaggcagggtttctcc	taagggaatctggtaagccga	367	62/40
Ex9	agcgaacacaaccctggcatt	acactcaggcacaactcagtg	320	64/40
Ex0	agcaaagcttacgtagtgcca	tattacatgtgcgcactctcc	322	64/40
Ex11	ggggccagggattgttactat	agtacagttccctctggcttc	548	62/40
Ex12	tcttaaactggcgtggtggtg	ttcctttctgtggtcccagtg	396	64/40
Ex13	aatgtctctgaactgcatccc	aaacctccactgctgatgtca	384	64/40
Ex14a	agtgcttttgcccttgaccat	gtgtggccatgaatctgtaac	523	64/40
Ex14b	gctcggaggtttaatcaccat	ggttaaggattcgagaaggct	443	64/40
Ex15a	gcagctgtttgcatgtgtctt	caggaatgagaccggagtatt	414	62/40
Ex15b	cagtgaccagatcccaattct	tagaatgcttgctcactgacc	200	64/40
Ex16a	ccagcagttaggctaacatga	tctactctgtgacagagcatg	352	62/40
Ex16b	ccatttgaatgcctcccctat	atgattctgaggtgtgggatg	302	62/40
Ex17a	ctcatcttgactctggttcac	tagcagatagtgctcgaggaa	302	62/40
Ex17b	caccagggaaggatgctttat	atagtgctcgaggaacctaca	334	62/40
Ex18a	ttcctcgagcactatctgcta	aaaacctcggtcatattggcc	461	62/40
Ex18b	ctctatccagcagtaactcaa	atccaccatgtcaaagtctga	353	62/40
Ex19	cctgatgcgctttaaagacca	tgtagcaggtactagttcacc	315	62/40
Ex20a	tctttccattggggtagagtg	aagctatgtcccagtatagcc	329	62/40
Ex20b	tgtttagttggctgcccagta	agaagagctatatggtagccc	323	62/40
Ex21	atcacactcagtgagctacag	caaaataccagtaggcagcga	400	62/40
3'a	gggctacttggttgtaggagt	ttctagccttccctgggaaga	375	62/40
3'b	gagtgtgcacggatgctgaat	gccttctcaagggcacataga	421	62/40
3'c	ccctgctactgaggagaaaga	accatagtacaggaaaggcgc	395	62/40
3'd	agttctggctactgatgcagc	ggcattccgactgccacaata	346	62/40
3'e	gctgtgaatgtagctatgggg	gagaccaataccgcattgcag	400	62/40
3'f	ggccttctgtccctttctttg	caagagggccagcttactgaa	361	58/40
3'g	aatggtgtcagatggtgaccc	gagctactacagacgctgcat	430	64/40

Region	Forward Primer	Reverse Primer	Amp (bp)	Ta/Cycles
3'h	gcttcctggtagtgtggaaga	ccctgttccaaccctatctag	420	64/40
3'i	aagctctctaggagtccaagc	agaccacaatccaatcagccc	383	64/40
3'j	ccgatctgatctgtgaaccag	agaacagcaaggcaccaagac	346	62/40
3'k	acccatttctgtcctgtgtgg	cagatgccacttgtggcaaac	486	62/40
3'l	gcattctgtccactcactgtc	gcatgccaagggcattctgaa	442	64/40
3'm	caccctgagtcttggcacatt	atgccttcacagactggcatg	426	62/40
3'n	cttagggactggagaagtgga	atcctcctcagtttgccagca	414	64/40
3'o	tcagaggcaactgtgatcctg	ccaaaccacacctcactgaca	374	62/40

Mitochondrial Ribosomal Protein L45 (*Mrpl45*)				
Region	Forward Primer	Reverse Primer	Amp (bp)	Ta/Cycles
Ex1	cagagggaagcacttttcg	tagaggggatcgcatacacc	598	58/40
Ex2	ccaaatcacctatacgctaac	acccgctaagtcatatctcc	344	58/40
Ex3	agtccaccttgtatgaccac	ttgcatgttcttctcagccc	230	62/40
Ex4	cctgaggttgaactcaggct	ggtggcacacgtgcttaatc	255	58/40
Ex5	aacaccatctgcaggcttggt	caaccacatggtggctcacaa	259	62/40
Ex6	cacttcctgttggttgcagca	gcttagatctcaccggtgctt	325	58/40
Ex7	aaattcctctgacgggccaga	gtggagcctaagaagagcgtt	304	50/40
Ex8	gacatcctgggtaaacagtag	agacagggtttctctgtgtag	308	58/40
3'a	cagaggcaggtggatttctgt	aaagctgtgggtctgatgcca	413	64/40
3'b	tcagctagcctgatggcgtta	ccaaatgctgactcggcctat	527	62/40
3'c	gccttggagcatcttctgttt	cagacagaacactcaggcata	460	62/40
3'd	agagtgtctacaaactagggc	atcctcttctggtgtgtctga	371	58/40
3'e	ctgcaagagcaacaggtattc	gtggggaagctaaagaccaat	490	58/40
3'f	ttcttacccactgagccatct	agagaaactctgtctgtggca	346	64/40

AK030625 clone (*AK*)				
Region	Forward Primer	Reverse Primer	Amp (bp)	Ta/Cycles
Pro	ggaactcactctgtagaccag	ccagagagagatgaatccagg	412	65/40
Ex1a	catggtactagtgacagggtg	gttgagaaagttggcagcctg	479	65/40
Ex1b	ttcaacggctgtcaggagcaa	gccctcatgacattccaggaa	515	65/40
Ex1c	caaggtacaggaagagactcc	atggtctctgcatagtgcagg	330	65/40
Ex2	gcctctgtgctaatgtgtgca	aagaggaatcctggagtgctg	472	65/40

Aminopeptidase Puromycin Sensitive (*Npepps*)				
Region	**Forward Primer**	**Reverse Primer**	**Amp (bp)**	**Ta/Cycles**
Ex1	cctcgccgcgatgccggaga	gggcgcggcctaactgctcg	199	62/40
Ex2	gtgcatgaaacattagcccag	tacaggaatgtatcagcgtgc	311	58/40
Ex3	cctaactgtggcagttgagat	gagcggcttacatggattctt	426	52/40
Ex4	tgaatgtagtgtcttgagggc	ggacacatagtgagacctatg	285	52/40
Ex5	catgaaacaacctctgagatt	tctcctacttaatcaagagag	199	52/40
Ex6	gcctataggtttttgcctagt	accgaaccagtaactgatgat	372	52/40
Ex7	gcagctctcctttgtgggttt	gccactcaactgtgaacagag	401	62/40
Ex8	gcagctctcctttgtgggttt	gccactcaactgtgaacagag	401	62/40
Ex9	gtcaccaggcagcacactaa	ttgctctggatgcaactcac	574	62/42
Ex10	cagtaatgcagtgactattcc	aaatcagtcacccaaaggaag	341	52/40
Ex11	gagttagaagggttttcctag	agcttcccattcttaccacaa	353	52/40
Ex12	ggatgcatgcttttcagcata	tgaatgcagacagtgtactca	257	50/40
Ex13a	gtaagccatgcaatgttaaaa	ttatctccttcaaagtacaga	450	54/40
Ex13b	gagcctctgtatgatggacc	aactgtctggctaggtagcc	525	62/40
Ex14	aatttgtactgcttccctgcc	agtgcacatagtcagagccac	375	62/40
Ex15	tcttggttacagcgtggcagt	ccacaaagacataggagtaag	313	58/40
Ex16a	cagaacagccagggttacata	acaggaaggaccatatccttc	330	58/40
Ex16b	cctgtctcacgaaaagtaagg	acaggaaggaccatatccttc	302	50/40
Ex17	ttgctagcagtagataatgcc	ctattaccttctccaggtttg	320	58/40
Ex18	ccgtagacttggtatcacagt	cctgagtactgggattaaagg	305	62/40
Ex19	gtacaacagtaggcctttgcc	gctctcctccacctctaagta	246	62/40
Ex20	ccacctcagtggaagagaagc	cccaagctcagagatcctcct	304	62/40
Ex21	gcgcagttttccaacagtctg	ggaaggttgggaaccaatggt	331	62/40
Ex22	gggtaagtggaagtttctgtc	gggtatcaagcaagtatggag	360	62/40
Ex23	tgatgagtcagttagtccaca	actggtgtaagactccagatt	353	52/40
3'a	attcaccagtacctccttcag	attctgcacaggctccactat	531	62/42
3'b	tgacaagccgggtatgtccat	gttttgagcagaaggcctagc	469	58/40
3'c	gaaccctgacatgcataagag	tcctgtaattctgaggcacag	542	58/40
3'd	tttagttctgcccagccctga	gggaaagggctgagacttagt	378	58/40
3'e	gaaccctgacatgcataagag	ctcacaatctgatgaccttcc	386	65/40

Supressor of Cytokine Signalling 7 (*Socs7*)				
Region	**Forward Primer**	**Reverse Primer**	**Amp (bp)**	**Ta/Cycles**
Ex1a	ggaatcggaggccgagagcct	cgctgagcctcccatgtcggt	400	62/42
Ex1b	gctgctggtcctggagggctt	gaaggcctcttgccggtccca	396	65/40
Ex1c	agcctccgggtcccgaactac	agtggggccggaacagggatg	621	65/40
Ex2	gattcaggaggtctggaatcc	atgcaagggtgtttgctgcga	208	64/42
Ex3	tcccttgttcagggaccctct	agatgcccgcccatctaagtg	409	64/42
Ex4	tgacttgcccgtgcataaagg	acagggatggagactgaagct	342	62/40
Ex5	agcttctaatgccttgccctc	aaggacaccacagacagagct	308	64/40
Ex6a	taagacagactgtgctcggga	cgtatacatacactcaggccc	363	64/40
Ex6b	gctatggtcggcacaagtgtt	agctccaggagacttaacacc	471	62/40
Ex7	agtctaccctctagctcagat	ggctaccctgaaatacaagag	377	64/40
Ex8	acagcacttcttctgggagct	agcgtcaaaggcacttccact	275	65/40
Ex9	ggctcagcaagagatgtattc	ggccttcatgactgttgtgtt	384	58/40
3'	ctgtgggtctactactctttg	caccaccttcaattcaatggg	347	58/40

Rho GTPase Activating Protein 23 (*Arhgap23*)				
Region	**Forward Primer**	**Reverse Primer**	**Amp (bp)**	**Ta/Cycles**
5'a	acatgagccctgtcatcaagc	gggaggagacagggaagataa	267	65/40
5'b	aacccataggaaatgccagcc	ctgcccctagacactcagtat	297	65/40
5'c	tgggaactggtgattggatgc	gcttcttccgtttgcggttga	174	65/40
Ex1	acacagtggtggtgcagagcc	aactccagcctgccacaccag	376	65/40
3'a	catcactgccatctggggacc	acaaacttggggctaaggtgc	676	51/40
3'b	gcaccttagccccaagtttgt	aaagactgacagacctgggca	417	64/40
3'c	tgtatagagtctcagctgggc	gagacacatccctcagatagc	362	64/40

Hypothetical Protein LOC103551 (*HypPro*)				
Region	**Forward Primer**	**Reverse Primer**	**Amp (bp)**	**Ta/Cycles**
Ex1a	aggaagcgcgaccgatcgcac	ttggcaagggcgcagaaggcg	404	65/40
Ex1b	atggagactctgtgtcctcct	ggactgctagctgcatcaaga	509	62/40
Ex1c	tcctcaggactctccgaccaa	aaggtgctcgatgtaggaagc	474	65/40
Ex1d	tttggtgttacgcgaaggggt	ttcagaatcgatgctccctcc	454	62/40

P140 (*P140cap*)				
Region	**Forward Primer**	**Reverse Primer**	**Amp (bp)**	**Ta/Cycles**
Ex2	ttgtgggagatgggcagctct	caactccaggctccctgttct	445	65/40
Ex3	ctgggaacatccatccctgtc	gggagatgtgaatccagggtg	263	65/42
Ex4	tgagtcccgagagtctctgac	gtgagaagcatgtgcaaggcg	190	65/40
Ex5	tatctggccggagctccggag	gggagtgacagccgctagagg	410	65/40
Ex6	ctgagggctcaccacactctc	cctagggaaggaccaccaagg	358	65/40
Ex7	aagggttctagctgctgccct	ctagggcaccttgtctcagac	284	65/40
Ex8a	ggtgctggcttctcaagcaag	tcctcatctggcttcacgtcg	382	65/40
Ex8b	ggcccaggatagactggaaga	ataggagaggcgtgaacgcga	297	62/40
Ex8c	tcgcgttcacgcctctcctat	agccatagccgtctccgtaga	424	65/40
Ex8d	gcatcgcacctagcatctagc	ttgtacagcgagtcctccagg	461	62/40
Ex8e	tgcgctctctcagcacctact	agatactgccacccctctgca	463	65/40
Ex8f	cgacgtgaagccagatgagga	cccgaatctttgcggaaggac	423	62/40
Ex9	gtaggaagtaggttgggcagg	gctcgcccatgatgtagctac	535	65/40
Ex10	gtaggaagtaggttgggcagg	gctcgcccatgatgtagctac	535	65/40
Ex11a	aaccagacagtgcctctctgg	gggcagcatttgcagagaggt	381	65/40
Ex11b	gtagctacatcatgggcgagc	tgagcaatgagggactccgct	503	62/40
Ex12	tctgcccacccttcccaaca	cctgcaccttccatatgagcc	364	65/40
Ex13	tcccagctgctcgatttctgg	ctgggtaggcagactgaggaa	284	65/40
Ex14	ggcgaggctgacctaagtgtt	atctctgccgaggagtcagga	321	65/40
Ex15a	gatgcctgcaggttcagttcc	cgtgctccttcagtacctgac	398	64/40
Ex15b	tcctgcaagttcccagagcct	aagagcccacgtgctccttca	432	62/40
Ex16a	cttagcactagtggctggagg	ggcaatcgctctccagtgctt	408	64/40
Ex16b	gaggggccaagtctcgtgtaa	ttctctggcagtgtggctacc	467	58/40
Ex17a	tgacctgagctgtcctcttgg	gctgtggggtcagaacaacac	367	62/40
Ex17b	tggcaggcatggggaaatgga	aagttgggttgccctggctga	383	65/40
Ex18a	gtgttgttctgaccccacagc	agggtcctgggctaacaaagg	341	62/40
Ex18b	tcagccagggcaacccaactt	ctcgcttcccacttcacagtg	422	64/40
Ex19a	gcttaaggaggtcctaacccc	agcactaggctcacaaggagg	395	62/40
Ex19b	gcttggagttccacactggac	caggggctcgtgtctatacca	381	64/40
Ex20a	gttcagaggagcactctctcc	ggaagtcaggggaagttggtg	563	62/42
Ex20b	ccctctggttctcgcttttgc	ggtagagcgggcatgaaagga	352	64/40
3'a	tgcccactctcacgcctgaaa	cttcgaaggctggacagacag	476	64/40
3'b	cctctggttccagaacctcca	gtctccgtggctcagagtttg	485	64/40
3'c	ctgggttccttcctggaggaa	tctaggcccttccatcttccc	488	64/40
3'd	cttcccctctgctctttcacc	ttctcccctggcacctagtgt	401	64/40

Hypothetical Protein LOC103551 (*HypPro*)				
Region	**Forward Primer**	**Reverse Primer**	**Amp (bp)**	**Ta/Cycles**
Ex1a	aggaagcgcgaccgatcgcac	ttggcaagggcgcagaaggcg	404	65/40
Ex1b	atggagactctgtgtcctcct	ggactgctagctgcatcaaga	509	62/40
Ex1c	tcctcaggactctccgaccaa	aaggtgctcgatgtaggaagc	474	65/40
Ex1d	tttggtgttacgcgaaggggt	ttcagaatcgatgctccctcc	454	62/40

Myeloid/Lymphoid or Mixed Lineage-Leukemia Translocation to 6 Homolog (*Mllt6*)				
Region	**Forward Primer**	**Reverse Primer**	**Amp (bp)**	**Ta/Cycles**
Proa	aggcagacaatgggtctgaag	agtgtgtgggtcaggcagtaa	351	65/40
Prob	tgttctgtaggccacgcagat	cgtgagtgactcttctcttcc	397	65/40
5'	ggtcctcatctggcttcacgt	tcgcacctagcatctagctcc	238	65/40
Ex2	tggctttagtaggctgggtct	gagtgacagagcttagtcctg	289	65/40
Ex3	ctctttgctctacagcctcag	ctcccaacaccaagctgtaga	313	62/40
Ex4	ctcctgttggtacaggaaggt	tgtgacctatgagcaaccctc	327	64/40
Ex5	tggcattgaggacaggccaaa	tggacccaagacctaagcatg	301	65/40
Ex6	gtcacctggtgagatctcaga	ctgtcacagacagagttcctg	403	65/40
Ex7	caggagttgcttctaggatcc	aagctctgtgcctcaagctgt	424	65/40
Ex8	ccctctgtagattgagagcac	tggtggcagcagaggtaacat	371	65/40
Ex9	tagagcttccttcccacagct	gtactcacctgcaggctgaaa	358	65/40
Ex10a	taactagggtctgcggttcct	ttctccttcagggtggtctca	447	65/40
Ex10b	ccccttcacctggagactata	gataatggccacctccgttct	511	62/40
Ex11	ggcatgctgtgttctctgaag	acagttgtactgtgtggtggg	398	65/40
Ex12a	tctgcttccatctccaccact	tctctgtgcaatggagtggca	449	65/40
Ex12b	gatcccatctctcatggtgga	gaggtaaattcagagggaggg	508	64/40
Ex13	aagaaggaggtgtgagctgag	aaagcacctagcacctagctc	313	65/40
Ex14	tggattgtgacatcctggtgg	aaggccagtgaagaggcttga	346	65/40
Ex16	cctatggactgcttcctcaag	agcagctgctggttagtcact	278	65/40
Ex17a	gctatgggagaatgctggtgg	accctcccagaagcccattga	360	65/40
Ex17b	cagctcttcgctctccttcca	cttaagtcgacagactgccag	462	nd
Ex18	cctactggaggtcttctagac	ctcaactctcactgggatgtg	372	65/40
Ex19a	agattgtctccctgttgtggc	ttggtctgagcagtgaggact	452	65/40
Ex19b	tccagcagatgcagcagaaac	agagacatagctgctgctgct	410	65/40
Ex20	ggcttgaccactcagcttctt	tccaaccaaccctccatctct	469	65/40
3'a	ggcttgaccactcagcttctt	tccaaccaaccctccatctct	469	65/40
3'b	tcactgcactggctgcttcag	aagtgctgtcctgcccttcct	379	65/40
3'c	ggcctatccctgtgtggaaat	aaaggagcagagttggtgagg	539	64/40
3'd	catttcttcctctggacctgg	ggaaggtagggtattaccctg	269	65/40

Polycomb Group Ring Finger (*Pcgf2*)				
Region	**Forward Primer**	**Reverse Primer**	**Amp (bp)**	**Ta/Cycles**
Pro	cagtacccttcacgttgagca	agctcgattatccggcctgaa	454	65/40
Ex1	tctcgactcctcgcttcctat	gttcgctcactccagctgaat	302	65/40
Ex4	catccctgctccaaggtgtta	gctacagtaggcatctgacct	333	65/40
Ex5	caagctggtatccagttgcac	tctactttccagggcagcaag	363	65/40
Ex6	cctgagctactgtgagctatc	ttcagacccagcattcaggca	294	65/40
Ex7a	tgcctgaatgctgggtctgaa	gctgggagatctgttggaagt	414	64/40
Ex7b	aagaaggaaggggtacagagc	cagtcacgttgcttcaggaac	335	62/40
Ex8a	tgcctgaatgctgggtctgaa	gctgggagatctgttggaagt	414	64/40
Ex8b	aagaaggaaggggtacagagc	cagtcacgttgcttcaggaac	335	62/40
Ex9a	atctctgagctgccctacttc	ctcaacagtggggctagagta	626	64/40
Ex9b	tacagtactgtccagtgggga	ttgtccccatctccattctcc	384	58/40
Ex10a	atctctgagctgccctacttc	ctcaacagtggggctagagta	626	64/40
Ex10b	atctctgagctgccctacttc	cccagctatccaactctgtga	596	62/40
Ex11a	atctctgagctgccctacttc	ctcaacagtggggctagagta	626	64/40
Ex11b	ggagaatggagatggggacaa	cccagctatccaactctgtga	263	62/40
Ex12a	ctcctggagtccacctttcaa	cagggatggagtgtctgacat	311	64/40
Ex13a	gaaccttggttgggtataggg	gtttgcaggcagttcgaagtg	311	64/40
Ex13b	ctggtccgtctttgttctgac	ggagcgccattaacagtcatc	421	62/40
Ex13c	gcatcagagtgtgagtcagtc	aaagacccccctagacctagac	570	64/40
Ex13d	gtgtgagtcagtcagcgacaa	acacacgagtttcctgtggca	500	62/40

Proteasome (Prosome, Macropain) Subunit, Beta Type 3 (*Psmb3*)				
Region	**Forward Primer**	**Reverse Primer**	**Amp (bp)**	**Ta/Cycles**
Pro	acagccgaacgcgctaaccga	ctggcgcttaccgtggtgct	660	60/40
Ex1	agaatgggcgccttcggtatac	ggtactcccatgtgcattctact	630	60/40
Ex2	cacgggtatatgagctttgggg	gtgttcagctgagtctcacact	380	60/40
Ex3	tgttccttggtagggacagaatc	gaggagttgcaggctagccag	370	60/40
Ex4	ggtgaacacatcttagacattgc	agccgtggctggcttgcttg	420	60/40
Ex5	tcccaagtaaggagctgagagg	acctggctgcagtcagtcacc	380	60/40
Ex6	gcttattacacttgctctgtagg	atgggaccagagcacaggttagt	290	60/40

Appendix 2.2 Chromosome 8

Zinc Finger Protein 423 (*Zfp423*)				
Region	**Forward Primer**	**Reverse Primer**	**Amp (bp)**	**Ta/Cycles**
Ex2	taaatactcccacagggctcc	ctggactagacacaggaatgc	290	62/40
Ex3	gaccccaggaggtagagtaat	gggtacccaagacaccacaat	459	62/40
Ex4a	tgtgtgtccacttacttccgg	tggccaggtgttccttgttct	638	62/40
Ex4b	aagtaccactgtcacgagtgc	caggtgtagcactgctcatgg	541	62/40
Ex4c	ccacgccaaccagaaacacaa	aatgtgctcctgcaggctgtt	547	62/40
Ex4d	caacctcaatgagcatgtgcg	ggtctggaagctctcgaagtt	586	62/40
Ex4e	cagcaagaagtccaaggctga	aagatgcacttgtgggccttg	570	62/40
Ex4f	gagaagaagatgtaccgctgc	cgttacacttatggctgccct	565	62/40
Ex4g	agcctacaccatggaggtgtt	cctgcttgctacggaactctt	554	62/40
Ex4h	ccatggcacctttcacatgca	cctaggaagcacacatgcaag	474	62/40
Ex5	ccagacattctgggccatctt	cccactgaaatgtcacagacc	298	62/40
Ex6	gtgttccgggactaatacagg	ctatgggacagctctgcatga	352	62/40
Ex7	atgcctgggtgatccctactt	atctgagtgaggagcctagtg	359	65/40
Ex8	atgatcgagccgctttctgca	ctagaaatgtagtctgcggcg	404	62/40
3'a	aatgatttggccatgaggcgc	actgtccggtgaactggcaaa	430	62/40
3'b	cgccgcagactacatttctag	tgtgtgagcccattggaactc	512	62/40

Hypothetical Protein LOC382030 (*HypP*)				
Region	**Forward Primer**	**Reverse Primer**	**Amp (bp)**	**Ta/Cycles**
Pro	tactgcccagaagttagtggg	gcggaagacacactctaccttt	446	62/40
5'	ggtctggatgagctacccaat	ataactcgcaagggctcgtca	352	62/40
Ex1	ggtctggatgagctacccaat	ataactcgcaagggctcgtca	352	62/40
Ex2	gatgtgcaagacctgttggag	agggagtcgttcctacttagg	250	62/40
Ex3	ggctgtgtctcttaagcactg	cagccaactagagcttccctt	333	62/40
Ex4	gaagttttcatgtccttgtgg	tctcaggtattgaatccacag	329	62/40
3'a	aagctgaagaaccttccctgg	agagggccaaacgtcatcaac	365	62/40
3'b	caggagacagtgaagggttca	ccttgccttccaaaggtagag	414	62/40

HEAT Repeat Containing 3 (*Heatr3*)				
Region	**Forward Primer**	**Reverse Primer**	**Amp (bp)**	**Ta/Cycles**
Pro	gcttaaagtactagaggtgcc	gcacacaactggtacacagat	492	62/40
5'	acattcccagggacatccagg	gacgtcagagtcgcgtagtga	501	64/40
Ex1	acattcccagggacatccagg	gacgtcagagtcgcgtagtga	501	64/40
Ex2	ttcaagcgacctcagttctcc	agaagtagagaatgcatcggg	485	58/42
Ex3	ctgtggttagacatacagggc	agggacacataagacgacacc	292	64/40
Ex4	gggatggaccatgtagagaac	ctcaagtcatcagattgcccc	398	64/40
Ex5	ggagagatggactgagagatc	agtaacagtcgggctgttagc	388	64/40
Ex6	catcctggaagtgaagcctct	acagagcattgtagagctggg	363	64/40
Ex7a	atagcctaagccctgtggaaa	tcgaacatccatctgactcac	534	64/40
Ex7b	ccatctaagagtcaggcagaa	cctgctgaaggaaactgatgt	493	62/40
Ex8	gcctgttctagcctccatcta	tctgctttacacccaagcctc	567	62/40
Ex9	gcctgttctagcctccatcta	tctgctttacacccaagcctc	567	62/40
Ex10	cctcctgaccaccttaacttg	gaacacaaccttctgcagggt	308	64/40
Ex11	cagtaccgcaaatcagtaggc	ctactgacacaccctgactgt	384	64/40
Ex12	tgtaagctaacattcgcatgc	tctacaaagctctgtatctcc	330	58/40
Ex13	cccacacacatgagcactcat	taaggcttgcctctgtggtgt	458	58/40
Ex14	ccttcttccctggtgtctttg	tttccagagctgctgagacct	513	62/40
Ex15	ggccacattctcattttcctc	ctcagcactaaatccatcagg	422	62/40
3'a	ccagctgtgtgttctcgacaa	atgtggggcattttcagtggc	501	62/40
3'b	aacaccacacctgacctccaa	acccagagtaactgctcagac	501	62/40
3'c	gccctcaggtggttcttaatg	taggaaggcggatacttaggc	616	62/40

Adenylate Cyclase 7 (*Adcy7*)				
Region	**Forward Primer**	**Reverse Primer**	**Amp (bp)**	**Ta/Cycles**
Pro	taccatcacggtgaggaaacc	tttccccgcatccttgtgtct	489	65/40
5'a	ggcagacgagatctggaggaa	agaaagcttcagaggggaagc	545	62/40
5'b	ggaggtggagctgaactgttt	cagacccagcttagaactcct	339	58/40
5'c	caccatgacatgaggagctgt	aatgcaggtcctctgctagag	283	62/40
5'd	tatgcccaggtactgtgtgga	ggtgagccggtacttctcata	426	62/40
Ex1a	tctgtccagtcctgcctgata	caacccacctagcagttcaca	415	58/40
Ex1b	tctgtccagtcctgcctgata	aggcatcaacatgccgaagct	370	65/40
Ex2	gtgtggagggtgcttgttatg	tgtcacgagtgggcagaatgt	385	58/40
Ex3	agagatgagaggtcccaggtt	agcagttaagacagaccggac	316	58/40
Ex4	cagatgccaccatgttctcac	catgccatccctctctccaaa	396	54/40
Ex5	gctagcctagggcctcataat	gggccaatcctgtatagactg	336	65/40
Ex6	tacctcttctggcctttggag	catgccactcacacagagtac	378	65/40
Ex7	agctgctgagcgacagttgaa	tatggcacgctgtgagaatcc	324	65/40
Ex8	ttgaggaagctctgtctccct	gctgaggagacacatgtcaga	389	65/40
Ex9	gatgtgtggtcccatgatgtg	ccacagtcttgagggtcaatg	407	65/40
Ex10	cagcccatgctcgaagaatac	taccttctcctgtccagaagg	465	62/40
Ex11a	ccttctggacaggagaaggta	gcattccaccccaaccattca	264	62/40
Ex11b	tgccccttagctgcattgtg	agacagagattgctcagggca	395	65/40
Ex12	tgctggcttcatgaactcagg	ggccagagccagtactcaata	294	62/40
Ex13	agtagctccttcccttgcact	aacacccagtgcagagattcc	282	62/40
Ex14	aatgactgtgtggagcaccac	tgctagccttgccagtttctg	326	62/40
Ex15	aggtgaccatgtgctggagaa	gggactcagttatcctgaagg	276	62/40
Ex16	ccttcaggataactgagtccc	gactgggattctggaatctgg	368	62/40
Ex17	tagttgtcttgggtcacctcc	ccatgagatgtccactctgac	284	62/40
Ex18	tgctggaaagagagcaatggg	ctgctctgatcaggtgctatg	392	65/40
Ex19a	ctttagaccctcactcagcag	ctgtcacacctgtgacatacc	356	65/40
Ex19b	ttctggagtgacccataggtc	accagcccatctgcaatactg	376	62/40
Ex20	cagtattgcagatgggctggt	tcaggcggtacttctggatag	339	62/40
Ex21	tttcacagtcacagcccacac	aggactaaggatggagcctga	385	62/40
Ex22a	cgtgcatgccatgtgtctgta	gtctccaggctatgccacaaa	310	62/40
Ex22b	atgttgtcacctgcagccatg	actccatgcagccttgactga	410	65/40
Ex23	tttgtggcatagcctggagac	agggtctgccgaaacctcata	317	62/40
Ex24	gagtgtgggcaagaactctca	aaccacacagccaagtgatgg	306	62/40
Ex25	ccatcacttggctgtgtggtt	gaacacagcctgtagtagacc	457	62/40
3'a	ggctgatcaacgtcaaaggca	agcagcaacccatgctagtca	444	62/40
3'b	ggctgatcaacgtcaaaggca	ctcctgtagccagtagagctt	442	65/40

Region	Forward Primer	Reverse Primer	Amp (bp)	Ta/Cycles
3'c	ggtctactacaggctgtgttc	ttagaactctgtccctgcagc	497	62/40
3'd	tgactagcatgggttgctgct	gtttgagaccaagctaggctg	532	62/40
3'e	gctgcagggacagagttctaa	ttcacaggccagagtcctgaa	402	62/40
3'f	tctgtgggaaagcctgtgtag	aaacctgctggttagcaccct	393	62/40
3'g	gcacgactatctccagctgtt	aaacctgctggttagcaccct	414	65/40

Bromodomain Containing 7 (*Brd7*)				
Region	**Forward Primer**	**Reverse Primer**	**Amp (bp)**	**Ta/Cycles**
Pro a	aagtactgggaaccgaaccca	agctcactgttgcatgtgcag	439	62/40
Pro b	ttacaggtgctgtgagctggt	agctcactgttgcatgtgcag	470	62/40
Ex3	ccagtagatggcagcaaaata	agttgtgagtcaagctaatgc	361	62/40
Ex4	tcctgctgcatgagagctctt	tttgctgccaggcaaggtact	370	62/40
Ex5	tctgtcttctgcttctgtgcc	gggacaactctgtagagttgg	508	62/40
Ex6	cccaaatttttgcagggccta	tatggtttgccaacgaggaac	278	62/40
Ex7	tcctcctggactggagattgt	aagaagggcagcactgactca	457	62/40
Ex8	gtagggcaagtgtctccattg	cccaggacagtaatacctgac	354	62/40
Ex9	agcctgtggcatgcatctgat	acccacctattctacctctgc	367	62/40
Ex10	atagagagcgccttgcagtag	catcaagaaagccagtggacg	365	62/40
Ex11	ggggtgactgtatctattggg	tccagcaacaggctggtatgt	533	62/40
Ex12	gtgtggtctatgaaccaaggg	ggagttcagctgtcatactgg	320	62/40
Ex13	gtatgctgcttttctcttgcc	aagcatctttacctgctgagc	261	62/40
Ex15	gaagctaaccatagcagagcc	ttcatggtgtggtactcgctc	333	62/40
Ex16	tgactacaggaaccacttcgg	cacactcacagccaaggagaa	453	62/40
Ex17	ttctccttggctgtgagtgtg	aaaggctggtgtgtgtcctag	420	62/40
3'	ttctccttggctgtgagtgtg	aaaggctggtgtgtgtcctag	420	62/40

Selectin Ligand Interactor Cytoplasmic-1 (*Slic1*)				
Region	**Forward Primer**	**Reverse Primer**	**Amp (bp)**	**Ta/Cycles**
5'	cgtggcctgtatgatgtactg	aaggacagcccatactctcac	368	62/40
Ex1	ggcatcattgtcattcctccc	ttaagacagctgcctggctac	330	62/40
Ex2	gatatccattccatcccacgc	ccctttctctggaagactgtg	379	58/40
Ex3	ttgagcgcgtgcgcgtgcaca	agtcgaggaactcgcgcgagc	357	64/40
3'a	ttgagcgcgtgcgcgtgcaca	agtcgaggaactcgcgcgagc	357	64/40
3'b	tacgcgctgggcaaggacttc	ggagcgaagggaagatctggg	612	65/40
3'c	tcgtctgcttgcgcgacctcg	aggagcccctcaagccaggct	362	65/40

Naked Cuticle 1 Homolog (*Nkd1*)				
Region	**Forward Primer**	**Reverse Primer**	**Amp (bp)**	**Ta/Cycles**
Ex2a	ccttcccttcactctctggta	gaacaatgtgcaagcgggatg	317	64/40
Ex2b	aagtctttactctccgggctg	aagcatagggcacaagtaggg	414	64/40
Ex3	ttaccaccacctgtgcagtct	gtggatgtaaccctgagtgct	277	64/40
Ex4	atggaaggatgtggagcatgg	taagaggtgagaactcctccc	318	64/40
Ex5	cactagagattacctgtgccc	aggacccttccaacaaccttt	462	64/40
Ex6	accatcttgcctccagatctc	caagggtttgctgaagccttg	412	64/40
Ex7	gctgcagagctgttgtgaact	caggatggaacctgctactca	286	65/40
Ex8	gaagaagtgatgaagctgccg	cctctgacctgtccagtagaa	327	58/40
Ex9a	tgtttctccctacaggactgc	aagtgcttgctcccatcctga	345	58/40
Ex9b	ctgtcggattggttcctagga	tgcttgtgtttcttgtgcccc	407	65/40
3'a	agggcaagaacatgggtatgg	gtcttctacatgaaggctggc	504	65/40
3'b	ttctatcagccctagacccca	gctctcctggaagaactgaag	335	65/40
3'c	tcaccaagaagtgactctggg	cttaaacacaggtgcatccttcc	464	58/40
3'd	gacaccttagctgtgtttccg	tttcatctgatggacgggcag	501	58/40
3'e	taaagggaactagcccttggc	agacggaggtggctgttttca	477	64/40

Caspase Recruitment Domain Family Member 15 (*Card15*)				
Region	**Forward Primer**	**Reverse Primer**	**Amp (bp)**	**Ta/Cycles**
Pro	ccttctgggaatgcctccatt	ctcctttccacatatccaccc	434	58/40
5'	tccctagagggaaatcaggag	gacttgtgacggtcgtgatct	307	58/40
Ex1a	tcctccttgcctgtgctcttt	gcttgctcagcctgctttctt	240	58/40
Ex1b	cccttctcctcagcatcttag	cagagcccggtgtcttagtca	683	65/40
Ex2	gcatacgttgctccctacagt	ggctgactcaacaagagtcac	628	65/40
Ex3	cttgggaccttcagattaggg	atgcaggaactgagtctggag	328	65/40
Ex4a	cttccacacattgcattcccc	gtgcaaacgctgcagaagagt	386	65/40
Ex4b	tggaggacctctttgataccc	tctcaggtacagttggatgcc	539	65/40
Ex4c	aacctgctgaagaatgcctgc	cactactttgggcacgtacca	535	65/40
Ex4d	ggccatgagctgctatgtgtt	ggacaacagacctgctaggaa	376	65/40
Ex4e	agagtcaagaagggcagcgaa	tacgtccagccttgacagtag	569	62/40
Ex5	cagaagcacagtgaggttgtc	aaggatcaccagccaccattg	525	65/40
Ex6	cagaagcacagtgaggttgtc	aaggatcaccagccaccattg	525	65/40
Ex7	gcagcatgtcactactacacc	tgaacacagaggcagctcaga	341	65/40
Ex8	atggtgtggtaggtccacgtt	tcacctccaaattcaccgcca	375	65/40
Ex9	tcactcgcccttcataggtca	attagcagtgaagcaccaggg	299	54/40
Ex10	ccctcaccactcttgtctact	ttccctaccagacacctcagt	323	65/40
Ex11	ctctcatgggtcatctcacag	gcctactgtgtgcagaatacc	330	65/40

Region	Forward Primer	Reverse Primer	Amp (bp)	Ta/Cycles
Ex12	actgagcattagctcccatcc	agcagagggattctgcctgat	271	65/40
3'a	atccaaacactgagctccagg	aagacgctggagtctgctgtt	494	62/40
3'b	catgtgggtgacacaatcctc	gggaggagaaagggaacttct	326	62/40
3'c	caggagaatgctggcaaggaa	cagctggagtgtggtcacatt	490	62/40
3'd	caggactcaacttcgacaacc	ttggttttgtcccctgcaagc	386	62/40
3'e	gagtcggtgcctatgaactga	tcaccatgggttagactctgc	549	62/40

Cylindromatosis (*Cyld*)				
Region	**Forward Primer**	**Reverse Primer**	**Amp (bp)**	**Ta/Cycles**
Pro	tgggagttccccgtgttac	cgtgcgctctgattgggtttt	416	65/40
5'a	gattggctagcgcggcattta	agagaaagacggagtcctgca	460	65/40
5'b	cgattggctagcgcggcatct	tgaggcagagcaggaacactg	280	58/40
Ex1a	ctgcaaatgctttgctactgg	actgtcctatactccctttgg	496	62/40
Ex1b	ctgtcacaatgagttcaggcc	gtctacctggaggcctttact	386	65/40
Ex1c	ttggagcaaccgcatgcagtt	tagatcagtggtagagggtcc	463	65/40
Ex2a	cccaactgcaactgttagtca	tcctagactctcttttcctgg	406	62/40
Ex2b	actgtggcgtgtttgttgcat	agcacatgcattctgtgtctg	412	62/40
Ex3	gggcaaagtagttaaaggttc	cctaggagacaacaatgtaac	468	58/40
Ex4a	gaatcgacttcctctgactag	tgcaccctcacaatcatgtac	506	65/40
Ex4b	cgacttcctctgactagcttt	acaattcatggggtggccatt	535	58/40
Ex5	ctgttatctgtacagcagctg	gcatgtcagcaatggtctact	335	65/40
Ex6a	ctgtgagcatacttgcaaagg	gggggaaatctagacaaaacc	569	65/40
Ex6b	gggatcatgtgctcagttaga	ctagacaaaacctcatgcagg	552	58/40
Ex7	ctacctcgtcagctagtcagt	cctgagatactgagaagcagc	384	65/40
Ex8a	aatagtgagagtcaagcaggg	cacgtcccaataaggcactat	566	58/40
Ex8b	ctgaaggaagcaatgttgaaa	agtcagtttctctactcaaag	455	65/40
Ex8c	ctgaaggaagcaatgttgaaa	cacgtcccaataaggcactat	384	65/40
Ex9	atgcattgctctcctatgcat	acagaagcagaagactaaagg	383	51/40
Ex10	gcgcttcccatgttaggattg	atctactgtagggtcagccac	489	65/40
Ex11	gggacaacatgacaacaaaat	agcagggatttcattcctatt	363	58/40
Ex12	gcagagctgcacatctgtatc	gggtagtatgtacaagccctg	344	65/40
Ex13	gccctgtaggactgtgatttc	ctcttcaggtactgcactgca	282	58/40
Ex14	gacttcttcctcccctttctg	ctcacacacacacaccaacag	299	58/40
Ex15	ggctcagtgaaagtggctaga	gttccttagtctgggtagctg	470	58/40
Ex16	ctctcagaagccaaggagact	ctttgctgaagggccatcatc	361	58/40
3'a	tccaaccatgagcctgtacaa	cagcacaccttcaacaattgg	502	58/40
3'b	atggaccagggatatgaaatc	cttatcgctcagtcatttcag	423	58/40

Region	Forward Primer	Reverse Primer	Amp (bp)	Ta/Cycles
3'c	tttctgtgttcctgcagcagt	gactgtgggtctgtataagaa	480	58/40
3'd	gcatgtctgtactttgctgag	actctgagccagcttcacttt	524	58/40
3'e	ctgaaatgactgagcgataag	aagcagtcctaagatgacatc	524	58/40
3'f	gacaacatgcagtggtttctg	gagacagccataccacaaaac	615	58/40
3'g	gtactctctggtgtcagtttg	gtctgtgcacagtatacacac	433	58/40

Sal-Like 1 (*Sall1*)				
Region	**Forward Primer**	**Reverse Primer**	**Amp (bp)**	**Ta/Cycles**
Pro a	ggagcacaccatccacttgat	cttctgttctgaggcctggtt	427	58/40
Pro b	ccgcaattaattcgtctctgc	aacgtgatcagaccggaaca	433	65/40
5'	cgagatagggcaaggattgtg	tttccgacacttgctacgtgc	320	65/40
Ex1	cgccgctcgatttccgtaatt	taaaatcagacgcgccgagtg	406	65/40
Ex2a	tagacaggagttcctcggcat	gtagagaggttgtgatcgctg	622	65/40
Ex2b	ttactgacagtctgtcctcgc	agaagttgcccagtgtcgtca	545	65/40
Ex2c	ttgacagggaagagtccatgg	tgcttcacaccgctgatgttg	592	65/40
Ex2d	cctctatcccgtctcaaggta	aagaccttcgcacagaacctg	574	65/40
Ex2e	ccgcagaagatttgaactccc	cacttttgactgagccttggg	546	65/40
Ex2f	cattgcctccaactctcccaa	ggccgcagatcttacacttga	543	65/40
Ex2g	aagaaggccacggatcccaat	ccaggccagcattgatcatct	535	64/40
Ex2h	atcccagacacacccaagtca	ctgacaagcaaaggtcttgcc	531	64/40
Ex2i	agtgaacggaggtgctttgga	gtcctgaggagaaacgtgtac	406	64/40
Ex2j	tcagatgcgagatctgccatc	aggtccccttttccagaacctt	504	64/40
Ex3a	tcgggtcacttgctttgtcga	cgccgttctgaatgacagaga	352	64/40
Ex3b	ctaggaggcaatcctgtcaag	gtgtagttcatagtcccaggg	457	65/40
3'a	aaactgggcaattcggaaccc	gtatcacggaggcattgcatc	497	64/40
3'b	tgcttcctctcagaatgtcgc	gaggcattgcatcaacaccag	352	65/40
3'c	tggactagagtgctcctagct	cctacaaggccaaaatgctac	550	64/40
3'd	gaacatttggaaggcttaggg	tacctgctcttgatcaagagg	467	65/40
3'e	caggctgaacatttggaaggc	acctgctcttgatcaagaggc	472	65/40
3'f	cttgaacgaccttcagtggag	cccatgcatgcccaattctgt	456	64/40

Appendix 2.3 Chromosome 9

Heat Shock Protein 8 (*Hspa8*)				
Region	**Forward Primer**	**Reverse Primer**	**Amp (bp)**	**Ta/Cycles**
5'a	gcgtgaaagttccagaacgcc	cggatctgctgcagtctctgt	412	64/40
Ex2	gcagtgataggcactaaggag	ggttggcaaattcccgatcag	343	65/40
Ex3	caggtgccatttgagatgggt	ttcctttcagctccgacctgt	350	65/40
Ex4a	accaactgctgctgctattgc	tcaactcctcaaatcgagccc	474	65/40
Ex4b	gctggcctcaatgtacttcga	ttctctacagggtccagtgtg	546	64/40
Ex4c	agtgagaacaagagagctgtc	catcacagcgaatcttacagg	425	65/40
Ex5a	gtagactgcagttacagtgcg	atcacagcgaggaacttccct	316	65/40
Ex5b	ccttggatgtctgagcgaatg	tccatcatcacagcgaggaac	360	64/40
Ex6	gcttaagccacacgagcagta	tcttccttactcaagcggcct	380	65/40
Ex7a	caccatcaccaatgacaaggg	atcattgtgacccctctcagc	297	65/40
Ex7b	ggtaagtatggacctgctgct	gagtcactcagacatccaagg	478	64/40
Ex8 & 3'a	ggcttagttgtcagtctcctc	caggacaactgtatggtgcca	354	65/40

Appendix 3 qRT-PCR Primers

SYBR Green Dye					
Gene	**Primer (F=Forward & R=Reverse)**	**Tm (°C)**	**%GC**	**Length**	**Amplicon (bp)**
Mapt	F=aggagacatggaccatggctt	59.4	52.4	21	66
	R=tcctccgctccatcatcg	59.2	61.1	18	
Vtn	F=tcagagcgtctatttcttctctgga	59.6	44	25	151
	R=agtgggctctgattcctacttctc	58.1	50	24	
Ngfr	F=ccatcttggctgctgtggtt	59.7	55	22	102
	R=tcaccggccggctgt	59.2	73.3	17	
Adcy7	F=atggtactaggctccgtgctgat	60	52.2	23	114
	R=gagaggcagtagtgcatacaccac	58.5	54.2	24	
Cyld	F=gagttgtacgcttcagaggacctt	59	50	24	156
	R=acacgccacagtcctcatca	58.7	55	20	
Sall1	F=tgtggaagagcattcacaacaaa	59.2	39.1	23	56
	R=atatgggtgcccatgtgga	58	52.6	19	
Slic1	F=agagccgctggaaacatgtc	58.9	55	20	115
	R=aagctcccggtctggatga	59.2	57.9	19	
Card15	F=agccagtacgagtgtgaggagat	58.1	52.2	23	114
	R=tagaaggaaggcagccagtcc	59.4	57.1	21	

Dual-Labelled Fluorogenic Probes					
Gene	**Primer (F=Forward & R=Reverse)**	**Tm (°C)**	**%GC**	**Length**	**Amplicon (bp)**
Mcp1	F=gttggctcagccagatgca	59.5	57.9	19	81
	R=agcctactcattgggatcatcttg	59.5	45.8	24	
	P=ttaacgccccactcacctgctgctact	69	55.6	27	
Sp6	F=atacgctaagacgtcgca	51.5	50	18	78
	R=aaaagccagttgcacacgaa	58	45	20	
	P=gtggcacagcggtgaccgacc	68.9	71.4	21	

Appendix 4 Allele Discrimination Primers

Gene	Primer (F=Forward & R=Reverse)	Tm (°C)	%GC	Length	Amplicon (bp)
Adcy7	F=ttgtggtgtatgcactactgcct	59.6	45.8	24	132
	R=acgtctggaaggctcttgtca	58.5	52.4	21	
	Probe (P1 & P2)	**Tm (°C)**	**%GC**	**Length**	
	P1=tcacgcctaccacgat	66	56.2	16	
	P2=acgcctgccacgat	66.8	64.3	14	
Card15	**Primer (F=Forward & R=Reverse)**	**Tm (°C)**	**%GC**	**Length**	87
	F=acgaggctgctgagtgtcaga	59.8	57.1	21	
	R=acccatcgtaagtactgaggaagc	58.8	50	24	
	Probe (P1 & P2)	**Tm (°C)**	**%GC**	**Length**	
	P1=agactgagtcaacacc	66.8	50	16	
	P2=actgagccaacacc	67	57.1	14	
Sp6	**Primer (F=Forward & R=Reverse)**	**Tm (°C)**	**%GC**	**Length**	123
	F=cccactcttgctctcttctctc	56.1	54.5	22	
	R=acacgcatacacacactcacacc	59.5	52.2	23	
	Probe (P1 & P2)	**Tm (°C)**	**%GC**	**Length**	
	P1=ccagaaccttctgcagg	50.7	58.8	17	
	P2=ccagaaccctctgca	46.4	60	15	

Genetics: Published Articles Ahead of Print, published on August 20, 2008 as 10.1534/genetics.108.090894

Investigation of *Mcp1* as a Quantitative Trait Gene for Prion Disease Incubation Time in Mouse

Marie O'Shea, Emma G. Maytham, Jackie M. Linehan, Sebastian Brandner, John Collinge and Sarah E. Lloyd[1]

MRC Prion Unit and Department of Neurodegenerative Diseases, Institute of Neurology, University College, London, WC1N 3BG, UK

Running head: *Mcp1* and prion disease incubation time

Keywords: prion disease incubation time, Quantitative Trait Gene, prion strain, *Mcp1*, microglia

[1]*Corresponding author*: Sarah E. Lloyd

MRC Prion Unit, Institute of Neurology, Queen Square, London, WC1N 3BG, UK

E-mail: s.lloyd@prion.ucl.ac.uk

Phone: +44 (0)20 7676 2187

Fax: +44 (0)20 7676 2180

ABSTRACT

The genetic basis of prion disease incubation time is principally determined by polymorphisms in the prion protein gene, *Prnp*. However, it is now known that other genetic factors are important. Several quantitative trait loci (QTL) have been identified across the genome including a broad region of linkage on Mmu11. Monocyte chemoattractant protein 1 (MCP-1) maps to this region and has been associated with microglial activation and reduced survival in the ME7 mouse scrapie model of prion disease. We have identified 10 polymorphisms, 3 of which are nonsynonomous, in *Mcp1* between "long" (CAST) and "short" (SJL or NZW) incubation time mouse strains. Crosses between these strains and *Mcp1*$^{-/-}$ mice inoculated with the Chandler/RML mouse scrapie prion strain formed the basis of a quantitative complementation test. In these models loss of *Mcp1* did not show an increase in incubation time suggesting that the effects of *Mcp1* may be specific to the ME7 prion strain and that *Mcp1* does not contribute to the QTL described on Mmu11.

Prion diseases or transmissible spongiform encephalopathies are fatal neurodegenerative disorders of humans and animals that include Creutzfeldt-Jakob disease (CJD), bovine spongiform encephalopathy (BSE) and scrapie (COLLINGE 2001). They are characterized by prolonged incubation periods, deposition of an abnormal form of the prion protein (PrP^{Sc}), and histologically by vacuolation (spongiosis) of the neuropil, gliosis and neuronal loss.

The main genetic determinant of incubation time in mouse is variation in the prion protein gene, *Prnp*, (MOORE *et al.* 1998; WESTAWAY *et al.* 1987; CARLSON *et al.* 1988; CARLSON *et al.* 1993) however, quantitative trait locus (QTL) mapping studies have successfully identified multiple loci across the genome that influence incubation time. (LLOYD *et al.* 2001; LLOYD *et al.* 2002; STEPHENSON *et al.* 2000; MANOLAKOU *et al.* 2001; MORENO *et al.* 2003).

Using the Chandler/RML mouse adapted scrapie prion strain two independent studies identified QTL on chromosome 11 (LLOYD *et al.* 2001; STEPHENSON *et al.* 2000). Both studies mapped broad and overlapping regions of linkage which may contain multiple QTL. Stephenson et al used a CAST/Ei and SJL/J F2 mouse intercross with the peak of linkage at *D11Mit219* while a larger F2 intercross with CAST/Ei and NZW/OlaHsd found the peak of linkage near *D11Mit36* (LLOYD *et al.* 2001). The extent of the overlap between these two regions suggests that they may share at least some QTL especially as CAST/Ei was used in both cases. Identifying individual

candidate genes within these large regions is especially challenging. However it has been reported that monocyte chemoattractant protein-1 (MCP-1), which maps within this region of chromosome 11, plays a role in the onset of late-stage clinical signs of prion disease (FELTON *et al.* 2005).

MCP-1 belongs to the CC family of chemokines and is thought to have a pro-inflammatory role within the CNS recruiting monocytes and activating resident microglia (GU *et al.* 1997; GU *et al.* 1999). Prion diseases display an atypical inflammatory response dominated by microglial activation suggesting a role for MCP-1 in this process (PERRY *et al.* 2002). Although the inflammatory response is an early occurrence in disease pathogenesis (GIESE *et al.* 1998), preceding neuronal death and the onset of severe clinical signs by several weeks, Felton et al showed that late-stage clinical signs were delayed by 4 weeks and survival time increased by 2-3 weeks in *Mcp1*$^{-/-}$ mice inoculated intracerebrally with the ME7 prion strain. The onset of early behavioral changes was not delayed in the knockout mice as compared to wild type neither were there any differences in microglial activation or neuronal death. It is suggested that MCP-1 is not necessarily required for microglial priming but may stimulate their further activation thus exacerbating neuronal damage (FELTON *et al.* 2005)

.

To assess whether *Mcp1* is a potential quantitative trait gene (QTG) for prion disease incubation time we identified polymorphisms between our "long" (CAST/Ei) and "short" (NZW/OlaHsd and SJL/J) incubation time mouse strains. *Mcp1*$^{-/-}$ mice were also used in

a quantitative complementation test to ascertain whether *Mcp1* is a QTG or influences the phenotype independently of the QTL (FLINT and MOTT 2001) .

MATERIALS AND METHODS

Mice: *Mcp1* knockout mice (B6.129S4-*Ccl2*^{tm1Rol}/J) were obtained as homozygotes from The Jackson Laboratory (Bar Harbor, Maine, USA). These mice were created by B. Rollins (Dana-Farber Cancer Institute, Harvard Medical School, Boston, USA) and backcrossed to C57BL/6J for 10 generations (LU *et al.* 1998). Control C57BL/6J mice were also obtained from The Jackson Laboratory to ensure uniformity of genetic background. CAST/Ei mice were obtained from the MRC Mammalian Genetics Unit (Harwell, UK), NZW/OlaHsd and SJL/JOlaHsd were obtained from Harlan (Bicester, UK).

Hemizygous mice were generated by crossing *Mcp1*$^{-/-}$ mice to C57BL/6J using both males and females from each strain. These F1 progeny (males and females from both directions of the cross) were further crossed to either CAST/Ei, NZW/OlaHsd or SJL/JOlaHsd to produce mice that were hemizygous or wild type at the *Mcp1* locus on a genetic background that was 50% C57BL/6J and 50% from one of the other strains.

Genotyping: DNA was extracted from 0.5cm tail biopsies using a Promega DNA extraction kit and re-suspended in 50µl TE (10mM Tris.HCL, 1mM EDTA, pH 7.5). A 1:10 dilution of this stock was used as template for subsequent PCRs. DNA for SJL/J was purchased from The Jackson Laboratory and used at a concentration of 10ng/µl in subsequent PCRs. All PCRs were carried out using a PTC-225 (MJ Research) thermal cycler. Wild type and knockout alleles were distinguished using two PCR reactions as designed by The Jackson Laboratory. Reaction A amplifies an 888bp product from the wild type allele while reaction B amplifies an approximately 1300bp product specific to

the knockout allele. 10µl PCR reactions were carried out in MegaMix Blue (Microzone, Ltd) according to the manufacturer's instructions using 5 pmoles of forward and reverse primers. Both reactions share the same forward primer (Forward – GGAGCATCCACGTGTTGGC) but are differentiated by the reverse primer. Reverse primer reaction A: ACAGCTTCTTTGGGACACC; reverse primer reaction B: TCCTCGTGCTTTACGGTATCG. Reaction A cycling conditions were: 94° for 3 min, 45° 30s, 72° 40s for one cycle; 94° 60s, 55° 30s, 72° 3 mins, for 30 cycles; 72° for 2 min. For reaction B cycling conditions were: 94° for 3 min, 45° 30s, 72° 40s for one cycle; 94° 60s, 62° 30s, 72° 3 mins, for 35 cycles; 72° for 2 min. Fragments were resolved on a 1% agarose gel and visualised with ethidium bromide.

Sequencing: PCR products were generated as above using primers and conditions as detailed in Supplementary Material - Table 1. Cycling conditions were determined empirically but in general were 94° for 15 min; 94° 30s, 45s, 72° 60s for 40 cycles; 72° 5 mins. PCR products were cleaned using Microclean (Microzone Ltd) according to the manufacturer's instructions and re-suspended in H_2O. 100-200ng PCR product was added to a 15µl sequencing reaction including 5pmoles of either the forward or reverse primer, 1µl BigDye Terminator v1.1 Cycle Sequencing Kit (Applied Biosystems) and 5µl Better Buffer (Microzone Ltd). Cycling conditions were: 95° 30s, 50° 15s, 60° 120s, for 30 cycles. Reactions were ethanol precipitated, washed in 70% ethanol and re-suspended in 10µl MegaBACE loading solution (Amersham Biosciences). Products were detected on a MegaBACE1000 capillary sequencer (Amersham Biosciences). Samples were injected at 3KV for 40s and run at 9KV for 100 minutes.

Inoculation and phenotyping: The inoculum was generated from Chandler/RML mouse adapted scrapie (obtained from A. Aguzzi, Institute of Neuropathology, University of Zurich, Zurich) by a single passage in CD-1 Swiss mice. Brains from terminally sick mice were used to generate a 1% homogenate in PBS (LLOYD *et al.* 2001). This was used as the inoculum in all subsequent experiments. Mice were anaesthetized with isofluorane/O_2 and inoculated intracerebrally into the right parietal lobe with 30µl inoculum. All groups of mice included both males and females derived from each direction of the crosses. Incubation time was calculated retrospectively after a definite diagnosis of scrapie had been made and defined as the number of days from inoculation to the onset of clinical signs. This was assessed by daily examination for neurological signs of disease. Early indicators of prion disease include erect ears, rigid tail, pilo-erection and un-groomed appearance, slight hunched posture and clasping of hind limbs when lifted however a definitive diagnosis was not made until a confirmatory sign was seen such as ataxia, generalized tremor, loss of righting reflex or limb paralysis. Animals were culled as soon as clinical scrapie was confirmed or if showing signs of distress or loss of up to 20% or body weight. All procedures were conducted in accordance with UK regulations and international standards on animal welfare.

RNA extraction: RNA was extracted from whole brains from either uninfected or RML terminally sick mice. In both cases, tissue was homogenized using a Ribolyser according to the manufacturer's instructions. RNA from uninfected brains was prepared using the RNeasy Maxi (Qiagen) kit according to the manufacturer's instructions. RNA from prion

infected tissue was extracted using TRIreagent (Ambion) according to the manufacturer's instructions. Samples were treated with DNaseI (Qiagen) and purified further using RNeasy Mini (Qiagen) columns according to the manufacturer's instructions.

Real-time RT-PCR: 4 µg total RNA was reversed transcribed with AMV reverse transcriptase and random primers from the Reverse Transcription System (Promega) according to the manufacturer's instructions. Reactions with no reverse-transcription were also carried out for each sample to ensure no genomic DNA contamination. *Mcp1* real-time PCR was carried out on a 7500 Fast Real-time PCR System (Applied Biosystems) in a total volume of 15µl using 1µl cDNA (200-300ng) and ROX MegaMix~Gold (Microzone Limited) according to the manufacturer's instructions. Primers (6 pmoles) and probe (3 pmoles) were as described by Felton *et al* and supplied by Sigma Genosys. Rodent GAPDH (Applied Biosystems) was duplexed within the reaction as an endogenous control according to the manufacturer's instructions. All reactions were carried out in triplicate. Standard curves were derived for both probes and used to calculate the quantity of gene specific cDNA in the reaction. *Mcp1* values were normalized by dividing with the quantity of GAPDH.

Neuropathology and immunohistochemistry: Tissue was fixed in 10% buffered formal saline (BFS) and prion infectivity was inactivated by incubation in 98% formic acid for one hour. After further washing for 24hrs in 10% BFS, tissue samples were processed and paraffin wax embedded. Sagittal sections were cut at a nominal thickness of 4µm, treated with 98% formic acid for 5 mins and then boiled in EDTA-Tris-citrate buffer pH

7.8 for 20 minutes. Immunohistochemical staining was performed with anti-PrP monoclonal antibody ICSM35 (D-Gen Limited, London) (ASANTE *et al.* 2002) for prion distribution, Glial Fibrillary Acid Protein (GFAP) (Dako) for gliosis on a Ventana automated immunohistochemical staining machine using a basic diaminobenzidine detection system according to the manufacturers instructions (Ventana Medical Systems, Tucson, Azizona). Spongiosis was determined using a serial section stained with haematoxylin and eosin (H&E). Activated microglia were stained with anti-Iba1 polyclonal antibody (Wako) on an automated immunohistochemical staining machine as above

RESULTS

***Mcp1* polymorphisms:** To determine whether *Mcp1* is a plausible QTG for prion disease incubation time we established its physical position on Mmu11 as 81,851,769-81,853,421 (NCBI Build 36). This locates *Mcp1* between *D11Mit219* (72,135,165) and *D11Mit36* (83,658,790) which represent the peaks of linkage as determined by Stephenson et al and Lloyd et al respectively. These data are consistent with *Mcp1* being a candidate QTG.

Mcp1 (NM_011333) is also known as Chemokine (C-C motif) Ligand 2 (*Ccl2*) and Small Inducible Cytokine A2 (*Scya2*), spans 1.65kb of genomic DNA and has a predicted mRNA transcript of 806bp that encodes a protein of 148 amino acids. If *Mcp1* has a role in influencing incubation time in the F2 intercrosses described then one would expect to see polymorphisms between the "long" incubation time strain (CAST/Ei) and the "short" incubation time strains (NZW/OlaHsd or SJL/J). Therefore we sequenced all three exons of the gene including some flanking sequence to ensure coverage of the whole transcript including untranslated regions, open reading frames and splice sites. In addition we sequenced a 240bp enhancer region, 2.3kb upstream of the transcription start site, that contains two platelet-derived growth factor (PDGF)-responsive promoter motifs that bind NF-κB (FRETER *et al.* 1995).

Ten polymorphisms were identified, two in the 5'UTR and eight within the open reading frame, three of which cause amino acid changes (Table 1). The insertion/deletion polymorphism in the 5'UTR occurs within a putative α-CP2 binding site (KIM *et al.* 1990). Although this transcription factor has been implicated in the activation of the α-globin gene it is uncertain whether it would influence the transcription of *Mcp1*. The

variation seen between the three strains is however consistent with the possibility that this polymorphism is a functional variant in both crosses.

The three nonsynonymous polymorphisms were found at codons 6, 50 and 92. The S50G change occurs between NZW/OlaHsd and CAST/Ei but is not seen in SJL/J suggesting that it could be a candidate QTN for the NZWxCAST F2 cross but not the SJLxCAST F2 cross. Conversely, the R92Q variant is seen only between CAST/Ei and SJL/J which makes it a candidate only for the SJLxCAST QTL. In contrast, the M6T polymorphism could be a candidate for both crosses with the threonine seen in the "long" and the methionine in the "short" incubation time strains respectively. Alternatively, these codons may not act independently but may influence incubation time together thus providing different haplotypes (MSR, TGR and MGQ) and incubation times for each of the three mouse strains.

One polymorphism in the 5'UTR and five in the ORF were silent changes. Although no known function could be ascribed to these nucleotides they cannot be excluded as potential QTN as they may influence other unexplored functions such as gene expression.

Quantitative complementation of *Mcp1*: Quantitative complementation has been used successfully by others to determine whether a candidate gene can interact with known functional alleles to influence a quantitative phenotype (YALCIN *et al.* 2004). Therefore, to test whether *Mcp1* is a QTG for prion disease incubation time a quantitative complementation test was designed (Figure 1). *Mcp1*$^{-/-}$ were crossed to C57BL6/J mice to produce hemizygous mice *Mcp1*$^{-/+}$ on a C57BL/6J genetic background. These mice were further crossed to CAST/Ei, NZW/OlaHsd and SJL/JOlaHsd. From previous work it is

known that CAST carries the chromosome 11 allele driving a longer incubation time ("increaser" QTL) while NZW and SJL carry the shorter incubation time alleles ("decreaser" QTL). The resulting offspring from this cross will have either one or two copies of *Mcp1* (Figure 1). Where two copies are present, one will be derived from the reference strain (C57BL/6J) while the other will carry either an "increaser" or "decreaser" allele (Figure 1 A and B). In the hemizygous mice the single *Mcp1* copy will either be an "increaser" or "decreaser" allele (Figure 1 C and D). If *Mcp1* knockout has no effect on incubation time then no difference will be observed between the wild type and hemizygous mice for each genetic background (no difference between A and C or B and D). If *Mcp1* affects the phenotype but not the QTL there should be no difference between the increaser and decreaser alleles. If *Mcp1* affects the QTL there will not only be a difference between the wild type and hemizygous mice but there should also be a difference between the effects of the increaser and decreaser QTL alleles (FLINT and MOTT 2001).

Hemizygous and wild type mice for each mouse cross were inoculated intracerebrally with 30µl 1% Chandler/RML inoculum. Additional groups of $Mcp1^{-/-}$, C57BL/6J and their F1 progeny, $Mcp^{-/+}$ were inoculated as controls. C57BL/6J were also inoculated with PBS as a negative control. All groups challenged with prions developed classical signs of mouse scrapie. No clinical differences were observed between any of the groups. These signs included early non-specific symptoms such as erect ears, rigid tail, pilo-erection and un-groomed appearance progressing to more definitive signs such as ataxia

and limb paralysis. Animals were culled at this stage and not allowed to develop more severe signs of disease. No clinical signs were observed in the PBS control group.

Group incubation times (Table 2) were compared by Kaplan-Meier log-rank survival analysis. For the control C57BL/6J background, no significant difference was observed between the hemizgygous and wild type mice. Unexpectedly, the knockout mice showed a reduced incubation time (161±0.5 days) compared to the wild type controls (166±3.9 days) which was statistically significant (P=0.0175). This is in direct contrast to the results reported by Felton et al for the ME7 model of murine prion disease where they described a significant increase in survival for *Mcp1*$^{-/-}$ mice. A significant difference was also seen between the hemizygous (167±3.0) and knockout mice (P=0.0027). For each of the "increaser" (CAST) and "decreaser" (NZW and SJL) crosses no significant differences were observed between the hemizygous and *Mcp1* wild type mice. Taken together these data suggest that in the Chandler/RML model total knockout of *Mcp1*, but not loss of a single copy, results in a small (mean difference of 5 days) decrease in incubation time and is unlikely to contribute to the observed Mmu11 QTL.

Neuropathology and Immunocytochemistry: The neuropathological phenotype was also compared between *Mcp1*$^{-/-}$, *Mcp1*$^{-/+}$ and C57BL/6J groups. Mice were culled and the brains removed at the terminal stage of disease once a definitive diagnosis of mouse scrapie had been made. PrP^{Sc} deposition was determined by immunohistochemistry with the monoclonal antibody ICSM35 (ASANTE *et al.* 2002). No differences were seen between the groups (Figure 2). PrP^{Sc} is deposited extensively throughout the brain with

the most intense staining seen in the cortex, hippocampus and thalamus with less deposition in the cerebellum, brain stem, tectum and basal ganglia (Figure 2, E-H). This PrP^{Sc} distribution pattern is characteristic of the Chandler/RML prion strain in inbred lines of mice such as C57BL/6J. Gliosis, (GFAP staining- data not shown) and spongiosis (Figure 2, A and B - H&E staining) mirrored the distribution pattern of PrP^{Sc} and did not differ between groups. Activated microglia were specifically detected with an anti-Iba1 (polyclonal) antibody (Figure 2, C and D). The distribution mirrored that of the general gliosis and PrP^{Sc} and showed no differences between the groups. No neuronal loss was detected in the hippocampus by H&E staining (data not shown).

***Mcp1* expression:** *Mcp1* is known to play a role in the activation of microglia which are postulated to contribute to end-stage prion disease by exacerbating neuronal injury (FELTON *et al.* 2005). According to this hypothesis, $Mcp1^{-/-}$ mice would be expected to exhibit an increase in incubation time. This was observed by Felton *et al* using the ME7 model but the opposite was seen in this study with RML. Microglial activation was detected in both ME7 and RML models with no differences between wt and knockout mice suggesting that *Mcp1* alone is not necessary for microglial activation. Nevertheless, it has been suggested that the presence of high levels of *Mcp1* at later stages of disease may be required to drive the microglia to an increased level of activation sufficient to aggravate already damaged neurons. Therefore we determined the level of *Mcp1* mRNA expression in our inbred mouse strains before inoculation and at end-stage disease to see whether the *Mcp1* expression profile is comparable in the ME7 and RML models.

RNA was extracted from whole brains for normal and RML infected C57BL/6, CAST, NZW and SJL mice. Following reverse transcription, cDNA was used for quantitative real-time PCR using primers and probes as previously described. Expression levels were normalized against GAPDH and expressed as a relative quantity (arbitrary units) (Figure 3). *Mcp1* levels were very low in uninfected tissues but as described for ME7 (FELTON *et al.* 2005), significantly raised in terminal disease ($P \leq 0.01$ for all strains, Mann-Whitney test). Comparison of mouse strains showed no significant differences between "long" and "short" incubation time strains for uninfected samples but did show significance (P=0.01, Mann-Whitney test) for both CAST/NZW and CAST/SJL comparisons in RML infected samples.

DISCUSSION

Mcp1 has been implicated in various models of neuronal damage such as prion disease, stroke and experimental allergic encephalomyelitis (HUGHES *et al.* 2002; TEUSCHER *et al.* 1999; FELTON *et al.* 2005). The finding that *Mcp1*$^{-/-}$ mice show a delay in the onset of late-stage clinical signs and an increased survival time after ME7 prion infection (FELTON *et al.* 2005) and the localization of *Mcp1* within QTL regions of linkage (STEPHENSON *et al.* 2000; LLOYD *et al.* 2001) strongly suggested that *Mcp1* was a plausible candidate QTG for prion disease incubation time. Sequence analysis of *Mcp1* in inbred mice further supported this suggestion with polymorphisms in both 5'UTR and ORF segregating between mouse strains in patterns consistent with the observed incubation times.

Quantitative complementation is a strategy based on techniques developed in Drosophila, adapted and used successfully for identifying QTL in mice (MACKAY 2001; FLINT and MOTT 2001; YALCIN *et al.* 2004). Our data show that in the Chandler/RML model of murine prion disease, *Mcp1* does not delay onset of clinical signs of disease nor increase survival time but rather shows a small decrease in incubation time. Although statistically significant, the mean difference in incubation time between the two groups was only five days. Although highly speculative, it is possible that this difference occurs because chemokines affect different neuronal populations which are differentially targeted in the ME7 and Chandler/RML model. No differences were seen between wild type and knockout crosses suggesting that *Mcp1* has no effect on the phenotype and does not contribute to the QTL. Based on the control data, any effect of *Mcp1* in this model would

only be seen in full knockout and not hemizygous mice. Our original studies (LLOYD *et al.* 2001) identified a broad region of linkage on Mmu11 and suggested the potential for multiple modifiers in this region. If the influence of a single gene such as *Mcp1* on incubation time in this model is small it is possible that the quantitative complementation assay presented here may not be sensitive enough to detect such an effect especially as the effect of C57BL6/J alleles on the Mmu11 modifiers is unknown. Thus, it is not possible to completely exclude *Mcp1* as a QTG however, it remains unlikely that *Mcp1* is an important QTG because the genotype mean incubation times calculated for linked markers on Mmu11 are consistent with an additive model of inheritance while *Mcp1* appears to be dominant (LLOYD *et al.* 2001). Although all crosses in this study were set up using both males and females in each direction and both sexes were using in the inoculated groups the numbers were of necessity small therefore we are unable to exclude any imprinting effects.

Although differences in *Mcp1* expression were observed at end-stage disease between different mouse strains this does not correlate with incubation time as the highest level of expression was observed in CAST/Ei and the model of MCP1 action would suggest that higher levels of *Mcp1* mRNA would reduce rather than increase the incubation time. However, it should be noted that mRNA levels may not necessarily correlate with protein levels. Significant differences (P=0.01, Mann-Whitney test) in *Mcp1* expression at end stage were seen between CAST and both NZW and SJL which correlates with some of the polymorphisms described therefore although *Mcp1* does not seem to be a major gene

affecting incubation time these polymorphisms may influence a differential response to scrapie infection.

The increased survival seen by Felton *et al* in *Mcp1*$^{-/-}$ mice was not replicated in our study. Not only was the onset of clinical signs not delayed, but our knockout mice displayed the full range of typical scrapie symptoms whereas in the previous study not all the knockout mice displayed signs of scrapie but rather were sacrificed following loss of >15% body weight. One possible explanation is the mouse model itself. Although both studies used a knockout line which originated in the same laboratory, the line was first described by Gu *et al* in 1999 and has subsequently been maintained by others. The mice used by Felton *et al* were obtained from Novartis (H. Perry, personal communication) while those used in this study were purchased from the Jackson Laboratory. Over time it is possible that differences may have been introduced into these independent colonies. The C57BL6/J control animals were also acquired from different sources: Harlan, UK in the Felton *et al* study and The Jackson Laboratory in this study, which may further compound the differences. An alternative and possibly more likely explanation for these differences is the choice of prion strains. While Chandler/RML and ME7 are both mouse-adapted scrapie prion strains, they were independently derived and are distinct strains with differing biological and biochemical characteristics. Naturally occurring scrapie is associated with multiple strains (BRUCE *et al.* 1991; BRUCE *et al.* 2002). Chandler/RML was derived from goat scrapie and subsequently passaged in sheep and CD-1 mice (CHANDLER 1961). In contrast, ME7 was derived from the spleen of a scrapie infected Suffolk sheep passaged in Swiss white mice and subsequently passaged

in C57BL mice (DICKINSON *et al.* 1969; ZLOTNIK and RENNIE 1963). In inbred mice, ME7 and RML have different incubation times, show different patterns of neuropathology, and *in-vitro,* cells show differential susceptibility to both strains (WESTAWAY *et al.* 1987; BRUCE 1993, 2003; KLOHN *et al.* 2003). Furthermore, biochemical analysis has established that ME7 and RML have different conformations of PrP^{Sc} (THACKRAY *et al.* 2007). Although *Mcp1* is similarly up-regulated in both ME7 and RML models it appears that its role in disease pathogenesis may be prion strain specific.

Both pro- and anti-inflammatory molecules have been implicated in prion disease incubation time (FELTON *et al.* 2005; SCHULTZ *et al.* 2004; THACKRAY *et al.* 2004) and their results are all consistent with the hypothesis that inflammation may accelerate neuronal loss. However, our results demonstrate that the effects of individual molecules are likely to be prion strain specific and therefore it may not be possible to extrapolate to human prion diseases where their role remains uncertain..

ACKNOWLEDGEMENTS

We thank Michelle Ahmet, Catherine O'Malley, and Caroline Powell for preparation of histological slides. We also thank David Key and team for animal care and Ray Young for preparation of figures.

This work was supported by the Medical Research Council, UK.

FIGURE 1

Schematic of chromosome 11 for the offspring of quantitative complementation crosses. All mice are the result of a cross between *Mcp1*$^{-/+}$ mice (C57BL/6J background, black panel) and an inbred mouse strain carrying either an "increaser" (CAST, white panels, A and C) or "decreaser" (NZW or SJL, grey panels, B and D) QTL. Mice represented by panels A and B have two copies of *Mcp1*: one allele from C57BL6/J and the other representing an increaser (A) or decreaser (B) allele. Panels C and D depict mice carrying only one *Mcp1* allele derived from the increaser (C) or decreaser (D) strain respectively. The hatched box represents the null *Mcp1* allele on a C57BL/6J background.

FIGURE 2

Neuropathology and immunohistochemistry for C57BL/6J (A,C,E) and *Mcp1*$^{-/-}$ (B,D,F) mice. The scale bar represents 50μm for panels A and B and 2mm for panels C-F. Panels A and B are stained with haematoxylin and eosin and show evidence of spongiosis (vacuolation). Distribution of activated microglia is shown in panels C and D stained with polyclonal antibody Iba1. Sections E and F are stained with monoclonal antibody ICSM-35 to show abnormal PrP deposition. PrP staining is diffuse in both strains. Schematic representation of PrP deposition in the brain is shown for C57BL/6J (G) and *Mcp1*$^{-/-}$ (H). Red represents areas of intense staining, dark pink areas of moderate staining and light pink areas of light staining. For both strains, the cortex, hippocampus and thalamus show intense staining (red) with light staining (light pink) in the cerebellum, brain stem, tectum and basal ganglia. No significant differences are seen between the groups. Data for *Mcp1*$^{-/+}$ mice not shown as results are indistinguishable from C7BL/6J and *Mcp1*$^{-/-}$.

FIGURE 3

Quantification of *Mcp1* mRNA expression in whole brain by real-time RT-PCR for C57BL/6, CAST, NZW and SJL mouse strains. Dark and light shaded bars represent uninfected mice and mice at the terminal stage of disease following inoculation with Chandler/RML scrapie prions respectively. N=6 for each group except CAST-RML (n=4) and NZW-RML (n=5). All samples were tested in triplicate. Units are arbitary and represent quantity of *Mcp1* transcript normalizsed by quantity of GAPDH. Error bars represent the standard error of the mean. * signifies P=0.01 when compared to other strains for infected samples only (Mann-Whitney test). No highly significant differences were detected between strains for uninfected mice. *Mcp1* mRNA expression is significantly increased in end-stage disease in all strains ($P \leq 0.01$ Mann-Whitney test).

LITERATURE CITED

ASANTE, E. A., J. M. LINEHAN, M. DESBRUSLAIS, S. JOINER, I. GOWLAND *et al.*, 2002 BSE prions propagate as either variant CJD-like or sporadic CJD-like prion strains in transgenic mice expressing human prion protein. EMBO J. **21:** 6358-6366.

BRUCE, M. E., 1993 Scrapie strain variation and mutation. Br. Med. Bull. **49:** 822-838.

BRUCE, M. E., 2003 TSE strain variation. Br. Med. Bull. **66:** 99-108.

BRUCE, M. E., A. BOYLE, S. COUSENS, I. MCCONNELL, J. FOSTER *et al.*, 2002 Strain characterization of natural sheep scrapie and comparison with BSE. J. Gen. Virol. **83:** 695-704.

BRUCE, M. E., I. MCCONNELL, H. FRASER and A. G. DICKINSON, 1991 The disease characteristics of different strains of scrapie in Sinc congenic mouse lines: implications for the nature of the agent and host control of pathogenesis. J. Gen. Virol. **72:** 595-603.

CARLSON, G. A., C. EBELING, M. TORCHIA, D. WESTAWAY and S. B. PRUSINER, 1993 Delimiting the Location of the Scrapie Prion Incubation Time Gene on Chromosome 2 of the Mouse. Genetics **133:** 979-988.

CARLSON, G. A., P. A. GOODMAN, M. LOVETT, B. A. TAYLOR, S. T. MARSHALL *et al.*, 1988 Genetics and polymorphism of the mouse prion gene complex: control of scrapie incubation time. Mol. Cell Biol. **8:** 5528-5540.

CHANDLER, R. L., 1961 Encephalopathy in mice produced by inoculation with scrapie brain material. Lancet **1:** 1378-1379.

COLLINGE J, 2001 Prion diseases of humans and animals: their causes and molecular basis. Annu. Rev. Neurosci. **24:** 519-550.

DICKINSON, A. G., V. M. MEIKLE and H. FRASER, 1969 Genetical control of the concentration of ME7 scrapie agent in the brain of mice. J. Comp. Path **79:** 15-22.

FELTON, L. M., C. CUNNINGHAM, E. L. RANKINE, S. WATERS, D. BOCHE *et al.*, 2005 MCP-1 and murine prion disease: Separation of early behavioural dysfunction from overt clinical disease. Neurobiol. Dis. **20:** 283-295.

FLINT, J. and R. MOTT, 2001 Finding the molecular basis of quantitative traits: successes and pitfalls. Nat. Rev. Genet. **2:** 437-445.

FRETER, R. R., J. A. ALBERTA, K. K. LAM and C. D. STILES, 1995 A new platelet-derived growth factor-regulated genomic element which binds a serine/threonine phosphoprotein mediates induction of the slow immediate-early gene MCP-1. Mol. Cell Biol. **15:** 315-325.

GIESE, A., D. R. BROWN, M. H. GROSCHUP, C. FELDMANN, I. HAIST *et al.*, 1998 Role of microglia in neuronal cell death in prion disease. Brain Pathol. **8:** 449-457.

GU, L., B. RUTLEDGE, J. FIORILLO, C. ERNST, I. GREWAL *et al.*, 1997 In vivo properties of monocyte chemoattractant protein-1. J. Leukoc. Biol. **62:** 577-580.

GU, L., S. C. TSENG and B. J. ROLLINS, 1999 Monocyte chemoattractant protein-1. Chem Immunol **72:** 7-29.

HUGHES, P. M., P. R. ALLEGRINI, M. RUDIN, V. H. PERRY, A. K. MIR *et al.*, 2002 Monocyte chemoattractant protein-1 deficiency is protective in a murine stroke model. J. Cereb. Blood Flow Metab. **22:** 308-317.

KIM, C. G., S. L. SWENDEMAN, K. M. BARNHART and M. SHEFFERY, 1990 Promoter elements and erythroid cell nuclear factors that regulate alpha-globin gene transcription in vitro. Mol. Cell Biol. **10:** 5958-5966.

KLOHN P, L. STOLTZE, E. FLECHSIG, M. ENARI and C. WEISSMANN, 2003 A quantitative, highly sensitive cell-based infectivity assay for mouse scrapie prions. Proc. Natl. Acad. Sci U. S. A **100:** 11666-11671.

LLOYD S, O. N. ONWUAZOR, BECK J, G. MALLINSON, M. FARRALL *et al.*, 2001 Identification of multiple quantitative trait loci linked to prion disease incubation period in mice. Proc. Natl. Acad. Sci. USA **98:** 6279-6283.

LLOYD, S. E. and J. COLLINGE, 2005 Genetic susceptibility to prion diseases in humans and mice. Current Genomics **6:** 1-12.

LLOYD, S. E., J. B. UPHILL, P. V. TARGONSKI, E. M. FISHER and J. COLLINGE, 2002 Identification of genetic loci affecting mouse-adapted bovine spongiform encephalopathy incubation time in mice. Neurogenetics **4:** 77-81.

LU, B., B. J. RUTLEDGE, L. GU, J. FIORILLO, N. W. LUKACS *et al.*, 1998 Abnormalities in monocyte recruitment and cytokine expression in monocyte chemoattractant protein 1-deficient mice. J. Exp. Med. **187:** 601-608.

MACKAY, T. F., 2001 Quantitative trait loci in Drosophila. Nat. Rev. Genet. **2:** 11-20.

MANOLAKOU, K., J. BEATON, I. MCCONNELL, C. FARQUAR, J. MANSON *et al.*, 2001 Genetic and environmental factors modify bovine spongiform encephalopathy incubation period in mice. Proc. Natl. Acad Sci U. S. A **98:** 7402-7407.

MOORE, R. C., J. HOPE, P. A. MCBRIDE, I. MCCONNELL, J. SELFRIDGE *et al.*, 1998 Mice with gene targetted prion protein alterations show that *Prnp, Sinc* and *Prni* are congruent. Nature Genet. **18:** 118-125.

MORENO, C. R., F. LANTIER, I. LANTIER, P. SARRADIN and J. M. ELSEN, 2003 Detection of new quantitative trait Loci for susceptibility to transmissible spongiform encephalopathies in mice. Genetics **165:** 2085-2091.

PERRY, V. H., C. CUNNINGHAM and D. BOCHE, 2002 Atypical inflammation in the central nervous system in prion disease. Curr. Opin. Neurol. **15:** 349-354.

SCHULTZ, J., A. SCHWARZ, S. NEIDHOLD, M. BURWINKEL, C. RIEMER *et al.*, 2004 Role of interleukin-1 in prion disease-associated astrocyte activation. Am. J . Pathol. **165:** 671-678.

STEPHENSON, D. A., K. CHIOTTI, C. EBELING, D. GROTH, S. J. DEARMOND *et al.*, 2000 Quantitative trait loci affecting prion incubation time in mice. Genomics **69:** 47-53.

TEUSCHER, C., R. J. BUTTERFIELD, R. Z. MA, J. F. ZACHARY, R. W. DOERGE *et al.*, 1999 Sequence polymorphisms in the chemokines Scya1 (TCA-3), Scya2 (monocyte chemoattractant protein (MCP)-1), and Scya12 (MCP-5) are candidates for eae7, a locus controlling susceptibility to monophasic remitting/nonrelapsing experimental allergic encephalomyelitis. J. Immunol. **163:** 2262-2266.

THACKRAY, A. M., L. HOPKINS, M. A. KLEIN and R. BUJDOSO, 2007 Mouse-adapted ovine scrapie prion strains are characterized by different conformers of PrPSc. J. Virol. **81:** 12119-12127.

THACKRAY, A. M., A. N. MCKENZIE, M. A. KLEIN, A. LAUDER and R. BUJDOSO, 2004 Accelerated prion disease in the absence of interleukin-10. J. Virol. **78:** 13697-13707.

WESTAWAY, D., P. A. GOODMAN, C. A. MIRENDA, M. P. MCKINLEY, G. A. CARLSON *et al.*, 1987 Distinct prion proteins in short and long scrapie incubation period mice. Cell **51:** 651-662.

YALCIN, B., S. A. WILLIS-OWEN, J. FULLERTON, A. MEESAQ, R. M. DEACON *et al.*, 2004 Genetic dissection of a behavioral quantitative trait locus shows that Rgs2 modulates anxiety in mice. Nat. Genet. **36:** 1197-1202.

ZLOTNIK, I. and J. C. RENNIE, 1963 Further observations on the experimental transmission of scrapie from sheep and goats to laboratory mice. J. Comp. Path. **73:** 150-162.

TABLE 1

Mcp-1 polymorphisms

Region	Position	Codon	Polymorphism (Amino Acid)		
			NZW/OlaHsd (108±1)	CAST/Ei (188±3)	SJL/J (122±1)
5'UTR	81851811	-	C	T	C
	81851812-81851817	-	nc	ACCAGC Del	ACCAGC Ins
Exon 1	81851873	6	T (Met)	C (Thr)	T (Met)
	81851887	11	C	C	T
Exon 2	81852688	29	C	C	T
	81852742	47	G	A	G
	81852749	50	A (Ser)	G (Gly)	G (Gly)
Exon 3	81853194	90	C	T	C
	81853199	91	T	C	T
	81853201	92	G (Arg)	G (Arg)	A (Gln)

Numbering based on genome sequence NCBI Build 36 (NM_011333)

Prion disease incubation times are shown for each strain following intracerebral inoculation of Chandler/RML prions ± sem (LLOYD and COLLINGE 2005).

Amino acids are shown only for nonsynonomous polymorphisms.

nc = No change when compared to database sequence for *Mcp-1*,

Del = Deletion, Ins = Insertion

TABLE 2

Incubation times for Chandler/RML prions

Mouse Strain	Genotype	Mean (days) ± sem (n)
Mcp1$^{-/-}$	ko/ko	161 ± 0.5 (10)
Mcp1$^{-/+}$	wt/ko	167 ± 3.0 (9)
C57BL/6	wt/wt	166 ± 3.9 (8)
CASTxC57BL/6	wt/wt	206 ± 5.8 (9)
	wt/ko	205 ± 2.0 (9)
NZWxC57BL/6	wt/wt	181 ± 3.8 (9)
	wt/ko	178 ± 9.5 (9)
SJLxC57BL/6	wt/wt	148 ± 2.6 (10)
	wt/ko	152 ± 4.3 (10)

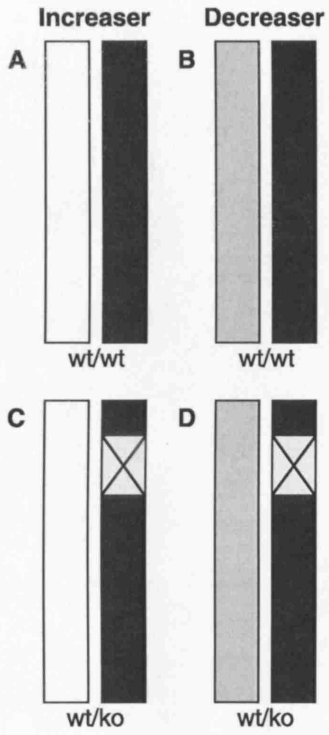
Increaser
Decreaser
A
B
wt/wt
wt/wt
C
D
wt/ko
wt/ko

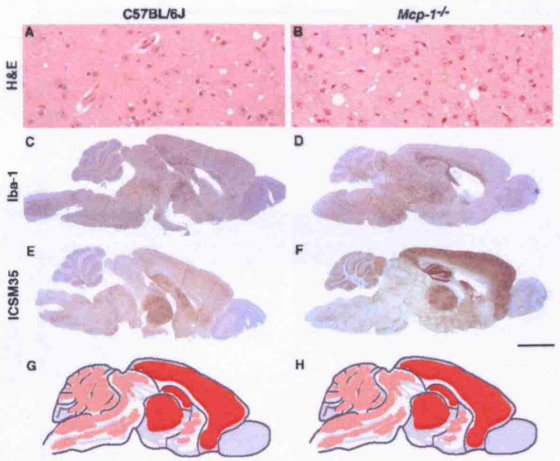
C57BL/6J
Mcp-1-/-
A
B
H&E
C
D
Iba-1
E
F
ICSM35
G
H

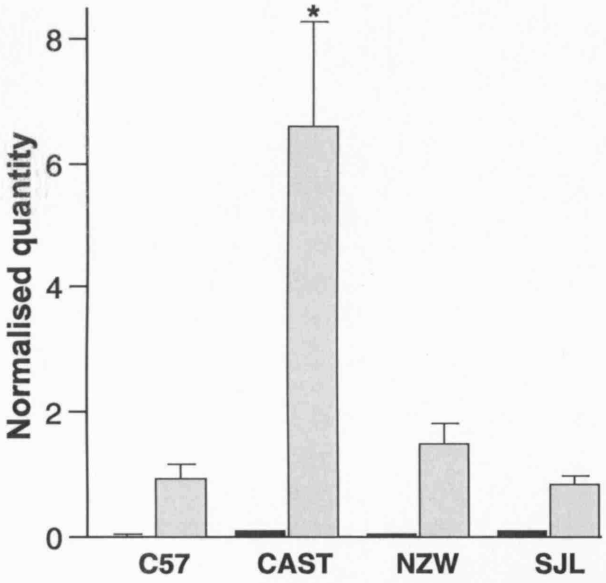
Normalised quantity
8
6
4
2
0
*
C57
CAST
NZW
SJL